



# NANOPARTICLES AND THE INTESTINE:

*in vitro* and *in vivo* investigations on genotoxic  
and inflammatory effects

Inaugural-Dissertation

zur Erlangung des Doktorgrades  
der Mathematisch-Naturwissenschaftlichen Fakultät  
der Heinrich-Heine-Universität Düsseldorf

vorgelegt von

**Kirsten Britta Gerloff**

aus Detmold

Düsseldorf, Mai 2010



aus dem Institut für umweltmedizinische Forschung an  
der Heinrich-Heine Universität Düsseldorf

Gedruckt mit der Genehmigung der  
Mathematisch-Naturwissenschaftlichen Fakultät der  
Heinrich-Heine-Universität Düsseldorf

Referent: Prof. Dr. J. Abel  
Koreferent: Prof. Dr. M. Braun

Tag der mündlichen Prüfung: 22.06.2010



Der Beginn aller Wissenschaften  
ist das Erstaunen,  
dass die Dinge sind, wie sie sind

Aristoteles  
384 - 322 v.Chr.

**Für meine Eltern**

---



# Table of contents

	Page
<b>Chapter 1</b>	<b>1</b>
<i>General Introduction</i>	
1 Introduction	1
1.1 The gastrointestinal tract	1
1.1.1 The Anatomy of the gastrointestinal tract	1
1.1.2 Caco-2 cells	5
1.1.3 The immune system in the gastrointestinal tract	6
1.1.3.1 Neutrophilic granulocytes	8
1.1.4 Oxidative stress, free radicals and the formation of reactive oxygen or nitrogen species	10
1.1.5 Ulcerative colitis	12
1.1.5.1 The role of neutrophils in ulcerative colitis	13
1.1.6 Genomic instability and carcinogenesis	13
1.2 Nanoparticles	15
1.2.1 Ambient particulate matter	16
1.2.2 Nanoparticles and the lung	17
1.2.2.1 Mechanisms of nanoparticle toxicity	18
1.2.3 Nanoparticles and the gut	19
1.2.3.1 Intestinal uptake of engineered nanoparticles	21
1.2.3.2 Toxicity of ingested nanoparticles	22
1.3 Aim of the thesis	25
1.4 References	27
<b>Chapter 2</b>	<b>35</b>
<i>Cytotoxicity and oxidative DNA damage by nanoparticles in human intestinal Caco-2 cells</i>	
2.1 Introduction	36
2.2 Methods	38
2.3 Results	42
2.4 Discussion	50
2.5 References	55
<b>Chapter 3</b>	<b>59</b>
<i>Specific surface area independent effects of titanium dioxide particles in human intestinal Caco-2 cells</i>	
3.1 Introduction	60
3.2 Methods	62
3.3 Results	64
3.4 Discussion	69
3.5 References	73

<b>Chapter 4</b>		<b>75</b>
	<i>Influence of simulated gastrointestinal digestion on particulate mineral oxide-induced cytotoxicity and interleukin-8 regulation in differentiated and undifferentiated Caco-2 cells</i>	
4.1	Introduction	77
4.2	Methods	80
4.3	Results	85
4.4	Discussion	95
4.5	References	101
<b>Chapter 5</b>		<b>105</b>
	<i>In vitro and in vivo investigations on the effect of amorphous silica on DNA damage in the inflamed intestine</i>	
5.1	Introduction	107
5.2	Methods	110
5.3	Results	115
5.4	Discussion	125
5.5	References	131
<b>Chapter 6</b>		<b>135</b>
6	General discussion	135
6.1	Conclusions	143
6.2	References	145
6.3	Summary	149
6.4	Zusammenfassung	150
6.5	Abbreviations	151
Publications		155
Presentations		157
Danksagung		159



# CHAPTER 1

---

## 1 Introduction

The human intestinal tract is challenged daily by a broad diversity of solid or liquid substances, containing essential nutrients such as carbohydrates, proteins, fats, minerals or vitamins, but also pathogens that easily find their way into this open, tubular system. Throughout a total surface area of 200-300 m<sup>2</sup> (Wells *et al.*, 1995) the healthy gut is well prepared to protect the body against possibly harmful substances, viruses, microorganisms or antigens by a tight mucosal lining, a well developed innate immune system and a variety of immune tissue and resident immune cells (Taniguchi *et al.*, 2009; Garrett *et al.*, 2010).

The adverse effects of nanoparticles (NP) in the lung are a long-standing field of research and the underlying mechanisms are nowadays well understood (Oberdörster *et al.*, 2005, Borm *et al.*, 2006, Nel *et al.*, 2006). In contrast, the use of NP in food and food related products is recently gaining increasing interest. Several types of microparticles are well established as food additives, known to be inert and therefore harmless to the human body. However, the number of nanoparticle-containing food products increases immensely (homepage nanoproject.org), but yet little is known about the cytotoxic or inflammatory potential of these novel materials and their impact on the human intestine. Patients suffering from intestinal diseases that are accompanied by disturbance of the epithelial layer, such as inflammatory bowel diseases, might be even more susceptible to possible harmful NP effects.

### 1.1 The gastrointestinal tract

#### 1.1.1 The Anatomy of the gastrointestinal tract

The gastrointestinal (GI) tract is a complex system, designed to ensure optimal nutrition and water absorption from ingested food. The human diet consists of a wide range of soluble to macromolecular structures, and the GI tract is challenged to handle not only this broad variety of substances that needs to be prepared for

optimal uptake of the containing nutrients. It also needs to deal with potentially harmful substances that can invade this long, tubular system via our daily food. A first barrier for the invasion of undesirable organisms, such as bacteria, is sterilisation by the acidic milieu of the stomach. The pH ranges from 1.5-2.0 in the fasting state and might rise up to 7.0 after ingestion of a meal. However, re-acidification takes place rapidly via increased secretion of gastric acid, mainly consisting of hydrochloric acid, sodium chloride and pepsin, by the gastric glands (Powell *et al.*, 1994; Lindahl *et al.*, 1997; Hörter and Dressman, 2001; Kwiecien and Konturek, 2003). Upon increasing motility of the stomach, the meal is transported to the small intestine. Here, the duodenum is the first segment and the regulator of digestion, as it is involved in inhibiting gastric secretion. Furthermore, pancreatic bicarbonate secretion leads to neutralisation of the chyme to a pH ranging from 6.4 to 7.5, depending on the intestinal section. This influences the solubility of certain nutrients and protects the intestinal mucosa (Evans *et al.*, 1988; Powell *et al.*, 1994; Hörter and Dressman, 2001; Kwiecien and Konturek, 2003). The small intestine further consists of the jejunum and, the most distal section, the ileum. Together with the duodenum, the jejunum is the major site of nutrient absorption. It is responsible for secretion of mucins, lactoferrin, albumin and other factors that are capable of mineral chelation to prevent nutrients, solubilised at the low gastric pH, from polymerising (Powell *et al.*, 1994, 1999). Its surface area is amplified immensely due to the presence of crypts, named the crypts of Lieberkühn, and projections called villi. Upon differentiation, the epithelial cells develop microvilli on the apical side, around 3000-7000 per cell in the small intestine (DeSesso and Jacobson, 2001). These villi further enhance the surface area to provide optimal nutrient absorption (Sancho *et al.*, 2004). Altogether, the intestine features a surface area of 200-300 m<sup>2</sup> (Wells *et al.*, 1995). The anatomy of the small intestine, including the villi and a schematic epithelial cell with microvilli, is illustrated in Figure 1.1.

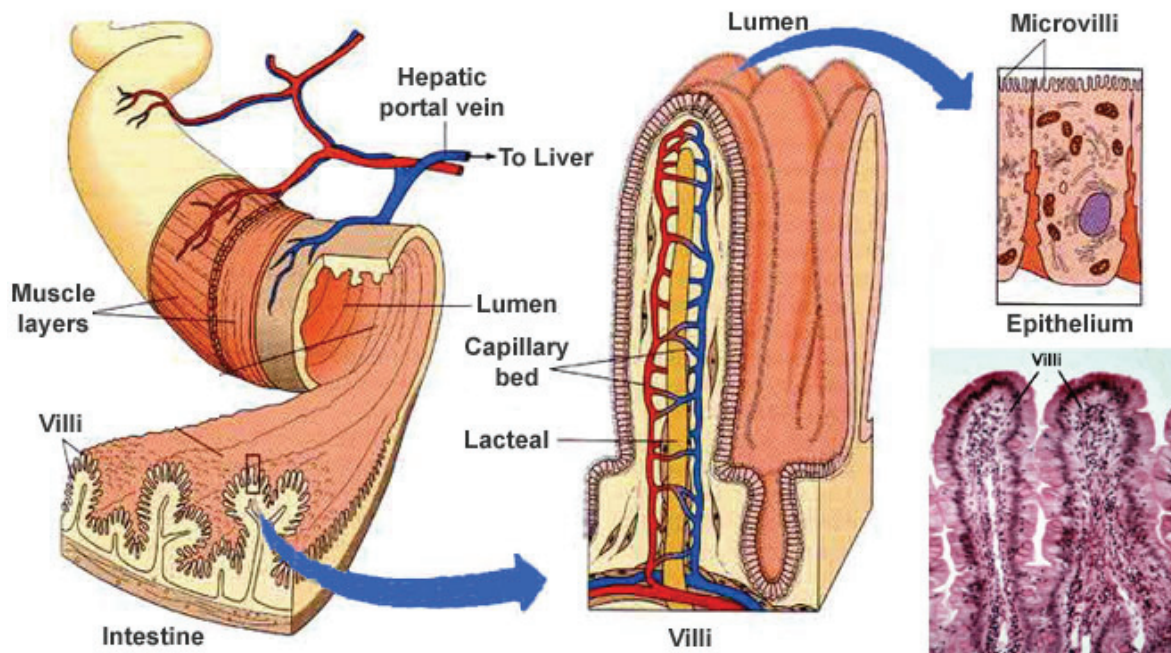


**Figure 1.1** Illustration of a cross section through the small intestine with villi and crypts and an exemplary epithelial cell, featuring microvilli. Taken from the homepage of the University of Colorado

The length of the villi decreases within the ileum. Finally, the colon, or the large intestine, marked by a considerably larger diameter, mainly consists of a smooth surface interspersed with crypts. The colon is divided into several segments, namely the ascending, the transverse, the descending and the sigmoid colon, terminating in the rectum. It is responsible for the storage of indigestible materials and waste products, the maintenance of the water balance as well as Vitamin K absorption. Three types of differentiated cells are present in the colon: enterocytes for nutrient absorption and secretion of hydrolases, goblet cells for mucus secretion, and the rare enteroendocrine cells that secrete several hormones, such as secretin or serotonin (Hollander *et al.*, 1977; Christensen, 1985; Powell *et al.*, 1994; Sancho *et al.*, 2004). Overall, the transit time of ingested food or beverages through the intestine varies between 3 to 8 hours and is driven by movement of the haustra, which are pouches caused by sacculations. Not only propulsive, but also non-propulsive haustra-activity was reported, and ensures homogenisation of the chyme and intensifies the contact with the mucosal surface for optimal nutrient absorption (Ritchie, 1968; Powell *et al.*, 1994).

The intestinal epithelial cells underlie constant renewal. Around four to six multipotent Leucine-rich repeat-containing G-protein coupled receptor 5 (Lgr5)-

expressing stem cells are located near (small intestine), or in (large intestine), each crypt bottom and constantly produce proliferating cells. These cells migrate either to the crypt bottom to differentiate to Paneth cells, exclusively found in the small intestine, or along the crypt-villus axis to proliferate several times and finally differentiate to enterocytes, enteroendocrine cells or goblet cells. The life span of a normal epithelial cell amounts to around five days, before it undergoes apoptosis, followed by cell shedding, at the tip of the villi or the surface epithelium in the colon, as depicted in Figure 1.4 (Ramachandran *et al.*, 2000; Sancho *et al.*, 2004; Sato *et al.*, 2009). The epithelium directly overlies a thin layer of loose connective tissue, the lamina propria (LP), which contains blood and lymph capillaries. Underneath the LP lies the submucosa followed by a circular and a longitudinal smooth muscle layer for optimal intestinal motility (DeSesso and Jacobson, 2001). The various layers are shown in Figure 1.2 by a cross-section of a healthy murine colon.

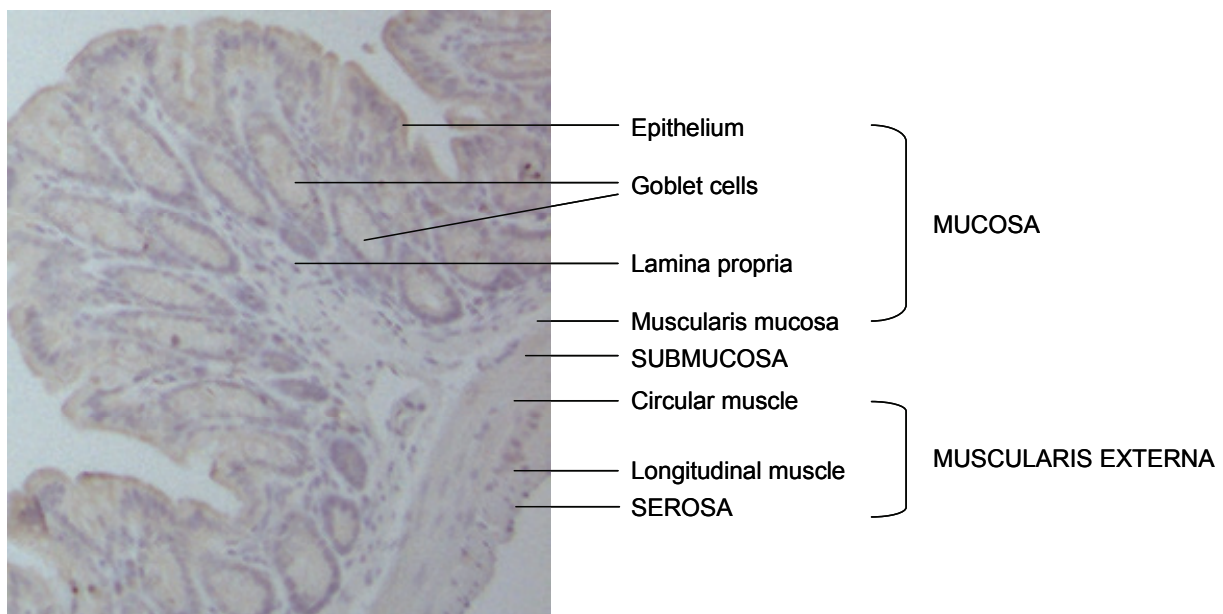


**Figure 1.2** Cross section through a healthy murine colon, the cell nuclei were stained using haematoxylin (blue) (The picture is from a 9 weeks old C57BL/6 mouse as used in the study described in Chapter 5)

### 1.1.2 Caco-2 cells

As an *in vitro* model of the human intestine, Caco-2 cells are widely used in the laboratory. In 1974, they were established from the primary colon tumor, an adenocarcinoma, of a 72-year-old Caucasian man. Upon cell-cell contact, Caco-2 cells accumulate in the  $G_0/G_1$  phase of the cell cycle and then undergo spontaneous enterocytic differentiation at standard culture conditions after reaching confluency (Mariadason *et al.*, 2002; Chopra *et al.*, 2010). Although isolated from colonic tissue, upon differentiation a loss of the colonic phenotype is detected, and expression of several markers of small intestine-like enterocytes increase, such as expression of villin and various brush-border associated hydrolases (e.g. sucrase, lactase, dipeptidylpeptidase 4 (DPP4), aminopeptidase N, and alkaline phosphatase), displaying their unique property of developing an apical brush border (Chantret *et al.*, 1988; Engle *et al.*, 1998; Mariadason *et al.*, 2002). Caco-2 cells, as shown in Figure 1.3, are also useful tools for studying differentiation processes occurring physiologically upon migration along the crypt–villus axis (Chopra *et al.*, 2010). Furthermore, undifferentiated cells might represent an inflamed intestinal epithelium, as hyperproliferative epithelial cells are known to occur during ulcerative colitis e.g. (Huang *et al.*, 1997). They also resemble human colon cancer cells in a wide range of their gene expression patterns (Sääf *et al.*, 2007). However, next to their various characteristics of small intestinal cells, gene expression patterns of differentiated Caco-2 cells appear similar to normal human colonic epithelial cells (Sääf *et al.*, 2007).

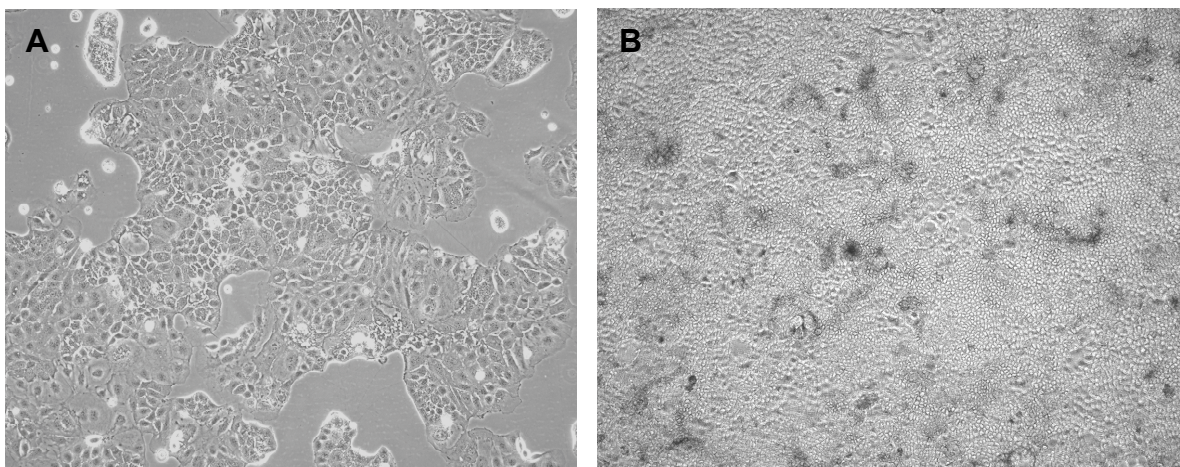


**Figure 1.3** Undifferentiated (A, 2 days after seeding) and differentiated (B, 11 days after seeding) Caco-2 cells (100 x magnification)

### 1.1.3 The immune system in the gastrointestinal tract

The intestinal tract constitutes the largest immune system of the body. While the small intestine is only sparsely populated, the large intestine hosts around  $10^{14}$  microorganisms. The gastrointestinal microbiota is composed of 500-1000 species, including eukarya, archaea and bacteria (Taniguchi *et al.*, 2009; Wells *et al.*, 2010). The human body highly benefits from most of these, as many live in a homeostatic symbiosis with the host. The bacteria are capable of providing nutrient and energy metabolism, influence tissue development and repair, protect against harmful microbiota and are responsible for infant immune development (Leser and Mølbak, 2009; Barbosa and Rescigno, 2010). Upon ingestion however, potential pathogens constantly enter the intestinal lumen. Therefore, the epithelium is permanently challenged with the discrimination between friend and foe. The mucus layer acts as the first barrier of undesired invasion of substances and organisms, and the gut epithelium consists of several immune tissues: the Peyer's patches (PP), which are gut-associated lymphoid tissue (GALT), the lamina propria, mesenteric lymph nodes (MLN) or intraepithelial lymphocytes (IEL) to maintain homeostasis. PP are covered with an epithelial layer rich of microfold (M)-cells. These M-cells are highly specialised for uptake of pathogens or other substances that need to be transported towards the underlying phagocytes (Powell *et al.*, 2010), and are shown to be upregulated in the presence of pathogens (Borghesi *et al.*, 1999).

The innate immune system of the intestine is well orchestrated by various pathogen-recognising receptors and immune cells. Thus, Toll-like receptors (TLR) play a key role in the innate gut immunity. They recognise so-called pathogen-associated molecular patterns (PAMP), which are common structures on microorganisms. TLR are not only present on the epithelial cells of the intestine, but also on dendritic cells, macrophages or Paneth cells (Taniguchi *et al.*, 2009; Wells *et al.*, 2010; Garrett *et al.*, 2010). Binding of PAMP to TLR can activate, amongst others, nuclear factor- $\kappa$ B (NF- $\kappa$ B), leading to an upregulation of chemokines and inflammatory cytokines, such as tumor necrosis factor- $\alpha$  (TNF- $\alpha$ ), interleukins or proteases (Medzhitov *et al.*, 1997). Upon cytokine secretion, polymorphonuclear neutrophils (PMN) that amongst others, circulate in the capillaries of the LP, can become activated and migrate towards the centre of inflammation. PMN are potent phagocytes, but they also lead to pathogen destruction upon oxidative bursting and

are for their part capable of pro-inflammatory cytokine production as well. The mechanisms underlying neutrophilic host defence are described in more detail in paragraph 1.1.3.1. Alongside neutrophils, dendritic cells (DC) and macrophages ( $m^\phi$ ) are the other important team players in intestinal host defence, and both are resident in PP, MLN and the lamina propria, as depicted in Figure 1.4. DC have a key role in antigen-processing and -presenting and are characterised by a high migratory capacity. Upon stimulation, they are able to induce proliferation and differentiation of both naïve and memory T cells, which is known to be uniquely for DC (Ng *et al.*, 2010; Garrett *et al.*, 2010). Next to DC,  $m^\phi$  are able to internalise partially degraded luminal products from absorptive enterocytes as well as apoptotic epithelial cell fragments even without prior activation. Similar to DC, they can directly induce the differentiation of regulatory T cells.  $m^\phi$  are widely unreactive upon repeated stimulation with the bacterial compound lipopolysaccharide (LPS) or endotoxins both *in vitro* and *in vivo* when pre-exposed with low doses of the respective substances. Thus, this tolerance development is considered a key role in maintaining homeostasis (West and Heagey, 2002; Ng *et al.*, 2010).

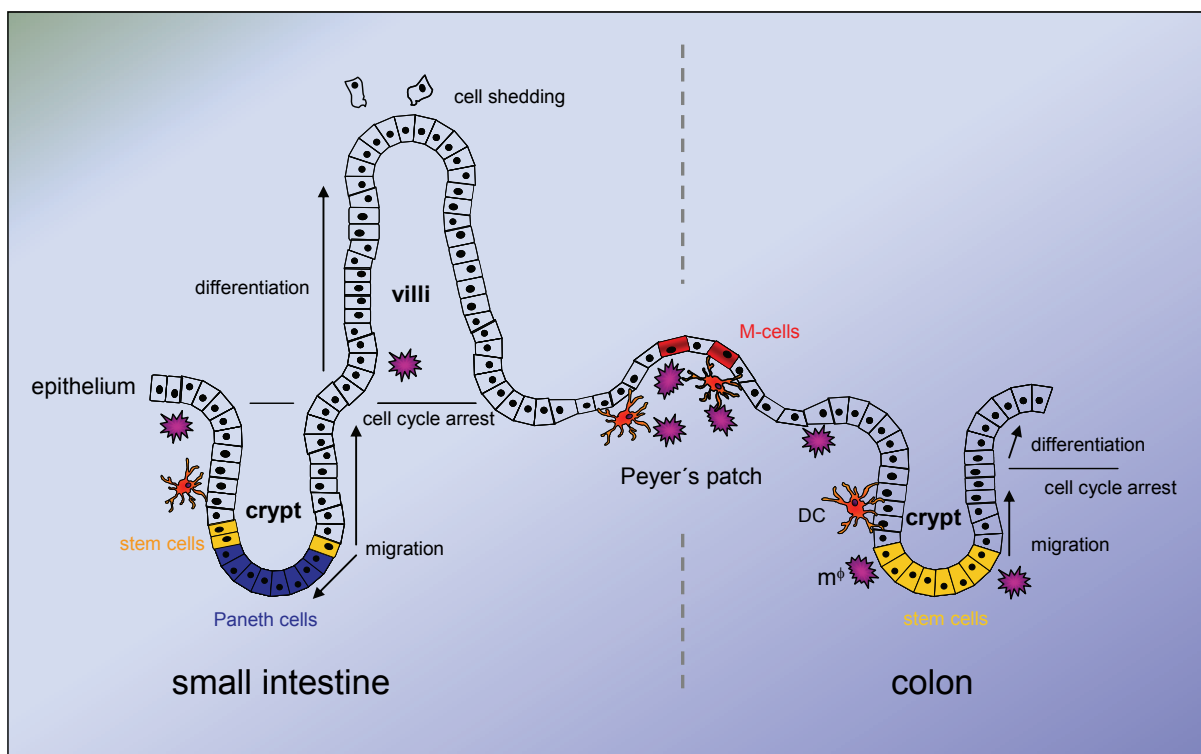


**Figure 1.4** Schematic intestinal construction with crypts and villi representing the small intestine, a Peyer's patch with M-cells, and the colon, solely exhibiting crypts. DC and macrophages are resident in the PP and LP.

### 1.1.3.1 Neutrophilic granulocytes

Neutrophilic granulocytes, or polymorphonuclear neutrophils (PMN), are counted among the most important phagocytes, and are in the first line of host defence. They circulate in the blood and have a life span of only 7-12 hours. Therefore, around  $1-2 \times 10^{11}$  PMN are produced daily in the human body. Neutrophils account for about 50-70 % of all blood leukocytes in the human body (Freitas *et al.*, 2009; Wessels *et al.*, 2010). Upon an inflammatory event, neutrophil production is upregulated, and its lifetime increases as a response to platelet activating factor (PAF), granulocyte-colony stimulating factor (G-CSF) or various pro-inflammatory cytokines, such as interleukin-1 $\beta$  (IL-1 $\beta$ ) (Wessels *et al.*, 2010). The crucial role of PMN in the human immune system is long known. In 1968, Baehner and Karnovsky described a link between a reduced PMN activity and the development of chronic granulomatous disease (CGD) (Baehner and Karnovsky, 1968). The important peroxidase-mediated bactericidal role of PMN and the formation of superoxide radicals as one of the main bactericidal mechanisms was already described more than 30 years ago (Klebanoff, 1967; Babior *et al.*, 1973; Klebanoff and Rosen, 1978). A strong negative correlation between the chemotactic ability of PMN and patients with increased bacterial sepsis was demonstrated (Christou and Meakins, 1979), and clinical morbidity from infections is clearly increased with a reduced number of circulating PMN in the blood (Nauseef, 2007).

Various endothelial adhesion molecules, such as the intercellular adhesion molecule 1 (ICAM-1), mediate neutrophil adhesion to endothelial cells. ICAM-1 expression on the luminal surface of the capillary is increased during inflammation, and interacts with  $\beta$ 2 integrin, which is expressed on the surface of PMN. Subsequent to adhesion, neutrophils begin to migrate across the endothelium and towards the centre of inflammation (Drost and MacNee, 2002; Wang *et al.*, 2004). Interleukin-8 (IL-8) is known to be one of the most potent chemoattractants for the recruitment and activation of neutrophils into various organs (e.g. lung, intestine), and binds to the human CXC chemokine receptor 1 (CXCR1) and CXC chemokine receptor 2 (CXCR2) on the surface of the PMN (Kunkel *et al.*, 1991; Mitsuyama *et al.*, 1994; Buanne *et al.*, 2007). IL-8 is mainly regulated by the NF- $\kappa$ B signalling pathway (Wang *et al.*, 2009). Upon incubation with IL-8, increased PMN deformability and upregulation of the adhesion receptor CD11b was observed (Drost and MacNee,



2002). The neutrophilic cytosol contains granules that are filled with a variety of proteins, such as defensins, bactericidal-permeability-increasing protein, proteases (e.g. elastase, cathepsins), and myeloperoxidase (MPO) that consumes hydrogen peroxide ( $H_2O_2$ ) and generates hypochlorous acid (HOCl), the most bactericidal oxidant that is produced by PMN (Hampton *et al.*, 1998; Nauseef, 2007; Freitas *et al.*, 2009). Activated neutrophils are capable of producing a variety of pro-inflammatory cytokines, e.g. IL-1 $\beta$ , IL-6, IL-12 and IL-23, and transport internalised pathogens to lymph nodes to support macrophages and DC in antigen presentation (Silva, 2010). Also, contact with pathogens results not only in phagocytosis, but also in the so-called oxidative burst, marked by an increased consumption of molecular oxygen and resulting production of reactive oxygen species (ROS) and reactive nitrogen species (RNS) (Babior, 2000). ROS generation by PMN is catalysed by nicotinamide adenine dinucleotide phosphate (NADPH) oxidase, a membrane-bound enzyme complex that can be stimulated *ex vivo* by phorbol myristate acetate (PMA) (Suzuki and Lehrer, 1980). The NADPH oxidase complex consists of various subunits that are located in the cytosol and in the membranes of intracellular vesicles and organelles. The cytosolic subunits migrate towards the membrane bound subunits upon activation, to bind and configure the active enzyme complex (Knaapen *et al.*, 2006).

In PMN, the catalytic subunit of the predominantly expressed NADPH oxidase is NOX2 (gp91phox), and the active enzyme complex is completed by the regulatory subunit p22phox, the cytosolic subunits p40phox, p47phox, and p67phox and the guanosine triphosphate hydrolase (GTPase) Rac. Moreover, several human homologs of NOX2 are present in nonphagocytic cells, such as NOX1, NOX3, NOX4, NOX5, and the dual oxidases Duox1 and Duox2 (Frey *et al.*, 2009).

The crucial role of the NADPH oxidase *in vivo* is shown in mice deficient in specific subunits of this enzyme complex as well as in chronic granulomatous disease (CGD) patients; animals lacking a functional NOX2 have been shown to rapidly develop spontaneous multi-organ bacterial and fungal infections early in life and their life-expectancy has been reduced to a few months only, even when raised under specific pathogen-free (SPF) conditions (Ostanin *et al.*, 2007). p47phox deficient mice develop CGD, a genetic childhood disease that is marked by non-functional phagocytes, thus leading to severe infections and early death (Jackson *et al.*, 1995), and a lack of either NOX2, p22phox, p47phox or p67phox is linked to CGD development in humans (Krause and Bedard, 2008; Matute *et al.*, 2009).

#### 1.1.4 Oxidative stress, free radicals and the formation of reactive oxygen or nitrogen species

The concept of oxidative stress describes the imbalance between oxidants and antioxidants in favour of the oxidants, which might result in cell or tissue damage (Sies, 1997). In healthy conditions, formation of oxidants is balanced by the presence of a variety of antioxidants. Oxidants can be generated by the reduction of molecular oxygen to water, leading to the formation of the intermediates superoxide anion radical ( $O_2^{\cdot-}$ ),  $H_2O_2$  or the hydroxyl radical ( $HO^{\cdot}$ ). Furthermore, free radicals in general are considered oxidants. Free radicals are molecules or molecular fragments that possess an unpaired electron, which is conventionally indicated by a superscript bold dot and responsible for the high reactivity and the paramagnetism of the radical. Free radicals can be charged positively or negatively or be electrically neutral. They are formed from a normal molecule by either homolytic cleavage of a covalent bond, requiring high energy input (e.g. ultrasound, UV-radiation), or addition or loss of a single electron. In biological processes, the electron transfer plays a major role in the generation of free radicals, as it can be initiated by enzymatic reactions (Slater, 1984; Cheeseman and Slater, 1993).

In healthy conditions, oxidants formation is scavenged by various antioxidant mechanisms. Some of the main antioxidant enzymes are superoxide dismutase (SOD) or catalase. Moreover, an important intracellular antioxidant is glutathione (GSH; L- $\gamma$ -glutamyl-L-cysteinyl-glycine), a tripeptide containing a thiol group. Upon reaction with an oxidant such as  $H_2O_2$  GSH is oxidised to glutathione disulfide (GSSG), and  $H_2O_2$  is reduced to water:



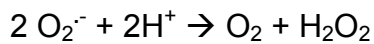
Subsequently, GSH is recovered by the GSSG reductase (Sies, 1997, 1999). Determination of the changes in intracellular GSH content and the GSH/GSSG ratio is a widely used marker for cellular response to oxidative stress in particle toxicity (Li *et al.*, 2008).

ROS but also reactive nitrogen species (RNS) formation may occur via a multitude of chemical reactions (Barthel and Klotz, 2005; Knaapen *et al.*, 2006; Freitas *et al.*, 2009):

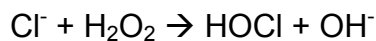
$O_2^{\cdot -}$  is a short-living radical and directly generated upon reaction of oxygen with NADPH oxidase:



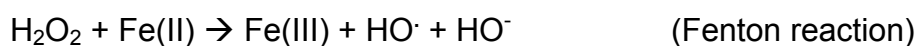
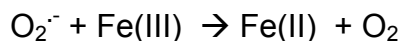
Either spontaneously or through catalysis by SOD  $O_2^{\cdot -}$  is dismutated into  $H_2O_2$ , which is relatively stable and capable of intracellular diffusion:



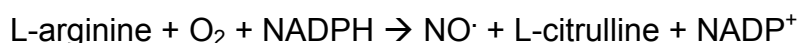
In PMN, the highly abundant enzyme MPO catalyses the formation of hypochlorous acid (HOCl), a highly bactericidal oxidant, and directly consumes up to 70 % of the formed  $H_2O_2$ :



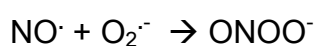
The hydroxyl radical ( $HO^{\cdot}$ ) is a highly reactive and very short living radical. It is formed according to the Haber Weiss-reaction, which includes the Fenton reaction, and is catalysed by iron:



Furthermore, neutrophils and, more importantly macrophages, are capable of producing reactive nitrogen species (RNS), especially nitric oxide ( $NO^{\cdot}$ ), via the inducible nitric oxide synthase (iNOS) by consumption of NADPH and conversion of L-arginine to L-citrulline:



The resulting  $NO^{\cdot}$  can further react with  $O_2^{\cdot -}$  to generate the highly mutagenic and cytotoxic peroxynitrite anion ( $ONOO^-$ ):



### 1.1.5 Ulcerative colitis

A disturbance of the well balanced immune system of the intestine can lead to the development of inflammatory bowel diseases (IBD), such as ulcerative colitis (UC) or Crohn's disease (CD). CD may affect parts of the whole gastro-intestinal system, including the oral cavity, whereas UC is reduced to the large intestine, starting from the rectum and continuing up the colon. Both diseases are characterised by periodic exacerbation and remission of the symptoms. Patients suffering from CD or UC experience chronic diarrhoea, sometimes with blood, weight loss and abdominal pain (Fatahzadeh, 2009)

UC mainly occurs in early adulthood and again between the ages of 50-70 years. Environmental, hereditary or immunological factors play a role in the outbreak and progression of the disease. Therapeutic approaches nowadays involve treatment with steroids, immunosuppressive drugs or heparin and, in severe cases, a colectomy. UC is marked by crypt abscesses, ulceration of the colonic epithelium and epithelial barrier dysfunction, accompanied by neutrophilic infiltration. A pronounced and long-lasting UC can also contribute to an increased risk for colorectal cancer (Itzkowitz and Yio, 2004; Wirtz and Neurath, 2007; Fatahzadeh, 2009; Wang *et al.*, 2009). The main cause for exacerbation of UC is discussed to be the imbalance of the intestinal immune system, marked by continuous migration of activated lymphocytes, granulocytes and macrophages into the mucosa. Increased levels of inflammatory cytokines and chemokines are found in the tissue of UC patients. IL-8 levels are found significantly increased in colitic tissue. Further cytokines that are upregulated in UC are IL-1 $\beta$ , IL-6 or TNF- $\alpha$  e.g. T-cell response was found to be mainly type 2 helper cell (Th2) dominant in UC, marked by an increase in IL-5 and IL-13 secretion, in contrast to CD, where T-cell response appeared to be mainly Th1 dominant (Mazzucchelli *et al.*, 1994; Mitsuyama *et al.*, 1994; Rogler and Andus, 1998; MacDermott, 1999; Shih and Targan, 2008).

Various animal models are nowadays used to induce experimental colitis. For example, intestinal inflammation can occur by disturbance of the epithelial barrier. Feeding with the widely used dextrane sulphate sodium (DSS), a substance that is directly toxic to epithelial cells, leads to induction of colitic symptoms, such as bloody diarrhoea, ulcerations and neutrophil infiltration. Multi drug resistant 1 (MDR1) gene deficient mice are known to develop spontaneous bowel inflammation triggered by

the bacterial flora. In addition to this, animals with a disturbed immune response, such as signal transducer and activator of transcription 3 or 4 (STAT3 / STAT4) gene deficient mice (Gaudio *et al.*, 1999; Wirtz and Neurath, 2007), develop spontaneous enterocolitis.

#### **1.1.5.1 The role of neutrophils in ulcerative colitis**

Neutrophils play a major role in the exacerbation of ulcerative colitis. The number of neutrophils present in colitic tissue correlates directly to the amount of secreted IL-8 and the grade of local inflammation (Mazzucchelli *et al.*, 1994; Mitsuyama *et al.*, 1994). Neutrophilic bursting is known to directly leading to an increased production of ROS (Knaapen *et al.*, 2006), which in turn is closely related to the amplification of the inflammatory response in UC (Babbs, 1992). Polymorphisms in the ICAM-1 encoding gene as well as elevated levels of ICAM-1 were found in tissues of UC patients (Dippold *et al.*, 1993; Vainer, 2005; Naito *et al.*, 2007). Neutrophil infiltration is also known to play a crucial role in DSS induced experimental colitis. DSS-treated CXCR2<sup>-/-</sup> mice did not exhibit PMN infiltration into the mucosa, and the clinical colitis conditions were noticeably improved in comparison to wild type (WT) mice (Buanne *et al.*, 2007). Specific depletion of neutrophils in a DSS-colitic rat model, using the monoclonal antibody RP-3, reduced the colitic symptoms significantly (Natsui *et al.*, 1997), whereas this attenuating effect seems to be mainly dependent on the depletion of iNOS and not on a defective NADPH oxidase (Kriegelstein *et al.*, 2001).

#### **1.1.6 Genomic instability and carcinogenesis**

Colorectal cancer (CRC) mainly arises from genomic instability such as chromosomal instability (CIN) or microsatellite instability (MSI). Aneuploidy, i.e. an abnormal number of chromosomes, as well as loss of heterozygosity arise from CIN. This can lead to large-scale chromosomal losses and therefore also loss or mutation of essential tumour suppressor genes such as p53 or adenomatous polyposis coli (APC), a key suppressor in the human colon. CRC in the colitic colon is evident by the presence of multifocal areas, unlike sporadic colorectal carcinoma (SCC), where dysplastic lesions usually develop in one or two focal areas. Additionally, these areas

are found to arise within tissue areas that are already affected by colonic inflammation (Boland *et al.*, 2005; Itzkowitz *et al.*, 2004).

The epithelial cells in active UC are known to be hyperproliferative, marked by increased apoptosis and an accelerated cell turnover that might contribute to carcinogenesis (Arai *et al.*, 1999). Further, the ongoing inflammation, accompanied by constant influx of activated phagocytes and permanent ROS/RNS generation, is an important risk factor for cancer development. Thus, DNA damage can be induced by oxidation, nitration, depurination, methylation and deamination (Knaapen *et al.*, 2006). The hydroxyl radical is the most reactive radical that directly interacts with the DNA by H-atom abstraction, to generate manifold products with all four bases (Pryor, 1988). One of the most important and well-studied oxidative lesions generated by HO $\cdot$  is 8-hydroxydeoxyguanosine (8-OHdG), generated by oxidation of guanine in DNA at C8, as shown in Figure 1.5.

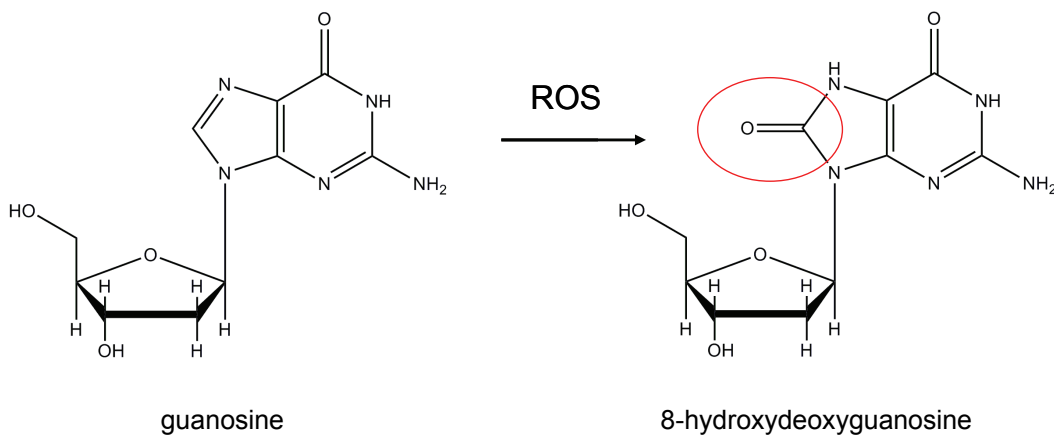


**Figure 1.5** ROS-induced formation of 8-hydroxydeoxyguanosine (8-OHdG) from guanosine

It is found to be elevated in colonic tissues of patients with long-lasting UC (Itzkowitz *et al.*, 2004) and well known for its mutagenic potential, as dAMP, instead of dCMP, might be incorporated wrongly opposite 8-OHdG (Shibutani *et al.*, 1991). The analysis of alterations in 8-OHdG sites is discussed to find use as a marker of oxidative stress in carcinogenesis (Kasai, 1997). Important enzymes for repair of oxidative base damage are 8-oxoguanine DNA glycosylase (OGG1) and its bacterial homologue formamidopyrimidine glycosylase (Fpg) that has found use in the laboratory to specifically detect and quantify oxidative lesions (Pflaum *et al.*, 1997; Burrows and Muller, 1998).

## 1.2 Nanoparticles

The use of engineered nanoparticles (ENP) is a rapidly growing economic field. These particularly small materials are characterised by a size range between 1 and 100 nm, with one or more external dimensions in the nanoscale (Stone *et al.*, 2009). Thus, the classification as a “nano” structure does not only include spherical particles, but also nanofibres, single- and multiwalled nanotubes, nanowires, nanorings, nanostructured surfaces and composite materials (Oberdörster *et al.*, 2005; Borm *et al.*, 2006). Not only size is a main feature of ENP, but also their large specific surface area (SSA), that increases exponentially with decreasing primary particle size (Oberdörster *et al.*, 2005). It is well known that NP tend to form aggregates by fusion of primary particles, and agglomerates, defined as undispersed clusters of aggregates during their production or generation as well as in suspension (Donaldson *et al.*, 2005; Zhang *et al.*, 2008). Particles are commonly discriminated between particles with inherent toxic activity, such as welding fume, quartz dust or hard-metal dusts, and poorly soluble low toxicity particles (PSP) such as titanium dioxide (TiO<sub>2</sub>) or carbon black (CB) (Borm *et al.*, 2004).

Nanotechnology will gain significant importance in the near future, in particular in the fields of optics, fabrics, displays and pigments, as well as in industries such as space, automotive, and microelectronics. In recent years, increasing research is focused on using ENP in medicine and pharmacology, for cosmetics, food or food related products (Oberdörster *et al.*, 2005; Borm *et al.*, 2006; Chaudhry *et al.*, 2008; Geiser and Kreyling, 2010). For example, nano-enabled products worth \$147 billion were produced in 2007, whereas the sales volume of nano-containing products is expected to be around \$3.1 trillion in 2015 (luxresearchinc.com).

Humans can be exposed to ENP intentionally by use of new drugs to deliver medical agents to specific target organs or by the use of quantum dots for *in vivo* targeting of tumour cells e.g. (Gao *et al.*, 2004; Mühlfeld *et al.*, 2008; Matsusaki and Akashi, 2009). Furthermore, various functional foods are launched regularly that promise enhanced nutrient absorption, or general increased well-being, by consuming nanoparticle-enriched products (homepage nanotechproject.org).

Unintentional uptake of ENP often occurs at the workplace simply by inhalation, and potentially through the skin by use of novel cosmetic products. Food and toothpaste can contain ENP, thus ingestion is another important route of

nanoparticle exposure, and the impact on human health is still under discussion. NP exposure of the brain is another very recent field of interest. There is evidence that NP might be taken up by the olfactory bulb upon inhalation and nasal deposition, and subsequently be transported directly to the brain (Hautot *et al.*, 2003; Oberdörster *et al.*, 2005). Also, systemic NP uptake can be an issue, either upon inhalation, ingestion or uptake by the skin, and high doses of ingested NP are already found to cause DNA damage in blood and bone marrow cells, suggesting that there may be significant translocation (Trouiller *et al.*, 2009). Possible routes of NP uptake are illustrated in Figure 1.6.

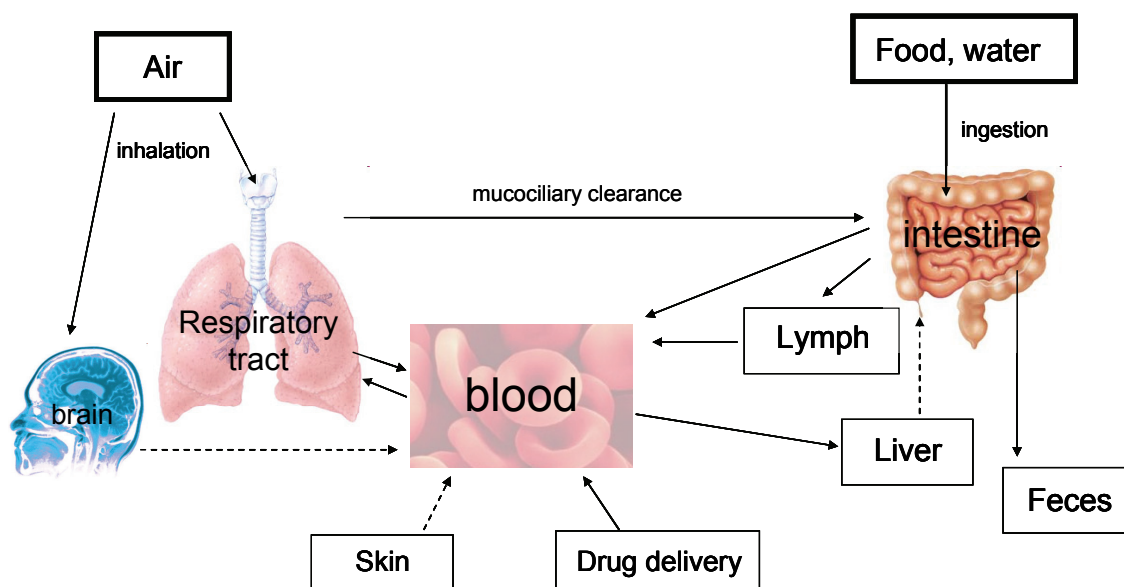


**Figure 1.6** Possible routes of human NP-uptake, allocation and excretion. Modified from Oberdörster *et al.*, 2005

### 1.2.1 Ambient particulate matter

Not only intentionally produced nanoparticles are a source for human exposure, but also a wide range of particulate matter (PM) challenge human health and the lung tissue is the first organ to get in contact with these materials. Forest fires and volcanoes, but also viruses and pollen are considered natural PM sources to which humans were constantly exposed throughout their evolution. In contrast, combustion or engine exhausts, power plants or welding applications are examples for anthropogenic sources for PM. Ambient particulate matter is divided into different categories in accordance to their aerodynamic diameters, namely the diameter of a



spherical particle with a density of  $1 \text{ g/cm}^3$ .  $\text{PM}_{10}$  is defined as having coarse, fine and ultrafine particles with aerodynamic diameters between  $2.5\text{-}10 \text{ }\mu\text{m}$ , hence  $\text{PM}_{2.5}$  are particles  $< 2.5 \text{ }\mu\text{m}$ , and  $\text{PM}_{0.1}$  are NP  $< 0.1 \text{ }\mu\text{m}$ . (Oberdörster *et al.*, 2005; Mühlfeld *et al.*, 2008).

## 1.2.2 Nanoparticles and the lung

Occupational exposure to inhaled nanoparticles and the discovery of its link to fibrosis originated the first nanotoxicological inquiries (Borm, 2002). Epidemiological studies with coal miners and silica-exposed workers further revealed a correlation between fibrosis and lung cancer (Borm *et al.*, 2004). Nowadays, inhaled particles are known to play an important role not only in fibrosis or cancer development, but also in chronic obstructive pulmonary disease (COPD) and asthma.  $\text{PM}_{10}$  are further discussed to exacerbate cardiovascular effects in predisposed individuals (Donaldson *et al.*, 2000; 2009). The mechanisms underlying toxicological NP effects and their impact on carcinogenicity and cancer development in the lung are partly understood. Nevertheless, particle hazard is often hard to predict, as their numerous properties (e.g. size, specific surface area (SSA), chemical composition, solubility) each might influence their toxic potential. However, studies on the lung and lung epithelial cells have shown that carbon black and  $\text{TiO}_2$  particles of the same composition and crystalline structure display elevated toxicity and pro-inflammatory potential with an increasing SSA (Oberdörster *et al.*, 2005; Monteiller *et al.*, 2007; Johnston *et al.*, 2009).

According to their size and mass, inhaled ENP or PM tend to invade and deposit differently into the three major regions of the respiratory tract. Upon nose breathing and during rest, a mathematical model predicts deposition of particles  $> 1000 \text{ nm}$  or  $< 1 \text{ nm}$  mainly in the nasal, pharyngeal and laryngeal region. Particles of a size between  $1\text{-}100 \text{ nm}$  tend to deposit in the tracheobronchial region but also in the alveoli (Oberdörster *et al.*, 2005). Clearance of particles in the lung can occur either by chemical processes, if the material is biodegradable, or by physical translocation, such as mucociliary clearance, whereupon after swallowing these particles finally reach the gastrointestinal tract (Oberdörster *et al.*, 2005).

Different mechanisms of cellular NP uptake are currently discussed. Amongst others, phagocytosis, macropinocytosis, clathrin- and nonclathrin-mediated endocytosis or diffusion can play a role. However, cellular uptake is dependent on particle size or chemical composition as well as the exposed cell type (Unfried *et al.*, 2007).

### 1.2.2.1 Mechanisms of nanoparticle toxicity

The main contributor to NP toxicity is considered to be their ability to induce ROS (Donaldson *et al.*, 2005; Oberdörster *et al.*, 2005). Molecular oxygen can be converted into ROS directly on the surface of metal-containing particles or by particle contaminants such as iron, via the Fenton-like reaction (paragraph 1.1.4). Indirectly, and upon single electron transfer, this may be catalysed by the NADPH oxidase, or it may occur as a side reaction of electron transport along the mitochondrial respiratory chain. Oxygen can react to  $O_2^-$  resulting in formation of  $H_2O_2$  (paragraph 1.1.4) (Unfried *et al.*, 2007). Likewise, photoactivation leads to the formation of singlet oxygen ( $^1O_2$ ) followed by transformation into  $O_2^-$ , and is discussed to play a role for NP-containing cosmetics as sun creams and thus NP toxicity to the skin. But also in the laboratory, photoactivation can play a role in inducing ROS by particles such as  $TiO_2$ , which might lead to positive outcomes in *in vitro* toxicology tests. Obviously however, it is not expected to play a role *in vivo* when exposed to inner organs such as lung or intestine (Nakagawa *et al.*, 1997; Sayes *et al.*, 2006; Johnston *et al.*, 2009).

Low amounts of ROS can induce activation of various signalling cascades within the cell, such as the phosphoinositide 3'-kinase (PI 3-kinase)/protein kinase B (PKB) pathway (Barthel and Klotz, 2005). Excessive ROS formation however can induce genotoxicity, leading to DNA strand breakage, oxidative lesions, micronucleus formation or sister chromatid exchanges, and thus induce carcinogenicity (Schins and Knaapen, 2007). DNA damage and oxidative stress was found *in vitro* and *in vivo* after exposure to both PM (Risom *et al.*, 2003; Gallagher *et al.*, 2003; Albrecht *et al.*, 2005) and ENP (Johnston *et al.*, 2000; Gurr *et al.*, 2005; Falck *et al.*, 2009).

Next to the primary particle toxicity described above, inflammation plays an important role in particle induced lung injury and is referred to as secondary particle

toxicity when the inflammatory processes overwhelm the antioxidant and DNA damage repair capacities in the lung (Schins and Knaapen, 2007; Figure 1.7). Resident alveolar macrophages, that usually phagocyte microorganisms or particles will be activated when overwhelmed by the amount of invading pathogens and release inflammatory cytokines and chemokines. Consequently, neutrophils are recruited and activated, leading to enhanced generation of reactive oxygen and nitrogen species by mechanisms as described above, thus featuring a high mutagenic potential by induction of genotoxicity (Driscoll *et al.*, 1997; Knaapen *et al.*, 1999; 2006).

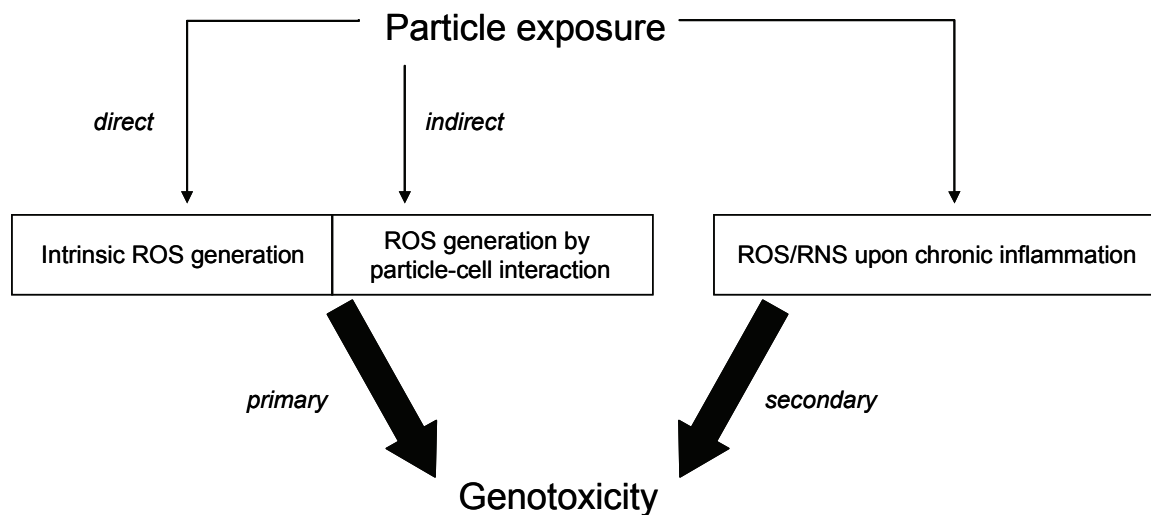


**Figure 1.7** Primary versus secondary particle induced genotoxicity mechanisms

### 1.2.3 Nanoparticles and the gut

Inorganic microparticles have a long-standing use in the food industry. They are appreciated for being inert within the human body and are approved as food additives, finding use in both conventional and functional food (homepage food.gov.uk). Several materials, their E numbers and applications are listed in Table 1.1.

E Number	Material	Application
171	Titanium dioxide	Colouring
172	Iron oxides / hydroxides	Colouring
173	Aluminium	Colouring
174	Silver	Colouring
175	Gold	Colouring
529	Calcium oxide	Acidity regulator
530	Magnesium oxide	Acidity regulator / Release agent
551	Silicon dioxide	Anticaking agent

**Table 1.1** Metals and metal oxides used as food additives (homepage food.gov.uk)

Nowadays, the use of ENP for food and food related products (food packaging/wraps, food storage containers, refrigerators, kitchenware e.g.) gains increasing attention (homepage nanotechproject.org). The reduction of particle size involves changing of the physico-chemical properties. Consequently, ENP often possess different colours, solubility, or thermal behaviour compared to their microparticulate equivalents (Tiede *et al.*, 2008). Titanium dioxide (TiO<sub>2</sub>) for example is popular as a whitener when utilised in the micro-size range and was already approved as a food additive by the FDA in 1966. Food products may contain up to 1 % of TiO<sub>2</sub> by weight (homepage cfsan.fda.gov). Nano-sized TiO<sub>2</sub> however has a different refractive index leading to loss of its white colour and therefore allowing it to be applied as transparent films. This can either prevent confectionary products from melting, improve shelf life when applied to food directly (Chaudhry *et al.*, 2008; Mars Inc.'s US Patent US 5741505), or act as an oxygen barrier or UV absorber in (plastics) food packaging (Chaudhry *et al.*, 2008; Arora and Padua, 2010). Taking into account that the first official approval already took place more than 40 years ago, and that nanotechnology was then a relatively young science, it is not surprising that the size of food additives was originally not regulated. However, international efforts have been made recently to address this issue and if deemed necessary, regulations were put in place to make up for previous omissions (homepage fda.gov; EFSA scientific opinion 2009).

Besides TiO<sub>2</sub>, various other metal or metal oxide nanoparticles are already used in food packaging. Silver (Ag), zinc oxide (ZnO) or magnesium oxide (MgO)

nanoparticles are potent antimicrobial agents, whereas silicon dioxide (SiO<sub>2</sub>), alumina (Al<sub>2</sub>O<sub>3</sub>), iron oxides (Fe<sub>3</sub>O<sub>4</sub>, Fe<sub>2</sub>O<sub>3</sub>) and, again, ZnO, are appreciated as UV absorbers in plastics that prevent UV-degradation of the food (Chaudhry *et al.*, 2008; Bouwmeester *et al.*, 2009). Several of these materials however can also be directly applied to functional or conventional food, such as TiO<sub>2</sub> or MgO in confectionary products, SiO<sub>2</sub> in slim shakes, as fluxing agents or for coatings, or selenium in a so-called nano-tea (Chaudhry *et al.*, 2008; Schmid and Riediker, 2008; homepage nanotechproject.org). In this case, one needs to distinguish between products that might contain ENP for improvement of the product properties, and that nowadays do not need to be specifically labelled as “nano-containing food”. This may lead to unintentional ingestion. Functional food in turn is promoted especially for its nano-contents. Therefore, the containing nanomaterials are ingested intentionally.

Besides, great effort is made to develop organic and biodegradable nanoparticles that can be used in medical approaches, for example for targeted drug delivery (Lamprecht *et al.*, 2001; Bouwmeester *et al.*, 2009). Furthermore, self-assembling nanotubes can be made of milk proteins, and liposomal vesicles are used as nutritional carriers (Das *et al.*, 2009). Upon their biodegradability, these nanomaterials are generally considered as safe to use in food and are regarded to be less contrary in comparison to metal and metal oxide particles that are often biopersistent.

Taken together the several sources of ENP, a daily ingestion of 10<sup>12</sup>-10<sup>14</sup> particles per day is suggested, with an increasing tendency (Lomer *et al.*, 2001; 2004). Currently there are major research initiatives including EU projects aiming to improve detection of NP in food and in the GI tract in order to further improve exposure assessment aspects (e.g. Nanolyse project, Inlivotox project; homepage European commission).

### **1.2.3.1 Intestinal uptake of engineered nanoparticles**

At present, the actual amount of nanoparticulate uptake within the intestine is still unclear and dependent on the applied material as well as their unique properties (size, surface structure, chemical composition e.g.). Generally, intestinal particle-absorption appears to be below 10% (Jani *et al.*, 1994; Hillery *et al.*, 1994), whereas

the uptake of small particles (~110-120 nm) within the small intestine *in situ* is shown to be 15-250 fold higher in comparison to larger particles (~510-550 nm, Desai *et al.*, 1996). The M-cells of the intestinal PP are specialised for absorption of macromolecules and particles (Powell *et al.*, 2010). Nonetheless, after ingestion of 60 nm polystyrene particles, only 60 % of the absorbed materials could be recovered in the PP, whereas 40 % were found in non-lymphoid tissue of Sprague-Dawley rats after 5 days of gavaging (Hillery *et al.*, 1994). This suggests that next to absorption via the M-cells additional uptake mechanisms play a role in the intestinal epithelium. Epithelial particle uptake can occur via manifold mechanisms such as phagocytosis, macropinocytosis, clathrin- and nonclathrin-mediated endocytosis or diffusion (Unfried *et al.*, 2007), depending on both the type of material and the exposed cell type. Also, persorption was described as a mechanism for particle translocation and that it can occur upon cell shedding, which might be associated with formation of epithelial “gaps”. However, this mechanism seems to be of minor importance (Volkheimer, 1974; Powell *et al.*, 2010). Nonetheless, nanoparticles tend to accumulate at the site of inflammation in IBD and can be efficiently taken up by macrophages within the affected tissue (Ashgar and Chandran, 2006).

### 1.2.3.2 Toxicity of ingested nanoparticles

Even though the uptake of nanoparticles into the gastrointestinal tract appears low, the health risks of ingested ENP are still unclear. Not much data is currently available that face the toxic or inflammatory potential of these novel materials, and very few studies deal with their impact on existing diseases or their outbreak, such as IBD. Powell *et al.* analysed the effect of a microparticulate (200 nm) TiO<sub>2</sub>-LPS conjugate to stimulate peripheral blood mononuclear cells from healthy controls and CD patients (Powell *et al.*, 2000). They found the strongest increase of IL-1 secretion after incubation with the conjugate, compared to TiO<sub>2</sub> or LPS alone, with a slightly higher response in cells from CD patients. Contrasting however, stimulation of colonic explants of both healthy controls and CD patients resulted in comparable IL-1 levels and the response in general appeared low. Ambiguous outcomes were also found in patients studies when IBD patients received a low particle diet. A pilot study pointed towards a positive effect as promotion of disease remission by avoiding

particle-containing food, whereas these findings could not be confirmed in a follow-up study (Lomer *et al.*, 2001; 2004).

Only very few *in vitro* approaches are nowadays published that determine metal or metal oxide particle toxicity in intestinal cell lines. Nano-vanadium oxide was found cytotoxic to Caco-2 cells (Rhoads *et al.*, 2010). Furthermore, the cytotoxic effects of nano-ZnO and its potential to induce oxidative stress in human colon carcinoma LoVo cells (De Berardis *et al.*, 2010) and human colon-derived RKO cells (Moos *et al.*, 2010) were recently confirmed.

To date, only few *in vivo* studies have addressed possible DNA damage and toxicity of NP in mice and rats. Dybdahl and co-workers exposed rats orally to diesel exhaust particles for 21 days. DNA strand breaks and oxidative stress were found both locally in colon epithelial cells and systemically in the liver (Dybdahl *et al.*, 2003). Furthermore, oral administration of single high doses (5 g Zn/kg) of nano-ZnO to mice were found to induced death in two cases as well as growth retardation in the first days after treatment. Various systemic effects were reported, such as renal damage and anaemia (Wang *et al.*, 2006). By gavaging of a single high dose (5 g/kg) of different sized nano-TiO<sub>2</sub> hepatic injury as well as Ti distribution into various tissues such as liver or kidneys was further observed (Wang *et al.*, 2007). Moreover, the study by Trouiller *et al.* revealed systemic DNA damage after ingestion of TiO<sub>2</sub>. After 5 days oral exposure to high particle concentrations, dose dependent double strand breaks could be detected in bone marrow by measure of  $\gamma$ -H2AX foci. By using the alkaline comet assay for detection of double and single strand breaks and/or strand breaks induced by alkali-labile sites, increasing damage could be found in white blood cells from peripheral blood after incubation with the highest dose (500 mg/kg). Moreover, blood-derived erythrocytes revealed an increased number of micronuclei at high dose treatment, and increased levels of 8-OHdG, a marker for oxidative DNA damage, were detected in the liver (Trouiller *et al.*, 2009).

Overall, knowledge of possible adverse effects of ingested ENP and their impact on intestinal health is very low in the research community, and more research is urgently needed to obtain a better understanding of possible adverse effects and the underlying mechanisms.





### 1.3 Aim of the thesis

The toxicological mechanisms of nanoparticles (NP) in the respiratory tract are reasonably well understood. Many metal oxide nanoparticles (e.g. TiO<sub>2</sub>) as well as carbonaceous nanoparticles derived from combustion processes, such as diesel engine exhaust particles and carbon black are known to be capable of generating reactive oxygen species that can induce intracellular oxidative stress (Oberdörster *et al.*, 2005; Donaldson *et al.*, 2005).

This in turn may lead to cytotoxicity or induction of pro-inflammatory cytokines. Oxidative stress and inflammation in the lung are implicated in various lung diseases including COPD and asthma. Particle-induced DNA damage may occur either directly, referred to as primary genotoxicity, or in an indirect way by activation of phagocytes such as neutrophils or macrophages, hence inducing inflammatory effects that further lead to DNA damage (secondary genotoxicity) (Schins and Knaapen, 2007). Elevated DNA strand breakage and oxidative DNA damage, also resulting from oxidative stress, is further known to contribute to carcinogenicity. An increased lung cancer risk is linked to inhalation of ambient particulate matter and diesel exhaust particles (Knol *et al.*, 2009; HEI research report, 1995), as well as chronic inhalation of nano-sized metal oxide particles (Donaldson *et al.*, 2005).

Industrial application of nano-sized materials in food and food products have increased dramatically. However, possible adverse effects of particles in the human intestine are poorly investigated to date and these might play a role in the development and progression of chronic inflammatory bowel diseases or bowel cancer.

The present thesis aimed to investigate whether primary and/or secondary genotoxic mechanisms were induced by ingested NP, and their relevance for the gastrointestinal tract was to be evaluated. Therefore, the induction of oxidative stress as well as the cytotoxic and DNA damaging potential of food relevant nanomaterials on the intestinal epithelium was determined *in vitro* and *in vivo*. Further, evaluations were conducted on the pro-inflammatory effects and the arising relevance of inflammatory processes in (nano)particle toxicology.

The particles used in these studies and their potential applications were

TiO <sub>2</sub>	potentially present in food
SiO <sub>2</sub> (amorphous)	
ZnO	potentially present in food / food packaging
MgO	
carbon black (CB)	model of an environmental NP

In **Chapter 2**, a subset of four food relevant (nano)particles, as well as carbon black as a model of an environmental combustion-derived nanomaterial, were analysed for their cytotoxic potential on the intestinal epithelial cell line Caco-2. The induction of oxidative stress and the resulting level of oxidative DNA damage were evaluated. Selected materials were further analysed for the influence of size on their DNA damaging and cytotoxic properties.

To follow up on the previous studies, and to gain deeper insight in size and specific surface area dependent adverse effects of TiO<sub>2</sub>, five different samples were characterised in detail in **Chapter 3**. The materials were compared for their cytotoxic and DNA damaging potential in Caco-2 cells with regard to their major physico-chemical properties (e.g. size, crystalline structures, aggregation).

The influence of gastric and intestinal pH conditions that impact on ingested nanoparticles was evaluated in **Chapter 4**. Two food relevant materials, namely SiO<sub>2</sub> and ZnO were analysed for solubility and size distribution within suspension. Uptake into Caco-2 cells was determined, and the influence of cell differentiation and simulated particle digestion was evaluated with regard to cytotoxicity and pro-inflammatory cytokine induction.

Activated primary human neutrophils (PMN) were co-cultured with Caco-2 cells, and in **Chapter 5** the generation of ROS within this model as well as the impact of PMN on the DNA integrity of the intestinal cells were evaluated. The influence of SiO<sub>2</sub> on PMN induced ROS generation and on DNA damage in the co-culture model was determined. An acute and chronic mouse model of colitis was used for the evaluation of DNA integrity and oxidative stress upon ingestion of SiO<sub>2</sub> in the intestinal epithelium *in vivo*.

## 1.4 References

- Albrecht C, Knaapen AM, Becker A, Höhr D, Haberzettl P, van Schooten FJ, Borm PJ, Schins RP. The crucial role of particle surface reactivity in respirable quartz-induced reactive oxygen/nitrogen species formation and APE/Ref-1 induction in rat lung. *Respir Res* 2005;6:129
- Arai N, Mitomi H, Ohtani Y, Igarashi M, Kakita A, Okayasu I. Enhanced epithelial cell turnover associated with p53 accumulation and high p21WAF1/CIP1 expression in ulcerative colitis. *Mod Pathol* 1999;12(6):604-11
- Arora A, Padua GW. Review: Nanocomposites in Food Packaging. *J Food Sci* 2010;75(1):43-49
- Asghar LF, Chandran S. Multiparticulate formulation approach to colon specific drug delivery: current perspectives. *J Pharm Pharm Sci* 2006;9(3):327-38
- Babbs CF. Oxygen radicals in ulcerative colitis. *Free Radic Biol Med* 1992;13(2):169-81
- Babior BM, Kipnes RS, Curnutte JT. Biological defense mechanisms. The production by leukocytes of superoxide, a potential bactericidal agent. *J Clin Invest* 1973;52(3):741-4
- Babior BM. Phagocytes and oxidative stress. *Am J Med* 2000;109(1):33-44
- Baehner RL, Karnovsky ML. Deficiency of reduced nicotinamide-adenine dinucleotide oxidase in chronic granulomatous disease. *Science* 1968;162(859):1277-9
- Barbosa T, Rescigno M. Host-bacteria interactions in the intestine: homeostasis to chronic inflammation. *Syst Biol Med* 2010;2(1):80-97
- Barthel A, Klotz LO. Phosphoinositide 3-kinase signaling in the cellular response to oxidative stress. *Biol Chem* 2005;386(3):207-16
- Boland CR, Luciani MG, Gasche C, Goel A. Infection, inflammation, and gastrointestinal cancer. *Gut* 2005;54(9):1321-31
- Borghesi C, Taussig MJ, Nicoletti C. Rapid appearance of M cells after microbial challenge is restricted at the periphery of the follicle-associated epithelium of Peyer's patch. *Lab Invest* 1999;79(11):1393-401
- Borm PJ. Particle toxicology: from coal mining to nanotechnology. *Inhal Toxicol* 2002;14(3):311-24
- Borm PJ, Schins RP, Albrecht C. Inhaled particles and lung cancer, part B: paradigms and risk assessment. *Int J Cancer* 2004;110(1):3-14
- Borm PJA, Robbins D, Haubold S, Kuhlbusch T, Fissan H, Donaldson K, Schins RPF, Stone V, Kreyling W, Lademann J et al. The potential risks of nanomaterials: a review carried out for ECETOC. *Part Fibre Toxicol* 2006;3:11
- Bouwmeester H, Dekkers S, Noordam MY, Hagens WI, Bulder AS, de Heer C, ten Voorde SE, Wijnhoven SW, Marvin HJ, Sips AJ. Review of health safety aspects of nanotechnologies in food production. *Regul Toxicol Pharmacol* 2009;53(1):52-62
- Buane P, Di Carlo E, Caputi L, Brandolini L, Mosca M, Cattani F, Pellegrini L, Biordi L, Coletti G, Sorrentino C, Fedele G, Colotta F, Melillo G, Bertini R. Crucial pathophysiological role of CXCR2 in experimental ulcerative colitis in mice. *J Leukoc Biol* 2007;82(5):1239-46
- Burrows CJ, Muller JG. Oxidative Nucleobase Modifications Leading to Strand Scission. *Chem Rev* 1998;98(3):1109-1152
- <http://www.cfsan.fda.gov/~dms/opa-col2.html> (May 2010)

- Chantret I, Barbat A, Dussaulx E, Brattain MG, Zweibaum A. Epithelial polarity, villin expression, and enterocytic differentiation of cultured human colon carcinoma cells: a survey of twenty cell lines. *Cancer Res* 1988;48(7):1936-42
- Chaudhry Q, Scotter M, Blackburn J, Ross B, Boxall A, Castle L, Aitken R, Watkins R. Applications and implications of nanotechnologies for the food sector. *Food Addit Contam Part A Chem Anal Control Expo Risk Assess* 2008;25(3):241-58
- Cheeseman KH, Slater TF. An introduction to free radical biochemistry. *Br Med Bull* 1993;49(3):481-93
- Chopra DP, Dombkowski AA, Stemmer PM, Parker GC. Intestinal epithelial cells in vitro. *Stem Cells Dev* 2010;19(1):131-42
- Christensen J. The response of the colon to eating. *Am J Clin Nutr* 1985;42,1025-1032
- Christou NV, Meakins JL. Neutrophil function in surgical patients: Two inhibitors of granulocyte chemotaxis associated with sepsis. *J Surg Res* 1979;26(4):355-364
- Das M, Saxena N, Dwivedi PD. Emerging trends of nanoparticles application in food technology: Safety paradigms. *Nanotoxicol* 2009;3(1):10-18
- De Berardis B, Civitelli G, Condello M, Lista P, Pozzi R, Arancia G, Meschini S. Exposure to ZnO nanoparticles induces oxidative stress and cytotoxicity in human colon carcinoma cells. *Toxicol Appl Pharmacol*. 2010 28 [Epub ahead of print]
- Desai MP, Labhassetwar V, Amidon GL, Levy RJ. Gastrointestinal uptake of biodegradable microparticles: effect of particle size. *Pharm Res* 1996;13(12):1838-45
- DeSesso JM, Jacobson CF. Anatomical and physiological parameters affecting gastrointestinal absorption in humans and rats. *Food Chem Toxicol* 2001;39(3):209-28
- Dippold W, Wittig B, Schwaeble W, Mayet W, Meyer zum Büschenfelde KH. Expression of intercellular adhesion molecule 1 (ICAM-1, CD54) in colonic epithelial cells. *Gut* 1993;34(11):1593-7
- Donaldson K, Gilmour MI, MacNee W. Asthma and PM10. *Respir Res* 2000;1(1):12-5
- Donaldson K, Tran L, Jimenez LA, Duffin R, Newby DE, Mills N, MacNee W, Stone V. Combustion-derived nanoparticles: a review of their toxicology following inhalation exposure. *Part Fibre Toxicol* 2005;2:10
- Donaldson K, Borm PJ, Castranova V, Gulumian M. The limits of testing particle-mediated oxidative stress in vitro in predicting diverse pathologies; relevance for testing of nanoparticles. *Part Fibre Toxicol* 2009;6:13
- Driscoll KE, Deyo LC, Carter JM, Howard BW, Hassenbein DG, Bertram TA. Effects of particle exposure and particle-elicited inflammatory cells on mutation in rat alveolar epithelial cells. *Carcinogenesis* 1997;18(2):423-30
- Drost EM, MacNee W. Potential role of IL-8, platelet-activating factor and TNF-alpha in the sequestration of neutrophils in the lung: effects on neutrophil deformability, adhesion receptor expression, and chemotaxis. *Eur J Immunol* 2002;32(2):393-403
- Dybdahl M, Risom L, Møller P, Autrup H, Wallin H, Vogel U, Bornholdt J, Daneshvar B, Dragsted LO, Weimann A, Poulsen HE, Loft S. DNA adduct formation and oxidative stress in colon and liver of Big Blue rats after dietary exposure to diesel particles. *Carcinogenesis* 2003;24(11):1759-66
- EFSA scientific opinion: <http://www.food.gov.uk/multimedia/pdfs/committee/acm949a.pdf>

- Engle MJ, Goetz GS, Alpers DH. Caco-2 cells express a combination of colonocyte and enterocyte phenotypes. *J Cell Physiol* 1998;174(3):362-9
- European commission: [http://cordis.europa.eu/fp7/home\\_en.html](http://cordis.europa.eu/fp7/home_en.html) (May 2010)
- Evans DF, Pye G, Bramley R, Clark AG, Dyson TJ, Hardcastle JD. Measurement of gastrointestinal pH profiles in normal ambulant human subjects. *Gut* 1988;29(8):1035-41
- Falck GC, Lindberg HK, Suhonen S, Vippola M, Vanhala E, Catalán J, Savolainen K, Norppa H. Genotoxic effects of nanosized and fine TiO<sub>2</sub>. *Hum Exp Toxicol* 2009;28(6-7):339-52
- Fatahzadeh M. Inflammatory bowel disease. *Oral Surg Oral Med Oral Pathol Oral Radiol Endod* 2009;108(5):e1-10
- <http://www.fda.gov/ScienceResearch/SpecialTopics/Nanotechnology/NanotechnologyTaskForceReport2007/default.htm> (May 2010)
- <http://www.food.gov.uk/safereating/chemsafe/additivesbranch/enumberlist> (May 2010)
- Freitas M, Lima JL, Fernandes E. Optical probes for detection and quantification of neutrophils' oxidative burst. A review. *Anal Chim Acta* 2009;649(1):8-23
- Frey RS, Ushio-Fukai M, Malik AB. NADPH oxidase-dependent signaling in endothelial cells: role in physiology and pathophysiology. *Antioxid Redox Signal* 2009;11(4):791-810
- Gallagher J, Sams R 2nd, Inmon J, Gelein R, Elder A, Oberdörster G, Prahalad AK. Formation of 8-oxo-7,8-dihydro-2'-deoxyguanosine in rat lung DNA following subchronic inhalation of carbon black. *Toxicol Appl Pharmacol* 2003;190(3):224-31
- Garrett WS, Gordon JI, Glimcher LH. Homeostasis and inflammation in the intestine. *Cell* 2010;140(6):859-70
- Gao X, Cui Y, Levenson RM, Chung LW, Nie S. In vivo cancer targeting and imaging with semiconductor quantum dots. *Nat Biotechnol* 2004;22(8):969-76
- Gaudio E, Taddei G, Vetuschi A, Sferra R, Frieri G, Ricciardi G, Caprilli R. Dextran sulfate sodium (DSS) colitis in rats: clinical, structural, and ultrastructural aspects. *Dig Dis Sci* 1999;44(7):1458-75
- Geiser M, Kreyling WG. Deposition and biokinetics of inhaled nanoparticles. *Part Fibre Toxicol* 2010;7:2
- Gurr JR, Wang AS, Chen CH, Jan KY. Ultrafine titanium dioxide particles in the absence of photoactivation can induce oxidative damage to human bronchial epithelial cells. *Toxicology* 2005;213(1-2):66-73
- Hampton MB, Kettle AJ, Winterbourn CC. Inside the neutrophil phagosome: oxidants, myeloperoxidase, and bacterial killing. *Blood* 1998;92(9):3007-17
- Hautot D, Pankhurst QA, Khan N, Dobson J. Preliminary evaluation of nanoscale biogenic magnetite in Alzheimer's disease brain tissue. *Proc Biol Sci* 2003;270 Suppl 1:S62-4
- HEI: Diesel exhaust: a critical analysis of emissions, exposure and health effects. A special report of the Institute's diesel working group. HEI research report 1995
- Hillery AM, Jani PU, Florence AT. Comparative, quantitative study of lymphoid and non-lymphoid uptake of 60 nm polystyrene particles. *J Drug Target* 1994;2(2):151-6
- Hollander D, Rim E, Ruble PE Jr. Vitamin K<sub>2</sub> colonic and ileal in vivo absorption: bile, fatty acids, and pH effects on transport. *Am J Physiol* 1977;233(2):E124-9

- Hörter D, Dressman JB. Influence of physicochemical properties on dissolution of drugs in the gastrointestinal tract. *Adv Drug Deliv Rev* 2001;46(1-3):75-87
- Huang N, Katz JP, Martin DR, Wu GD. Inhibition of IL-8 gene expression in Caco-2 cells by compounds which induce histone hyperacetylation. *Cytokine* 1997;9(1):27-36
- Itzkowitz SH, Yio X. Inflammation and cancer IV. Colorectal cancer in inflammatory bowel disease: the role of inflammation. *Am J Physiol Gastrointest Liver Physiol* 2004;287(1):G7-17
- Jackson SH, Gallin JI, Holland SM. The p47phox mouse knock-out model of chronic granulomatous disease. *J Exp Med* 1995;182(3):751-8
- Jani PU, McCarthy DE, Florence AT. Titanium dioxide (rutile) particle uptake from the rat GI tract and translocation to systemic organs after oral administration. *J Pharm* 1994;105(2):157-168
- Johnston CJ, Driscoll KE, Finkelstein JN, Baggs R, O'Reilly MA, Carter J, Gelein R, Oberdörster G. Pulmonary chemokine and mutagenic responses in rats after subchronic inhalation of amorphous and crystalline silica. *Toxicol Sci* 2000;56(2):405-13
- Johnston HJ, Hutchison GR, Christensen FM, Peters S, Hankin S, Stone V. Identification of the mechanisms that drive the toxicity of TiO<sub>2</sub> particulates: the contribution of physicochemical characteristics. *Part Fibre Toxicol* 2009;6:33
- Kasai H. Analysis of a form of oxidative DNA damage, 8-hydroxy-2'-deoxyguanosine, as a marker of cellular oxidative stress during carcinogenesis. *Mutat Res* 1997;387(3):147-63
- Klebanoff SJ. Iodination of bacteria: a bactericidal mechanism. *J Exp Med* 1967;126(6):1063-78
- Klebanoff SJ, Rosen H. The role of myeloperoxidase in the microbicidal activity of polymorphonuclear leukocytes. *Ciba Found Symp* 1978;(65):263-84
- Knaapen AM, Seiler F, Schilderman PA, Nehls P, Bruch J, Schins RP, Borm PJ. Neutrophils cause oxidative DNA damage in alveolar epithelial cells. *Free Radic Biol Med* 1999;27(1-2):234-40
- Knaapen AM, Güngör N, Schins RP, Borm PJ, Van Schooten FJ. Neutrophils and respiratory tract DNA damage and mutagenesis: a review. *Mutagenesis* 2006;21(4):225-36
- Knol AB, de Hartog JJ, Boogaard H, Slottje P, van der Sluijs JP, Lebret E, Cassee FR, Wardekker JA, Ayres JG, Borm PJ, Brunekreef B, Donaldson K, Forastiere F, Holgate ST, Kreyling WG, Nemery B, Pekkanen J, Stone V, Wichmann HE, Hoek G. Expert elicitation on ultrafine particles: likelihood of health effects and causal pathways. *Part Fibre Toxicol* 2009;6:19
- Krause KH, Bedard K. NOX enzymes in immuno-inflammatory pathologies. *Semin Immunopathol* 2008;30(3):193-4
- Kriegelstein CF, Cerwinka WH, Laroux FS, Salter JW, Russell JM, Schuermann G, Grisham MB, Ross CR, Granger DN. Regulation of murine intestinal inflammation by reactive metabolites of oxygen and nitrogen: divergent roles of superoxide and nitric oxide. *J Exp Med*. 2001;194(9):1207-18
- Kunkel SL, Standiford T, Kasahara K, Strieter RM. Interleukin-8 (IL-8): the major neutrophil chemotactic factor in the lung. *Exp Lung Res* 1991;17(1):17-23
- Kwiecien S, Konturek SJ. Gastric analysis with fractional test meals (ethanol, caffeine, and peptone meal), augmented histamine or pentagastrin tests, and gastric pH recording. *J Physiol Pharmacol* 2003;54 Suppl 3:69-82

- Lamprecht A, Ubrich N, Yamamoto H, Schäfer U, Takeuchi H, Maincent P, Kawashima Y, Lehr CM. Biodegradable nanoparticles for targeted drug delivery in treatment of inflammatory bowel disease. *J Pharmacol Exp Ther* 2001;299(2):775-81
- Leser TD, Mølbak L. Better living through microbial action: the benefits of the mammalian gastrointestinal microbiota on the host. *Environ Microbiol* 2009;11(9):2194-206
- Li N, Xia T, Nel AE. The role of oxidative stress in ambient particulate matter-induced lung diseases and its implications in the toxicity of engineered nanoparticles. *Free Radic Biol Med* 2008;44(9):1689-99
- Lindahl A, Ungell AL, Knutson L, Lennernäs H. Characterization of fluids from the stomach and proximal jejunum in men and women. *Pharm Res* 1997;14(4):497-502
- Lomer MC, Harvey RS, Evans SM, Thompson RP, Powell JJ. Efficacy and tolerability of a low microparticle diet in a double blind, randomized, pilot study in Crohn's disease. *Eur J Gastroenterol Hepatol* 2001;13(2):101-6
- Lomer MC, Hutchinson C, Volkert S, Greenfield SM, Catterall A, Thompson RP, Powell JJ. Dietary sources of inorganic microparticles and their intake in healthy subjects and patients with Crohn's disease. *Br J Nutr* 2004;92(6):947-55
- [http://www.luxresearchinc.com/press/RELEASE\\_Nano-SMR\\_7\\_22\\_08.pdf](http://www.luxresearchinc.com/press/RELEASE_Nano-SMR_7_22_08.pdf)
- MacDermott. Chemokines in the inflammatory bowel disease. *J Clin Immunol* 1999;19(5):266-72
- Mariadason JM, Arango D, Corner GA, Arañes MJ, Hotchkiss KA, Yang W, Augenlicht LH. A gene expression profile that defines colon cell maturation in vitro. *Cancer Res* 2002;62(16):4791-804
- Mars Inc.'s US Patent US 5741505
- Matsusaki M, Akashi M. Functional multilayered capsules for targeting and local drug delivery. *Expert Opinion on Drug Deliv* 2009, Vol. 6, No. 11, Pages 1207-1217
- Matute JD, Arias AA, Wright NA, Wrobel I, Waterhouse CC, Li XJ, Marchal CC, Stull ND, Lewis DB, Steele M, Kellner JD, Yu W, Meroueh SO, Nauseef WM, Dinauer MC. A new genetic subgroup of chronic granulomatous disease with autosomal recessive mutations in p40 phox and selective defects in neutrophil NADPH oxidase activity. *Blood* 2009;114(15):3309-15
- Mazzucchelli L, Hauser C, Zraggen K, Wagner H, Hess M, Laissue JA, Mueller C. Expression of interleukin-8 gene in inflammatory bowel disease is related to the histological grade of active inflammation. *Am J Pathol* 1994;144(5):997-1007
- Medzhitov R, Preston-Hurlburt P, Janeway CA Jr. A human homologue of the Drosophila Toll protein signals activation of adaptive immunity. *Nature* 1997;388(6640):394-7
- Mitsuyama K, Toyonaga A, Sasaki E, Watanabe K, Tateishi H, Nishiyama T, Saiki T, Ikeda H, Tsuruta O, Tanikawa K. IL-8 as an important chemoattractant for neutrophils in ulcerative colitis and Crohn's disease. *Clin Exp Immunol* 1994;96(3):432-6
- Monteiller C, Tran L, MacNee W, Faux S, Jones A, Miller B, Donaldson K. The pro-inflammatory effects of low-toxicity low-solubility particles, nanoparticles and fine particles, on epithelial cells in vitro: the role of surface area. *Occup Environ Med* 2007;64(9):609-15
- Moos PJ, Chung K, Woessner D, Honegg M, Cutler NS, Veranth JM. ZnO particulate matter requires cell contact for toxicity in human colon cancer cells. *Chem Res Toxicol* 2010;23(4):733-9

- Mühlfeld C, Rothen-Rutishauser B, Blank F, Vanhecke D, Ochs M, Gehr P. Interactions of nanoparticles with pulmonary structures and cellular responses. *Am J Physiol Lung Cell Mol Physiol* 2008;294(5):L817-29
- Naito Y, Takagi T, Yoshikawa T. Neutrophil-dependent oxidative stress in ulcerative colitis. *J Clin Biochem Nutr* 2007;41(1):18-26
- Nakagawa Y, Wakuri S, Sakamoto K, Tanaka N. The photogenotoxicity of titanium dioxide particles. *Mutat Res* 1997;394(1-3):125-32
- <http://www.nanotechproject.org/inventories/consumer/browse/> (May 2010)
- Natsui M, Kawasaki K, Takizawa H, Hayashi SI, Matsuda Y, Sugimura K, Seki K, Narisawa R, Sendo F, Asakura H. Selective depletion of neutrophils by a monoclonal antibody, RP-3, suppresses dextran sulphate sodium-induced colitis in rats. *J Gastroenterol Hepatol* 1997;12(12):801-8
- Nauseef WM. How human neutrophils kill and degrade microbes: an integrated view. *Immunol Rev* 2007;219:88-102
- Nel A, Xia T, Mädler L, Li N. Toxic potential of materials at the nanolevel. *Science* 2006;311(5761):622-7
- Ng SC, Kamm MA, Stagg AJ, Knight SC. Intestinal dendritic cells: Their role in bacterial recognition, lymphocyte homing, and intestinal inflammation. *Inflamm Bowel Dis* 2010 Mar 10 [Epub ahead of print]
- Oberdörster G, Oberdörster E, Oberdörster J. Nanotoxicology: an emerging discipline evolving from studies of ultrafine particles. *Environ Health Perspect* 2005;113(7):823-39
- Ostanin DV, Barlow S, Shukla D, Grisham MB. NADPH oxidase but not myeloperoxidase protects lymphopenic mice from spontaneous infections. *Biochem Biophys Res Commun* 2007;355(3):801-6
- Pflaum M, Will O, Epe B. Determination of steady-state levels of oxidative DNA base modifications in mammalian cells by means of repair endonucleases. *Carcinogenesis* 1997;18(11):2225-31
- Powell JJ, Whitehead MW, Lee S, Thompson RPH. Mechanisms of gastrointestinal absorption: dietary minerals and the influence of beverage ingestion. *Food Chem* 1994; 51 381-388
- Powell JJ, Jugdaohsingh R, Thompson RP. The regulation of mineral absorption in the gastrointestinal tract. *Proc Nutr Soc* 1999;58(1):147-53
- Powell JJ, Harvey RS, Ashwood P, Wolstencroft R, Gershwin ME, Thompson RP. Immune potentiation of ultrafine dietary particles in normal subjects and patients with inflammatory bowel disease. *J Autoimmun* 2000;14(1):99-105
- Powell JJ, Faria N, Thomas-McKay E, Pele LC. Origin and fate of dietary nanoparticles and microparticles in the gastrointestinal tract. *J Autoimmun* 2010;34(3):J226-33
- Pryor WA. Why is the hydroxyl radical the only radical that commonly adds to DNA? Hypothesis: it has a rare combination of high electrophilicity, high thermochemical reactivity, and a mode of production that can occur near DNA. *Free Radic Biol Med* 1988;4(4):219-23
- Ramachandran A, Madesh M, Balasubramanian KA. Apoptosis in the intestinal epithelium: its relevance in normal and pathophysiological conditions. *J Gastroenterol Hepatol* 2000;15(2):109-20



- Rhoads LS, Silkworth WT, Roppolo ML, Whittingham MS. Cytotoxicity of nanostructured vanadium oxide on human cells in vitro. *Toxicol In Vitro* 2010;24(1):292-6
- Risom L, Dybdahl M, Bornholdt J, Vogel U, Wallin H, Møller P, Loft S. Oxidative DNA damage and defence gene expression in the mouse lung after short-term exposure to diesel exhaust particles by inhalation. *Carcinogenesis* 2003;24(11):1847-52
- Ritchie JA. Colonic motor activity and bowel function. II. Distribution and incidence of motor activity at rest and after food and carbachol. *Gut* 1968;9(5):502-11
- Rogler G, Andus T. Cytokines in inflammatory bowel disease. *World J Surg* 1998;22(4):382-9
- Sääf AM, Halbleib JM, Chen X, Yuen ST, Leung SY, Nelson WJ, Brown PO. Parallels between global transcriptional programs of polarizing Caco-2 intestinal epithelial cells in vitro and gene expression programs in normal colon and colon cancer. *Mol Biol Cell* 2007;18(11):4245-60
- Sancho E, Battle E, Clevers H. Signaling pathways in intestinal development and cancer. *Annu Rev Cell Dev Biol* 2004;20:695-723
- Sato T, Vries RG, Snippert HJ, van de Wetering M, Barker N, Stange DE, van Es JH, Abo A, Kujala P, Peters PJ, Clevers H. Single Lgr5 stem cells build crypt-villus structures in vitro without a mesenchymal niche. *Nature* 2009;459(7244):262-5
- Sayes CM, Wahi R, Kurian PA, Liu Y, West JL, Ausman KD, Warheit DB, Colvin VL. Correlating nanoscale titania structure with toxicity: a cytotoxicity and inflammatory response study with human dermal fibroblasts and human lung epithelial cells. *Toxicol Sci* 2006;92(1):174-85
- Schins RP, Knaapen AM. Genotoxicity of poorly soluble particles. *Inhal Toxicol* 2007;19 Suppl 1:189-98
- Schmid K, Riediker M. Use of nanoparticles in Swiss Industry: a targeted survey. *Environ Sci Technol* 2008;42(7):2253-60
- Shibutani S, Takeshita M, Grollman AP. Insertion of specific bases during DNA synthesis past the oxidation-damaged base 8-oxodG. *Nature* 1991;349(6308):431-4
- Shih DQ, Targan SR. Immunopathogenesis of inflammatory bowel disease. *World J Gastroenterol* 2008;14(3):390-400
- Sies H. Oxidative stress: oxidants and antioxidants. *Exp Physiol* 1997;82(2):291-5
- Sies H. Glutathione and its role in cellular functions. *Free Radic Biol Med* 1999;27(9-10):916-21
- Silva MT. Neutrophils and macrophages work in concert as inducers and effectors of adaptive immunity against extracellular and intracellular microbial pathogens. *J Leukoc Biol* 2010;87(5):805-13
- Slater TF. Free-radical mechanisms in tissue injury. *Biochem J* 1984;222(1):1-15
- Stone V, Johnston H, Schins RP. Development of in vitro systems for nanotoxicology: methodological considerations. *Crit Rev Toxicol* 2009;39(7):613-26
- Suzuki Y, Lehrer RI. NAD(P)H oxidase activity in human neutrophils stimulated by phorbol myristate acetate. *J Clin Invest* 1980;66(6):1409-18
- Taniguchi Y, Yoshioka N, Nakata K, Nishizawa T, Inagawa H, Kohchi C, Soma G. Mechanism for maintaining homeostasis in the immune system of the intestine. *Anticancer Res* 2009;29(11):4855-60

- Tiede K, Boxall AB, Tear SP, Lewis J, David H, Hasselov M. Detection and characterization of engineered nanoparticles in food and the environment. *Food Addit Contam Part A Chem Anal Control Expo Risk Assess* 2008;25:795-821
- Trouiller B, Reliene R, Westbrook A, Solaimani P, Schiestl RH. Titanium dioxide nanoparticles induce DNA damage and genetic instability in vivo in mice. *Cancer Res* 2009;69(22):8784-9
- Unfried K, Albrecht C, Klotz LO, von Mikecz A, Grether-Beck S, Schins RPF. Cellular responses to nanoparticles: target structures and mechanisms. *Nanotoxicol* 2007;1:52-71
- University of Colorado: <http://www.colorado.edu/intphys/Class/IPHY3430-200/image/villi.jpg>  
(April 2010)
- Vainer B. Intercellular adhesion molecule-1 (ICAM-1) in ulcerative colitis: presence, visualization, and significance. *Inflamm Res* 2005;54(8):313-27
- Volkheimer G. Passage of particles through the wall of the gastrointestinal tract. *Environ Health Perspect* 1974;9:215-25.
- Wang Q, Doerschuk CM, Mizgerd JP. Neutrophils in innate immunity. *Semin Respir Crit Care Med* 2004;25(1):33-41
- Wang B, Feng WY, Wang TC, Jia G, Wang M, Shi JW, Zhang F, Zhao YL, Chai ZF. Acute toxicity of nano- and micro-scale zinc powder in healthy adult mice. *Toxicol Lett* 2006;161(2):115-23
- Wang J, Zhou G, Chen C, Yu H, Wang T, Ma Y, Jia G, Gao Y, Li B, Sun J, Li Y, Jiao F, Zhao Y, Chai Z. Acute toxicity and biodistribution of different sized titanium dioxide particles in mice after oral administration. *Toxicol Lett* 2007;168(2):176-85
- Wang S, Liu Z, Wang L, Zhang X. NF-kappaB signaling pathway, inflammation and colorectal cancer. *Cell Mol Immunol* 2009;6(5):327-34
- Wells CL, Jechorek RP, Erlandsen SL. Inhibitory effect of bile on bacterial invasion of enterocytes: possible mechanism for increased translocation associated with obstructive jaundice. *Crit Care Med* 1995;23(2):301-7
- Wells JM, Loonen LM, Karczewski JM. The role of innate signaling in the homeostasis of tolerance and immunity in the intestine. *Int J Med Microbiol* 2010;300(1):41-8
- Wessels I, Jansen J, Rink L, Uciechowski P. Immunosenescence of polymorphonuclear neutrophils. *ScientificWorldJournal* 2010;10:145-60
- West MA, Heagy W. Endotoxin tolerance: A review. *Crit Care Med*. 2002;30(1 Supp):S64-S73
- Wirtz S, Neurath MF. Mouse models of inflammatory bowel disease. *Adv Drug Deliv Rev* 2007;59(11):1073-83
- Zhang Y, Chen Y, Westerhoff P, Hristovski K, Crittenden JC. Stability of commercial metal oxide nanoparticles in water. *Water Res* 2008;42(8-9):2204-12

## CHAPTER 2

---

### **Cytotoxicity and oxidative DNA damage by nanoparticles in human intestinal Caco-2 cells**

Kirsten Gerloff<sup>1</sup>, Catrin Albrecht<sup>1</sup>, Agnes W. Boots<sup>1</sup>, Irmgard Förster<sup>2</sup>, Roel P.F. Schins<sup>1</sup>

<sup>1</sup> Particle Research and <sup>2</sup> Molecular Immunology, Institut für Umweltmedizinische Forschung (IUF) at the Heinrich Heine University Düsseldorf, Germany.

#### **Abstract**

The use of engineered nanoparticles in the food sector is anticipated to increase dramatically, whereas their potential hazards for the gastrointestinal tract are still largely unknown. We investigated the cytotoxic and DNA damaging effects of several types of nanoparticles and fine particles relevant as food additives (TiO<sub>2</sub> and SiO<sub>2</sub>) or for food packaging (ZnO and MgO) as well as carbon black on human intestinal Caco-2 cells.

All particles, except for MgO, were cytotoxic (LDH and WST-1 assay). ZnO, and to lesser extent SiO<sub>2</sub>, induced significant DNA damage (Fpg-comet), while SiO<sub>2</sub> and carbon black were the most potent in causing glutathione depletion. DNA damage by TiO<sub>2</sub> was found to depend on sample processing conditions. Interestingly, application of different TiO<sub>2</sub> and ZnO particles revealed no relation between particle surface area and DNA damage. Our results indicate a potential hazard of several food-related nanoparticles which necessitate investigations on the actual exposure in humans.

## 2.1 Introduction

Engineered Nanoparticles (ENP) have gained strong interest in various fields of research and industry, since their small size offers new features and enhanced reactivity in comparison to larger particles of the same chemical composition. Their use can be found in a broad field, for instance as pigments and resins, as UV-filters in cosmetics, in strategies to improve drug delivery, or for applications in medical diagnostics (Borm *et al.*, 2006). The food industry is starting to use various nanoparticles as food additives or to improve food packaging in an attempt to optimise their products. While microparticles, such as Titanium dioxide or Silicon dioxide have had a long-standing use as food additives, for example as whiteners (e.g.  $\text{TiO}_2$ ) or enhancers of viscosity and fluxing agents (e.g.  $\text{SiO}_2$ ) (Schmid and Riediker, 2008; Chaudhry *et al.*, 2008), in the future nanoparticles of this composition will be finding their way into foods, i.e. as coatings of confectionary products (e.g.  $\text{SiO}_2$ ,  $\text{MgO}$  and  $\text{TiO}_2$ ; Chaudhry *et al.*, 2008) or as additives for functional food (e.g. amorphous  $\text{SiO}_2$ ; Nanotechproject homepage). Specific ENP are also considered as promising components of novel food packaging materials in view of their ability to enhance gas exchange and their antimicrobial properties (e.g.  $\text{ZnO}$  and  $\text{MgO}$ ). More advanced approaches in the food industry include nanoparticle-based sensors to monitor food edibility or nano-encapsulation applications to improve nutrient stability and delivery (Taylor *et al.*, 2005; Asuri *et al.*, 2007; Kaittanis *et al.*, 2007). Little is known, however, about the potential risks of ENP application to the human body. Especially the effects of ENP within the gastrointestinal tract are poorly investigated.

In the field of nanotoxicology research, inhalation and ingestion are considered as two major uptake routes of nanoparticles to the human body (Oberdörster *et al.*, 2005a, 2007). Depending on their physicochemical properties, nanoparticles can be taken up by different types of cells via active or passive uptake mechanisms (reviewed in Unfried *et al.*, 2007). Within biological systems, they are able to generate reactive oxygen species (ROS) like superoxide ( $\text{O}_2^{\cdot-}$ ), hydroxyl radicals ( $\text{OH}^{\cdot}$ ) or hydrogen peroxide ( $\text{H}_2\text{O}_2$ ) as well as reactive nitrogen species (RNS) like nitric oxide ( $\text{NO}^{\cdot}$ ) and peroxynitrite ( $\text{ONOO}^-$ ) in a direct or indirect manner (Unfried *et al.*, 2007). The surface chemistry of particles can lead to direct ROS formation (Brown *et al.*, 2001; Stoeger *et al.*, 2009), whereas cellular targets such as Nicotinamide adenine dinucleotide phosphate (NADPH)-like enzymes, mitochondria, or intracellular calcium stores can be activated to produce ROS in an indirect way (Brown *et al.*, 2004; Singh *et al.*, 2007). Alternatively, particles can lead to

indirect ROS generation by inducing inflammation characterised by the recruitment and activation of ROS producing phagocytic cells such as monocytes and neutrophils (Schins and Knaapen, 2007).

The ability of particles to generate ROS and to induce oxidative stress has been proposed as a unifying mechanism of their toxicity (Oberdörster *et al.*, 2005a, 2007; Xia *et al.*, 2006). Such properties have been associated not only with the activation of inflammatory mediators, but also with the induction of oxidative DNA damage and associated mutagenesis (Oberdörster *et al.*, 2007; Schins and Knaapen, 2007). In the respiratory tract, the potential adverse effects of inhaled particles are well recognised and relevant toxicity mechanisms have been identified. Previous studies have for instance shown that combustion derived nanoparticles (including carbon black and diesel exhaust) elicit inflammation in the respiratory tract and may result in chronic inflammatory diseases such as fibrosis or chronic obstructive pulmonary disease (Donaldson *et al.*, 2005).

Possible harmful effects of (engineered) nanoparticles in the gastrointestinal tract are still largely unknown. Lomer and co-workers have estimated that around  $10^{12}$ - $10^{14}$  microparticles are ingested daily per person (Lomer *et al.*, 2004). However, nanofood applications are expected to increase dramatically in the near future and this strengthens the need for research to increase knowledge on the potential toxicological effects of nanoparticles to the gut.

The aim of our present study was to investigate the cytotoxic and DNA damaging properties of several types of ENP and fine particles to the human colon epithelial cell-line Caco-2, recognised as an *in vitro* model of the human small intestinal epithelium. TiO<sub>2</sub> and SiO<sub>2</sub> particles were chosen as examples of food additives, while ZnO and MgO particles were selected as promising constituents of food packaging. Finally, carbon black was evaluated as a model of ambient air nanoparticles, since these can reach the gastrointestinal tract upon pulmonary clearance. For the determination of cytotoxicity, the LDH assay as well as the WST-1 assay was used. The reduction of total glutathione (GSH) content was determined as a marker for oxidative stress. To investigate oxidative DNA-damage, the formamidopyrimidine glycosylase (Fpg)-modified comet assay was used, which specifically detects oxidative lesions including 8-hydroxy-2-deoxyguanosine (8-OHdG).

## 2.2 Methods

**Materials.** The characteristics of all (nano)particles used in this study are listed in Table 1. Trypsin, Dulbecco's Ca<sup>2+</sup>/Mg<sup>2+</sup>-free phosphate buffered saline (PBS), agarose, low melting point (LMP) agarose, Triton X-100, Dimethyl sulfoxide (DMSO), ethidium bromide, Glutathione-reductase, reduced L-Glutathione, fetal calf serum (FCS), KH<sub>2</sub>PO<sub>4</sub>, K<sub>2</sub>HPO<sub>4</sub> and BCA-assay kit (bicinchoninic acid- and copper(II) sulphate solution) were all purchased from Sigma (Germany). Minimum essential Medium (MEM) with Earle's salts and non essential amino acids were obtained from invitrogen (Germany). Lactate dehydrogenase (LDH) Cytotoxicity Detection Kit and Cell Proliferation Reagent WST-1 were obtained from Roche (Switzerland). Formamidopyrimidine-glycosylase (Fpg)-enzyme was kindly provided by Dr. Andrew Collins, Institute for Nutrition Research, University of Oslo, Norway. All other chemicals were from Merck (Germany).

Code	Material specification	BET (m <sup>2</sup> /g) *	primary particle size range (nm) ***	Source
TiO <sub>2</sub> -F	TiO <sub>2</sub> fine (pure anatase)	10	40-300	Aldrich
TiO <sub>2</sub>	TiO <sub>2</sub> ultrafine (80% anatase, 20% rutile), p25	50	20-80	Degussa
TiO <sub>2</sub> -HSA	TiO <sub>2</sub> (anatase modified), Hombikat	> 300	< 10	Sigma
SiO <sub>2</sub>	Amorphous SiO <sub>2</sub> fumed	200	14	Sigma
CB	Carbon black, Printex 90	300	14	Degussa
MgO	MgO nanoactive**	600	8	Nanoscale Materials Inc., USA
ZnO	ZnO nanoactive**	70	10	Nanoscale Materials Inc., USA
ZnO-Ns	ZnO nanoscale	50	20	Nanostructured and Amorphous Materials Inc.
ZnO-F	ZnO fine	< 10	n.d.	Sigma

**Table 2.1 Characteristics of (nano)particles used in the present study**

\* Surface area according to Brunauer, Emmett and Teller, as provided by company

\*\* Specified as nanoactive particles by company (i.e. composed of aggregates with a geometric size above nano-size, but with specific properties of nanoscale particles)

\*\*\* As provided by company

n.d. no information provided

**Culture and treatment of the cells.** The human colon adenocarcinoma cell line Caco-2 was obtained from DSMZ (Deutsche Sammlung von Mikroorganismen und Zellkulturen GmbH, Germany) and grown in MEM with Earle's salts and Non Essential Amino Acids, supplemented with 20 % FCS, 1 % L-glutamine and 30 IU/ml penicillin–streptomycin. For experiments, cells were trypsinised at near confluency and  $4 \times 10^4$  cells per  $\text{cm}^2$  were seeded into 60 mm culture plates (Fpg comet assay), 6-well tissue culture plates (glutathione assay) or 96-well tissue culture plates (LDH- and WST-1 assay) and grown overnight to 70-80% confluency. Cells were then starved for 20 h in serum free medium. Experiments were always performed between cell passages 5 to 30. For treatment, all particles were suspended in starvation culture medium. The suspension was sonicated (Sonorex TK52 water-bath; 60 Watt, 35 kHz) for 7 min and then directly added to the cells at the indicated concentrations. For the Fpg comet assay and glutathione assay, cell monolayers were rinsed repeatedly with PBS after the end of the treatments. This was done to remove excess of extracellular particles that might interfere with the various assays, as well as to remove detached (dead) cells and their debris.

**Cytotoxicity.** Cytotoxicity was determined by the lactate dehydrogenase (LDH) assay as a marker of cell membrane integrity as well as the water-soluble tetrazolium salt (WST-1) as a measure of the metabolic activity of the cells. For both the LDH and the WST-1 assay 96-well tissue culture plates were used and cells were treated at the indicated concentrations and time intervals with the particles as described above. LDH was determined using a commercial diagnostic kit (Roche, Switzerland). The cleavage of the tetrazolium salt WST-1 to formazan dye via mitochondrial dehydrogenases was measured using a commercial WST-1 diagnostic kit (Roche). Cells were incubated for additional 2 h with WST-1 and analysed directly.

**Detection of oxidative DNA damage by Fpg-modified comet assay.** The Fpg-modified comet assay was used to measure DNA strand breaks and specifically oxidative DNA damage in the cells, based on the method as described by Speit *et al.* (2004). As a positive control, the photosensitiser Ro-19 8022 (Roche, Switzerland) was used, which induces specific oxidative damage after 2 min light exposure. On the basis of the kinetics of DNA damage induction and its repair in Caco-2 cells, a treatment of 4 h was chosen to reveal possible DNA damage by the particles with avoidance of effective DNA repair. After incubation, cells were rinsed twice with PBS, detached by

trypsinisation and immediately suspended in 1 ml culture medium. Cells were centrifuged for 10 min at 1300 rpm and 4 °C and resuspended in starvation medium at a concentration of  $1.5 \times 10^6$  cells/ml. A mixture of 10 µl cell suspension with 70 µl 0.5 % LMP agarose was added onto 1.5 % agarose precoated slides in duplicates. Following 10 min of solidification on ice, slides were lysed overnight at 4 °C in lysis buffer (2.5 M NaCl, 100 mM EDTA, 10 mM Tris-base, pH 10, containing 10% DMSO and 1% Triton X-100). The slides were washed three times for 5 min in Fpg-enzyme buffer (40 mM HEPES, 100 mM KCl, 0.5 mM EDTA, 0.2 mg/ml BSA, pH 8), covered with 100 µl of either buffer or Fpg in buffer, sealed with a coverslip and incubated for 30 min at 37 °C. All slides were then transferred into the electrophoresis tank. After alkaline unwinding (pH 13) for 20 min, electrophoresis was performed subsequently for 10 min at 270 mA, 26 V. Slides were neutralised three times for 5 min using neutralisation buffer (0.4 M Tris, pH 7.5). Before analysis, slides were dried on air for 10 min and stained with ethidium bromide (10 µg/ml, 40 µl per slide). Comet appearances were analyzed using an Olympus BX60 fluorescence microscope at 400× magnification. A comet image analysis software program (Comet Assay II, Perceptive Instruments, Haverhill, UK) was used for quantification of DNA damage by analysis of the % tail DNA. A total of 50 cells were analyzed per slide per experiment.

**Evaluation of comet assay sample processing conditions.** Since  $\text{TiO}_2$  is suspected to cause oxidative ROS production by photosensitising mechanisms, Caco-2 cells treated with  $\text{TiO}_2$  were applied to the comet assay slides in duplicates. For each individual experiment, two slides were processed as usual, with all washing and incubation steps in the dark, while two further slides were handled under normal laboratory light conditions from lysing until Fpg-incubation (daylight + additional illumination by standard neon tubes 18 W, Philips).

**Total glutathione content.** For measurement of total glutathione content of the Caco-2 cells, cells were treated for 4 hours after which they were rinsed twice with PBS and scraped in 1 ml KPE-buffer (1:6.25 phosphate buffer A [0.1 M  $\text{KH}_2\text{PO}_4$ ] and phosphate buffer B [0.1  $\text{MK}_2\text{HPO}_4 \cdot 3\text{H}_2\text{O}$ ], 10 mM EDTA, pH 7.5) plus 0.1% Triton-X-100 and 0.6% sulfosalicylic acid, sonicated and vortexed for 3 times (30 sec each). After centrifugation (6200 rpm, 5 min at 4 °C) supernatants were frozen at -20 °C until analysis. A mixture of 0.8 mM NADPH and 0.6 mM DTNB (1:1) was added to 50 µl samples or GSH standard



in a 96 well-plate, followed by the immediate addition of 50  $\mu$ l GSH reductase (4 units/ml). The absorbance was measured at 412 nm for 5 times during 2 min and the values were adjusted to the total protein content as determined by BCA-assay.

**Statistics.** All means were calculated from three independent experiments, and are expressed in the graphs as mean and standard deviation (SD). Analysis of statistical significance was done by Student's t-test with \* $p < 0.05$ , \*\* $p < 0.01$  and \*\*\* $p < 0.001$  as levels of significance.

## 2.3 Results

The cytotoxic potential of ZnO, TiO<sub>2</sub>, MgO, SiO<sub>2</sub> and CB was evaluated in dose- and time-dependent manner by measuring the LDH leakage as marker of the cell membrane integrity and the reduction of WST-1 as marker of changes in the metabolic activity. To this extent, cells were treated 4 and 24 hours with 20 and 80 µg/cm<sup>2</sup> particles. After 4 h incubation, 80 µg/cm<sup>2</sup> SiO<sub>2</sub> significantly increased LDH release in comparison to the controls (Figure 2.1 A). After 24 h incubation, SiO<sub>2</sub>, TiO<sub>2</sub> and ZnO induced a significant LDH release and thus loss of membrane integrity at both treatment concentrations (Figure 2.1 B). Notably, with CB significant LDH release could only be measured after 24 hours at the lower concentration. The absence of significant LDH increase at the higher treatment concentration may be an artefact due to the absorption of the LDH onto the large surface of the carbon black particles. MgO did not show any membrane-damaging effects at the concentrations and time points tested.

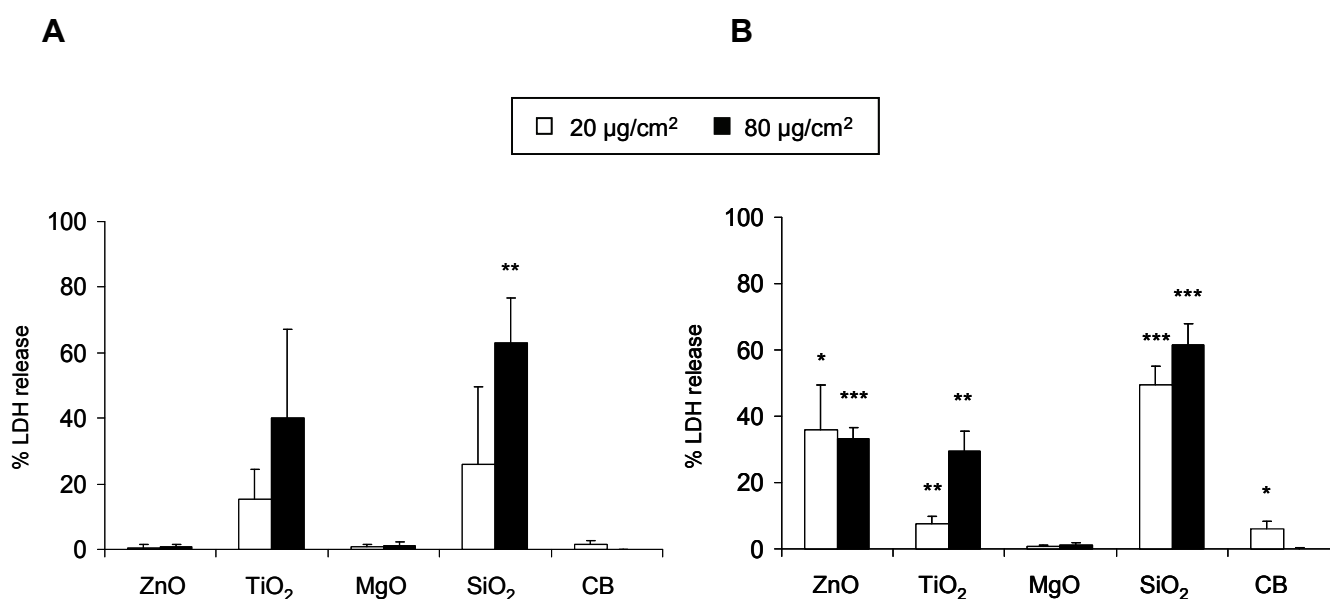


**Figure 2.1 Cytotoxic effects of several particles on Caco-2 cells.** Cells were incubated with 20 and 80 µg/cm<sup>2</sup> particles for 4 (A) and 24 (B) hours. LDH leakage from the cells was measured as marker of cell toxicity and is presented as percentage of the whole LDH content of the cells in the control incubation (ctr). Values are expressed as mean and standard deviation.

\* p < 0.05, \*\* p < 0.01 and \*\*\* p < 0.001 versus control

With the WST-1 assay, all particles with the exception of MgO, were found to reduce metabolic activity and thus induce toxicity. After 4 h incubation, the high dose of

all particles significantly decreased the metabolic activity of the Caco-2 cells (Figure 2.2 A), whereas after 24 h significant toxicity occurred at both concentrations tested (Figure 2.2 B). Interestingly, the 4 h incubation with 80  $\mu\text{g}/\text{cm}^2$  MgO, caused a significantly increased formazan dye formation compared to the control cells.

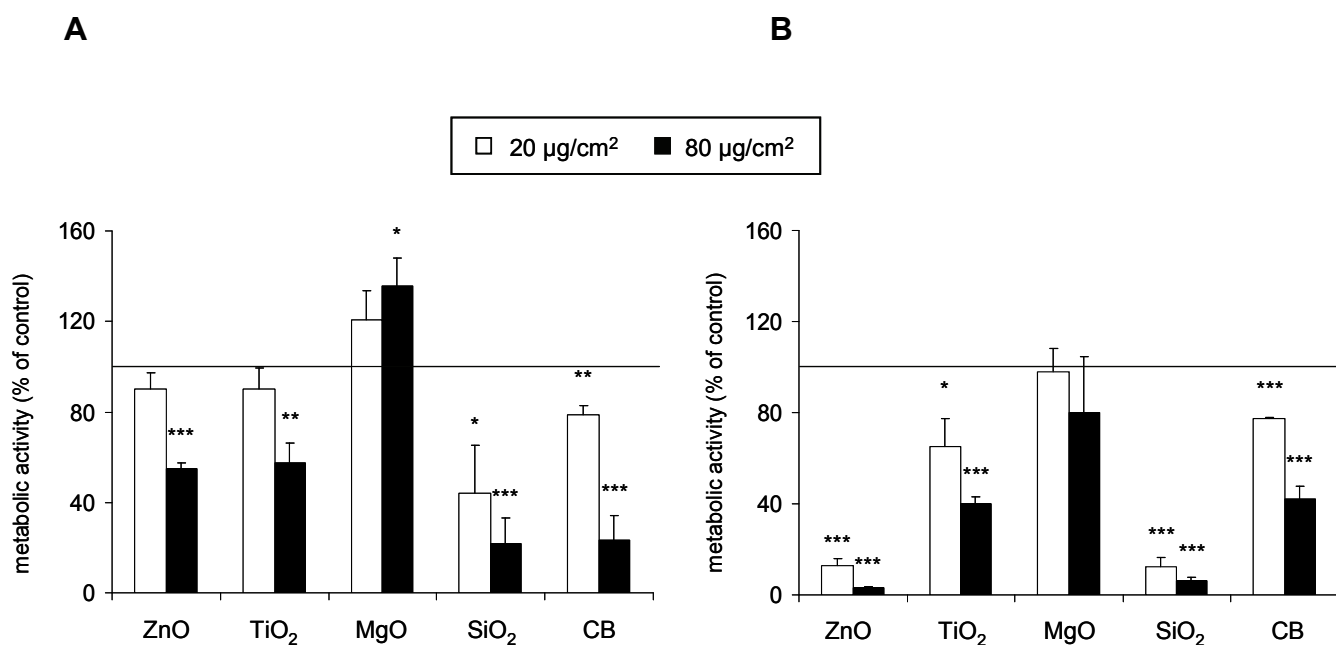


**Figure 2.2 Influences of several particles on the viability of Caco-2 cells.** Cells were incubated with 20 and 80  $\mu\text{g}/\text{cm}^2$  particles for 4 (A) and 24 (B) hours. Mitochondrial enzyme activity was measured via conversion of WST-1 as a marker of cell viability. Values are expressed as mean and standard deviation. The control level is indicated by the horizontal line for clarification.  
\*  $p < 0.05$ , \*\*  $p < 0.01$  and \*\*\*  $p < 0.001$  versus control

To investigate their dose-dependent cytotoxicity in more detail, the effects of additional concentrations of two of the strongly cytotoxic particles, i.e. TiO<sub>2</sub> and ZnO, were examined. Both the LDH and WST-1 assay revealed a clear dose dependent cytotoxic effect of both particle types after 24 hours incubation with an even more pronounced toxicity caused by ZnO in comparison to TiO<sub>2</sub> (Figure 2.3).

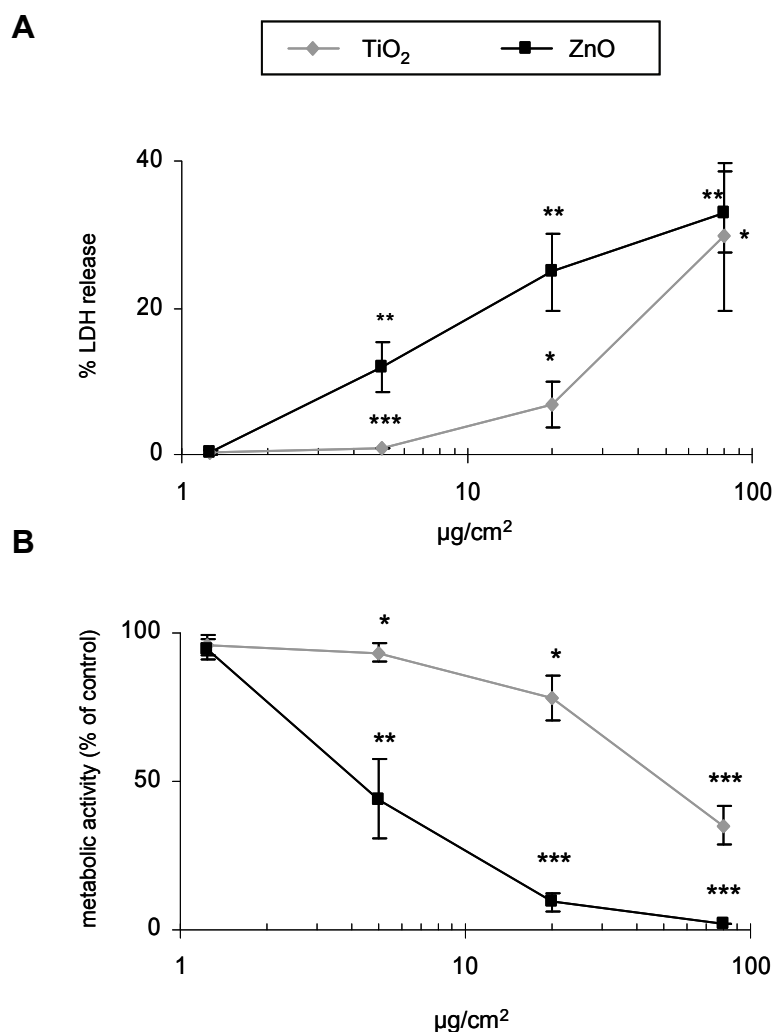


**Figure 2.3** Dose dependent cytotoxic effects of TiO<sub>2</sub> and ZnO on Caco-2 cells. Cells were incubated with 1.25, 5, 20 and 80 µg/cm<sup>2</sup> particles for 24 hours. LDH leakage (A) and mitochondrial activity (B) were measured as markers of cell toxicity. Values are expressed as mean and standard deviation. \* p < 0.05, \*\* p < 0.01 and \*\*\* p < 0.001 versus control

To determine the potential DNA damaging properties of the particles to colon cells, the Fpg modified comet assay was used. In this assay, after electrophoresis DNA damage becomes visible as a “tail” of DNA fragments behind the cell core and is scored by determination of the percentage of DNA in tail. The specific induction of oxidative DNA damage is determined by the incorporation in the assay of the Fpg-enzyme, which specifically cleaves oxidative DNA lesions, particularly 8-OHdG sites. The activity of the Fpg was verified by the treatment of the cells with Ro-19 8022, a photosensitiser known to induce oxidative DNA damage via generation of singlet oxygen (data not shown).

Already after 4 h incubation, ZnO caused a significant increase of both DNA strand breaks and oxidative DNA damage in the Caco-2 cells (Figure 2.4). Additionally, treatment with SiO<sub>2</sub> caused significant oxidative DNA damage to the cells. None of the

other particles were found to cause DNA strand breakage or oxidative DNA damage in the Caco-2 cells. However, TiO<sub>2</sub> treated Caco-2 cells that were processed in the presence of light (see methods section for details) showed increased DNA damage as well as significant oxidative damage in contrast to the dark-processed TiO<sub>2</sub> treated cells (see Figure 2.4).

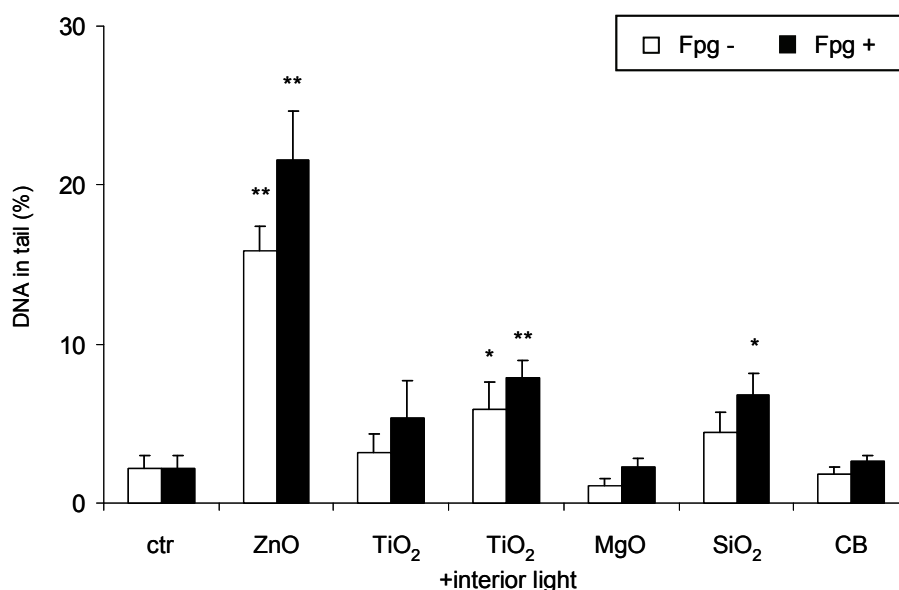


**Figure 2.4 Particle-induced DNA strand breakage and oxidative DNA damage in Caco-2 cells using Fpg comet assay.** DNA strand breakage and oxidative DNA damage was determined in Caco-2 cells by Fpg-modified comet assay following 4 h treatment with several particles at 20  $\mu\text{g}/\text{cm}^2$ . After treatment all samples were processed for comet assay in the dark, while additional samples of TiO<sub>2</sub>-treated cells were processed under normal interior light (see method section for details). Values are expressed as mean and standard deviation.  
\*  $p < 0.05$ , \*\*  $p < 0.01$  and \*\*\*  $p < 0.001$  versus control

Since it is known cells with diminished intracellular glutathione (GSH) levels may be more sensitive to oxidative DNA damage induction, the total GSH content of the Caco-2 cells was measured after 4 h particle incubation. Treatment of the Caco-2 cells with all particles, except for TiO<sub>2</sub>, led to significant GSH depletion with SiO<sub>2</sub> causing the strongest effect of 40 % depletion (Figure 2.5).

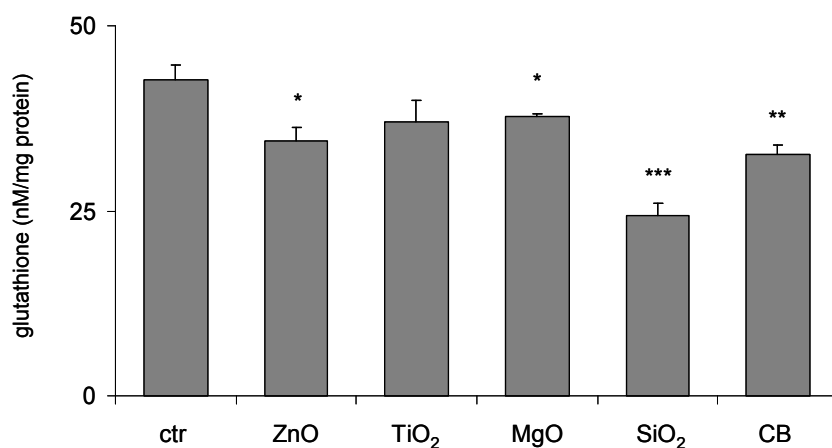


**Figure 2.5 Effects of several particles on total glutathione content of Caco-2 cells.** Cells were incubated with 20  $\mu\text{g}/\text{cm}^2$  particles for 4 hours. Total glutathione content of the Caco-2 cells is expressed as nM/mg protein. Values are expressed as mean and standard deviation. \*  $p < 0.05$ , \*\*  $p < 0.01$  and \*\*\*  $p < 0.001$  versus control

To investigate whether the cytotoxic and DNA damaging effects of the particles occurred in proportion to their surface area, multiple types of TiO<sub>2</sub> and ZnO particles were simultaneously tested for their cytotoxicity as well as their capability to induce DNA damage. To this extent, Caco-2 cells were incubated for 4 hours with the TiO<sub>2</sub> and ZnO samples used so far as well as with two further samples of both TiO<sub>2</sub> and ZnO with different surface area (see sample specifications in Table 2.1).

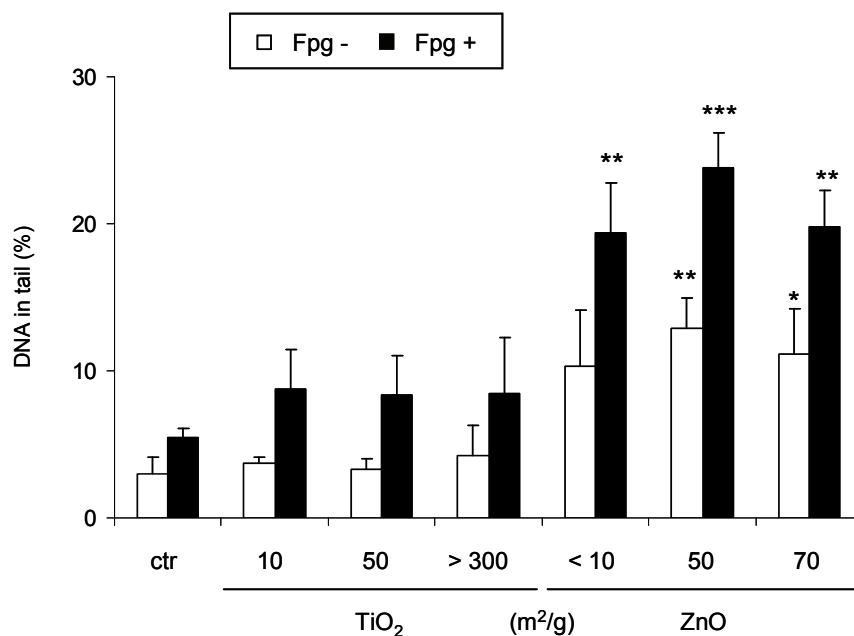


**Figure 2.6 Oxidative DNA damage in Caco-2 cells using Fpg comet assay induced by different-sized particles.** Damage was determined in Caco-2 cells using the Fpg-modified comet assay following 4 h treatment with TiO<sub>2</sub> and ZnO particles with BET-values of 10, 50, >300 m<sup>2</sup>/g (TiO<sub>2</sub>) and <10, 50, 70 m<sup>2</sup>/g (ZnO) at 20  $\mu\text{g}/\text{cm}^2$ . Values are expressed as mean and standard deviation. \*  $p < 0.05$ , \*\*  $p < 0.01$  and \*\*\*  $p < 0.001$  versus control

For TiO<sub>2</sub>, no significant DNA strand breaks or oxidative DNA lesions could be observed for any of the samples (Figure 2.6). In contrast to these findings, cytotoxicity was significantly induced by the highest doses of the two nano-TiO<sub>2</sub> samples (TiO<sub>2</sub> and TiO<sub>2</sub>-HSA) but not by fine TiO<sub>2</sub> (TiO<sub>2</sub>-F) (Figure 2.7 A). Additionally, fine TiO<sub>2</sub> only reduced metabolic activity of the cells in high doses, whereas both samples of nano-TiO<sub>2</sub> already showed effects at the treatment concentration 20 µg/cm<sup>2</sup> (Figure 2.7 B).

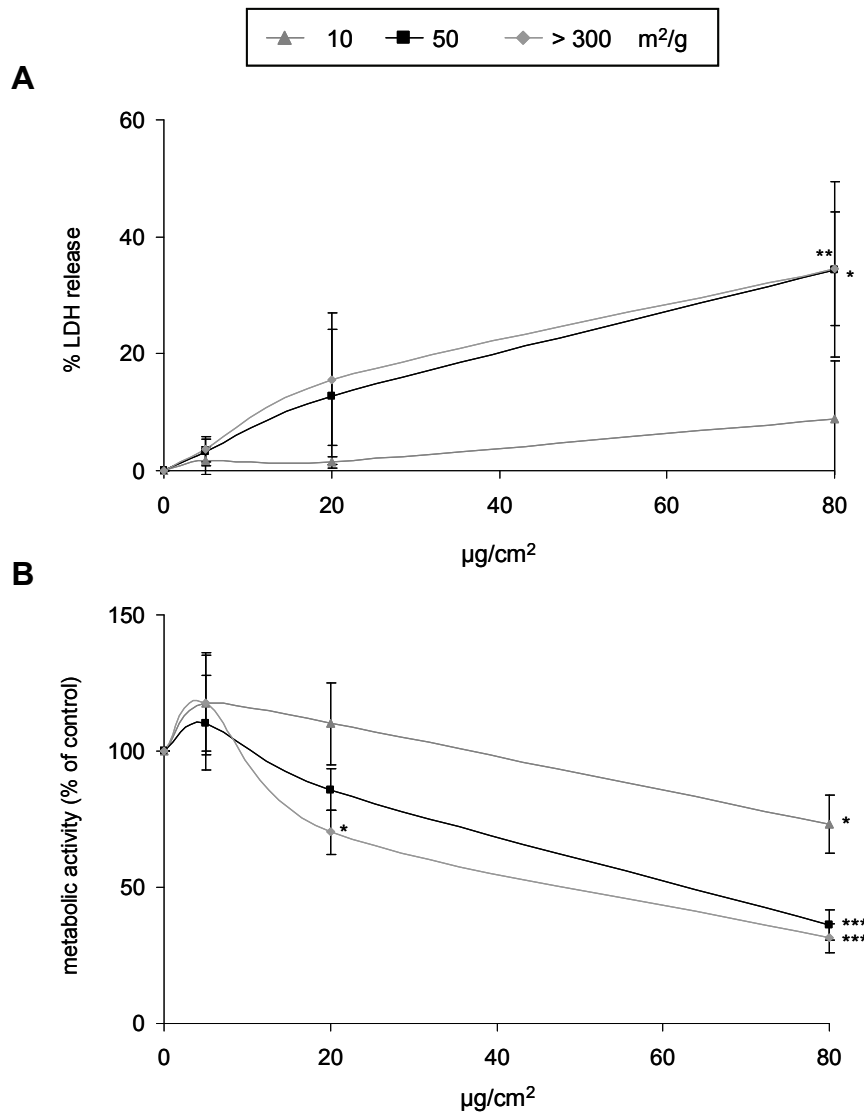


**Figure 2.7 Cytotoxicity of TiO<sub>2</sub> particles of with different surface area to Caco-2 cells.** Cells were incubated for 4 hours with 5, 20 and 80 µg/cm<sup>2</sup> of TiO<sub>2</sub> particles with BET-values of 10, 50 and > 300 m<sup>2</sup>/g. LDH leakage (A) and mitochondrial activity (B) were measured as markers of cell toxicity. Values are expressed as mean and standard deviation.

<sup>+</sup> p < 0.05 versus control for the 10 m<sup>2</sup>/g particles

\* p < 0.05 and \*\*\* p < 0.001 versus control for the 50 m<sup>2</sup>/g particles

## p < 0.01 and ### p < 0.001 versus control for the > 300 m<sup>2</sup>/g particles

For ZnO, all three samples caused a significant increase of DNA strand breaks as well as enhanced oxidative damage, with no significant differences in potency between the individual ZnO particles (Figure 2.6). In agreement with our earlier observations (see Figure 2.1 A), the ZnO sample with the surface area of 70 m<sup>2</sup>/g did not induce increased LDH leakage after 4 h. This also appeared true now for the fine ZnO sample (ZnO-F) as well as the ZnO sample with the BET surface area of 50 m<sup>2</sup>/g (ZnO-Ns) (see Figure 2.8 A).

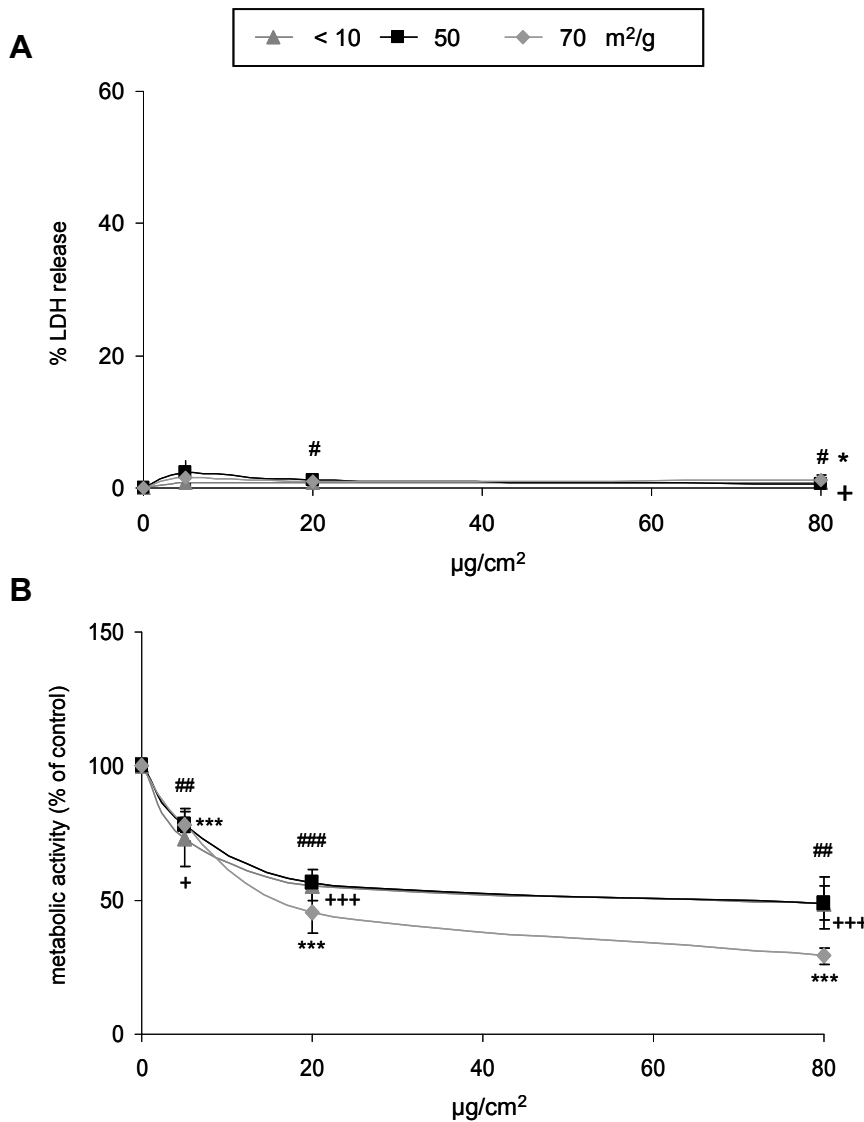


**Figure 2.8 Cytotoxicity of ZnO particles of different surface area to Caco-2 cells.** Cells were incubated for 4 hours with 5, 20 and 80 µg/cm<sup>2</sup> of ZnO particles with BET-values of <10, 50 or 70 m<sup>2</sup>/g. LDH leakage (A) and mitochondrial activity (B) were measured as markers of cell toxicity. Values are expressed as mean and standard deviation.  
 + p < 0.05 and +++ p < 0.001 versus control for the <10 m<sup>2</sup>/g particles  
 \* p < 0.05 and \*\*\* p < 0.001 versus control for the 50 m<sup>2</sup>/g particles  
 # p < 0.05, ## p < 0.01 and ### p < 0.001 versus control for the 70 m<sup>2</sup>/g particles



A slight, but significant LDH release could be shown for the ZnO-Ns at 20  $\mu\text{g}/\text{cm}^2$  as well as the highest dose (80  $\mu\text{g}/\text{cm}^2$ ) for all ZnO particles. Finally, irrespective of their surface area, all ZnO particles were found to reduce metabolic activity in a clear dose-dependent manner, already being significant at 5  $\mu\text{g}/\text{cm}^2$ . (Figure 2.8 B). The ZnO sample with the highest surface area tended to be more toxic than both other samples, but this difference was not statistically significant.

## 2.4 Discussion

In the present study, the toxic effects of a panel of fine and nano-size particles to the human colon epithelial cell line Caco-2 were evaluated. At first, we investigated the cytotoxic effects of the particles by measuring their influence on membrane integrity and metabolic activity of the cells. We found that both  $\text{TiO}_2$  and  $\text{SiO}_2$  already display significant dose-dependent membrane damage after 4 hours. ZnO and CB only revealed their membrane damaging properties after 24 hours. Analysis of changes in metabolic activity indicated cytotoxicity towards the Caco-2 cells for all samples, with the exception of MgO. Over all, the WST-1 assay tended to be more sensitive to detect particle toxicity when compared to the LDH assay, in concordance with previous findings by us in lung epithelial cells (Schins *et al.*, 2002) and macrophages (Albrecht *et al.*, 2009). Our data also highlight the importance of using more than one cytotoxicity assay; this is most notably shown by the contrasting effects with the CB nanoparticles, whereby the lacking -or even seemingly decreasing effect in the LDH in high concentrations- is considered to result from LDH absorption artefacts (Monteiro-Riviere *et al.* 2008; Stone *et al.*, 2009). In this regard it also remains to be investigated whether the enhanced formation of formazan dye in the WST-1 assay as observed with the MgO is due to increased cell proliferation, or an artefact.

Within the panel of tested particles, ZnO induced a significant amount of DNA strand breaks and oxidative damage in the Caco-2 cells, while  $\text{SiO}_2$  only induced oxidative DNA damage in the absence of a significant increase in DNA strand breakage. The lack of significance in the observations upon  $\text{SiO}_2$  treatment is in line with the recent study of Barnes *et al.* (2008) that could not find significant strand breaks in the conventional comet assays performed in two separate laboratories. It is also important to notice that the DNA strand breakage induction of  $\text{SiO}_2$  was measured at a concentration that also causes significant cytotoxicity (WST-1 assay). In contrast, the DNA damaging effects of ZnO were observed to occur in the absence of cytotoxicity (both LDH and WST-1 assay). Notably, to determine the true genotoxic potential of these and other particles, more detailed dose-response investigations will be required, i.e. according to testing guidelines and by employing independent genotoxicity assays (Stone *et al.*, 2009). However, such an approach was beyond the scope of our current study, which was aimed to provide first clues for the toxic properties of various nanoparticles in human colon epithelial cells.

In the present study, both SiO<sub>2</sub> and ZnO treatment also caused a clear depletion of total glutathione (GSH) within the Caco-2 cells, in association with the observed oxidative DNA damage induced by these particles. This indicates that, alongside GSH measurements (Oberdörster *et al.*, 2005b; Hussain *et al.*, 2005), oxidative DNA damage analysis by Fpg-comet assay can also be considered a highly sensitive marker of oxidative stress in the toxicity screening of nanoparticles. However, one should also be cautious about potential artefacts with this assay. For instance, we could observe that incubation with TiO<sub>2</sub> caused an obvious but not statistically significant increase of strand breaks and oxidative DNA damage when the comet assay was processed as usual in the dark. After handling of the already lysed slides by normal interior light, these damages became statistically significant. This reveals the necessity of careful handling when performing the comet assay to avoid false positive results, especially when photosensitising compounds such as TiO<sub>2</sub> are used.

The relevance of the photosensitising action of TiO<sub>2</sub> is under ongoing discussion, most importantly in relation to its application in skin formulations. Nakagawa *et al.* could demonstrate enhanced strand breaks detected by using the comet assay, but also increased cytotoxicity, in mouse lymphoma cells when treated with different TiO<sub>2</sub> particles and irradiated with UV light (Nakagawa *et al.*, 1997). On the other hand, Theogaraj and co-workers could not find increased chromosome aberrations after treatment of Chinese hamster ovary cells with several ultrafine TiO<sub>2</sub> particles and UV light irradiation (Theogaraj *et al.*, 2007).

Since toxic effects of nanoparticles are considered to be at least in part due to their increased surface area (Oberdörster *et al.*, 2005a), we also investigated cytotoxicity and DNA damaging properties in Caco-2 cells of TiO<sub>2</sub> and ZnO samples that differed in their surface area. Remarkably however, we could not find any surface area-dependent effects concerning DNA strand breaks or oxidative damage, neither by the three different TiO<sub>2</sub> particles nor by the various ZnO particles used. Only slightly increased cytotoxic effects of both nano-sized TiO<sub>2</sub> particles in comparison to fine TiO<sub>2</sub> could be observed. As such, our data are in contrast to observations on the DNA damaging effects of fine versus ultrafine TiO<sub>2</sub> in bronchial epithelial cells (Gurr *et al.*, 2005) and also differ from the hallmark observations in pulmonary toxicology where ultrafine TiO<sub>2</sub> causes increased inflammatory responses in comparison to fine TiO<sub>2</sub> at equal mass dose or lung burden (reviewed in Oberdörster *et al.* 2005a). Our findings therefore suggest that particle surface area may not necessarily be the best dose-metric to predict the

genotoxic properties of poorly soluble low toxicity particles and/or the over all toxic potency of particles to the gastrointestinal tract, unlike e.g. their inflammogenic potency as clearly demonstrated for the respiratory tract (Oberdörster *et al.*, 2005a; Donaldson *et al.*, 2008). Our data reveal marked differences in the responding of each single particle tested. Table 2 summarises the various outcomes of the toxic properties of the different types of particles that were investigated. The findings of our study demonstrate that the various properties are not predictable and points out the need of differentiated investigation of each single property for every particle.

	Membrane damage (LDH) 4 h		Membrane damage (LDH) 24 h		Impaired metabolic activity (WST-1) 4 h		Impaired metabolic activity (WST-1) 24 h		DNA strand breakage	Oxidative DNA damage	Glutathione depletion
	20	80	20	80	20	80	20	80			
$\mu\text{g}/\text{cm}^2$	20	80	20	80	20	80	20	80	20	20	20
TiO <sub>2</sub>	-	-	++	++	-	++	+	+++	-	-	-
SiO <sub>2</sub>	-	++	++	++	+	+++	+++	+++	-	+	+++
CB	-	-	+	-(a)	++	+++	+++	+++	-	-	++
MgO	-	-	-	-	-	+(†)	-	-	-	-	+
ZnO	-	-	+	++	-	+++	+++	+++	+++	+++	+

**Table 2.2 Overview of particle effects on different endpoints**

- : no significant effects found

+, ++ and +++ : significant effects found (number of symbols indicates the strength of significance)

(a) potential artefact

(†) opposite, i.e. possible proliferative effect

An estimated daily ingestion of  $10^{12}$ - $10^{14}$  particles per day has been reported (Lomer *et al.*, 2001, 2004), with an increasing tendency, while still very little is known about the possible cytotoxic or genotoxic effects of nanoparticles reaching the colon (Oberdörster *et al.*, 2007; Borm *et al.*, 2006; Chaudhry *et al.*, 2008). Nowadays, the actual daily ingestion of particles and its burden to the colon seems to be still below risk for the consumer. However, it is well anticipated that the occurrence of nanoparticles, i.e. novel materials as well as modified formulations of existing particles will increase in food products or contaminants in the near future (Chaudhry *et al.*, 2008; Tiede *et al.*, 2008; Bouwmeester *et al.*, 2009). Presently, it is still largely unclear to which extent ingested nanoparticles are actually taken up by the epithelial cells in relation to their physicochemical properties and to which extent they can translocate into the bloodstream. Earlier studies suggest an estimated particle-absorption of less than 10 % (Jani *et al.*, 1994). However, the uptake of small particles (~110-120 nm) by the small intestine *in situ* is shown to be 15-250 fold higher in comparison to larger particles

(~510-550 nm, Desai *et al.*, 1996). Studies with lung epithelial cells indicate that specific nanoparticles, depending on their primary size and aggregation status may be taken up by cells via various mechanisms including phagocytosis, pinocytosis and passive diffusion and thereby occasionally may reach important intracellular targets including mitochondria and the nucleus (Geiser *et al.*, 2005; Unfried *et al.*, 2007; Mühlfeld *et al.*, 2008).

In relation to our current observations it should also be kept in mind that many factors influence and possibly enhance the toxicity of ingested nanoparticles. For example, the acidic gastric fluid may modify the chemical composition or have an impact on solubility of the particles. Additionally, the recent observation by Ashwood *et al.* (2007), showing that interactions with the microflora of the colon can increase the toxicity of particles, suggests that the toxicity observed in our *in vitro* model might even be an underestimation of that occurring *in vivo* upon exposure to these compounds. Possible interactions between different ingested particles should also be kept in mind. Exemplary, MgO, which showed no cytotoxic effects in our experiments, might nevertheless render cells more susceptible to the effects of other particles due to its ability to decrease cellular GSH levels.

Finally, it should be kept in mind that our current *in vitro* study represents a model of healthy intestine, and that our current observations do not elaborate on the potential role of intestinal inflammation in the toxicity of ingested particles. On the one hand, it should be addressed to which extent specific particles can trigger pro-inflammatory processes in the gastrointestinal tract as this may increase their toxicity. For the respiratory tract it has been established that low-toxicity nanoparticles cause inflammation in proportion to their surface area, and this inflammatory response in turn, has been associated with tissue damage, remodelling and mutagenesis (Duffin *et al.*, 2007; Schins and Knaapen, 2007). On the other hand, it should also be investigated whether the toxic potency of ingested nanoparticles differs between healthy individuals and those with (chronic) inflammatory bowel diseases.

In conclusion, our results show that a variety of nanoparticles, which may occur in food or food packaging, can exert cytotoxic as well as DNA damaging effects in target cells of the human intestine. Presently, we cannot entirely rule out any harmful effect of such particles upon ingestion. Obviously, the results of our study should be interpreted in relation to the applied particle concentrations. However, the mere lack of information about in which products they can actually be found, to which extent they are used in

processed food and in which dose they will actually reach the intestine upon ingestion (Tiede *et al.*, 2008; Bouwmeester *et al.*, 2009) complicates an appropriate evaluation of the risks of nanoparticle ingestion.

### **Acknowledgements**

This study was financially supported by a grant from the German Research Council (Deutsche Forschungsgemeinschaft - Graduate College GRK-1427).

### **Declaration**

The manuscript is published at Nanotoxicology.

All experimental work presented was performed by Kirsten Gerloff. The impact on authoring this paper can be estimated in total with 90%.

## 2.5 References

- Albrecht C, Scherbart AM, Van Berlo D, Braunbarth CM, Schins RPF, Scheel J. Evaluation of cytotoxic effects and oxidative stress with hydroxyapatite dispersions of different physicochemical properties in rat NR8383 cells and primary macrophages. *Toxicol in Vitro* 2009;23:520-530
- Ashwood P, Thompson RP, Powell JJ. Fine particles that adsorb lipopolysaccharide via bridging calcium cations may mimic bacterial pathogenicity towards cells. *Exp Biol Med (Maywood)* 2007;232(1):107-17
- Asuri P, Karajanagi SS, Vertegel AA, Dordick JS, Kane RS. Enhanced stability of enzymes adsorbed onto nanoparticles. *J Nanosci Nanotechnol* 2007;7(4-5):1675-8
- Barnes CA, Elsaesser A, Arkusz J, Smok A, Palus J, Leśniak A, Salvati A, Hanrahan JP, Jong WH, Dziubałowska E *et al.* Reproducible comet assay of amorphous silica nanoparticles detects no genotoxicity. *Nano Lett* 2008;8(9):3069-74
- Borm PJA, Robbins D, Haubold S, Kuhlbusch T, Fissan H, Donaldson K, Schins RPF, Stone V, Kreyling W, Lademann J *et al.* The potential risks of nanomaterials: a review carried out for ECETOC. *Part Fibre Toxicol* 2006;3:11
- Bouwmeester H, Dekkers S, Noordam MY, Hagens WI, Bulder AS, de Heer C, ten Voorde SE, Wijnhoven SW, Marvin HJ, Sips AJ. Review of health safety aspects of nanotechnologies in food production. *Regul Toxicol Pharmacol* 2009;53:52
- Brown DM, Wilson MR, MacNee W, Stone V, Donaldson K. Size-dependent proinflammatory effects of ultrafine polystyrene particles: a role for surface area and oxidative stress in the enhanced activity of ultrafines. *Toxicol Appl Pharmacol* 2001;175:191-9
- Brown DM, Donaldson K, Borm PJ, Schins RP, Dehnhardt M, Gilmour P, Jimenez LA, Stone V. Calcium and ROS-mediated activation of transcription factors and TNF-alpha cytokine gene expression in macrophages exposed to ultrafine particles. *Am J Physiol Lung Cell Mol Physiol* 2004;286:L344-53
- Chaudhry Q, Scotter M, Blackburn J, Ross B, Boxall A, Castle L, Aitken R, Watkins R. Applications and implications of nanotechnologies for the food sector. *Food Addit Contam Part A Chem Anal Control Expo Risk Assess* 2008;25(3):241-58
- Desai MP, Labhsetwar V, Amidon GL, Levy RJ. Gastrointestinal uptake of biodegradable microparticles: effect of particle size. *Pharm Res* 1996;13(12):1838-45
- Donaldson K, Tran L, Jimenez LA, Duffin R, Newby DE, Mills N, MacNee W, Stone V. Combustion-derived nanoparticles: a review of their toxicology following inhalation exposure. *Part Fibre Toxicol* 2005;2:10
- Donaldson K, Borm PJ, Oberdörster G, Pinkerton KE, Stone V, Tran CL. Concordance between in vitro and in vivo dosimetry in the proinflammatory effects of low-toxicity, low-solubility particles: the key role of the proximal alveolar region. *Inhal Toxicol* 2008;20(1):53-62
- Duffin R, Tran L, Brown D, Stone V, Donaldson K. Proinflammatory effects of low-toxicity and metal nanoparticles in vivo and in vitro: highlighting the role of particle surface area and surface reactivity. *Inhal Toxicol* 2007;19(10):849-856.

- Geiser M, Rothen-Rutishauser B, Kapp N, Schürch S, Kreyling W, Schulz H, Semmler M, Im Hof V, Heyder J, Gehr P. Ultrafine particles cross cellular membranes by nonphagocytic mechanisms in lungs and in cultured cells. *Environ Health Perspect* 2005;113:1555-60
- Gurr JR, Wang AS, Chen CH, Jan KY. Ultrafine titanium dioxide particles in the absence of photoactivation can induce oxidative damage to human bronchial epithelial cells. *Toxicology* 2005;213(1-2):66-73
- Hussain SM, Hess KL, Gearhart JM, Geiss KT, Schlager JJ. In vitro toxicity of nanoparticles in BRL 3A rat liver cells. *Toxicol In Vitro* 2005;19:975-83
- Jani PU, McCarthy DE, Florence AT. Titanium dioxide (rutile) particle uptake from the rat GI tract and translocation to systemic organs after oral administration. *J Pharm* 1994;105(2):157-168
- Kaittani C, Naser SA, Perez JM. One-step, nanoparticle-mediated bacterial detection with magnetic relaxation. *Nano Lett* 2007;7:380-3
- Lomer MC, Harvey RS, Evans SM, Thompson RP, Powell JJ. Efficacy and tolerability of a low microparticle diet in a double blind, randomized, pilot study in Crohn's disease. *Eur J Gastroenterol Hepatol* 2001;13(2):101-6
- Lomer MC, Hutchinson C, Volkert S, Greenfield SM, Catterall A, Thompson RP, Powell JJ. Dietary sources of inorganic microparticles and their intake in healthy subjects and patients with Crohn's disease. *Br J Nutr* 2004;92(6):947-55
- Monteiro-Riviere NA, Inman AO, Zhang LW. Limitations and relative utility of screening assays to assess engineered nanoparticle toxicity in a human cell line. *Toxicol Appl Pharmacol* 2009;234:222-35
- Mühlfeld C, Gehr P, Rothen-Rutishauser B. Translocation and cellular entering mechanisms of nanoparticles in the respiratory tract. *Swiss Med Wkly* 2008;138(27-28):387-91
- Nakagawa Y, Wakuri S, Sakamoto K, Tanaka N. The photogenotoxicity of titanium dioxide particles. *Mutat Res* 1997;394(1-3):125-32
- Nanotechproject homepage,  
<http://www.nanotechproject.org/inventories/consumer/browse/products/5107/> (August 2009)
- Oberdörster G, Oberdörster E, Oberdörster J. Nanotoxicology: an emerging discipline evolving from studies of ultrafine particles. *Environ Health Perspect* 2005a;113(7):823-39
- Oberdörster G, Maynard A, Donaldson K, Castranova V, Fitzpatrick J, Ausman K, Carter J, Karn B, Kreyling W, Lai D *et al.*; ILSI Research Foundation/Risk Science Institute Nanomaterial Toxicity Screening Working Group. Principles for characterizing the potential human health effects from exposure to nanomaterials: elements of a screening strategy. *Part Fibre Toxicol* 2005b;2:8
- Oberdörster G, Stone V, Donaldson K. Toxicology of nanoparticles: a historical perspective. *Nanotoxicol* 2007;1:2-25
- Schins RPF, Duffin R, Höhr D, Knaapen AM, Shi T, Weishaupt C, Stone V, Donaldson K, Borm PJA. Surface modification of quartz inhibits toxicity, particle uptake, and oxidative DNA damage in human lung epithelial cells. *Chem Res Toxicol* 2002;15:1166-1173
- Schins RP, Knaapen AM. Genotoxicity of poorly soluble particles. *Inhal Toxicol* 2007;19 (Suppl 1):189-98
- Schmid K, Riediker M. Use of nanoparticles in Swiss Industry: a targeted survey. *Environ Sci Technol* 2008;42(7):2253-60



- Singh S, Shi T, Duffin R, Albrecht C, van Berlo D, Höhr D, Fubini B, Fenoglio I, Martra G, Borm PJA, Schins RPF. Endocytosis, oxidative stress and IL-8 expression in human lung epithelial cells upon treatment with fine and ultrafine TiO<sub>2</sub>: role of particle surface area and of surface methylation of the particles. *Toxicol Applied Pharmacol* 2007;222:141-151
- Speit G, Schütz P, Bonzheim I, Trenz K, Hoffmann H. Sensitivity of the FPG protein towards alkylation damage in the comet assay. *Toxicol Lett* 2004;146(2):151-8
- Stoeger T, Takenaka S, Frankenberger B, Ritter B, Karg E, Maier K, Schulz H, Schmid O. Deducing in vivo toxicity of combustion-derived nanoparticles from a cell-free oxidative potency assay and metabolic activation of organic compounds. *Environ Health Perspect* 2009;117:54-60
- Stone V, Johnston H, Schins RPF. Development of *in vitro* systems for Nanotoxicology - methodological considerations. *Crit Rev Toxicol* 2009; 39:613-626
- Taylor TM, Davidson PM, Bruce BD, Weiss J. Liposomal nanocapsules in food science and agriculture. *Crit Rev Food Sci Nutr* 2005;45(7-8):587-605
- Theogaraj E, Riley S, Hughes L, Maier M, Kirkland D. An investigation of the photo-clastogenic potential of ultrafine titanium dioxide particles. *Mutat Res* 2007;634(1-2):205-19
- Tiede K, Boxall AB, Tear SP, Lewis J, David H, Hasselov M. Detection and characterization of engineered nanoparticles in food and the environment. *Food Addit Contam Part A Chem Anal Control Expo Risk Assess* 2008;25:795-821
- Unfried K, Albrecht C, Klotz LO, von Mikecz A, Grether-Beck S, Schins RPF. Cellular responses to nanoparticles: target structures and mechanisms. *Nanotoxicol* 2007;1:52-71
- Xia T, Kovochich M, Brant J, Hotze M, Sempf J, Oberley T, Sioutas C, Yeh JI, Wiesner MR, Nel AE. Comparison of the abilities of ambient and manufactured nanoparticles to induce cellular toxicity according to an oxidative stress paradigm. *Nano Lett* 2006;6:1794-8



## CHAPTER 3

---

### Specific surface area independent effects of titanium dioxide particles in human intestinal Caco-2 cells

Kirsten Gerloff<sup>1</sup>, Ivana Fenoglio<sup>2</sup>, Emanuele Carella<sup>2</sup>, Catrin Albrecht<sup>1</sup>, Agnes W. Boots<sup>1</sup>, Irmgard Förster<sup>3</sup>, Roel P.F. Schins<sup>1</sup>

<sup>1</sup> Particle Research and <sup>3</sup> Molecular Immunology, Institut für Umweltmedizinische Forschung (IUF) at the Heinrich Heine University Düsseldorf, Germany.

<sup>2</sup> Dip. di Chimica Inorganica, Chimica Fisica e Chimica dei Materiali and Interdepartmental Centre "G. Scansetti" for Studies on Asbestos and Other Toxic Particulates and Interdepartmental Center for Nanostructured Interfaces and Surfaces University of Torino, Italy.

#### Abstract

Titanium dioxide (TiO<sub>2</sub>) has a long-standing use as a food additive. Micrometric powders are e.g. applied as whiteners in confectionary or dairy products. Conversely, possible hazards of nanometric TiO<sub>2</sub>-particles for humans and the potential influence of a varying specific surface area (SSA) are currently under discussion. To follow-up on our previous study (Gerloff *et al.*, 2009; *Nanotoxicology*) we have analysed five different samples of TiO<sub>2</sub> for crystallinity, primary particle size, SSA and aggregation/agglomeration. Their cytotoxic and DNA damaging potential was evaluated in human intestinal Caco-2 cells by LDH assay and Fpg-modified comet assay. Two anatase-rutile containing TiO<sub>2</sub> samples, in contrast to three pure anatase powders, caused mild membrane damage and DNA oxidation under exclusion of illumination. The effects could not be explained by the different SSA of the samples, and indicated that cytotoxic and DNA damaging properties of TiO<sub>2</sub> in this system are more likely driven by their chemical composition.

### 3.1 Introduction

The use of particles as food additives has been well established throughout the last decades. Titanium dioxide (TiO<sub>2</sub>) for example is well appreciated for its inert capacities and as such widely used as a white food coloring. Indeed, it can be found in many foods, as for example dairy products (GSFA online) and is accepted by the EU with the E-number 171. Currently, a lot of research is in progress to expand the application areas of this additive using nano TiO<sub>2</sub>-particles, for example as a coating in confectionary products to prevent melting or improve shelf life (Chaudhry *et al.*, 2008). Bulk TiO<sub>2</sub> is regarded as a highly biocompatible material. However, TiO<sub>2</sub> nanoparticles have been found to elicit toxic responses in various *in vivo* and *in vitro* systems (Oberdörster *et al.* 2005; Oberdörster *et al.* 2007; Johnston *et al.* 2009). The observed adverse effects in these studies have been contributed to the small particle size, the high specific surface area (SSA) and the reactivity of nanometric TiO<sub>2</sub> powders. Consequently, investigations on possible adverse effects of ingested TiO<sub>2</sub>-nanoparticles are necessary to rule out any health risks to humans consuming particle-containing products.

Previously, we have investigated the potential of different nano-sized materials to induce cytotoxicity and DNA damage in Caco-2 cells (Gerloff *et al.*, 2009). Amongst others, we have also aimed to address the influence of an increasing particle specific surface area (SSA evaluated by means of Brunauer, Emmett and Teller method) on both endpoints mentioned by comparative testing of three different types of TiO<sub>2</sub>-particles. In this study we did not observe a distinction with respect to DNA damage. Recently however, we have found out that the SSA value listed by the supplier in the catalogue as well as on the label of the specific batch was incorrect. Contrary to the provided SSA value of > 300 m<sup>2</sup>/g, this TiO<sub>2</sub> sample appeared to have a SSA value of about 50 m<sup>2</sup>/g, closely resembling that of one of the two other previously tested samples (Gerloff *et al.*, 2009). Accordingly, the statement on the apparent lack of a surface area dependent DNA damaging effect for TiO<sub>2</sub> on our previous paper could not be truly made.

To clarify on this matter, we have now further screened a broader range of TiO<sub>2</sub>-particles, by including two additional types of particles of high SSA values. In the present study, for all samples the SSA values were newly determined. The mean primary particle size as well as their organisation in aggregates was evaluated by

using transmission electron microscopy (TEM) and dynamic light scattering (DLS). Using both these novel and the earlier investigated materials, we re-evaluated the potential role of surface area of TiO<sub>2</sub>-particles on cytotoxicity and oxidative DNA damage in Caco-2 cells.

## 3.2 Methods

**Materials.** Trypsin, Dulbecco's  $\text{Ca}^{2+}/\text{Mg}^{2+}$ -free phosphate buffered saline (PBS), agarose, low melting point (LMP) agarose, Triton X-100, Dimethyl sulfoxide (DMSO), ethidium bromide and fetal calf serum (FCS) were all purchased from Sigma (Germany). Lactate dehydrogenase (LDH) Cytotoxicity Detection Kit was obtained from Hoffmann-LaRoche (Switzerland). Minimum essential Medium (MEM) with Earle's salts and non essential amino acids was purchased from invitrogen (Germany). [R]-1-[(10-Chloro-4-oxo-3-phenyl-4H-benzo[a]quinolizin-1-yl)-carbonyl]-2-pyrrolidinemethanol (Ro19-8022) was a gift from Hoffmann-LaRoche (Switzerland). Formamidopyrimidine-glycosylase (Fpg)-enzyme was kindly provided by Dr. Andrew Collins, Institute for Nutrition Research, University of Oslo, Norway. All other chemicals were from Merck (Germany).

**TiO<sub>2</sub> samples.** A set of five different TiO<sub>2</sub> samples was used. Three of the samples were already used in our previous study (Gerloff *et al.*, 2009). For the present investigations, two further samples were included, i.e. JRC 12, supplied by the Japan Catalysis Society, and Hombikat UV100, obtained from Sachtleben Chemie GmbH, Germany.

**XRD spectroscopy.** XRD spectra were collected on a diffractometer (PW1830, Philips) using  $\text{CoK}\alpha$  radiation, in the (20 – 90)  $2\theta$  range, with step width  $2\theta = 0.05$  and diffraction peaks have been indexed according to ICDD database (International Centre for Diffraction Data).

**Surface area measurements.** The surface area of the particles has been measured by means of the Brunauer, Emmett and Teller (BET) methods based on  $\text{N}_2$  adsorption at 77K (Micrometrics ASAP 2010).

**Morphological characterisation.** The mean size of primary particles as well as their organisation in aggregates/agglomerates has been evaluated by electron transmission microscopy TEM (JEOL 3010-UHR instrument operating at 300 kV, equipped with a  $2\text{k} \times 2\text{k}$  pixels Gatan US1000 CCD camera).

**Average hydrodynamic size.** TiO<sub>2</sub> particles were suspended in water at pH 9 to maximise the electrostatic repulsion between particles. The suspensions were sonicated for 2 min with a probe sonicator (100 W, 20 kHz, Sonoplus, Bandelin, Berlin, Germany). The average hydrodynamic size of particles or aggregates has been evaluated by means of dynamic light scattering (DLS) (Zetasizer Nano-ZS, Malvern Instruments, Worcestershire, UK). The detection limit for this technique is of 6 µm.

**Culture and treatment of the cells.** The human colon adenocarcinoma cell line Caco-2 was obtained from DSMZ (Deutsche Sammlung von Mikroorganismen und Zellkulturen GmbH, Germany) and grown in MEM with Earle's salts and Non Essential Amino Acids, supplemented with 20 % FCS, 1 % L-glutamine and 30 IU/ml penicillin–streptomycin. For LDH assay and Fpg-modified comet assay, cells were prepared and treated as described in Gerloff *et al.*, 2009.

**Cytotoxicity.** Cytotoxicity was determined by the lactate dehydrogenase (LDH) assay as a marker of cell membrane integrity. 96-well tissue culture plates were used and cells were treated at the indicated concentrations for 4 hours with the particles as described above. LDH was determined using a commercial diagnostic kit according to the manufacturer's instructions (Roche, Switzerland).

**Detection of oxidative DNA damage by Fpg-modified comet assay.** The Fpg-modified comet assay was used to measure DNA strand breaks and specifically oxidative DNA damage in the cells, based on the method described by Speit *et al.* (2004) with minor modifications described earlier (Gerloff *et al.*, 2009). As positive control, the photosensitiser Ro-19 8022 was used, which induces specific oxidative lesions after 2 min light exposure (Angelis *et al.*, 1999).

**Statistics.** All means were calculated from three independent experiments, and are expressed in the graphs as mean and standard deviation (SD). Analysis of statistical significance was done by unpaired Student's t-test with \*p<0.05 and \*\*p<0.01 as levels of significance.

### 3.3 Results

The characteristics of the samples used in this study are listed in Table 3.1.

Sample	Crystalline phases <sup>a</sup>	Particle specific surface area (m <sup>2</sup> /g) as reported in Gerloff <i>et al.</i> , 2009	Particle specific surface area (m <sup>2</sup> /g) as determined in current study	Primary particles mean diameter (nm)	Aggregates/ agglomerates size range (nm)
TiO <sub>2</sub> -F	100 % anatase	10	10	> 100 <sup>b</sup>	70 – 1000 <sup>d</sup>
TiO <sub>2</sub> (p25)	77 % anatase 23 % rutile	50	52.6 ± 0.1	25.2 ± 0.2 <sup>c</sup>	40 - 500 <sup>d</sup>
TiO <sub>2</sub> -HSA	90 % anatase 10 % rutile	> 300	52.8 ± 0.4	21.9 ± 0.3 <sup>c</sup>	20 - 2000 <sup>d</sup>
JRC 12	100 % anatase	-	282.3 ± 1.9	7 <sup>b</sup>	30 - 1000 <sup>d</sup>
UV100	100 % anatase	-	342.4 ± 1.3	3.94 ± 0.05 <sup>c</sup>	50 - 2000 <sup>d</sup>

**Table 3.1 Characterisation of different-sized titanium dioxide particles.**

<sup>a</sup> evaluated by means of XRD

<sup>b</sup> theoretical, calculated from the surface area value

<sup>c</sup> evaluated by TEM

<sup>d</sup> evaluated by Dynamic Light Scattering (DLS). This technique has an upper detection limit of 6000 nm, therefore the presence of larger aggregates may not be excluded.

The samples were found to differ to great extent in terms of their crystalline phases, SSA values and nanostructure. Two samples, i.e. TiO<sub>2</sub>(p25) and TiO<sub>2</sub>-HSA are composed of anatase and rutile phases in different proportions. The other three samples are pure anatase. TiO<sub>2</sub>-F is a micrometric powder as suggested by the low SSA which corresponds to a theoretical particle size larger than 100 nm. Although a fraction of single monodisperse particles is present, the powder is mainly composed by aggregates or agglomerates, as suggested by DLS evaluation. TiO<sub>2</sub>(p25) and TiO<sub>2</sub>-HSA exhibited similar SSA values. As already mentioned, TiO<sub>2</sub>-HSA, which was used in our previous study (Gerloff *et al.*, 2009) turned out to have a much lower BET value upon analysis than the value originally provided by the supplier. The TEM images of these two different samples show the presence of primary particles having a mean diameter of around 20 nm, mainly organised in nanometric and micrometric agglomerates (Figure 3.1 A, B). Single nanoparticles were also detected by TEM. The presence of agglomerates was confirmed by DLS measurements. Well defined crystallographic planes are visible in the HRTEM images (see inserts in Figure 3.1 A and B) suggesting a high degree of crystallinity of the materials. The XRD patterns (Figure 3.2) reveal the presence of very sharp peaks corresponding to anatase and rutile phases, which further confirms the crystallinity of both samples.



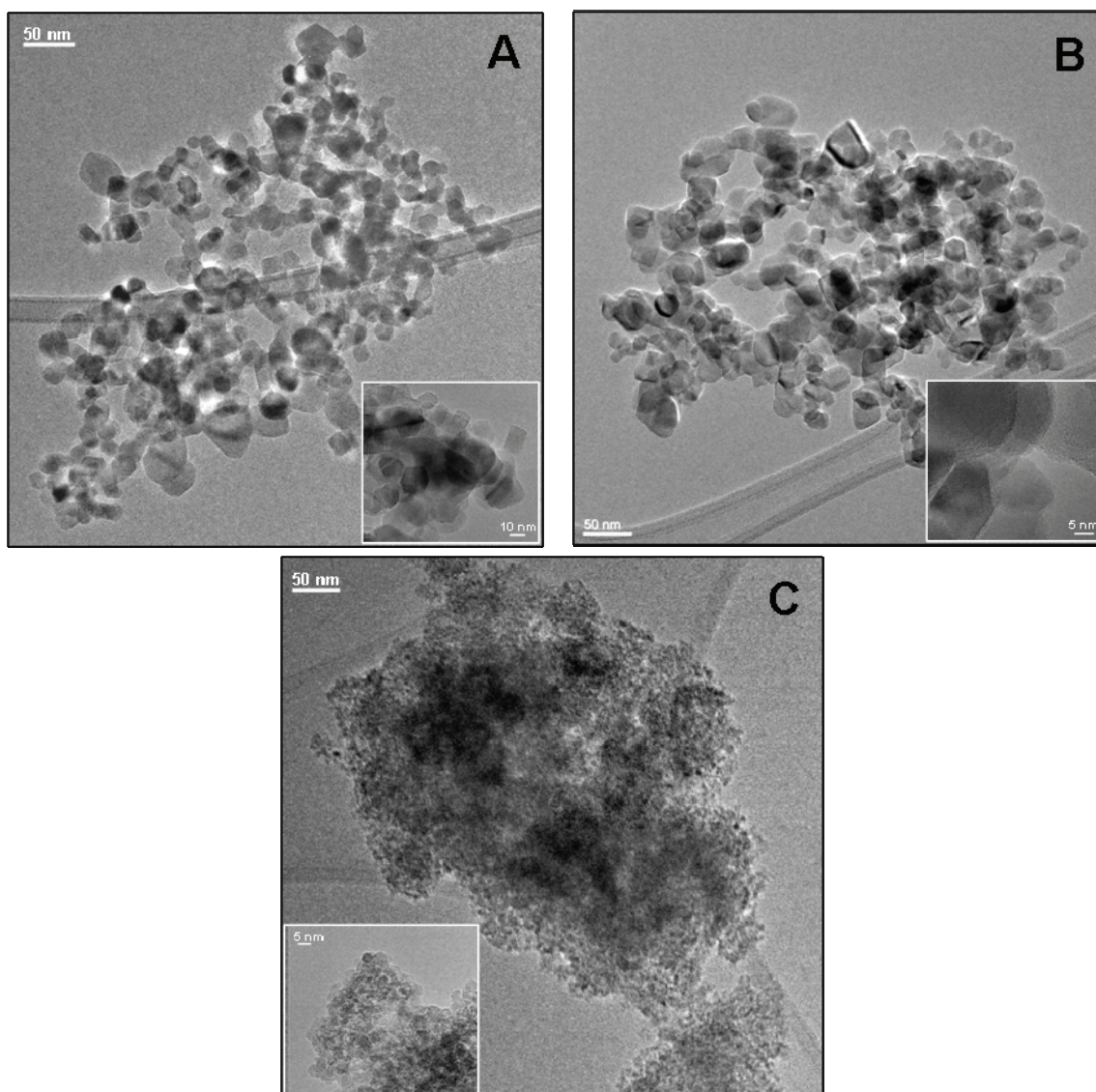


**Figure 3.1 Morphological characterisation of titanium dioxide particles.** TEM images of (A)  $\text{TiO}_2\text{-HSA}$ , 30kX; (B)  $\text{TiO}_2(\text{p25})$ , 40kX; (C) UV100, 40kX. In the insets the HRTEM images (200kX, 500kX and 300kX respectively) are shown.

The high surface area sample UV100 exhibits a very different structure: in this case nanometric primary particles are strongly bonded together to form nanometric and micrometric aggregates (Figure 3.1 C). No single monodisperse nanoparticles were detected in both TEM and DLS analysis. The broadening of the diffraction peaks corresponding to the anatase phase in the XRD pattern (Figure 3.2) reveals a highly disordered structure which is a direct consequence of the small size of primary particles.

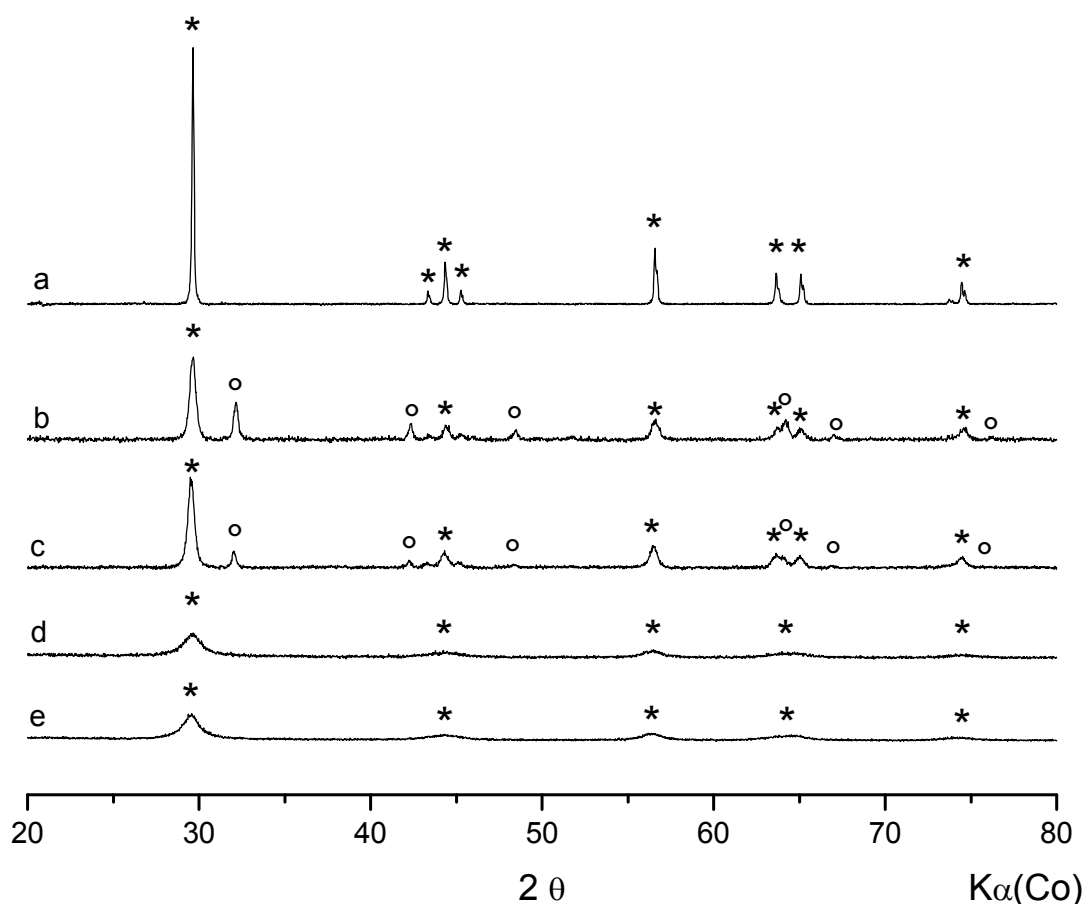


**Figure 3.2 Crystalline phases in titanium dioxide particles.** XRD patterns of (a)  $\text{TiO}_2\text{-F}$ ; (b)  $\text{TiO}_2(\text{p}25)$ ; (c)  $\text{TiO}_2\text{-HAS}$ ; (d) UV100; (e) JRC 12; in the  $20\text{-}80 = 2\theta$  range. The diffraction peaks of anatase (\*) and rutile (°) are indicated above the patterns.

The presence of amorphous  $\text{TiO}_2$  is confirmed by the low abundance of crystallographic planes in the HRTEM images (see insert of Figure 3.1 C). A similar structure is likely for the other high surface area sample JRC 12: the broad diffraction peaks in the XRD patterns are indicative of a disordered anatase structure while DLS analysis revealed the presence of nanometric and micrometric aggregates/agglomerates.

To determine whether the differences in primary particle size, surface area or crystalline phase of the  $\text{TiO}_2$  samples result in an altered cytotoxic or DNA damaging potential to Caco-2 cells, all five particle types were simultaneously tested in the LDH assay and the Fpg-modified comet assay. Cell membrane integrity was measured after incubation for 4 h with 20 and 80  $\mu\text{g}/\text{cm}^2$  particles respectively as the degree of LDH leakage in comparison to a positive (100 %) and negative control (0 %) (Figure 3.3). No cytotoxic effect was found after incubation with  $\text{TiO}_2\text{-F}$ . Moreover,

both particles of the highest surface area and the lowest primary particle size (JRC 12 and UV100) did also not induce any LDH leakage. In contrast, TiO<sub>2</sub>(p25) as well as TiO<sub>2</sub>-HSA, both rutile-containing particle types, induced significant cytotoxicity after incubation with 80 µg/cm<sup>2</sup>. Additionally, the incubation with 20 µg/cm<sup>2</sup> TiO<sub>2</sub>(p25) induced mild but statistically significant effects.

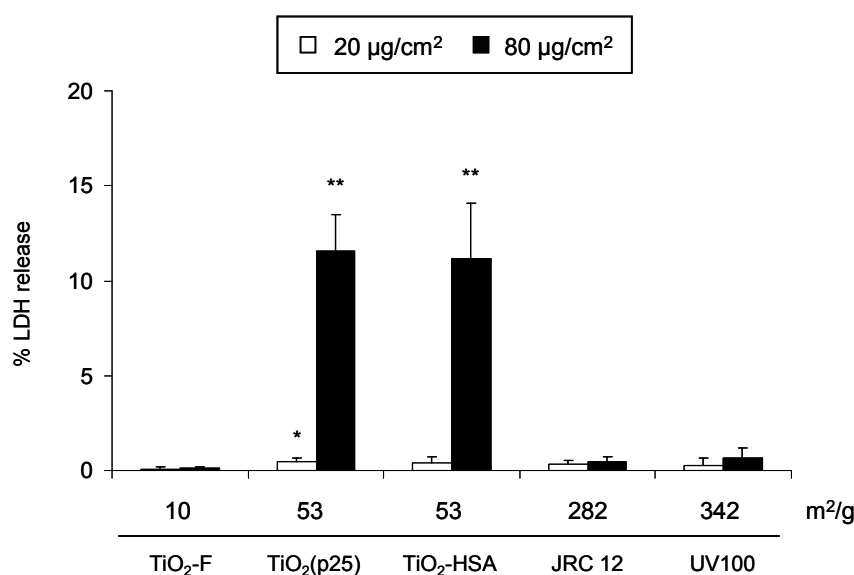


**Figure 3.3 Cytotoxic effects of different titanium dioxide particles on Caco-2 cells.** Cells were incubated with 20 and 80 µg/cm<sup>2</sup> of different TiO<sub>2</sub> particles for 4 hours. Specific surface area is indicated in m<sup>2</sup>/g (BET). Membrane integrity was measured as marker of cell toxicity using the LDH (lactate dehydrogenase) assay. Values are expressed as mean +/- standard deviation, n=3. \* p < 0.05 and \*\* p < 0.01 versus control

DNA strand breaks and alkali labile sites as well as specific oxidative DNA damage were analyzed by the Fpg-modified comet assay (Figure 3.4). In this assay, DNA damage becomes visible as a “tail” of DNA fragments behind the cell core after electrophoresis and is scored by determination of the percentage of DNA in tail. The Fpg-enzyme is used to specifically identify oxidative DNA damage by cleavage of oxidative DNA lesions, particularly 8-OHdG sites. As a positive control, the photosensitiser Ro-19 8022, known to induce oxidative DNA damage (Will *et al.*, 1999) was applied to verify the activity of the Fpg. Incubating the Caco-2 cells with 20 µg/cm<sup>2</sup> particles for 4 hours resulted in a damage for the different samples with tendencies similar to that observed for the cell integrity (Figure 3.3). Both particles of the highest surface area and the lowest primary particle size (JRC 12 and UV100) did not induce any significant DNA damage. Fine TiO<sub>2</sub> was able to slightly, but significantly induce DNA strand breaks but no oxidative lesions, whereas both

TiO<sub>2</sub>(p25) and TiO<sub>2</sub>-HSA led to significant oxidative DNA damage. Moreover, TiO<sub>2</sub>(p25) also caused significant DNA strand breaks. Compared to the positive control, the damage induced by all TiO<sub>2</sub> samples appeared very low.

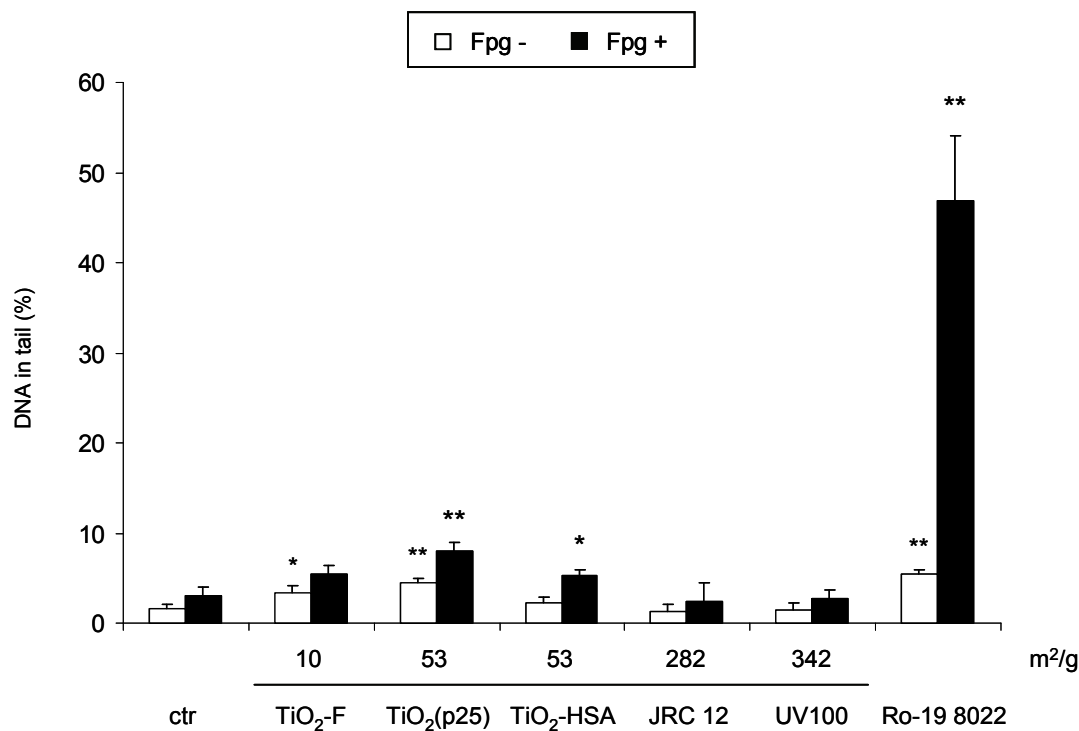


**Figure 3.4 Oxidative DNA damage in Caco-2 cells using Fpg-modified comet assay induced by different titanium dioxide particles.** DNA strand breakage and oxidative DNA damage were determined in Caco-2 cells using the Fpg-modified comet assay following 4 hours treatment with 20  $\mu\text{g}/\text{cm}^2$  of different TiO<sub>2</sub> particles. Specific surface area is indicated in m<sup>2</sup>/g (BET). ctr=control. Values are expressed as mean  $\pm$  standard deviation, n=3.

\* p < 0.05 and \*\* p < 0.01 versus control

### 3.4 Discussion

In our previous study (Gerloff *et al.*, 2009) we have investigated the possible hazards of food-related nanoparticles with respect to cytotoxicity and genome integrity in human intestinal cells. Additionally, in the previous study, we compared the potential cytotoxic and DNA-damaging effects of zinc oxide (ZnO) and titanium dioxide (TiO<sub>2</sub>) powders of different particle sizes and surface areas in more detail. To this extent, we included a specific TiO<sub>2</sub> sample with a very high SSA (TiO<sub>2</sub>-HSA), chosen especially to compare with our sample of interest, i.e. TiO<sub>2</sub>(p25). Since this specific sample was needed only for comparative analyses, we did not fully characterise it ourselves but instead relied on the SSA value provided by the supplier (> 300 m<sup>2</sup>/g).

After publication of our previous study, by chance we found new and contradictory information regarding the surface area of TiO<sub>2</sub>-HSA, which was confirmed upon our further inquiries by the supplier. To rule out any possible false conclusions about the absence of an influence of a high SSA on cytotoxicity and DNA damage, we therefore decided to characterise TiO<sub>2</sub>-HSA in detail. To our surprise, we found a SSA of only 52.8 ± 0.4 m<sup>2</sup>/g. Moreover, the sample was found to be composed of 90 % anatase and 10 % rutile (Table 3.1). Both characteristics thus turned out to be quite similar to those of TiO<sub>2</sub>(p25). Consequently, it is not surprising at all that we have shown similar levels of toxicity for both particles in our previous study (Gerloff *et al.*, 2009).

A thorough evaluation of the physicochemical properties and composition of the materials used is considered as a prerequisite for an appropriate interpretation of nanotoxicology studies (Warheit, 2008; Stone *et al.*, 2009). Our previous and current study provides a clear example of this, and that one should not rely solely on characterisation data provided by suppliers.

In order to verify our previous conclusions stating that there is no dependency on the specific surface area in terms of cytotoxicity and DNA damage in Caco-2 cells, we included two additional TiO<sub>2</sub> powders both having a very high SSA (around 300 m<sup>2</sup>/g) and a composition of 100 % anatase (Table 3.1) and repeated a set of experiments. The high SSA of the two new samples corresponded to a very low primary particle size (4 and 7 nm, respectively). However, the size distribution of particles was very similar to the other samples (Table 3.1), since primary particles appeared organised in nanometric and micrometric aggregates.

In accordance to our previous findings, only the rutile-containing TiO<sub>2</sub>-particles that also possess an intermediate specific surface area (i.e. TiO<sub>2</sub>(p25) and TiO<sub>2</sub>-HSA) induced cytotoxicity after 4 h treatment with the highest concentration. None of the other particles (TiO<sub>2</sub>-F, JRC 12 and UV100) showed cytotoxicity at the tested concentrations. A similar tendency was observed for the endpoints evaluated by the Fpg-modified comet assay, i.e. DNA strand breakage and oxidative DNA damage. In concordance with the cytotoxicity findings, no DNA damaging effect was found after incubation for 4 hours with JRC 12 and UV100. Surprisingly however, in our present study we detected a low, but nonetheless significant induction of DNA damage by TiO<sub>2</sub>-F. Likewise, TiO<sub>2</sub>-HSA was shown to induce a mild but significant oxidative DNA damage. For TiO<sub>2</sub>(p25) both oxidative damage and strand breakage were significantly induced. None of these current findings were observed in our previous study (Gerloff *et al.*, 2009). The most likely explanation for this phenomenon lies within the highly sensitive comet assay itself. The level of DNA damage induced by the TiO<sub>2</sub> samples was found to be relatively close to background in contrast to our positive control, and variations in comet assay measurements are well known to occur in relation to cell culture conditions (e.g. cell passage number) or gel to gel variations (Liao *et al.*, 2009). Obviously, our current observations also have to be interpreted in terms of statistical versus biological significance, in relation to the dose applied.

It has been shown that crystallinity influences the toxic potential of TiO<sub>2</sub>-particles with anatase usually showing a greater tendency to induce adverse effects such as cyto- or genotoxicity (reviewed in Johnston *et al.*, 2009). This may be related to the higher photocatalytic activity of the anatase phase in biological tests performed under UV irradiation, while no effect should be expected in tests performed in the dark. Some studies reported that free radical species may be generated at the surface of TiO<sub>2</sub> also in the dark or under ambient illumination (Sayes *et al.*, 2006; Fenoglio *et al.* 2009) but there are no evidences of a higher reactivity of anatase with respect to rutile or mixed phases in these conditions. Besides, rutile or TiO<sub>2</sub> powders composed by the two crystalline phases were reported to be more active than anatase in several studies. Gurr and co-workers compared the DNA-damaging effects of rutile- and anatase-TiO<sub>2</sub> particles of 200 nm primary particle size on human bronchial epithelial cells, BEAS-2B. They demonstrated a significant increase in the release of hydrogen peroxide in cells treated with rutile TiO<sub>2</sub>, but not with anatase

TiO<sub>2</sub> if incubated in the dark. Additionally, using the comet assay they found that a mixture of anatase and rutile particles showed a more pronounced DNA damaging effect in the absence of light, than pure anatase or pure rutile TiO<sub>2</sub> (Gurr *et al.*, 2005). More recently, Grassian and colleagues studied the possible influence of primary particle size on the inflammatory potential of nano-TiO<sub>2</sub> in mice. Two samples were considered, having different particle size and, consequently, different SSA. The sample having smaller primary particles consisted of pure anatase, while those having the larger particles contained both anatase and rutile crystalline phases. Stronger effects were expected after inhalation or instillation of the higher SSA TiO<sub>2</sub>. Interestingly however, exactly the opposite was observed: after a 4 hours low dose inhalation of the anatase/rutile-containing TiO<sub>2</sub> a significantly increased number of total cells in bronchoalveolar lavage was observed, whereas anatase-TiO<sub>2</sub> could cause this effect only at high exposure concentrations. A similar effect was found after instillation of mice with a medium and high concentration of anatase/rutile-containing TiO<sub>2</sub> but not by pure anatase-TiO<sub>2</sub>. Additionally, a significant release of LDH and IL-1 $\beta$  was induced by the highest, and an increased release of TNF- $\alpha$  by the medium and high concentration of anatase/rutile-TiO<sub>2</sub> (Grassian *et al.*, 2007). Toxic effects towards keratinocytes have been reported for both rutile and anatase (Braydic-Stolle *et al.* 2009), while micrometric rutile appeared more active in inducing IL-1 $\beta$  release in macrophage-like THP-1 cells than anatase TiO<sub>2</sub> (Morishige *et al.*, 2010).

In our study, a higher reactivity of the anatase-rutile containing TiO<sub>2</sub> in comparison to the anatase-TiO<sub>2</sub> was found while working under dark conditions. The significant induction of DNA strand breaks and oxidative DNA damage by TiO<sub>2</sub>(p25) and TiO<sub>2</sub>-HSA was surprising. However, it confirms our previous conclusion (Gerloff *et al.*, 2009) that the TiO<sub>2</sub>-reactivity in Caco-2 cells is independent of the specific surface area. In contrast, a hazardous potential of TiO<sub>2</sub> seems to be mainly associated with the crystalline phase of the particles. Moreover, JRC 12 and UV100 were characterised by a low degree of crystallinity, which may account for the observed absence of cytotoxicity and DNA damage induction of these specific samples despite their high SSA.

In conclusion, we were able to verify our previous observations on the absence of an association between the specific surface area of TiO<sub>2</sub> particles and their cytotoxic and DNA damaging effects in Caco-2 cells (Gerloff *et al.*, 2009).

Furthermore, our present study also highlights, once again, the need for a proper physico-chemical characterisation of the nanoparticles used in toxicity tests.

### **Acknowledgements**

The authors are grateful to Dr. Gianmario Martra, Dip. di Chimica IFM, University of Torino, for providing two of the TiO<sub>2</sub> samples and Dr. Giovanni Agostini, Dip. di Chimica IFM, University of Torino, for his kind help with TEM analysis.

This study was financially supported by a grant from the German Research Council (Deutsche Forschungsgemeinschaft - Graduate College GRK-1427)

### **Declaration**

The manuscript is submitted to a peer-review journal.

The cytotoxicity measurements and detection of DNA strand breakage and oxidative lesions were performed by Kirsten Gerloff. The impact on authoring this paper can be estimated in total with 90%.



### 3.5 References

- Angelis KJ, Dusinská M, Collins AR. Single cell gel electrophoresis: detection of DNA damage at different levels of sensitivity. *Electrophoresis* 1999;20(10):2133-8
- Braydich-Stolle L, Schaeublin NM, Murdock RC, Jiang J, Biswas P, Schlager JJ, Hussain SM. Crystal structure mediates mode of cell death in TiO<sub>2</sub> nanotoxicity. *J Nanopart Res* 2009; 11(6):1361-1374
- Chaudhry Q, Scotter M, Blackburn J, Ross B, Boxall A, Castle L, Aitken R, Watkins R. Applications and implications of nanotechnologies for the food sector. *Food Addit Contam Part A Chem Anal Control Expo Risk Assess* 2008;25(3):241-58
- Fenoglio I, Greco G, Livraghi S, Fubini B. Non-UV-induced radical reactions at the surface of TiO<sub>2</sub> nanoparticles that may trigger toxic responses. *Chem European J* 2009;15(18):4614-4621
- Gerloff K, Albrecht C, Boots AW, Förster I, Schins RPF. Cytotoxicity and oxidative DNA damage by nanoparticles in human intestinal Caco-2 cells. *Nanotoxicol* 2009;3(4):355-364
- Grassian VH, Adamcakova-Dodd A, Pettibone JM, O'shaughnessy PT, Thorne PS. Inflammatory response of mice to manufactured titanium dioxide nanoparticles: comparison of size effects through different exposure routes. *Nanotoxicol* 2007;1:211-226
- GSFA online:  
<http://www.codexalimentarius.net/gsaonline/additives/details.html?id=184> (March 2010)
- Gurr JR, Wang AS, Chen CH, Jan KY. Ultrafine titanium dioxide particles in the absence of photoactivation can induce oxidative damage to human bronchial epithelial cells. *Toxicology* 2005;213(1-2):66-73
- Johnston HJ, Hutchison GR, Christensen FM, Peters S, Hankin S, Stone V. Identification of the mechanisms that drive the toxicity of TiO<sub>2</sub> particulates: the contribution of physicochemical characteristics. *Part Fibre Toxicol* 2009;17:6:33
- Liao W, McNutt MA, Zhu WG. The comet assay: a sensitive method for detecting DNA damage in individual cells. *Methods* 2009;48(1):46-53
- Morishige T, Yoshioka Y, Tanabe A, Yao X, Tsunoda S, Tsutsumi Y, Mukai Y, Okada N, Nakagawa S. Titanium dioxide induces different levels of IL-1 $\beta$  production dependent on its particle characteristics through caspase-1 activation mediated by reactive oxygen species and cathepsin B. *Biochem Biophys Res Commun* 2010;5,392(2):160-5
- Oberdörster G, Oberdörster E, Oberdörster J. Nanotoxicology: an emerging discipline evolving from studies of ultrafine particles. *Environ Health Perspect* 2005;113(7):823-39
- Oberdörster G, Stone V, Donaldson K. Toxicology of nanoparticles: a historical perspective. *Nanotoxicol* 2007;1:2-25
- Sayes CM, Wahi R, Kurian PA, Liu Y, West JL, Ausman KD, Warheit DB, Colvin VL. Correlating nanoscale titania structure with toxicity: a cytotoxicity and inflammatory response study with human dermal fibroblasts and human lung epithelial cells. *Toxicol Sci* 2006;92(1):174-85
- Speit G, Schütz P, Bonzheim I, Trenz K, Hoffmann H. Sensitivity of the FPG protein towards alkylation damage in the comet assay. *Toxicol Lett* 2004;146(2):151-8

### *Chapter 3*

Stone V, Johnston H, Schins RPF. Development of in vitro systems for Nanotoxicology - methodological considerations. *Crit Rev Toxicol* 2009;39:613-626

Warheit DB. How meaningful are the results of nanotoxicity studies in the absence of adequate material characterization? *Toxicol Sci* 2008;101(2):183-185

Will O, Gocke E, Eckert I, Schulz I, Pflaum M, Mahler HC, Epe B. Oxidative DNA damage and mutations induced by a polar photosensitizer, Ro19-8022. *Mutat Res* 1999;435(1):89-1

## CHAPTER 4

---

### **Influence of simulated gastrointestinal digestion on particulate mineral oxide-induced cytotoxicity and interleukin-8 regulation in differentiated and undifferentiated Caco-2 cells**

Kirsten Gerloff<sup>1</sup>, Dora I.A. Pereira<sup>2</sup>, Nuno J.R. Faria<sup>2</sup>, Agnes W. Boots<sup>1</sup>, Irmgard Förster<sup>3</sup>, Catrin Albrecht<sup>1</sup>, Jonathan J. Powell<sup>2</sup>, Roel P.F. Schins<sup>1</sup>

<sup>1</sup> Particle Research and <sup>3</sup> Molecular Immunology, Institut für Umweltmedizinische Forschung (IUF) at the Heinrich Heine University Düsseldorf, Germany.

<sup>2</sup> Biomineral Research Section, MRC Human Nutrition Research, Elsie Widdowson Laboratory, Cambridge, United Kingdom.

#### **Abstract**

Novel aspects of engineered nanoparticles may offer many advantages for optimising food products and food packaging over bulk materials. However, their potential hazards in the gastrointestinal tract require further investigation. Here, we evaluated the uptake of two types of particles relevant to the food industry, namely silicon dioxide (SiO<sub>2</sub>) and zinc oxide (ZnO) in human intestinal Caco-2 cells. Furthermore, we have determined the ability of these particles to generate reactive oxygen species (ROS), induce cytotoxicity and affect interleukin-8 (IL-8) both mRNA expression and protein secretion by Caco-2 cells. The role of gastrointestinal digestion was assessed by pre-incubating the materials in simulated gastric and intestinal pH-conditions. We evaluated the solubility and agglomeration properties of both the native and the pre-incubated particles, and both particle suspensions were used for the incubation of undifferentiated and differentiated Caco-2 cells. Pre-treatment under gastrointestinal conditions reduced ROS formation but did not influence cytotoxicity (based on the WST-1 assay) or IL-8 expression for either material. In contrast, cell differentiation markedly determined the cytotoxic potential of the SiO<sub>2</sub> and ZnO particles, reflected as significantly lower TD<sub>50</sub> values in the undifferentiated Caco-2 cells. Interestingly,

the pro-inflammatory effects of SiO<sub>2</sub> on the cells appeared to be higher in the undifferentiated cells, whereas ZnO only induced IL-8 secretion in the differentiated Caco-2 cells. Further research is needed to determine the *in vivo* relevance of the state of differentiation of intestinal epithelial cells for the hazards of ingested particles.

## 4.1 Introduction

The production of functional foods is a fast growing field and the use of inorganic food additives herein as well as in conventional foods is widely accepted. Several microparticulate metal oxides have been used as food colouring agents (e.g. E171, titanium dioxide; E172, iron oxides and hydroxides), acidity regulators (e.g. E530, magnesium oxide) or anti-caking agents (e.g. 551, silicon dioxide) for many years (homepage food.gov.uk). However the use of similar mineral oxides, in smaller nanoparticulate sizes, is also receiving much interest as “nano-sizing” alters the properties of the materials and offers new applications for the food industry. Indeed, zinc oxide (ZnO) is already attracting attention in nanoparticulate form to develop novel food packaging products due to its antimicrobial and UV-absorbent properties (Chaudhry *et al.*, 2007). An average Western diet provides a large mineral oxide intake of microparticles, typically  $10^{12}$ - $10^{14}$  particles per day (Lomer *et al.*, 2001 and 2004), so nanoparticle intakes could similarly become significant if food applications grow.

The altered properties of nano-sized materials is generating some concern as it is well recognised that their decreased size in conjunction with a highly increased specific surface area considerably influences their reactivity and may, therefore, increase aspects of their toxicity and inflammatory potential (reviewed in Oberdörster *et al.* 2005, Borm *et al.* 2006). Certain nanoparticles (especially those based on reactive metals e.g. Fe, Zn) proffer a unique capability to generate reactive oxygen species (ROS) such as superoxide ( $O_2^{\cdot-}$ ), hydroxyl radicals ( $HO^{\cdot}$ ) or hydrogen peroxide ( $H_2O_2$ ) with the associated induction of cellular oxidative stress (Oberdörster *et al.*, 2005, 2007; Xia *et al.*, 2006; Unfried *et al.*, 2007). This ROS formation can be triggered both directly by the specific surface chemistry of particles (Brown *et al.*, 2001; Stoeger *et al.*, 2009), or indirectly, for example by acting on ROS-producing cellular components such as membrane bound NADPH oxidase enzymes and mitochondria (Unfried *et al.*, 2007). In turn, ROS formation and oxidative stress are implicated in the inflammatory effects of nanoparticles by activating pro-inflammatory signalling cascades. Particle-induced inflammation is typically characterised by the recruitment and activation of ROS producing phagocytic cells including monocytes and neutrophils, which exacerbates oxidative stress and tissue damage (Schins and Knaapen, 2007). One of the most prominent cytokines responsible for neutrophil-

recruitment is interleukin-8 (Kunkel *et al.*, 1991; Mitsuyama *et al.*, 1994; Kucharzik and Williams, 2002-2003). Toxic effects of particles are all described in the lung, whereas only few data are available concerning possible impacts of these compounds on the gastrointestinal tract. The uptake of nanoparticles can occur via different mechanisms (reviewed in Unfried *et al.*, 2007) and varies with the nature of the material and also the cell type. The gastrointestinal tract features Peyer's Patch lymphoid tissue, rich in 'M-cells' which are specialised and differentiated epithelial cells highly capable of taking up particles (reviewed in Powell *et al.*, 2010). Other mechanisms may also be relevant as, for example, previous work has shown that 40 % of 60 nm polystyrene particles that were taken up could be recovered in non-lymphoid tissue of Sprague-Dawley rats after 5 days of gavaging (Hillery *et al.*, 1994).

The human intestine undergoes constant regeneration, whereupon undifferentiated enterocytes generated from stem cells migrate from the crypts to the villus (small intestine) or the surface epithelium (colorectum) within 5 days. On their way, they begin to differentiate and become postmitotic before undergoing apoptosis followed by cell shedding (Ramachandran *et al.*, 2000; Sancho *et al.*, 2004). The Caco-2 cell line is derived from colonic epithelial adenocarcinoma cells. When grown under normal cell culture conditions, and after reaching confluence, they differentiate into small intestine enterocytes as the cells become polarised and express many of the characteristics of the enterocytes (e.g. tight junctions, microvilli, membrane transporters) (Chantret *et al.*, 1988; Chopra *et al.*, 2010). Therefore this cell line has been widely used as a model for *in vitro* studies looking at uptake of nutrients and pharmaceuticals. On the other hand, undifferentiated Caco-2 cells (i.e. prior to confluence in the exponential phase of growth) may resemble epithelial cells of the inflamed colon, as hyperproliferative epithelial cells have been shown to be present in ulcerative colitis (e.g. Huang *et al.*, 1997; Arai *et al.*, 1999), and they resemble human colonic cancer cells in a wide range of their gene expression patterns (Sääf *et al.*, 2007). Thus, Caco-2 cells are a useful *in vitro* model to investigate both the pathological and the normal intestine.

Recently, using undifferentiated Caco-2 cells, we have demonstrated the DNA damaging and cytotoxic potential of various types of nanoparticles that might in the future occur in food or food-related products (Gerloff *et al.*, 2009). Amongst other materials, we included amorphous silicon dioxide (SiO<sub>2</sub>) particles which, as noted

above, is a relevant additive in foods and pharmaceuticals (Schmidt and Riediker, 2008). Particulate zinc oxide (ZnO) was also investigated. In the undifferentiated Caco-2 cells, both SiO<sub>2</sub> and ZnO particles were found to induce cytotoxicity as well as oxidative DNA damage (Gerloff *et al.*, 2009). The aim of the present study was to study the cytotoxic and pro-inflammatory effects of SiO<sub>2</sub> and ZnO particles in (i) undifferentiated compared to differentiated Caco-2 cells, and (ii) to examine the impact of gastrointestinal digestion of the particles on cellular response.

## 4.2 Methods

**Materials.** Two types of particle were used in the present study: amorphous SiO<sub>2</sub> (fumed; Sigma, Germany) with a mean primary diameter of 14 nm and specific surface area (SSA) of 200 m<sup>2</sup>/g and ZnO (nanoactive: Nanoscale Materials Inc., US) with a reported crystallite size of ≤10 nm and SSA ≥ 70 m<sup>2</sup>/g. The ZnO sample was kindly provided by Dr. Duffin (University of Edinburgh) who reported a SSA of 48.3 m<sup>2</sup>/g by an independent analysis. Trypsin, Dulbecco's Ca<sup>2+</sup>/Mg<sup>2+</sup>-free phosphate buffered saline (PBS), ethylenediaminetetraacetic acid disodium salt dehydrate (EDTA), hydrogen peroxide (H<sub>2</sub>O<sub>2</sub>), nitric acid (HNO<sub>3</sub>), deferoxamine (DFO), sucrose, fetal calf serum (FCS) and bovine serum albumin (BSA) were all purchased from Sigma (Germany). Minimum essential Medium (MEM) with Earle's salts was obtained from Invitrogen (Germany). DC Protein Assay kit and iScript cDNA Synthesis Kit were purchased from BioRad Laboratories (USA). RNeasy Mini kit and QuantiFast SYBR Green PCR Kit were obtained from Qiagen (Germany). Calibration standard solutions (zinc or silicon solution 1000 ppm) were obtained from Fisher Scientific (UK), 1-hydroxy-3-carboxy-pyrrolidine (CPH) was purchased from Alexis Biochemicals (Germany). Cell Proliferation Reagent WST-1 and Lactate dehydrogenase (LDH) Cytotoxicity Detection Kit were purchased from Roche (Germany) and human IL-8 ELISA kit was obtained from Sanquin (The Netherlands). Spartan Syringe filters 0.2 µm were purchased from Whatman (Germany), ultrafiltration units (Vivaspin, 3kDa MWCO) were obtained from Sartorius Stedim Biotechnology (Germany). Interleukin-1β (IL-1β) was obtained from R&D Systems (USA). All other chemicals were from Merck (Germany). All assay kits were used according to the manufacturer's protocol.

**Solubility and aggregation or agglomeration of the particles.** The freshly-prepared particle suspensions were analysed using elemental mass analysis for both their soluble and insoluble (i.e. particulate) amounts. The latter was further subdivided into fractions < 200 nm, containing individual primary particles and/or smaller aggregates (generated by fusion of primary particles) and/or agglomerates (undispersed clusters of aggregates) (Donaldson *et al.*, 2005), and fractions above 200 nm, consisting of large aggregates and/or agglomerates. Therefore, (i) the initial particle suspension (1 mg/ml serum free cell culture media), (ii) the suspension after



10 min of sonication as detailed below, and (iii) the final dilution as used in the cell culture experiments (i.e.  $20 \mu\text{g}/\text{cm}^2$ ), were filtered through a  $0.2 \mu\text{m}$  syringe filter followed by ultrafiltration with a 3 kDa unit. This approach was applied to the original particles as well as to those that were subjected to the digestion simulation assay according to the procedure described below. Each fraction was analysed by inductively coupled plasma optical emission spectrometry (ICP-OES) for quantitative evaluation of elemental Si or Zn. The hydrodynamic size of the particle aggregates or agglomerates in suspension was also evaluated by means of laser diffraction using the Mastersizer 200 (Malvern Instruments). This measurement was performed only for the original (undigested) ZnO and SiO<sub>2</sub> suspensions immediately following sonication.

**Inductively coupled plasma optical emission spectrometry (ICP-OES).** The samples were digested in 5% HNO<sub>3</sub> and their elemental content was analysed using a JY2000-2 ICP Optical Emission Spectrometer (Jobin Yvon Horiba). External calibrations (0.1-20 ppm) were carried out for the determination of Si (251.611 nm) and Zn (202.551 nm).

**Culture and treatment of the cells.** The human colon adenocarcinoma cell line, Caco-2, was obtained from the Deutsche Sammlung von Mikroorganismen und Zellkulturen (DSMZ) GmbH, Germany, and grown in MEM with Earle's salts and Non Essential Amino Acids, supplemented with 20 % FCS, 1 % L-glutamine and 30 IU/ml penicillin–streptomycin. For the experiments, cells were trypsinised at near confluency and  $4 \times 10^4$  cells per  $\text{cm}^2$  were seeded into 6-well tissue culture plates (for particle cellular uptake, ELISA and qRT-PCR) or 96-well tissue culture plates (for the WST-1 assay) and grown overnight (undifferentiated cells) or for 10 days (differentiated cells). Prior to the experiments, the cells were incubated overnight (20 h) in serum free medium. All experiments were performed between cell passages 5 to 30. The SiO<sub>2</sub> and ZnO particles were suspended in serum-free culture medium. Two treatments were applied to the cells: (a) the suspension was sonicated (Sonorex TK52 water-bath; 60 Watt, 35 kHz) for 10 min and then directly added to the cells at the indicated concentrations or (b) particles were pre-incubated under simulated gastrointestinal pH-conditions (see below) and then applied to the cells.

**Particle uptake.** Cells were incubated in triplicate wells with 10, 20 or 40  $\mu\text{g}/\text{cm}^2$  particles at 37 °C for 1 h. The cell monolayer was washed three ( $\text{SiO}_2$ ) or four ( $\text{ZnO}$ ) times with DPBS containing 2 mmol EDTA to remove all loosely bound particles. To confirm removal of particles that were not taken up by the cells, the content of Si and Zn in the wash solutions was analysed by ICP-OES. For  $\text{SiO}_2$ , no remaining particles were detected in the wash solution from the second rinsing (data not shown). For  $\text{ZnO}$ , few particles (~6 %) could still be recovered within the 4<sup>th</sup> wash solution, but further washing repeats were not considered to prevent detachment of the cells. Then 2 ml  $\text{HNO}_3/\text{H}_2\text{O}_2$  was added to the culture disks to lyse the cells overnight. After homogenisation by shaking, the Si or Zn content was determined by ICP-OES. To ensure that particles were not taken up by cells due to permeation of membrane damaged cells the LDH content of the media supernatants, after treatment, was determined using a commercial diagnostic kit according to the manufacturer's instructions (LDH leakage in each treatment < 5 %; data not shown). Additionally, triplicate wells were lysed with 2 ml 0.5 M NaOH for 15 min and homogenised by shaking for determination of total cell protein by the DC (detergent compatible) protein assay. Particle uptake was expressed in  $\mu\text{g}$  of Si or Zn per mg of cell protein.

**Uptake inhibition.** Two independent methods were used to inhibit particle uptake into the differentiated Caco-2 cells. For the inhibition of active energy-dependent particle uptake by destruction of microtubules, cells were incubated at 4 °C with the particles for 1 h on an ice slab in the incubator and washed with ice cold buffer. To block clathrin AP2-mediated endocytosis, cells were treated in hypertonic serum free cell culture medium with 0.45 M sucrose for 1 h. After the incubation period the particle uptake was determined as described above.

**Simulation of gastrointestinal digestion.** The  $\text{SiO}_2$  and  $\text{ZnO}$  particles were used either directly after their suspension in serum-free medium and subsequent sonication (hereafter referred to as native particles, i.e.  $\text{SiO}_2$  and  $\text{ZnO}$ ) or, alternatively, were pre-treated under gastro- and intestinal pH-conditions (referred to hereafter as “digestion simulated” particles,  $\text{SiO}_2\text{-DS}$  and  $\text{ZnO-DS}$ ). The  $\text{SiO}_2$  and  $\text{ZnO}$  particles were incubated at a concentration of 1 mg/ml for 30 min in 25 ml gastric solution (NaCl (34 mM) / HCl solution, pH 2.7). Following this acidic incubation, a 3.75 ml sample was taken for characterisation of dispersability of the

particles (solubility and aggregation/agglomeration) as described above, and the remaining suspension was neutralised to pH 7.5-7.7 with 2.5 ml intestinal solution, (a carbonate/bicarbonate buffer (50 mM), at pH 9.5 including 1.68 g of NaCO<sub>3</sub>, 7.16 g NaHCO<sub>3</sub> and 4 g NaCl in 2 L H<sub>2</sub>O) and incubated for a further 30 min. After the second incubation period the suspensions were characterised for dispersability as before. The simulated digestion was conducted at 37 °C under constant shaking. Finally, the samples were appropriately diluted in serum-free media to obtain the final particle suspension that Caco-2 cells were incubated with.

**ROS measurements by Electron Paramagnetic Resonance (EPR).** For detection of reactive oxygen species (ROS) formation, induced by the particles, 20 and 80 µg/cm<sup>2</sup> of SiO<sub>2</sub>, ZnO, SiO<sub>2</sub>-DS and ZnO-DS particles were preincubated for 30 or 60 minutes with the spin probe CPH (0.5 mM CPH (1-hydroxy-3-carboxy-pyrrolidine) in 10 µM DFO) for specific superoxide detection and analysed using a MiniScope MS200 Spectrometer (Magnettech, Berlin, Germany) at room temperature. The following instrumental settings were used: Magnetic field: 3360 G; sweep width: 97 G; scan time: 60 sec; number of scans: 1; modulation amplitude: 2000 mG. Data shown are calculated from the average peak amplitude of CPH characteristic triplet spectrum and expressed in arbitrary units (AU).

**Cytotoxicity.** Cytotoxicity was determined by the tetrazolium salt WST-1 for measurement of the metabolic activity of the cells. The cleavage of the tetrazolium salt WST-1 to formazan dye via mitochondrial dehydrogenases in the cells was measured using a commercial WST-1 diagnostic kit (Roche, Germany) in 96-well culture plates. Cells were incubated with various particle concentrations at different time points as described above. After the incubation period with the particles, the cells were incubated for a further 2 h (undifferentiated Caco-2 cells) or 30 min (differentiated cells) with WST-1 and analysed as per the manufacturer's protocol.

**Enzyme-linked immunosorbent assay (ELISA).** To measure IL-8 release, cells were treated with 20 µg/cm<sup>2</sup> particles or the positive control IL-1β (10 ng/ml) for 4 and 24 h. After the treatment period, cell monolayers were washed two times with PBS to remove loosely membrane-bound particles and detached (dead) cells and cell debris. Cell culture medium was collected, centrifuged (14000 rpm, 5 min at 4 °C) and

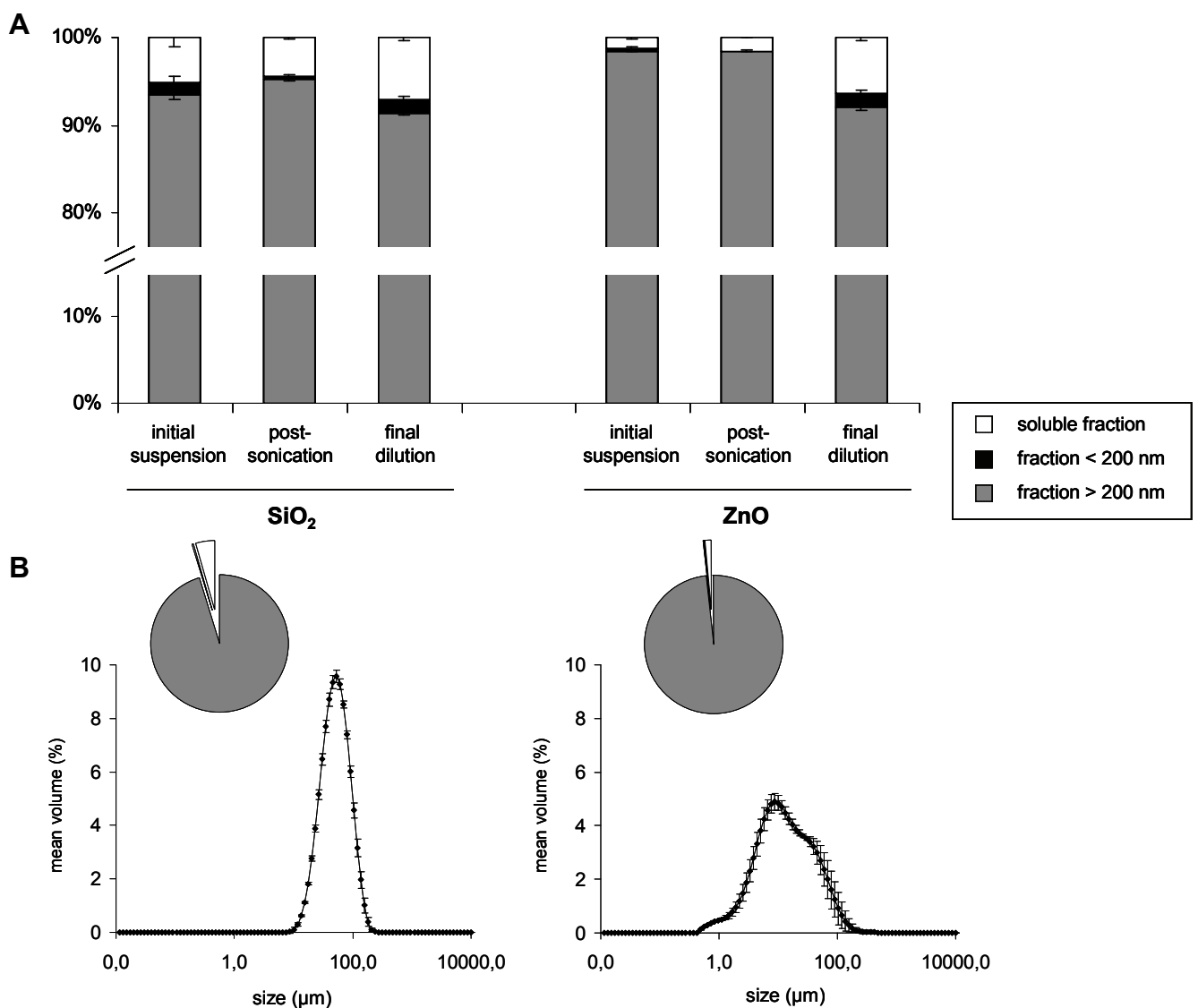
supernatants were frozen at -20 °C until analysis. IL-8 activity was determined by a commercial ELISA kit according to the recommendations of the supplier (Sanquin, The Netherlands).

**RNA isolation and quantitative Real-Time reverse-transcription polymerase chain reaction (qRT-PCR).** Cells were treated with 20 µg/cm<sup>2</sup> particles for 4 h as described above. Total RNA was isolated using a commercial RNeasy kit according to the manufacturer's instructions and 0.5 µg per sample was transcribed into complementary DNA using iScript cDNA Synthesis Kit according to the protocol. Total amount of mRNA was analysed in the Rotor-Gene Q (Qiagen) in 47 cycles, using 7.5 µl QuantiFast SYBR Green PCR Kit, 25 ng cDNA, and 0.5 µM primers. Human β-Actin was used as the internal reference gene. Primer sequences for IL-8 were 5'-ACT CCA AAC CTT TCC ACC C-3' (forward) and 5'-CCC TCT TCA AAA ACT TCT CCA C-3' (reverse), and for β-Actin 5'-CCC CAG GCA CCA GGG CGT GAT-3' (forward) and 5'-GGT CAT CTT CTC GCG GTT GGC CTT GGG GT -3' (reverse).

**Statistics.** All means were calculated from three independent cell experiments and each condition was investigated in triplicate wells in each experiment, with the error bars representing standard deviation (SD). Analysis of statistical significance was done by unpaired Student's t-test with \*p < 0.05, \*\*p < 0.01 and \*\*\*p < 0.001 as levels of significance. Cytotoxicity data were analysed using ANOVA with Dunnett post-hoc comparison with \*p < 0.01 and \*\*p < 0.001. TD<sub>50</sub> values were analysed by log-linear regression.

### 4.3 Results

Both particles used (i.e. amorphous SiO<sub>2</sub> and ZnO), were found to form large aggregates/agglomerates Figure 4.1 A shows the distribution of the amounts of Si or Zn quantified after fractionated filtration. For both types of material, the majority of particles were found to occur as large aggregates/agglomerates in each fraction (> 90 %). The amount of soluble material varied between 1 and 7 %. When considered on a mass basis, low to negligible amounts of Si or Zn were found to be in the < 200 nm fraction.



The presence of large aggregates/agglomerates in the post-sonicated fraction was confirmed by Mastersizer measurements as an independent method (Figure 4.1 B), revealing size ranges from 10-200  $\mu\text{m}$  for  $\text{SiO}_2$  and 1-100  $\mu\text{m}$  for ZnO, respectively.

The ability of differentiated Caco-2 cells to take up the particles within one hour incubation is shown in Figure 4.2.

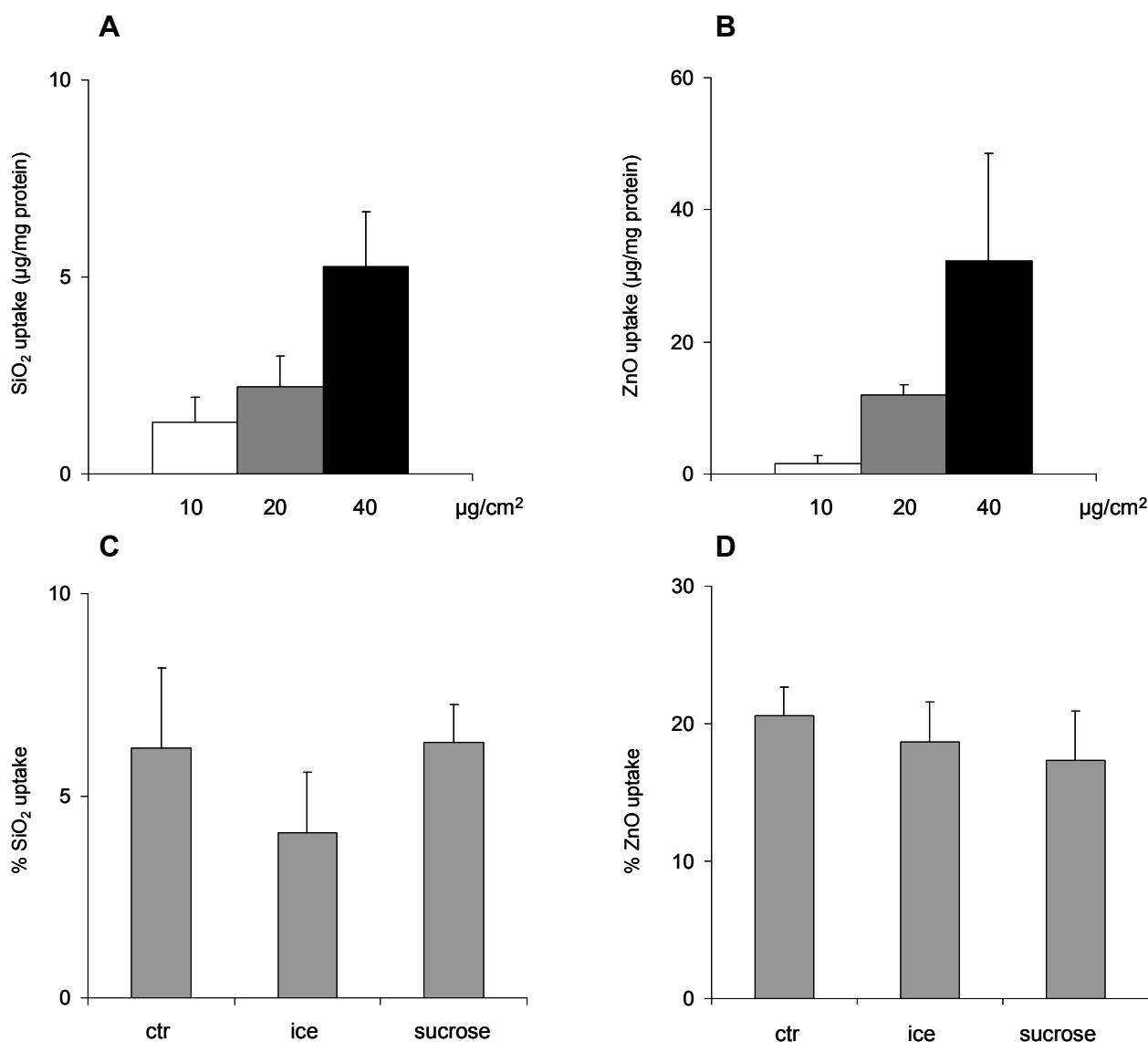


**Figure 4.2 Particle uptake and uptake inhibition in Caco-2 cells.** The uptake of  $\text{SiO}_2$  (A) or ZnO (B) was determined in differentiated Caco-2 cells after treatment for 1 h at 10, 20 and 40  $\mu\text{g}/\text{cm}^2$ . Inhibition of uptake of  $\text{SiO}_2$  (C) or ZnO (D) particles was determined after 20  $\mu\text{g}/\text{cm}^2$  treatment by incubation at 4°C (ice) or introducing hypertonic conditions (sucrose, B). Values are expressed as mean and standard deviation, n=3.

Both  $\text{SiO}_2$  and ZnO were taken up in a dose dependent manner, but ZnO uptake appeared to be much higher than uptake of  $\text{SiO}_2$  (Figure 4.2 A, B). The

particle uptake was not apparently due to increased cell permeability (i.e. membrane damage) as after one hour incubation none of the doses tested induced significant leakage of LDH or, therefore, disruption of the cell membrane (we used a cytotoxicity cut-off of 5 %). To investigate possible uptake mechanisms, the particle-treated cells were either incubated on ice to reduce microtubule-dependent endocytosis or incubated with 0.45 M sucrose, since hypertonic conditions are known to inhibit clathrin AP2-mediated endocytosis (Figure 4.2 C, 4.2 D). The incubation on ice caused a slight reduction of the SiO<sub>2</sub> uptake, although this did not reach statistical significance. There was no reduction on the uptake of the ZnO particles when the cells were incubated at 4 °C. Similarly, the hypertonic conditions did not influence the uptake of either type of particle. Overall, therefore, uptake of particles onto the cells was likely to dominate over uptake into the cells.

To simulate gastrointestinal digestion processes, which could potentially alter the toxicity of particles after their oral intake, we developed a gastrointestinal assay. The amount of Si and Zn was determined in samples collected during all steps of this assay, namely, the treatment in gastric buffer, the additional treatment in neutralised intestinal buffer and the final diluted particle suspension used for the cellular experiment (Figure 4.3).

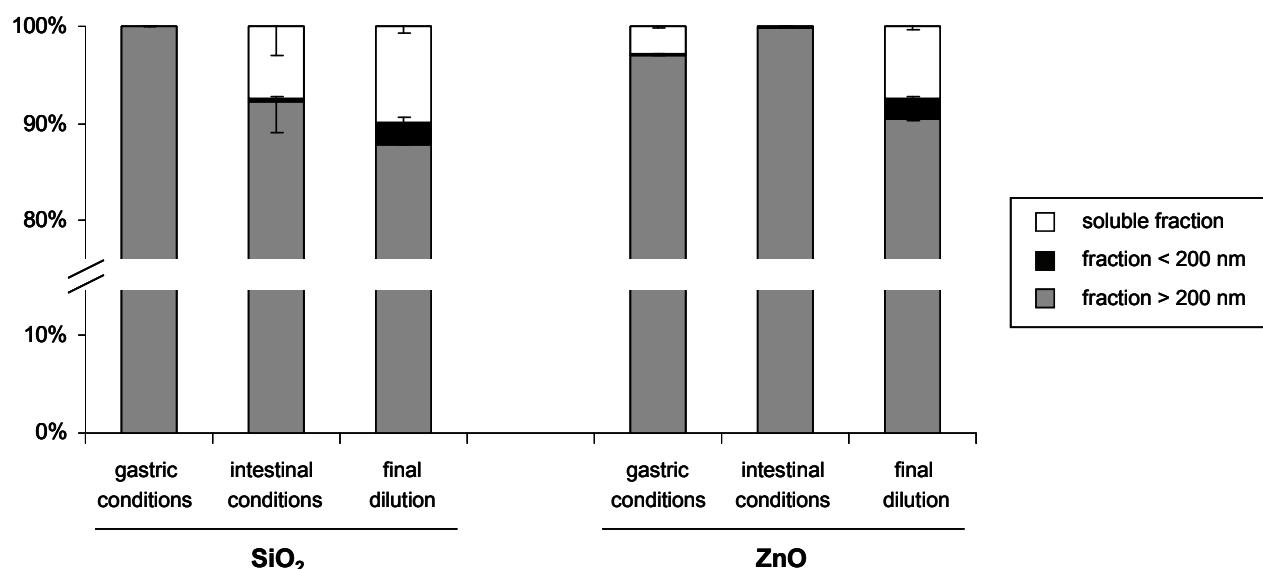


**Figure 4.3 Particle characterisation after gastrointestinal pH-treatment.** SiO<sub>2</sub> and ZnO particles were characterised for aggregate/agglomerate formation and solubility via fractionated filtration and quantitative element analysis after incubation in gastric pH-conditions followed by intestinal pH-conditions. Final dilution = particle concentration used for cell incubation (20 µg/cm<sup>2</sup>) in serum free cell culture medium. Values are expressed as mean and standard deviation, n=2-3.

The agglomeration patterns of the final dilutions of the digested particles ( $\text{SiO}_2\text{-DS}$  and  $\text{ZnO-DS}$ ; Figure 4.3) were similar to those of the un-digested ( $\text{SiO}_2$ , and  $\text{ZnO}$ ), as can be seen in Figure 4.1 A. Suggesting particles were mainly present as large aggregates or agglomerates.

To determine the effect of the digestion simulation treatment on the surface reactivity of both types of particles, their ability to generate superoxide anion radicals ( $\text{O}_2^{\cdot-}$ ) was determined by EPR spectroscopy using the spin probe CPH. Figure 4.4 A shows the time- and concentration dependent potential of both the native and the “digested”  $\text{SiO}_2$  and  $\text{ZnO}$  particles to generate  $\text{O}_2^{\cdot-}$ . Interestingly, the formation of superoxide was significantly reduced after gastrointestinal simulation treatment of both particles followed by 60 minutes pre-incubation with CPH. Representative spectra of CPH control, digested and undigested  $\text{SiO}_2$  ( $80 \mu\text{g}/\text{cm}^2$ , 60 min pre-incubation with CPH) are depicted in Figure 4.4 B.

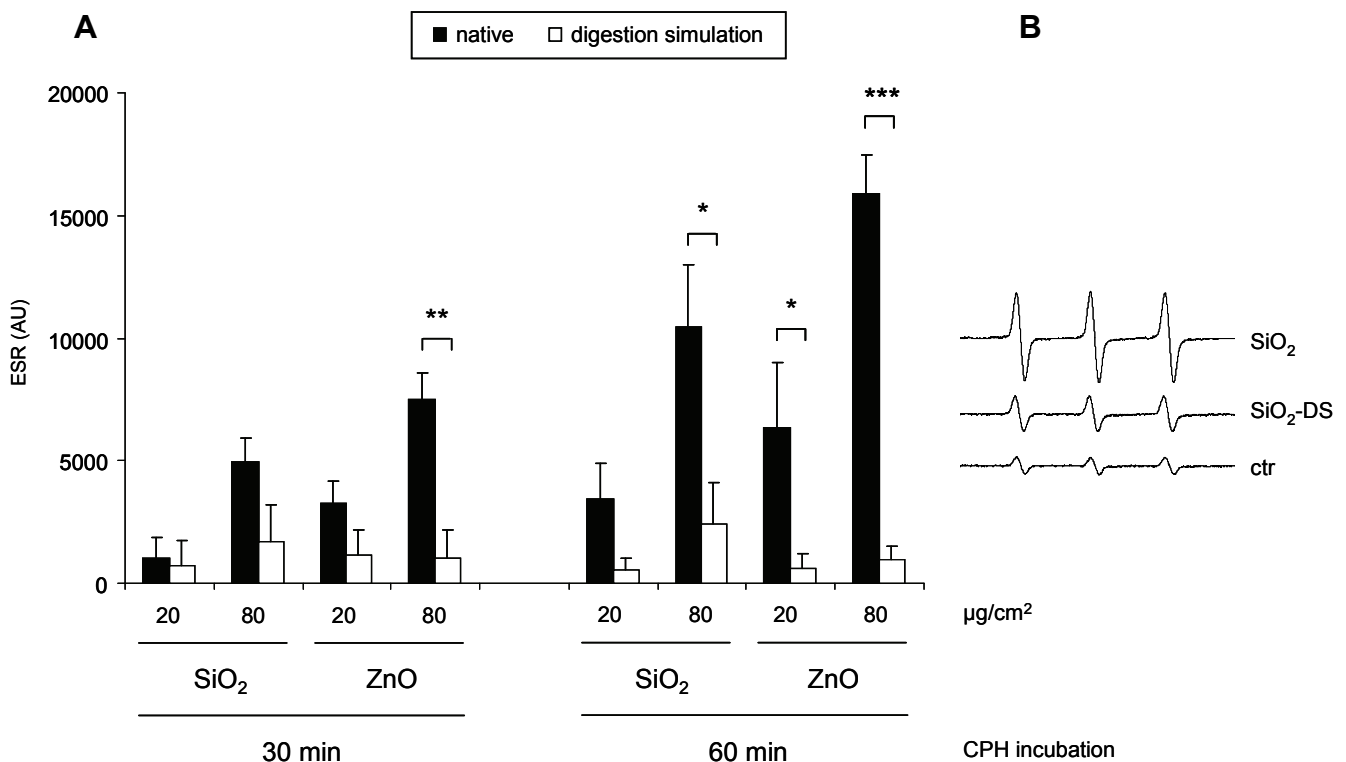


**Figure 4.4** **Acellular ROS formation by  $\text{SiO}_2$  and  $\text{ZnO}$  particles.** The formation of superoxide anion radicals was determined by EPR after 30 and 60 min pre-incubation with the spin probe CPH. 20 and  $80 \mu\text{g}/\text{cm}^2$  native or digestion buffers treated  $\text{SiO}_2$  or  $\text{ZnO}$  were used (A). Representative spectra of CPH-control,  $80 \mu\text{g}/\text{cm}^2$  native or digested  $\text{SiO}_2$  after 60 min pre-incubation (B). Values are expressed as mean and standard deviation,  $n=3$ .

\*  $p < 0.05$ , \*\*  $p < 0.01$  and \*\*\*  $p < 0.001$



To investigate whether the simulated gastric and intestinal digestion had an influence on cell viability, we performed the WST-1 assay after incubation of Caco-2 cells with the digested particle suspension for 4 (Figures 4.5, 4.6; A and C) or 24 h (Figures 4.5, 4.6; B and D). These experiments were performed both in undifferentiated and differentiated Caco-2 cells in order to address the possible impact of cell differentiation status on particle-induced toxicity. Results for the undifferentiated cells (i.e. at 70-80 % confluency) are shown in Panels A and B, while effects in the differentiated cells are depicted in Panels C and D of Figures 4.5 and 4.6.

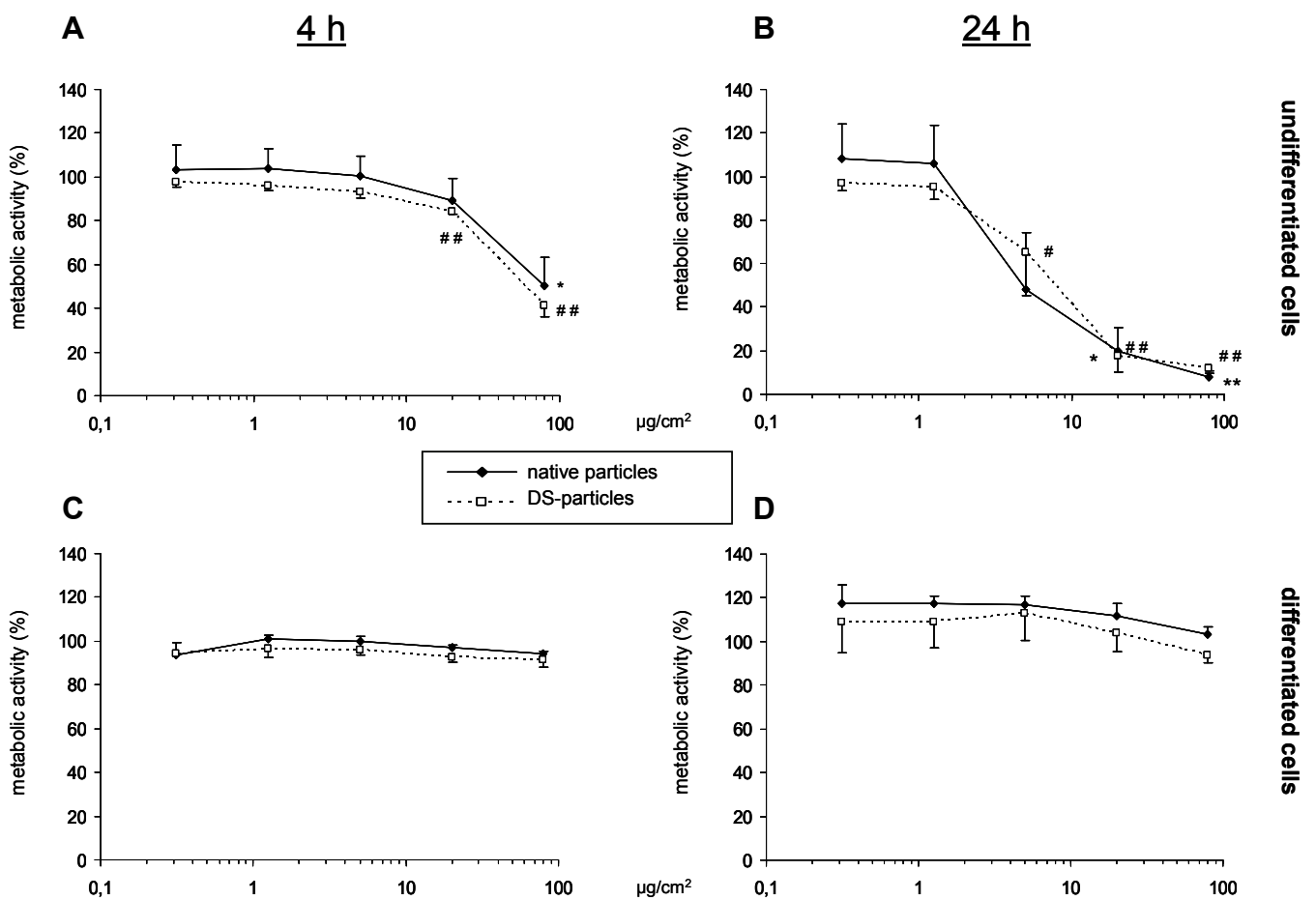


**Figure 4.5** Effects of SiO<sub>2</sub> on the viability of undifferentiated and differentiated Caco-2 cells. Undifferentiated (A, B) and differentiated (C, D) Caco-2 cells were incubated with 0.3125, 1.25, 5, 20 and 80 µg/cm<sup>2</sup> native or pH-treated SiO<sub>2</sub> particles for 4 (A, C) and 24 (B, D) hours. Metabolic competence of the cells was determined via conversion of WST-1 as a marker of cell viability. Values are expressed as mean and standard deviation, n=3.

\* p < 0.01 and \*\* p < 0.001 versus control for native particles

# p < 0.01 and ## p < 0.001 versus control for pH-treated particles

SiO<sub>2</sub> and SiO<sub>2</sub>-DS were both found to reduce cell viability only in undifferentiated cells. For the 24h incubation, significant effects in the undifferentiated Caco-2 cells were even observed at low concentrations (5 µg/cm<sup>2</sup>). In contrast, the differentiated cells were neither affected by SiO<sub>2</sub> nor by SiO<sub>2</sub>-DS (Figure 4.5). Contrary to these observations, ZnO was found to be cytotoxic to both undifferentiated and differentiated cells after 24 h incubation, although considerably more so in the former (Figure 4.6).

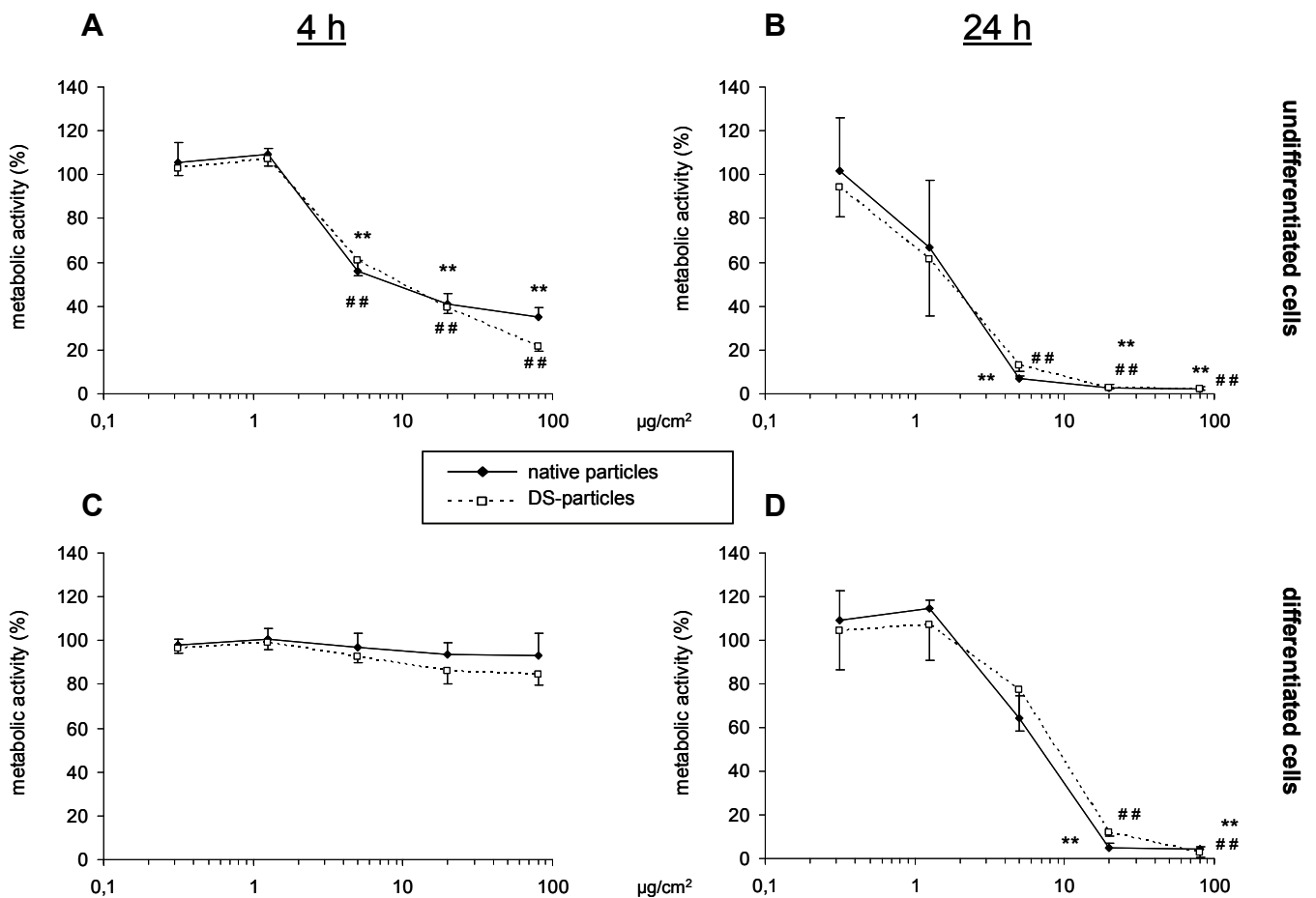


**Figure 4.6 Influences of ZnO on the viability of undifferentiated and differentiated Caco-2 cells.** Undifferentiated (A, B) and differentiated (C, D) Caco-2 cells were incubated with 0.3125, 1.25, 5, 20 and 80 µg/cm<sup>2</sup> native or pH-treated ZnO particles for 4 (A, C) and 24 h (B, D). Metabolic competence was measured as conversion of WST-1 as a marker of cell viability. Values are expressed as mean and standard deviation, n=3.

\* p < 0.01 and \*\* p < 0.001 versus control for native particles

# p < 0.01 and ## p < 0.001 versus control for pH-treated particles

The  $TD_{50}$  values (24 h) in the undifferentiated cells were  $1.74 \pm 1.74$  and  $1.77 \pm 1.6$  for ZnO and ZnO-DS, respectively. For the differentiated cells, significantly higher  $TD_{50}$  values were obtained being,  $8.99 \pm 1.05$  and  $9.82 \pm 2.98$  for ZnO and ZnO-DS, respectively. The  $TD_{50}$  values did not differ between the native and the digested ZnO, indicating that the toxicity of these particles may be mostly dependent on the cell differentiation status. At 4 h, only the undifferentiated cells showed significantly reduced viability after treatment with ZnO at doses of  $5 \mu\text{g}/\text{cm}^2$  or higher. For all conditions tested, the simulated digestion of the particles did not significantly influence their toxicity as evaluated by the WST-1 assay.

To address potential pro-inflammatory effects of the particles, the mRNA expression and protein secretion of IL-8 was determined in both undifferentiated and differentiated Caco-2 cells. Results are shown in Figure 4.7 for  $\text{SiO}_2$  and  $\text{SiO}_2$ -DS and in Figure 4.8 for ZnO and ZnO-DS, respectively.

In the undifferentiated Caco-2 cells,  $\text{SiO}_2$  strongly induced mRNA expression of IL-8, with levels that were similar to those provoked by the positive control IL-1 $\beta$ . The upregulation was even higher after treatment with the  $\text{SiO}_2$ -DS particles. In differentiated cells, however,  $\text{SiO}_2$  incubation could only induce a slight albeit non-significant upregulation of IL-8 mRNA expression. The effect was significantly lower than that induced in undifferentiated cells. IL-8 protein release from undifferentiated cells after 24 h was significantly increased after treatment with both the native and the digested  $\text{SiO}_2$  particles (Figure 4.7 B). In the differentiated cells, an increase of IL-8 upon treatment with  $\text{SiO}_2$  and  $\text{SiO}_2$ -DS was also observed, but this did not reach statistical significance.

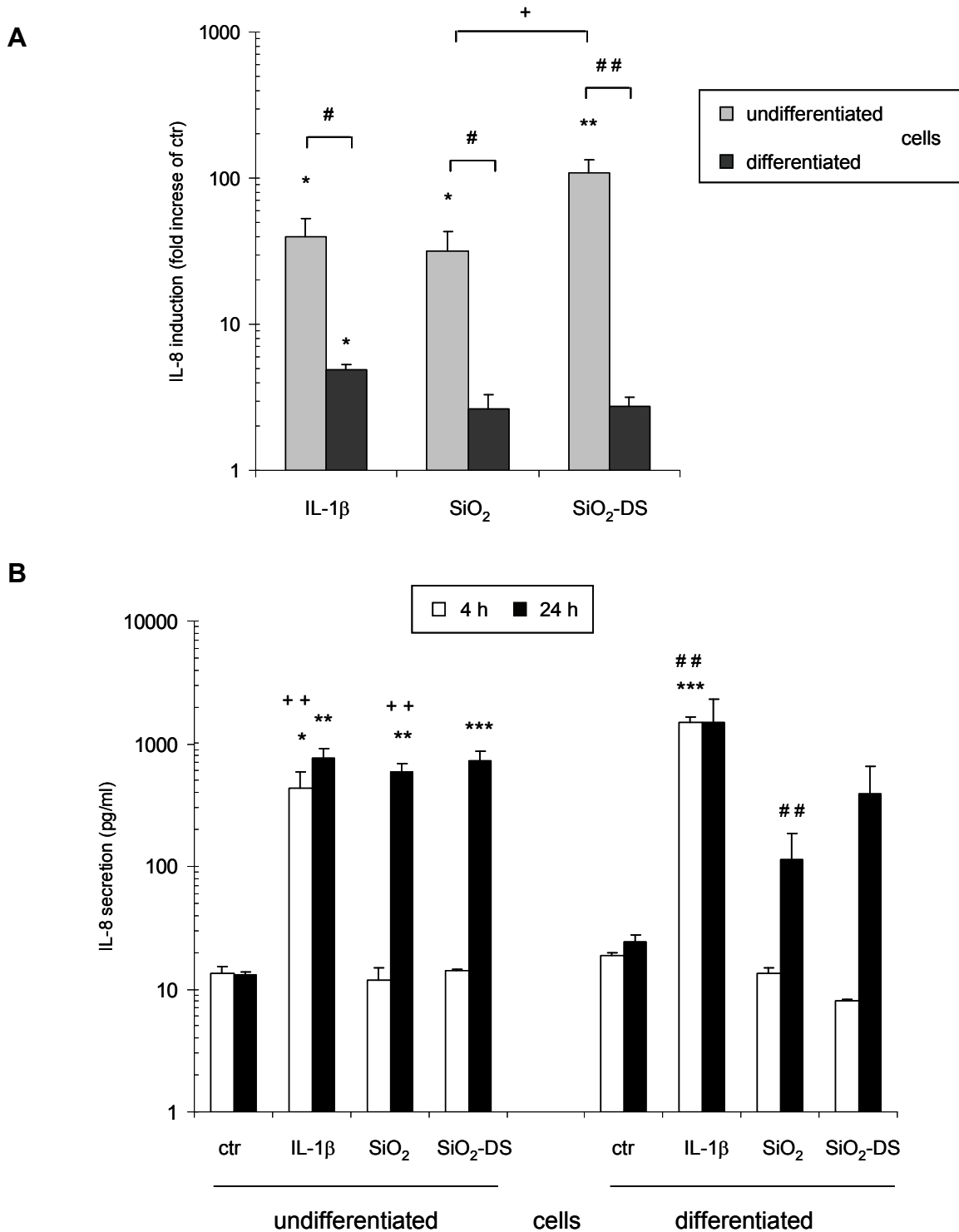


**Figure 4.7** Effects of SiO<sub>2</sub> particles on IL-8 mRNA expression and protein secretion after treatment of undifferentiated and differentiated Caco-2 cells. Induction of IL-8 mRNA after 4 h incubation with 20  $\mu\text{g}/\text{cm}^2$  native or pH-treated SiO<sub>2</sub> was determined in undifferentiated and differentiated Caco-2 cells via qRT-PCR (A). The secretion of IL-8 after 4 and 24 h incubation with 20  $\mu\text{g}/\text{cm}^2$  native or pH-treated SiO<sub>2</sub> was determined in undifferentiated and differentiated Caco-2 cells by ELISA (B). IL-1 $\beta$  was used as a positive control. Values are expressed as mean and standard deviation, n=3.

\* p < 0.05, \*\* p < 0.01 and \*\*\* p < 0.001 versus control

+ p < 0.05 and ++ p < 0.01 native versus pH-treated particles

# p < 0.05 and ## p < 0.01 differentiated versus undifferentiated cells

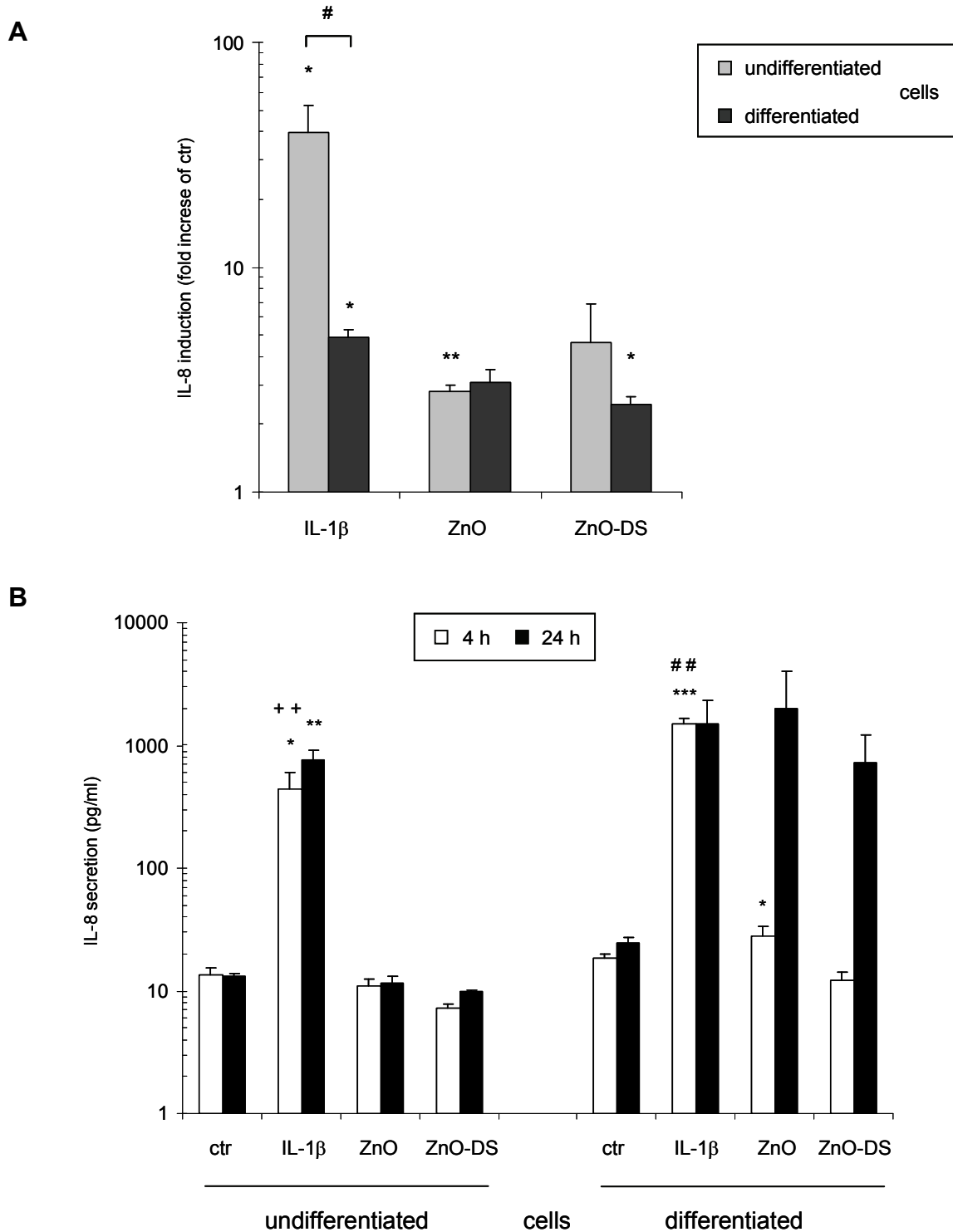


**Figure 4.8** Effects of ZnO particles on IL-8 mRNA expression and protein secretion after treatment of undifferentiated and differentiated Caco-2 cells. Induction of IL-8 mRNA after 4 h incubation with 20  $\mu\text{g}/\text{cm}^2$  native or pH-treated ZnO was determined in undifferentiated and differentiated Caco-2 cells via qRT-PCR (A). The total secretion of IL-8 after 4 and 24 h incubation with 20  $\mu\text{g}/\text{cm}^2$  native or pH-treated ZnO was determined in undifferentiated and differentiated Caco-2 cells by ELISA (B). IL-1 $\beta$  was used as a positive control. Values are expressed as mean and standard deviation, n=3.

\*  $p < 0.05$ , \*\*  $p < 0.01$  and \*\*\*  $p < 0.001$  versus control  
 ++  $p < 0.01$  native versus pH-treated particles  
 #  $p < 0.05$  differentiated versus undifferentiated cells

Incubation with ZnO resulted only in a slight upregulation of IL-8 mRNA levels in both undifferentiated and differentiated cells (Figure 4.8 A).

Significant increases in IL-8 mRNA expression were only found after treatment with the native ZnO in undifferentiated cells, and after treatment with the digested material (ZnO-DS) in differentiated cells. In contrast to the effects induced by SiO<sub>2</sub>, undifferentiated cells did not respond to stimulation by ZnO in terms of IL-8 secretion (Figure 4.8 B). Surprisingly however, non-significant but notable IL-8 levels were observed in differentiated cells after 24 h incubation upon treatment with ZnO and ZnO-DS.

## 4.4 Discussion

In the present study, we characterised particle suspension of silicon dioxide (SiO<sub>2</sub>) and zinc oxide (ZnO) particles and investigated their uptake, cytotoxic potential and pro-inflammatory properties on the intestinal Caco-2 cell line. Additionally, to mimic the behaviour of the particles after oral uptake, we have developed an assay to simulate the gastric and intestinal pH-conditions.

Particles were characterised by two independent methods, namely fractionated filtration combined with elemental analysis and laser diffraction. The first method revealed that both particle types were mostly present as large aggregates and/or agglomerates when suspended in serum free cell culture media. Less than 8 % of the material was soluble and only a negligible amount was present as small particles, aggregates and/or agglomerates (< 200 nm). Concordantly, size distribution measurement by using the Mastersizer revealed that both SiO<sub>2</sub> and ZnO particles are highly aggregated and/or agglomerated.

The uptake of both materials by the differentiated cells was clearly dependent on the treatment dose. Interestingly, ZnO particles were taken up more efficiently than SiO<sub>2</sub>. Possible uptake mechanisms include adsorptive (Apodaca, 2001) and clathrin-mediated endocytosis (San Martin *et al.*, 2008; Kalgaonkar *et al.*, 2009). Involvement of endocytotic processes was determined by microtubules depolymerising and lowering of the energy availability, thus slowing down the whole process, applying a low incubation temperature of 4°C (Moriya *et al.*, 2005). The latter was more specifically inhibited by introducing hypertonic conditions via addition of sucrose, since it is known that such circumstances prevent the interaction of clathrin with AP2 (San Martin *et al.*, 2008; Kalgaonkar *et al.*, 2009). Interfering with either of the uptake mechanisms did not significantly reduce particle internalisation of both SiO<sub>2</sub> and ZnO, favouring adsorptive mechanisms as the chief form of uptake. In the gut, natural dispersants (like acids, mucin etc) may help to keep particles disaggregated but apical cell adsorption will at least first occur, making these data physiologically relevant.

The intestinal uptake of soluble Zn<sup>2+</sup> ions can also be mediated by various other mechanisms, including transport via the human ZnT-like transporter 1 (hZTL1), which is also present on the apical membrane of Caco-2 cells (reviewed in Ford, 2004). However, involvement of this uptake pathway could only explain part of the

observed Zn uptake, since the solubility of the material used in our study is below 8 % whereas about 20 % of the ZnO was found to be associated with the cells. Moreover, this uptake mechanism could not explain our SiO<sub>2</sub> data since the uptake of the already low soluble SiO<sub>2</sub> fraction was found to be negligible (data not shown). This leads to the conclusion that presumably other mechanisms play an important role in the uptake of both materials, including phagocytosis, macropinocytosis or diffusion (Unfried *et al.*, 2007).

To evaluate the cytotoxic and pro-inflammatory potential of our materials upon passage through the gastrointestinal tract, we developed an *in vitro* gastrointestinal assay based upon physiological pH conditions. The gastric pH ranges from 1.5-2.0 in the fasting state and might rise up to pH 7.0 after ingestion of a meal, and sodium and chloride are the most prominent elements within gastric acid (Powell *et al.*, 1994; Lindahl *et al.*, 1997; Hörter and Dressman, 2001). Therefore, we used a sodium chloride-based HCl buffer with pH 2.7, thus simulating the pH conditions that arise upon ingestion of a light meal. To mimic the subsequent pancreatic bicarbonate output, the suspension was neutralised with a carbonate/bicarbonate buffer to a pH of 7.5, which is representative of the intestinal conditions (Evans *et al.*, 1988; Hörter and Dressman, 2001). To compare dispersibility of the digested particles to the undigested particles, fractionated filtration was performed after each digestion step as well as after preparing the final particle suspension. SiO<sub>2</sub> was only present as large aggregates and/or agglomerates at acidic pH, whereas at neutral pH around 8 % of the material was soluble. In the case of ZnO there was a small fraction of soluble material at acidic pH but again most of the material was present as large aggregates/agglomerates. In the final particle suspensions incubated with the cells, both particles showed similar dispersion behaviour (i.e. similar percentages of soluble, ca. 10 %; small aggregates/agglomerates, ca. 2 %; and large aggregates/agglomerates, ca. 90 %) and their dispersion was independent of the pre-digestion treatment.

The influence of the simulated digestion treatment on the behaviour of the particles in the cellular assay was investigated to determine if there were any alterations on the surface of the particle aggregates/agglomerates that could influence induction of ROS production, cytotoxicity or pro-inflammatory properties.

Firstly, we have observed that the superoxide-generating potential of both compounds was significantly reduced for the digested particles in comparison to the



native materials. This could be explained by surface modifications during acidic treatment, such as surface chemistry alterations and removal of possible contaminants including trace iron that might support  $O_2^{\cdot -}$  formation by these materials (Fubini, 1998). Comparable effects have been reported for cobalt chrome particles, for which cyto- and genotoxic properties were found to be largely decreased upon macrophage phagocytosis, presumably due to surface modifications induced by the acidic conditions in the lysosomes of these cells (Papageorgiou *et al.*, 2008). In contrast, for quartz particles (i.e. crystalline silica) an increased reactivity after chemical etching has been shown and this has been discussed as a relevant mechanism to explain its strong pulmonary toxicity after inhalation (reviewed in Fubini, 1998).

Secondly, in our study, the digestion treatment of the particles did not influence their cytotoxicity on Caco-2 cells as this was found to be mostly dependent on the cell's differentiation status.  $SiO_2$  only reduced cell viability in undifferentiated cells whereas ZnO appeared toxic to both undifferentiated and differentiated Caco-2 cells after 24 h treatment. For differentiated cells, a higher dose of particles seems to be required to achieve comparable toxic effects on the cells. It should be noted however that upon confluency and subsequent differentiation, a 2 to 3-fold higher amount of cells was counted than in undifferentiated (semi-confluent) Caco-2 cell cultures. Therefore more cells face the same amount of particles and, as such, this influences the toxic effect measured by the WST-1 assay. Our observations stand in line with the work of Anelli and colleagues, showing a 2-fold difference in cytotoxicity to undifferentiated versus differentiated Caco-2 cells after treatment with lymphokine-activated natural killer cells (Anelli *et al.*, 1993). This suggests that the state of differentiation might influence the response to toxic agents.

Differentiation of intestinal epithelial cells is a constant process in the healthy human gut (Huang *et al.*, 1997; Ramachandran *et al.*, 2000; Sancho *et al.*, 2004), whereas ulcerative colitis and other inflammatory states of the intestine are, amongst others, marked by hyperproliferative epithelial cells, resulting in an expansion of an undifferentiated cell population (Huang *et al.*, 1997). This process plays an important role in the immune response, as it is well known that differentiation of intestinal epithelial cells markedly reduces their pro-inflammatory response upon stimulation with  $IL-1\beta$  at early time points (2-12 hours) (Huang *et al.*, 1997; Böcker *et al.*, 2000). In our study we found similar effects after 4 h incubation with  $IL-1\beta$ , since the

induction of IL-8 mRNA expression was dramatically lower in differentiated Caco-2 cells in comparison to undifferentiated cells. However, these differential effects on the mRNA levels were not reflected on the secreted IL-8 protein level, as 24 h incubation with IL-1 $\beta$  led to a comparable IL-8 release for both differentiation states. Possibly, the gene expression of IL-8 in differentiated Caco-2 cells might be induced with slower kinetics than in undifferentiated cells, but nevertheless lead to comparable accumulated levels of secreted protein. Interestingly, we also observed a high pro-inflammatory potential of SiO<sub>2</sub> as the SiO<sub>2</sub>-induced up regulation of IL-8 mRNA in undifferentiated cells at 4 h was comparable to (or for SiO<sub>2</sub>-DS even higher than) the effects induced by IL-1 $\beta$ . After 24 hours, the IL-8 secretion induced by the native and digestion buffer treated particles was similar again. Although SiO<sub>2</sub> was capable of inducing IL-8 secretion from differentiated Caco-2 cells as well, this effect was not significant and lower than that found in undifferentiated cells. This low effect might be due to the increased amount of cells after confluency and differentiation, as discussed above. Surprisingly, ZnO only induced IL-8 secretion in differentiated cells, but mRNA up regulation was found to be low in both undifferentiated and differentiated cells.

The gastrointestinal assay applied in our current work allows a more reliable judgement regarding the possible hazards of particles that might be of relevance *in vivo*. Interestingly, the effects of conventionally prepared particles for cell culture experiments seemed to be comparable to more physiologically treated, (i.e. digested) particles for our endpoints. However, our current assay is limited to investigating pH effects of the gastrointestinal tract, and does not take into account the presence of proteins or various chemical or biological compounds including other endogenous or exogenous particles in the chyme, and bacterial flora that all might interact with our specifically tested materials. For example, it has been shown that bacterial components such as LPS can bind to nanoparticles which then, by serving as a carrier for these toxins, will lead to highly increased inflammatory responses, characterised by the release of IL-1 $\beta$ , IL-6 or TNF- $\alpha$  (Ashwood *et al.*, 2007). Interestingly, the inflammation induced by the LPS-particle complex is more pronounced than that caused by incubation with either the particles or LPS alone. So, certain components might be able to even elevate the cytotoxic or pro-inflammatory potential of particles, and this needs to be considered in the hazard assessment of ingested particles.

In this study we have shown that simulated gastrointestinal digestion of SiO<sub>2</sub> and ZnO particles did not markedly alter the cytotoxic or pro-inflammatory potential of the materials. The reduction in the ROS generating properties, widely accepted to be relevant in nanoparticle toxicity, did not influence the endpoints measured in our study. This also suggests that the cytotoxic and pro-inflammatory potential of specific particles in intestinal epithelial cells is not driven by intrinsic ROS formation. However, it remains to be investigated whether the genotoxic potential (Gerloff *et al.*, 2009) of the modified particles is altered. In contrast, cell differentiation appeared to play a far more important role in the toxic potential of SiO<sub>2</sub> and ZnO particles: undifferentiated Caco-2 cells were more sensitive towards particle toxicity and might therefore serve as an initial screening tool. The pro-inflammatory effects of particles on the cells appeared to be less dependent on cell differentiation than their cytotoxicity. Further research is needed to determine the relevance of the state of differentiation of intestinal epithelial cells for ingested particles *in vivo*, all the more since in patients suffering from inflammatory bowel disease this differentiation process is known to be imbalanced.

## **Acknowledgements**

This study was financially supported by a grant from the German Research Council (Deutsche Forschungsgemeinschaft - Graduate College GRK-1427). The authors thank Dr. Klaus Unfried (IUF, Düsseldorf) for providing primers for human IL-8 and  $\beta$ -Actin. K.G. thanks the MRC Human Nutrition Research Elsie Widdowson laboratory in Cambridge (UK) for hosting her during 3 months to conduct part of the research presented here.

## **Declaration**

The manuscript is currently in preparation.

The experimental work presented was performed by Kirsten Gerloff. The impact on authoring this paper can be estimated in total with 80%.

## 4.5 References

- Arai N, Mitomi H, Ohtani Y, Igarashi M, Kakita A, Okayasu I. Enhanced epithelial cell turnover associated with p53 accumulation and high p21WAF1/CIP1 expression in ulcerative colitis. *Mod Pathol* 1999;12(6):604-11
- Ashwood P, Thompson RP, Powell JJ. Fine particles that adsorb lipopolysaccharide via bridging calcium cations may mimic bacterial pathogenicity towards cells. *Exp Biol Med (Maywood)* 2007;232(1):107-17
- Anelli R, Placido R, Sambuy Y, Bach S, Di Massimo A, Colizzi V. Cytotoxic activity of human lymphocytes against differentiated intestinal tumour cell lines. *Immunology* 1993;78(1):166-9
- Apodaca G. Endocytic traffic in polarized epithelial cells: role of the actin and microtubule cytoskeleton. *Traffic* 2001;2(3):149-59
- Borm PJA, Robbins D, Haubold S, Kuhlbusch T, Fissan H, Donaldson K, Schins RPF, Stone V, Kreyling W, Lademann J *et al.* The potential risks of nanomaterials: a review carried out for ECETOC. *Part Fibre Toxicol* 2006, 3:11
- Böcker U, Schottelius A, Watson JM, Holt L, Licato LL, Brenner DA, Sartor RB, Jobin C. Cellular differentiation causes a selective down-regulation of interleukin (IL)-1beta-mediated NF-kappaB activation and IL-8 gene expression in intestinal epithelial cells. *J Biol Chem* 2000;275(16):12207-13
- Brown DM, Wilson MR, MacNee W, Stone V, Donaldson K. Size-dependent proinflammatory effects of ultrafine polystyrene particles: a role for surface area and oxidative stress in the enhanced activity of ultrafines. *Toxicol Appl Pharmacol* 2001;175:191-9
- Chantret I, Barbat A, Dussaulx E, Brattain MG, Zweibaum A. Epithelial polarity, villin expression, and enterocytic differentiation of cultured human colon carcinoma cells: a survey of twenty cell lines. *Cancer Res* 1988;48(7):1936-42
- Chaudhry Q, Scotter M, Blackburn J, Ross B, Boxall A, Castle L, Aitken R, Watkins R. Applications and implications of nanotechnologies for the food sector. *Food Addit Contam Part A Chem Anal Control Expo Risk Assess* 2008;25(3):241-58
- Chopra DP, Dombkowski AA, Stemmer PM, Parker GC. Intestinal epithelial cells in vitro. *Stem Cells Dev* 2010;19(1):131-42
- Evans DF, Pye G, Bramley R, Clark AG, Dyson TJ, Hardcastle JD. Measurement of gastrointestinal pH profiles in normal ambulant human subjects. *Gut* 1988;29(8):1035-41
- Ford D. Intestinal and placental zinc transport pathways. *Proc Nutr Soc* 2004;63(1):21-9
- Fubini B. Surface chemistry and quartz hazard. *Ann Occup Hyg* 1998;42(8):521-30
- Gerloff K, Albrecht C, Boots AW, Förster I, Schins RPF. Cytotoxicity and oxidative DNA damage by nanoparticles in human intestinal Caco-2 cells. *Nanotoxicol* 2009; 3(4):355-364
- Hillery AM, Jani PU, Florence AT. Comparative, quantitative study of lymphoid and non-lymphoid uptake of 60 nm polystyrene particles. *J Drug Target* 1994;2(2):151-6
- Hörter D, Dressman JB. Influence of physicochemical properties on dissolution of drugs in the gastrointestinal tract. *Adv Drug Deliv Rev* 2001;46(1-3):75-87
- Huang N, Katz JP, Martin DR, Wu GD. Inhibition of IL-8 gene expression in Caco-2 cells by compounds which induce histone hyperacetylation. *Cytokine* 1997;9(1):27-36

<http://www.food.gov.uk/safereating/chemsafe/additivesbranch/enumberlist>

- Kalgaonkar S, Lönnnerdal B. Receptor-mediated uptake of ferritin-bound iron by human intestinal Caco-2 cells. *J Nutr Biochem* 2009;20(4):304-11
- Kucharzik T, Williams IR. Neutrophil migration across the intestinal epithelial barrier-summary of in vitro data and description of a new transgenic mouse model with doxycycline-inducible interleukin-8 expression in intestinal epithelial cells. *Pathobiology* 2002-2003;70(3):143-9
- Kunkel SL, Standiford T, Kasahara K, Strieter RM. Interleukin-8 (IL-8): the major neutrophil chemotactic factor in the lung. *Exp Lung Res* 1991;17(1):17-23
- Lindahl A, Ungell AL, Knutson L, Lennernäs H. Characterization of fluids from the stomach and proximal jejunum in men and women. *Pharm Res* 1997;14(4):497-502
- Lomer MC, Harvey RS, Evans SM, Thompson RP, Powell JJ. Efficacy and tolerability of a low microparticle diet in a double blind, randomized, pilot study in Crohn's disease. *Eur J Gastroenterol Hepatol* 2001;13(2):101-6
- Lomer MC, Hutchinson C, Volkert S, Greenfield SM, Catterall A, Thompson RP, Powell JJ. Dietary sources of inorganic microparticles and their intake in healthy subjects and patients with Crohn's disease. *Br J Nutr* 2004;92(6):947-55
- Mitsuyama K, Toyonaga A, Sasaki E, Watanabe K, Tateishi H, Nishiyama T, Saiki T, Ikeda H, Tsuruta O, Tanikawa K. IL-8 as an important chemoattractant for neutrophils in ulcerative colitis and Crohn's disease. *Clin Exp Immunol* 1994;96(3):432-6
- Moriya M, Linder MC. Vesicular transport and apotransferrin in intestinal iron absorption, as shown in the Caco-2 cell model. *Am J Physiol Gastrointest Liver Physiol* 2006;290(2):G301-9
- Oberdörster G, Oberdörster E, Oberdörster J. Nanotoxicology: an emerging discipline evolving from studies of ultrafine particles. *Environ Health Perspect* 2005;113(7):823-39
- Oberdörster G, Stone V, Donaldson K. Toxicology of nanoparticles: a historical perspective. *Nanotoxicol* 2007; 1:2-25
- Papageorgiou I, Shadrick V, Davis S, Hails L, Schins R, Newson R, Fisher J, Ingham E, Case CP. Macrophages detoxify the genotoxic and cytotoxic effects of surgical cobalt chrome alloy particles but not quartz particles on human cells in vitro. *Mutat Res* 2008;643(1-2):11-9
- Powell JJ, Whitehead MW, Lee S, Thompson RPH. Mechanisms of gastrointestinal absorption: dietary minerals and the influence of beverage ingestion. *Food Chem* 1994; 51 381-388
- Powell JJ, Faria N, Thomas-McKay E, Pele LC. Origin and fate of dietary nanoparticles and microparticles in the gastrointestinal tract. *J Autoimmun* 2010;34(3):J226-33
- Ramachandran A, Madesh M, Balasubramanian KA. Apoptosis in the intestinal epithelium: its relevance in normal and pathophysiological conditions. *J Gastroenterol Hepatol* 2000;15(2):109-20
- San Martin CD, Garri C, Pizarro F, Walter T, Theil EC, Núñez MT. Caco-2 intestinal epithelial cells absorb soybean ferritin by mu2 (AP2)-dependent endocytosis. *J Nutr* 2008;138(4):659-66
- Sancho E, Batlle E, Clevers H. Signaling pathways in intestinal development and cancer. *Annu Rev Cell Dev Biol* 2004;20:695-723

- Sääf AM, Halbleib JM, Chen X, Yuen ST, Leung SY, Nelson WJ, Brown PO. Parallels between global transcriptional programs of polarizing Caco-2 intestinal epithelial cells in vitro and gene expression programs in normal colon and colon cancer. *Mol Biol Cell* 2007;18(11):4245-60
- Schins RP, Knaapen AM. Genotoxicity of poorly soluble particles. *Inhal Toxicol* 2007;19 (Suppl 1):189-98
- Schmid K, Riediker M. Use of nanoparticles in Swiss Industry: a targeted survey. *Environ Sci Technol* 2008;42(7):2253-60
- Stoeger T, Takenaka S, Frankenberger B, Ritter B, Karg E, Maier K, Schulz H, Schmid O. Deducing in vivo toxicity of combustion-derived nanoparticles from a cell-free oxidative potency assay and metabolic activation of organic compounds. *Environ Health Perspect* 2009;117:54-60
- Unfried K, Albrecht C, Klotz LO, von Mikecz A, Grether-Beck S, Schins RPF. Cellular responses to nanoparticles: target structures and mechanisms. *Nanotoxicol* 2007;1:52-71
- Xia T, Kovoichich M, Brant J, Hotze M, Sempf J, Oberley T, Sioutas C, Yeh JI, Wiesner MR, Nel AE. Comparison of the abilities of ambient and manufactured nanoparticles to induce cellular toxicity according to an oxidative stress paradigm. *Nano Lett* 2006;6:1794-807





## CHAPTER 5

---

### ***In vitro* and *in vivo* investigations on the effect of amorphous silica on DNA damage in the inflamed intestine**

Kirsten Gerloff<sup>1</sup>, Meike Winter<sup>2</sup>, Agnes W. Boots<sup>1</sup>, Damien van Berlo<sup>1</sup>, Julia Kolling<sup>1</sup>,  
Catrin Albrecht<sup>1</sup>, Irmgard Förster<sup>3</sup>, Roel P.F. Schins<sup>1</sup>

<sup>1</sup> Particle Research and <sup>2</sup> Molecular Immunology, Institut für Umweltmedizinische Forschung (IUF) at  
the Heinrich Heine University Düsseldorf, Germany.

#### **Abstract**

The discussion about possible adverse effects of ingested nanoparticles towards the human body is currently gaining much attention. One of the major contributors to regular nanoparticle ingestion includes amorphous SiO<sub>2</sub> which is already widely used in cosmetics, pharmaceutical products and foods. Recently we demonstrated that these particles can cause cytotoxicity and oxidative DNA damage to human intestinal Caco-2 cells, as well as upregulation of the expression of the potent neutrophil chemoattractant interleukin-8. To elaborate whether the toxic potency of ingested nanoparticles differs between healthy individuals and those with (chronic) inflammatory bowel diseases (IBD) we have investigated the oxidative DNA damaging properties of SiO<sub>2</sub> (i) *in vitro* in Caco-2 cells during co-exposure to primary human neutrophils (PMN) and (ii) *in vivo* by evaluation of the effects of SiO<sub>2</sub> enriched chow in acute and chronic dextrane sulphate sodium (DSS) induced colitis in mice. Genotoxicity was evaluated by the formamidopyrimidine glycosylase (Fpg)-modified comet assay and immunohistochemistry for 8-hydroxydeoxyguanosine (8-OHdG). It was found that activated human neutrophils potently induce DNA strand breakage and oxidative lesions *in vitro*. However, SiO<sub>2</sub> did not lead to PMN activation, and no

PMN mediated DNA damage was determined in a co-culture model with Caco-2 cells. The outcomes of the *in vivo* study were in support of these findings: analysis of DNA damage in whole colonic tissue by the *in vivo* Fpg-modified comet assay did not reveal elevated strand breakage after receiving a SiO<sub>2</sub> enriched chow. However, a mild increase of 8-OHdG lesions was shown by immunohistochemical staining after chronic, but not after acute colitis induction.

## 5.1 Introduction

Throughout the last few years, the discussion about possible adverse effects of ingested nanoparticles towards the human body is gaining much attention. The use of nanoparticles, defined by a size smaller 100 nm, for food and food-related products becomes more popular (Oberdörster *et al.*, 2005; Chaudhry *et al.*, 2008; Tiede *et al.*, 2008; Schmid and Riediker, 2008; homepage nanotechproject.org). A daily ingestion of  $10^{12}$ - $10^{14}$  particles per day has been suggested already several years ago, with increasing tendency each year (Lomer *et al.*, 2001, 2004). One of the major contributors to regular nanoparticle ingestion includes the amorphous SiO<sub>2</sub> which is already widely used in cosmetics, pharmaceutical products and foods (Johnston *et al.*, 2000; Chaudhry *et al.*, 2008). SiO<sub>2</sub> in general is accepted as a common food additive (E551) and mainly used as an anticaking agent (homepage food.gov.uk). The uptake of such nanoparticles into the intestinal epithelium is still not fully understood and appears to vary with different particle compositions and applications (Unfried *et al.*, 2007; Powell *et al.*, 2010). In general, particle uptake by intestinal tissue is low (< 10 %) (Jani *et al.*, 1994, Hillery *et al.*, 1994) but reported to be a 15-250 fold higher for small particles (~110-120 nm) compared to larger particles (Desai *et al.*, 1996). Intestinal particle internalisation is mainly driven by the so-called Peyer's Patches, i.e. lymphoid tissue rich of specified M-cells (reviewed in Powell *et al.*, 2010), but epithelial cells are also reported to be capable of considerable particle uptake (Hillery *et al.*, 1994). Trouiller and co-workers recently showed marked systemic DNA damage and mutagenesis in mice after oral uptake of TiO<sub>2</sub> nanoparticles and suggested that this may be due to uptake and subsequent induction of systemic inflammation (Trouiller *et al.*, 2009).

Recently, we have addressed the potential hazards of a selection of nanoparticles that are likely to find their way into engineered food or food packaging in the future. In these studies we observed for instance that nano-size SiO<sub>2</sub> and ZnO induce marked cytotoxicity, and also can cause oxidative DNA damage and the release of the pro-inflammatory mediator interleukin-8 from human intestinal Caco-2 cells. In contrast, TiO<sub>2</sub> only showed rather negligible cytotoxic and DNA damaging effects in our investigations (Gerloff *et al.*, 2009, Gerloff *et al.*, in preparation). Remarkably however and contrasting to findings in lung epithelial cells (e.g. Singh *et al.*, 2007; Monteiller *et al.*, 2007), the aforementioned effects could not be predicted

by the primary particle size or specific surface area of the different compounds (Gerloff *et al.*, 2009, Gerloff *et al.*, submitted). In the respiratory tract, particles of low solubility and toxicity, such as TiO<sub>2</sub> and carbon black, have been shown to cause inflammation in proportion to their specific surface area. This observation is of major importance for risk assessment of inhaled particles, since their adverse effects have been demonstrated to be associated with their intrinsic inflammatory potency (Oberdörster *et al.*, 2005; Duffin *et al.*, 2007). In contrast, relatively little is known about possible inflammatory properties and possibly associated effects of nanoparticles in the gut. In the respiratory tract, the particle-driven inflammatory response is associated with tissue damage, remodelling and mutagenesis (Donaldson *et al.*, 2005; Duffin *et al.* 2007; Schins and Knaapen, 2007). An important player in the relationship between inflammation and carcinogenesis is the formation of reactive oxygen species (ROS) during inflammatory phagocyte respiratory burst (Babbs, 1992; Knaapen *et al.*, 2006). Indeed, activated polymorphonuclear neutrophils (PMN) have been shown to cause oxidative DNA damage in rat lung epithelial cells (Knaapen *et al.*, 1999; Knaapen *et al.*, 2002a), and the amounts of recruited neutrophils was shown to be correlated with genotoxic and mutagenic effects in the lung epithelium of particle-exposed rats (Driscoll *et al.*, 1997; Knaapen *et al.* 2002b).

Inflammatory effects of particles might also play an important role in particle risk assessment for the intestine. For example, bacterial components such as LPS are shown to bind to TiO<sub>2</sub> particles which then, by serving as a carrier for these toxins, may lead to highly increased inflammatory responses in peripheral blood mononuclear cells, characterised by the release of various inflammatory cytokines. Interestingly, the inflammatory response induced by the LPS-particle complex is synergistic as it was shown to be more pronounced than that caused by incubation with either the particles or LPS alone (Ashwood *et al.*, 2007). Since large amounts of bacterial compounds are present, such particle-endotoxin complexes might be easily formed within the colon. Transportation of these bacterial composites into the mucosa via binding to nanoparticles might lead to aggravation of inflammatory events induced by unintentional ingestion of nanoparticles via food uptake and exacerbate inflammatory bowel diseases (IBD) as ulcerative colitis. However, the influence of particles on the etiopathology of IBD is currently under discussion but not yet confirmed (Lomer *et al.*, 2001, 2004; Schneider *et al.*, 2007).

The main hallmark of colitis is the imbalance of the intestinal immune system. This is characterised by continuous migration of activated lymphocytes, granulocytes and macrophages into the mucosa as well as an increased production of various pro-inflammatory cyto- and chemokines (Mitsuyama *et al.*, 1994; Rogler and Andus, 1998; MacDermott, 1999). In colonic tissue of colitis patients, increased levels of the potent chemoattractant interleukin-8 (IL-8), secreted by epithelial cells, macrophages or fibroblasts, are found. These elevated IL-8 levels are directly linked to the attraction and thus the infiltration of neutrophils, and therefore also correlate with the grade of local inflammation (Kunkel *et al.*, 1991; Mazzucchelli *et al.*, 1994; Mitsuyama *et al.*, 1994; Kucharzik and Williams, 2002-2003). The respiratory burst of activated neutrophils will lead to an increased production of reactive oxygen species (ROS) that can further enhance inflammation and may introduce DNA damage. Persistent activation of neutrophils and ROS has been considered to contribute to carcinogenesis in the respiratory tract as well as the intestine (Itzkowitz *et al.*, 2004; Knaapen *et al.*, 2006; Westbrook *et al.*, 2009).

Recently, we have found that amorphous SiO<sub>2</sub> is capable of inducing cytotoxicity, oxidative DNA lesions and pro-inflammatory responses in Caco-2 cells, including the upregulation of mRNA expression and protein secretion of IL-8 (Gerloff *et al.*, 2009, Gerloff *et al.*, in preparation), one of the most prominent cytokines expressed by these cells (Jung *et al.*, 1995). In the present study, we aimed to investigate the potential consequences of the pro-inflammatory properties of SiO<sub>2</sub> for DNA damage induction in intestinal cells using both an *in vitro* and *in vivo* model of intestinal inflammation. For the *in vitro* experiments, we used a co-incubation model composed of Caco-2 cells and primary human neutrophils. Using this co-incubation, we analysed the potential genotoxic effects of SiO<sub>2</sub> nanoparticles in Caco-2 cells in the presence or absence of neutrophils. For the *in vivo* experiments, we used a colitic mouse model using dextrane sulphate sodium (DSS), known to induce experimental ulcerative colitis by disturbance of the epithelial integrity (Wirtz and Neurath, 2007). Upon inducing either acute or chronic inflammation, the colon was analyzed for DNA strand breakage and oxidative DNA damage.

## 5.2 Methods

**Materials.** Trypsin, Dulbecco's  $\text{Ca}^{2+}/\text{Mg}^{2+}$ -free phosphate buffered saline (PBS), agarose, low melting point (LMP) agarose, Triton X-100, DMSO, ethidium bromide, fetal calf serum (FCS), phorbol-12-myristate-13-acetate (PMA) and deferoxamine (DFO) were all purchased from Sigma (Germany). Minimum essential Medium (MEM) with Earle's salts, Hanks' Balanced Salt Solution (HBSS), penicillin/streptomycin were purchased from Invitrogen (Germany). Lymphoprep was obtained from Axis-Shield (Norway). 1-hydroxy-3-carboxy-pyrrolidine (CPH) was purchased from Alexis Biochemicals (Germany), lucigenin (N,N'-Dimethyl-9,9'-biacridinium dinitrate) was obtained from Fluka and RNeasy Fibrous Tissue Mini Kit was from Qiagen (Germany). Dextran sulfate sodium (DSS; mol wt 36.000-50.000) was obtained from MP Biomedicals (USA). Hemocare was from Care Diagnostica (Germany). The antibody against 8-OHdG was obtained from the Japan Institute of Aging, mouse IgG was purchased from Vector Laboratories (USA). Histomouse™-SP Kit was sourced from Zymed Laboratories (USA) and DePex was obtained from Serva (Germany). Formamidopyrimidine-glycosylase (Fpg)-enzyme was kindly provided by Dr. Andrew Collins (Institute for Nutrition Research, University of Oslo, Norway). All other chemicals were from Merck (Germany).

**Nanoparticles.**  $\text{SiO}_2$  (amorphous Silica, fumed; Sigma, Germany) was used for all experiments in present study. The sample has been reported to have a surface area according to Brunauer, Emmett and Teller (BET) of  $200 \text{ m}^2/\text{g}$  and a mean primary particle diameter of 14 nm. For the *in vitro* studies,  $\text{SiO}_2$ -nanoparticles were suspended in HBSS, sonicated for 10 min (Sonorex TK52 water-bath; 60 Watt, 35 kHz) and then directly added to the cells at the indicated concentrations. Although the primary size of the  $\text{SiO}_2$  particles is well in the nano-size range, the material is well-known to occur as aggregates/agglomerates. This was also confirmed by Mastersizer analysis in the suspensions used for cell treatment (Gerloff *et al.*, submitted). For the *in vivo* study, chow was purchased from Ssniff (Germany), either supplemented with or without 0.1 % w/w  $\text{SiO}_2$  ( $\text{SiO}_2$ -chow).

**Animals.** C57BL/6 mice were originally purchased from Harlan-Winkelmann and bred at the IUF animal facility under specific pathogen free (SPF) conditions. The

animals were housed and maintained in an accredited on-site testing facility under SPF conditions, according to the guidelines of the Society for Laboratory Animals Science (GV-SOLAS). Food and water were available ad libidum. Female mice were used at 9 weeks of age. Mice were painlessly sacrificed in a CO<sub>2</sub> chamber, according to German guidelines. The experiment was performed with the permission of the Regierung von Nordrhein-Westfalen, Germany.

**Cell culture and co-incubation.** The human colon adenocarcinoma cell line Caco-2 was obtained from the *Deutsche Sammlung von Mikroorganismen und Zellkulturen* (DSMZ) GmbH, Germany and grown in MEM with Earle's salts and Non Essential Amino Acids, supplemented with 20 % FCS, 1 % L-glutamine and 30 IU/ml penicillin–streptomycin. For experiments, cells were trypsinised at near confluency and  $4 \times 10^4$  cells per cm<sup>2</sup> were seeded into 60 mm culture plates and grown overnight. Experiments were performed in HBSS between cell passages 5 to 30 after starvation of the cells for 20 h in serum free medium. Neutrophils (PMN) were isolated freshly from blood of healthy, non-smoking volunteers as described in Knaapen *et al.* (1999) using Lymphoprep. PMN were suspended in HBSS (+ Ca<sup>2+</sup>/Mg<sup>2+</sup>) and counted using a Neubauer chamber. Cell viability was tested via Trypan Blue staining (viability > 95%). PMA (100 ng/ml) was used for PMN-activation. For the co-incubation experiments, PMN were incubated with PMA or SiO<sub>2</sub> and added directly to the Caco-2 cells for 30 min at 37°C at the indicated ratios. SiO<sub>2</sub> particles were administered to the cell cultures at the indicated concentration immediately after sonication as described above. After treatment, cell monolayers were rinsed twice with PBS to remove excess of extracellular particles, neutrophils and detached (dead) cells or cell debris.

**ROS measurements by luminescence and Electron Paramagnetic Resonance (EPR).** ROS production was measured using either lucigenin-enhanced chemiluminescence or EPR spectroscopy. For luminescence, PMN (2.5 mil/ml) were stimulated with SiO<sub>2</sub> (31.25 and 312.5 µg/cm<sup>2</sup>) or PMA (100 ng/ml) in a white MaxiSorp™ 96-well plate (Nunc, Germany). Subsequently, 0.25 mM lucigenin was added to preferentially detect superoxide formation and chemiluminescence was recorded directly for 50 min at 37°C using a Luminometer (Multi-Bioluminat, Berthold,

Germany). Results were expressed as the area under the curve (RLU=relative light units).

For EPR spectroscopy the spin probe CPH was used. Caco-2 cells were previously seeded in a 96 well plate and grown to 70-80 % confluency before 30 min co-incubation with PMN (1.3 million/ml) at 37°C in the presence of 0.5 mM CPH in 10 µM DFO. Furthermore, PMN alone were preincubated with 20 or 80 µg/cm<sup>2</sup> SiO<sub>2</sub> for 30 min at 37°C in the presence of 0.5 mM CPH in 10 µM DFO. ROS generation was evaluated using a MiniScope MS200 Spectrometer (Magnettech, Berlin, Germany) at room temperature using the following instrumental settings: Magnetic field: 3360 G; sweep width: 97 G; scan time: 60 sec; number of scans: 1; modulation amplitude: 2000 mG. Data shown are calculated from the average peak amplitude of CPH characteristic triplet spectrum and expressed in arbitrary units (AU).

**Colitis induction in C57/BL6 mice.** Induction of chronic and acute colitis was performed by a method previously described, with some modifications (Okayasu *et al.*, 1990). In short, mice were pre-treated with conventional or SiO<sub>2</sub>-enriched chow for 14 days. Chronic colitis was induced by 3 cycles of DSS-treatment. Each cycle consisted of one week of 2 % (wt/vol) DSS in acidified drinking water ad libidum, while the mice received normal chow, followed by two weeks on normal drinking water and SiO<sub>2</sub>-chow. After the last cycle, mice were sacrificed on day 77 for further analysis. For induction of acute colitis, mice were pre-treated with SiO<sub>2</sub>-chow for 17 days. Then colitis was induced by 2 % DSS in drinking water for six days. During DSS-treatment, mice were offered normal breeding chow ad libidum. After day six, mice were left for additional two days, in which they were set on SiO<sub>2</sub> chow and normal drinking water, after which they were sacrificed for further analysis. Thus, both the acute and the chronic exposure model represented each 4 different treatment groups, i.e. the i.e. (i) animals without any treatment, (ii) animals treated with DSS, (iii) animals treated with SiO<sub>2</sub>, and finally, (iv) animals exposed to both DSS and SiO<sub>2</sub>. To evaluate the severity of disease, colon length was assessed as an established marked. A clinical score according to Cooper *et al.* (1993), which consists of bleeding intensity, weight loss and stool consistency was determined. Scores of these three categories were added and divided by three. In short, rectal bleeding was scored as 3, hemocare+ (i.e. the detection of minor amounts of haemoglobin in the faeces) as 2 and no bleeding was scored as 1. For weight loss,



more than 20% weight loss was scored as 4, 10 - 20% as 3, 0 – 10% as 2 no weight loss was scored as 1. For liquid stools 3 points were given, pasty, soft stools were scored as 2 and well-formed pellets were scored as 1.

**Detection of oxidative DNA damage in Caco-2 cells and in cells obtained from mouse small intestine or colon tissues by Fpg-modified comet assay.** The Fpg-modified comet assay was used to determine DNA strand breaks and alkali labile sites as well as specifically oxidative DNA damage in the Caco-2 cells, based on the method by Speit *et al.*, (2004) and modifications as described earlier (Gerloff *et al.*, 2009). Comet appearances were analyzed using an Olympus BX60 fluorescence microscope at 400× magnification. A comet image analysis software program (Comet Assay II, Perceptive Instruments, Haverhill, UK) was used for quantification of DNA damage by analysis of % DNA in tail. A total of 50 cells were analyzed per slide per experiment. A detailed description of the method in Caco-2 cells is provided in Gerloff *et al.* (2009). For the *in vivo* comet assay, after sacrificing the colons of the mice were removed and flushed with ice cold PBS. The entire colon was divided into 3 equal pieces, and one third of each piece was used to assess DNA strand breakage and oxidative DNA lesions. The tissue pieces of each colon were then pooled and processed for the *in vivo* Fpg-modified comet assay as described in Risom *et al.*, 2003 with minor modifications. Shortly, the tissue samples were minced with the plunger of a syringe in 1ml ice cold *in vivo* comet assay buffer (IVCAB, 0.14 M NaCl, 1.47 mM KH<sub>2</sub>PO<sub>4</sub>, 2.7 mM KCl, 8.1 mM Na<sub>2</sub>HPO<sub>4</sub> and 10 mM EDTA, pH 7.4). The cell-homogenate was filtered through a 40 µm sieve and subsequently centrifuged at 180 g for 10 min at 4°C. Supernatant was discarded and the pellet resuspended in 50µl IVCAB. Afterwards, 25 µl of the suspension were mixed with 235 µl 0.5 % low melting point agarose and applied to pre-coated slides (coated with 1.5 % agarose). From here, the Fpg-modified comet assay was performed as described for the *in vitro* measurements (Gerloff *et al.*, 2009). Data are shown as % comet tail values for each individual animal in the presence or absence of Fpg, i.e. % tail DNA<sub>+Fpg</sub> and % tail DNA<sub>-Fpg</sub>, respectively. Moreover, results are depicted as the calculated group means and standard deviations (SD) of the differences in % tail DNA as measured in the presence or absence of the Fpg enzyme:  $\Delta$ Fpg = [% tail DNA<sub>+Fpg</sub>] – [% tail DNA<sub>-Fpg</sub>].

**Colon fixation and immunohistochemistry of 8-hydroxydeoxyguanosine.** Three colonic sections of each animal were removed, fixed in 4% paraformaldehyde/PBS and paraffin embedded. The tissue sections were mounted on slides and stained for 8-OHdG. Mouse IgG staining was used as a negative control. RNA digestion was performed using RNase (100 µg/ml) in Tris buffer (5 mM Tris, 1 mM EDTA, pH 7.5; 60 min at 37 °C) and DNA-denaturation was conducted by 70 mM NaOH with 0.14 M NaCl and 40 % Ethanol. Zymed Histomouse<sup>TM</sup>-SP Kit was used according to the supplier's manual to block unspecific binding. The sections were then incubated over night with a primary antibody against 8-OHdG (1:250) or against IgG (1:250) as a negative control and counter stained with hematoxylin. After washing with water slides were dehydrated and covered in DePex. Slides were analysed using a light microscope (Olympus BX60).

**Statistics.** For all experiments, all means were calculated from three independent experiments, with the error bars representing standard deviation (SD). Analysis of statistical significance was done by unpaired Student's t-test with \*p < 0.05, \*\*p < 0.01 and \*\*\*p < 0.001 as levels of significance.

### 5.3 Results

The potential of human primary blood derived neutrophils (PMN) to induce DNA strand breakage and/or oxidative DNA damage in human intestinal Caco-2 cells was evaluated using a co-incubation model consisting of both cell types. As depicted in Figure 5.1, only activated neutrophils were able to induce both DNA strand breaks and, more pronounced, oxidative lesions. A non-significant induction of oxidative damage was already observed at a 1:1 ratio of both cell types, whereas a 3:1 ratio (PMN:Caco-2) resulted in significant DNA strand breakage and oxidative DNA damage.

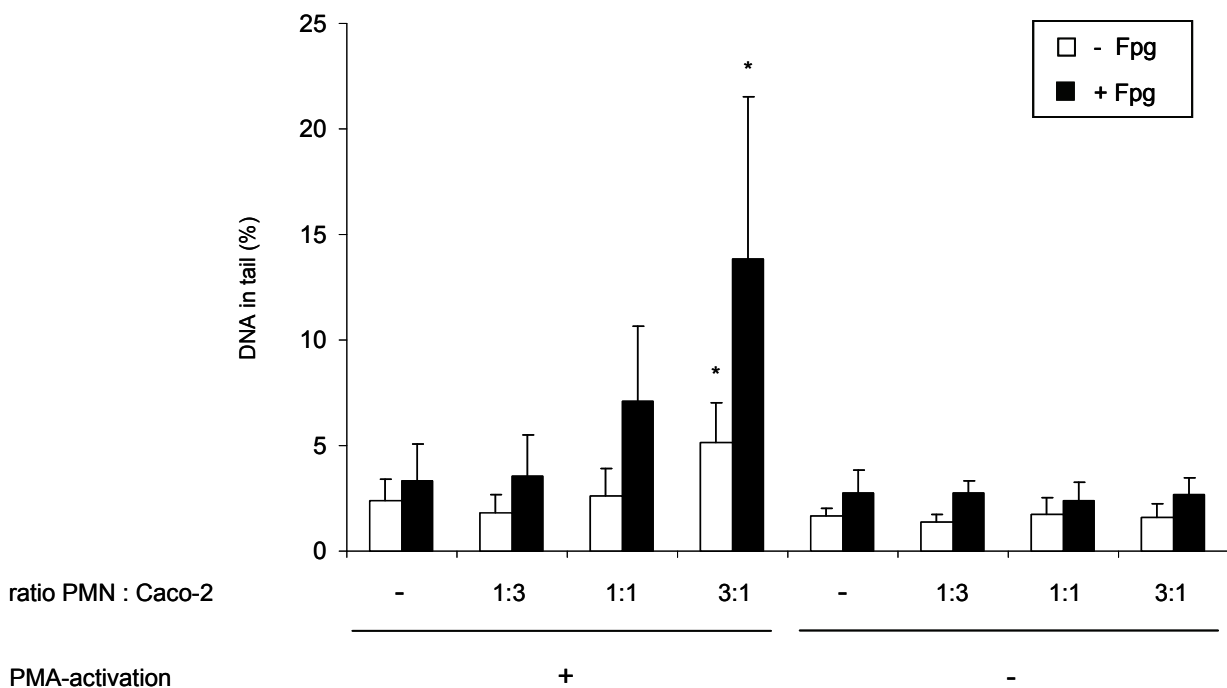


**Figure 5.1 DNA strand breakage and oxidative DNA damage in Caco-2 cells upon co-exposure to activated PMN.** DNA strand breakage and oxidative DNA damage were determined in Caco-2 cells using the Fpg-modified comet assay following 30 minutes co-incubation with PMA-activated or non-activated primary human neutrophils (PMN) at the indicated PMN:Caco-2 ratios in HBSS<sup>+/+</sup>. PMA=phorbol-12-myristate-13-acetate. Values are expressed as mean and standard deviation, n=3.

\* p < 0.05 versus control

Next, we investigated the ROS formation in this co-incubation model using EPR with the spin probe CPH, which has been introduced for the specific detection of superoxide anion radicals ( $O_2^{\cdot-}$ ). Caco-2 cells alone, either with or without the addition of PMA, did not induce any detectable  $O_2^{\cdot-}$  production (Figure 5.2). Non-

activated PMN were capable of mild ROS-formation, but this production could no longer be detected in the unstimulated co-incubation with Caco-2 cells. PMA-activated PMN did cause a pronounced and significant ROS generation, both in the absence and presence of Caco-2 cells. Interestingly, this PMN-induced ROS generation was slightly reduced in the presence of the intestinal epithelial cells although this reduction was not significant.

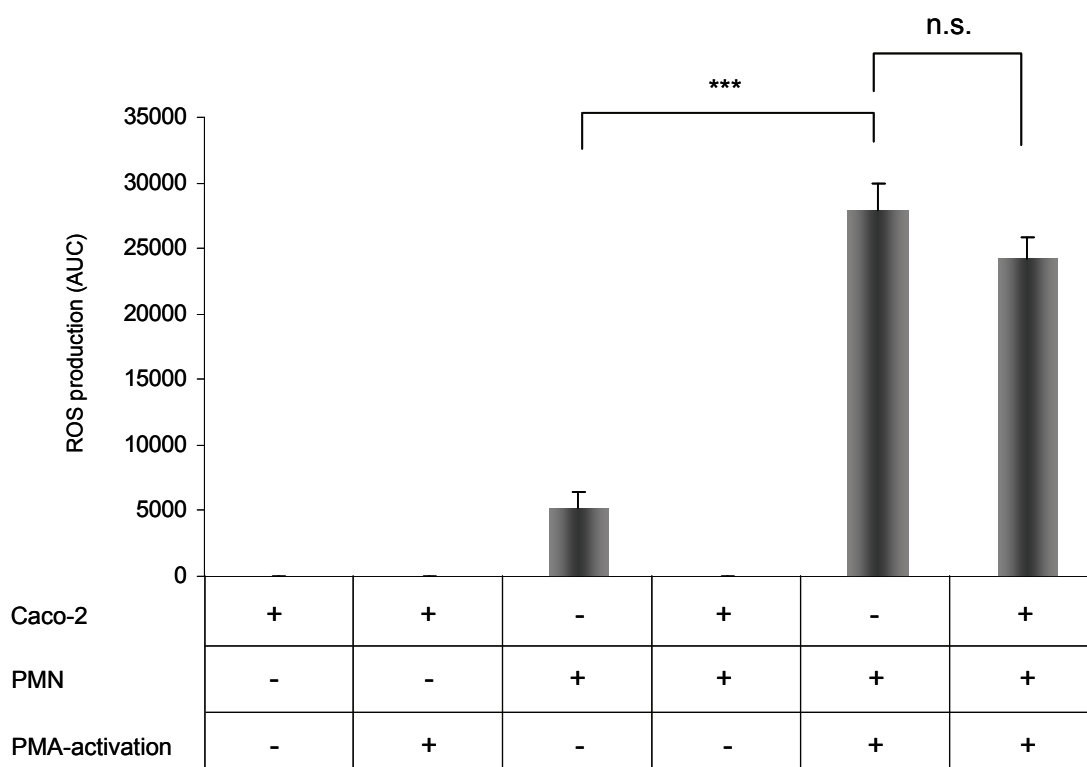


**Figure 5.2 ROS formation by PMN and Caco-2 cells.** The formation of superoxide anion radicals by Caco-2 cells alone, PMA activated or non-activated primary human neutrophils (PMN) alone or Caco-2 cells and PMN in co-incubation was determined via ESR after 30 minutes at 37°C using the spin probe CPH. PMA=phorbol-12-myristate-13-acetate. AU=arbitrary units. Values are expressed as mean and standard deviation, n=3. n.s.=not significant  
\*\*\* p < 0.001 versus control

The effect of PMN on SiO<sub>2</sub> induced DNA damage in Caco-2 cells is shown in Figure 5.3. The SiO<sub>2</sub> particles caused a significant induction of DNA damage in Caco-2 cells in the absence of PMN. Notably, the level of induction observed with the SiO<sub>2</sub> in the Caco-2 cells was similar to the effect observed with PMA-treated PMN used as positive control in these series of experiments. Surprisingly, the presence of PMN did not augment the SiO<sub>2</sub>-induced DNA strand breakage, but in fact resulted in markedly reduced effect in the intestinal epithelial cells. Application of the Fpg

enzyme revealed an increased, albeit not significant induction of oxidative lesions after SiO<sub>2</sub> incubation alone. In the presence of PMN however, a significant increase in oxidative DNA damage was detected.

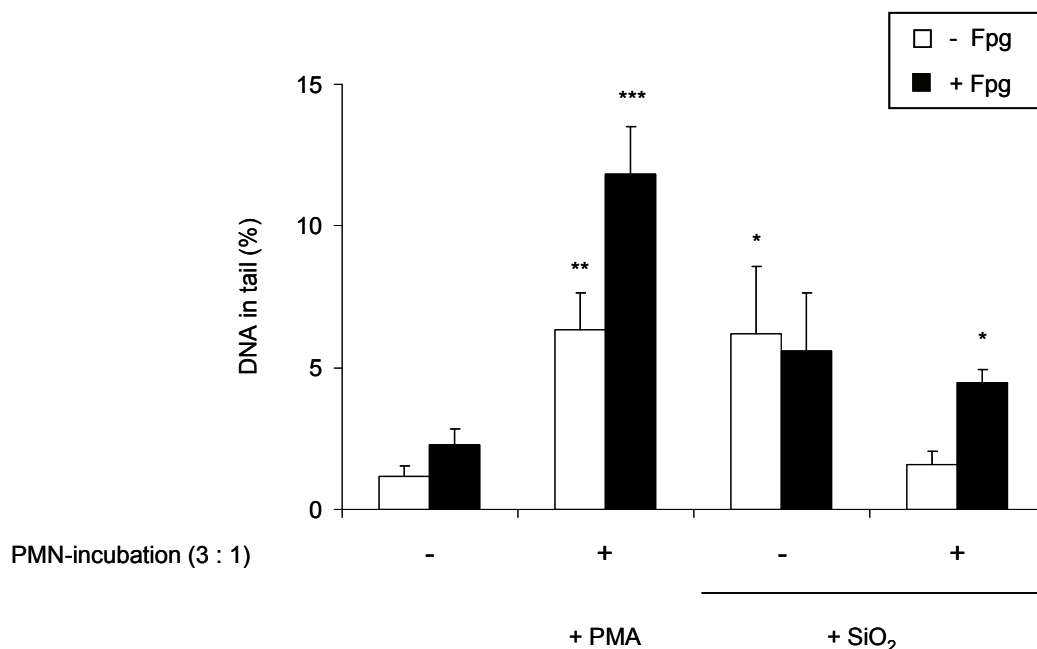


**Figure 5.3 DNA strand breakage and oxidative DNA damage in Caco-2 cells by activated PMN and SiO<sub>2</sub>.** DNA strand breakage and oxidative DNA damage were determined in Caco-2 cells using the Fpg-modified comet assay. Cells were (I) not incubated as controls, (II) 30 minutes co-incubated with PMA-activated primary human neutrophils (PMN), (III) 30 minutes incubated with SiO<sub>2</sub> alone or (IV) 30 minutes co-incubated with SiO<sub>2</sub> and PMN. SiO<sub>2</sub> concentration: 20 µg/cm<sup>2</sup>. PMN:Caco-2 ratio: 3:1. PMA=phorbol-12-myristate-13-acetate. Values are expressed as mean and standard deviation, n=3.  
\* p < 0.05, \*\* p < 0.01 and \*\*\* p < 0.001 versus control

Possible effects of SiO<sub>2</sub> on PMN-induced O<sub>2</sub><sup>-</sup> generation were analysed using two independent methods, i.e. both lucigenin-enhanced chemiluminescence (Figure 5.4 A) and EPR spectroscopy with CPH as spin probe (Figure 5.4 B). ROS detection via chemiluminescence occurs via constant measurement over 50 minutes and results in a typical curve as depicted in Figure 5.4 a. Compared to non-stimulated PMN, the presence of SiO<sub>2</sub> did not affect the overall formation of superoxide (area under the curve). In contrast, stimulation with PMA resulted in a significant ROS induction (Figure 5.4 A). EPR spectroscopy allows for a quantification of the amount of CPH that has reacted with superoxide anions over the 30 min incubation. Similar to our findings in chemiluminescence measurement, ESR confirmed that SiO<sub>2</sub> did not activate neutrophilic burst, since no increase in ROS formation was detected (Figure

5.4 B). In contrast, a clear effect was observed with the well-known neutrophil activator PMA. Figure 5.4 b shows representative EPR spectra of ROS formation.

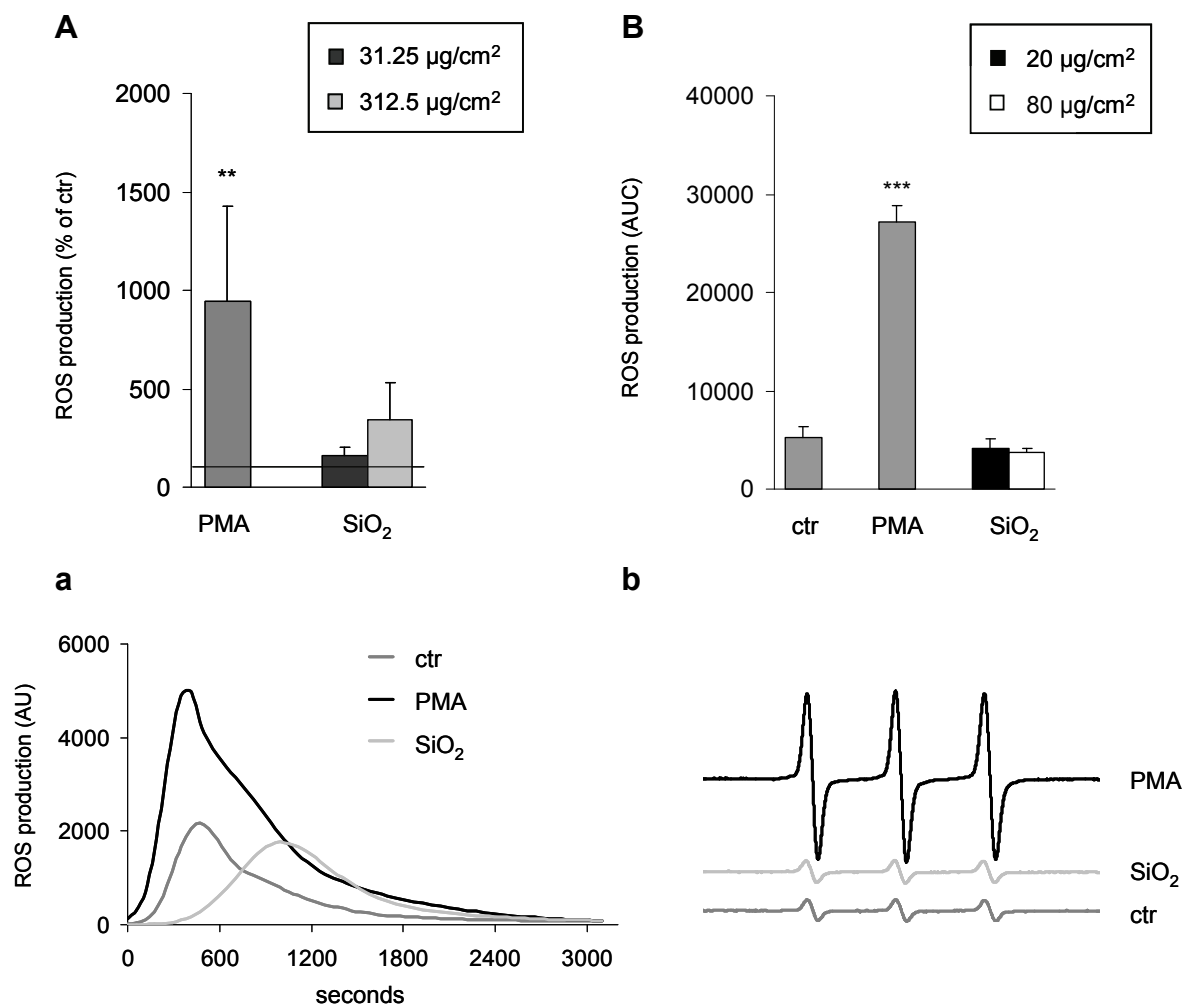


**Figure 5.4 ROS generation from PMN upon treatment with SiO<sub>2</sub>.** The formation of superoxide anion radicals by primary human neutrophils (PMN) was determined by chemiluminescence using lucigenin over an incubation period of 50 minutes (A) and ESR after 30 minutes pre-incubation with the spin probe CPH (B). (a) Representative luminescence curve and (b) representative ESR spectra by non-activated PMN (ctr=control), PMA-activated PMN (PMA) and SiO<sub>2</sub>-treated PMN (SiO<sub>2</sub>; (a) 312.5  $\mu\text{g}/\text{cm}^2$ , (b) 20  $\mu\text{g}/\text{cm}^2$ ). AU=arbitrary units. Values are expressed as mean and standard deviation, n=3.

\*\* p < 0.01 and \*\*\* p < 0.001 versus control

To analyse the genotoxic properties of SiO<sub>2</sub> *in vivo* in healthy intestine as well as during inflammation, mice were fed normal or SiO<sub>2</sub> chow for 14 days, followed by 3 alternating cycles of DSS or SiO<sub>2</sub> treatment for the induction of colitis. The occurrence of symptoms of colitic inflammation was confirmed by measure of colon length (Figure 5.5 A) and the clinical score, with 3 indicating severest symptoms (Figure 5.5 B). The colon lengths were reduced markedly after colitis induction,

whereas mice receiving SiO<sub>2</sub> exhibited normal colon lengths. The clinical score, reflecting bleeding intensity, weight loss and stool consistency, revealed an increase in symptoms after each DSS treatment followed by states of remission.

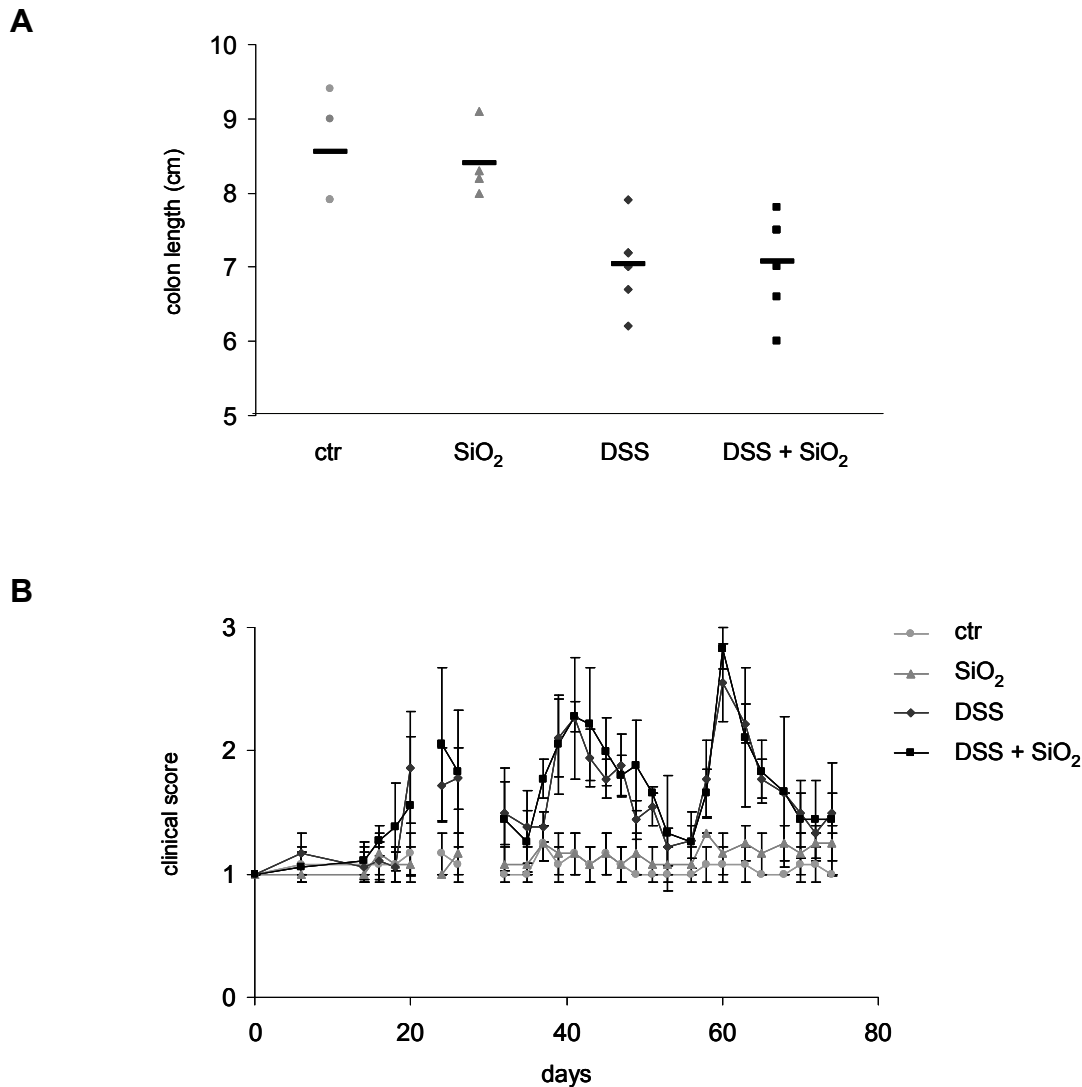


**Figure 5.5 Evaluation of the severity of the induced chronic colitis.** Colon lengths were determined as marker of colitic symptoms (A). The clinical score as a combined measure of changes in bleeding intensity, weight loss and stool consistency. 1 = no effect detectable to 3 = strongest colitic effects (B).

Interestingly, DNA damage as measured by *in vivo* Fpg-comet assay (see Figure 5.6) was already high in the colons of the control animals, i.e. the mice that were neither treated with SiO<sub>2</sub> nor with DSS. Consequently, chronic colitis did not result in an increased DNA damage in the colon of DSS-treated animals compared to these high controls (Figure 5.6 A). The SiO<sub>2</sub>-enriched diet even led to a reduced oxidative DNA damage, both in the colon tissues of healthy and colitic mice.

However, calculation of the  $\Delta$ Fpg showed that the reduction in oxidative lesions was not statistically significant, as a result of high individual variations (Figure 5.6 B).

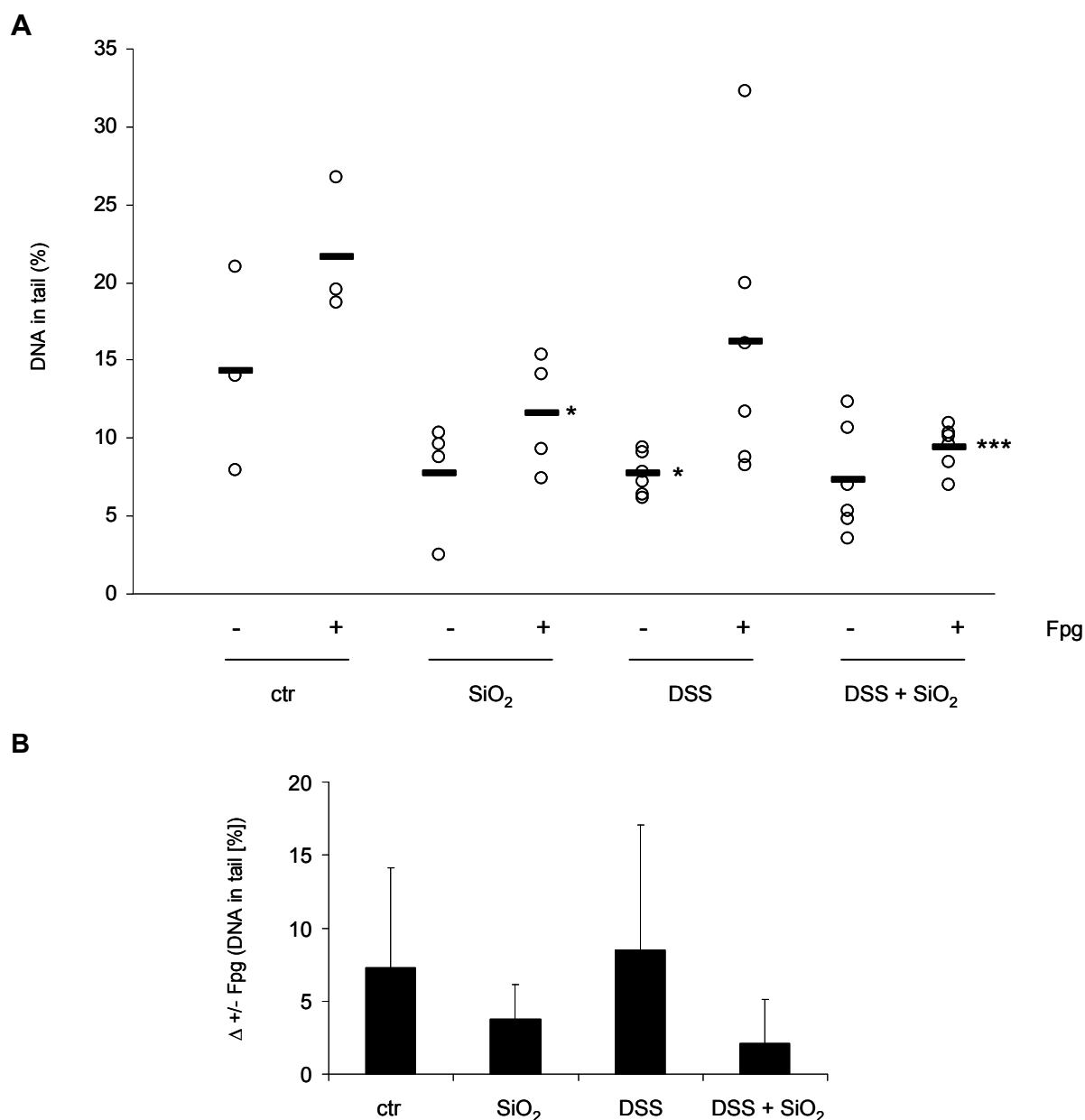


**Figure 5.6** Effect of oral SiO<sub>2</sub> on DNA strand breakage and oxidative DNA damage in murine colonic tissue in a chronic colitis model. DNA strand breakage and oxidative DNA damage were determined in whole murine colonic tissue using the *in vivo* Fpg-modified comet assay (A). The total amount of oxidative DNA damage is depicted as  $\Delta$ Fpg, calculated by the difference between + Fpg and – Fpg values (B). Treated mice were fed with either DSS to induce chronic colitic symptoms, SiO<sub>2</sub> or both DSS and SiO<sub>2</sub>. ctr=control, DSS=dextrane sulphate sodium. Values are expressed as mean and standard deviation, n=3 (ctr), n=4 (SiO<sub>2</sub>) and n=6 (DSS, DSS+SiO<sub>2</sub>).

\* p < 0.05 and \*\*\* p < 0.001 versus control



Interestingly, detection of 8-OHdG by immunohistochemistry (IHC, Figure 5.7) revealed a clear increase of oxidative lesions, mainly located in the nuclei of epithelial cells, in both SiO<sub>2</sub> (Figure 5.7 B) and DSS (Figure 5.7 C) treated mice when compared to the control animals (Figure 5.7 A). Combined treatment with SiO<sub>2</sub> and DSS (Figure 5.7 D) also induced increased 8-OHdG sites compared to the control, however, these appeared less pronounced than the lesions induced by SiO<sub>2</sub> or DSS alone. All IgG stained (control) slides were found to be without marked nuclear staining (not shown).

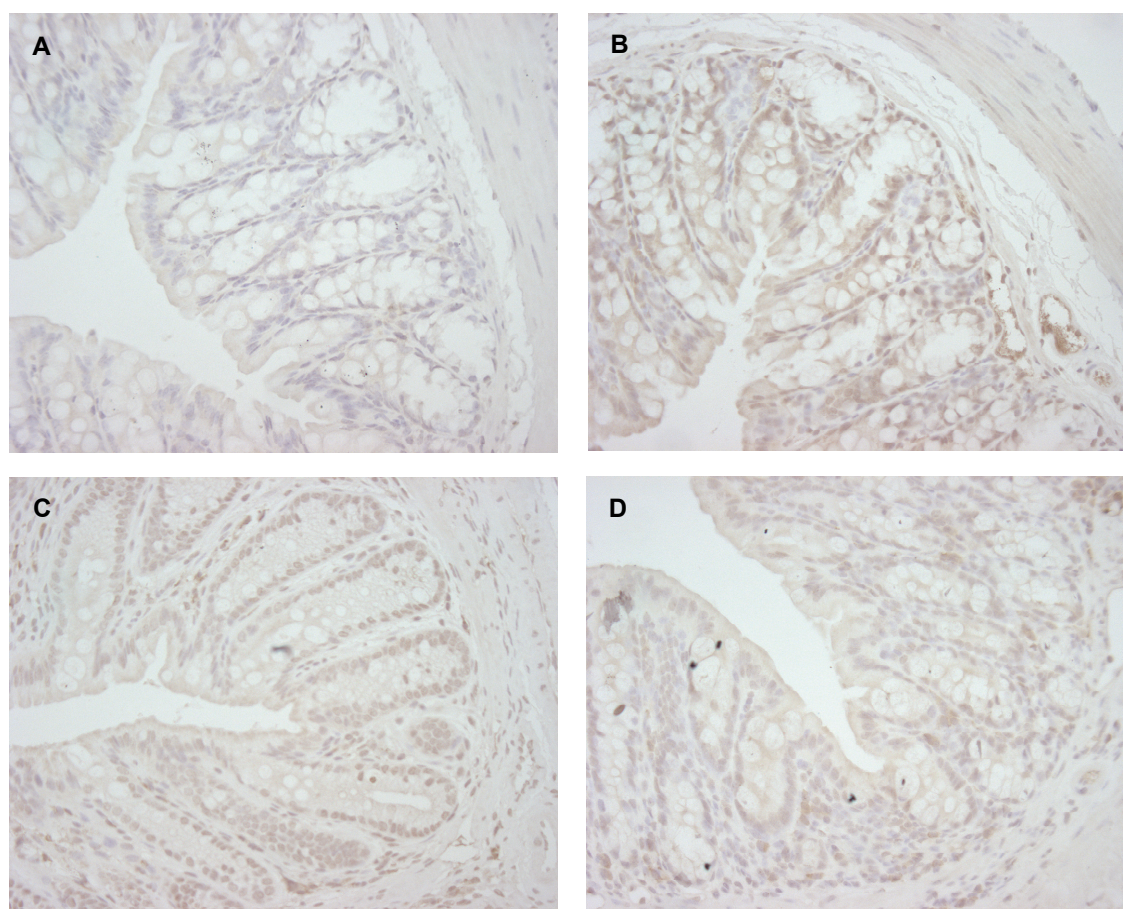


**Figure 5.7** Immunohistochemical analysis of 8-hydroxydeoxyguanosine in a murine colonic tissue in a chronic colitis model. Representative images of colonic sections, obtained from controls (A), mice after receiving SiO<sub>2</sub> enriched-chow (B) DSS treated mice receiving normal chow (C) or DSS treated mice receiving SiO<sub>2</sub> enriched-chow (D), stained with an antibody against 8-OHdG (original magnification × 400). n=3 (ctr), n=4 (SiO<sub>2</sub>) and n=6 (DSS, DSS+SiO<sub>2</sub>).

We also evaluated the small intestines from the same animals. In contrast to colon, no differences in DNA damage or induction of oxidative lesions were observed between any of the various treatments in the small intestine by Fpg-comet assay (Figure 5.8 A and B).

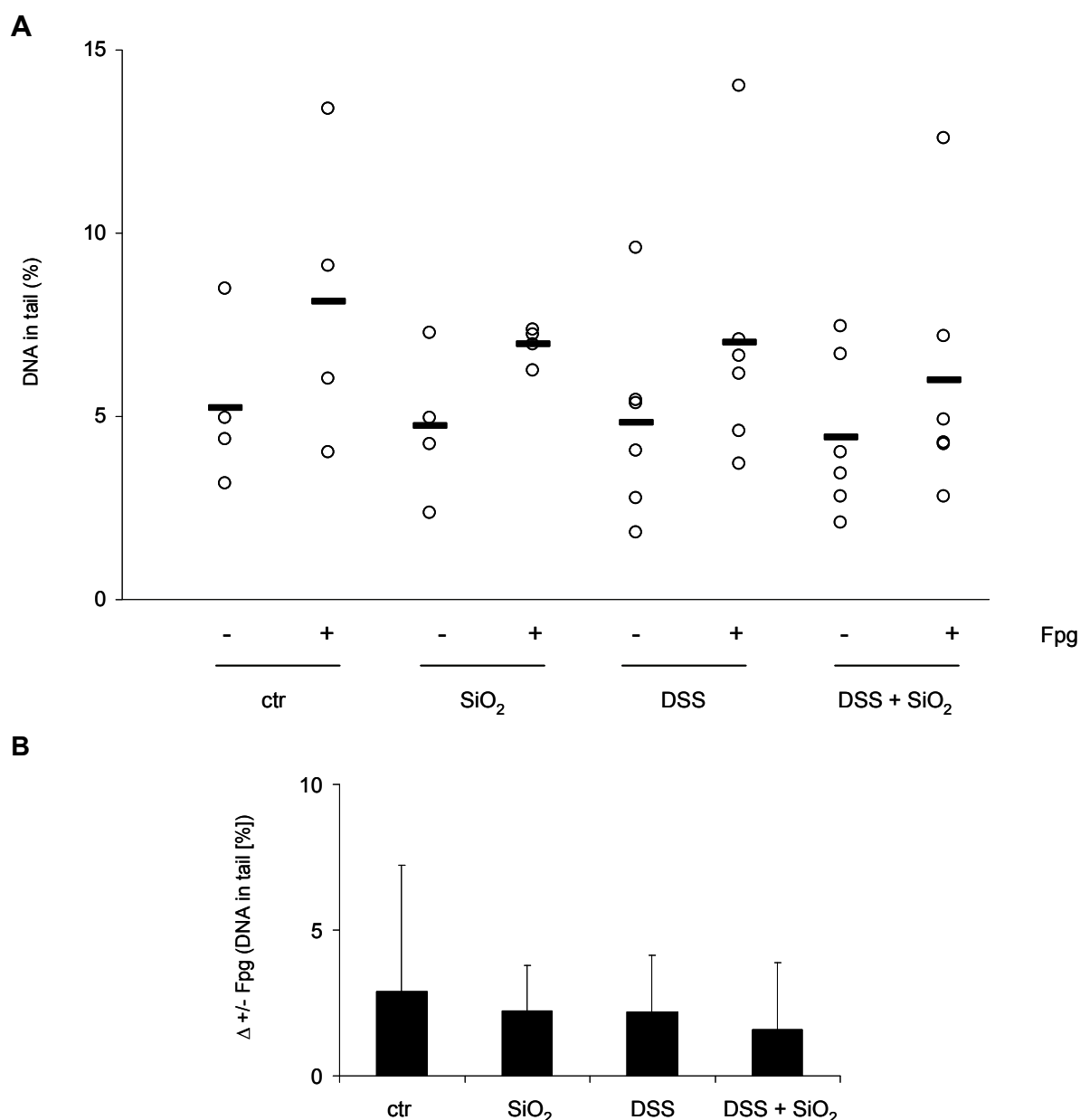


**Figure 5.8 Effect of oral SiO<sub>2</sub> on DNA strand breakage and oxidative DNA damage in murine small intestinal tissue in a chronic colitis model.** DNA strand breakage and oxidative DNA damage were determined in whole murine small intestinal tissue using the *in vivo* Fpg-modified comet assay (A). The total amount of oxidative DNA damage is depicted as  $\Delta$ Fpg, calculated by the difference between + Fpg and - Fpg values (B). Treated mice were fed with either DSS to induce chronic colitic symptoms, SiO<sub>2</sub> or both DSS and SiO<sub>2</sub>. ctr=control, DSS=dextrane sulphate sodium. Values are expressed as mean and standard deviation, n=4 (ctr, SiO<sub>2</sub>) and n=6 (DSS, DSS+SiO<sub>2</sub>).  
\* p < 0.05 and \*\*\* p < 0.001 versus control

Since the above findings in colon tissue during chronic colitis might have been due to feedback and/or adaptive response mechanisms we also evaluated the genotoxic effects of SiO<sub>2</sub> after shorter particle exposures and/or acute colitis. The treatment consisted of administration of DSS for 6 days (acute colitis animals)

following 17 days of normal or SiO<sub>2</sub> chow. Results of these investigations are shown in Figure 5.9.

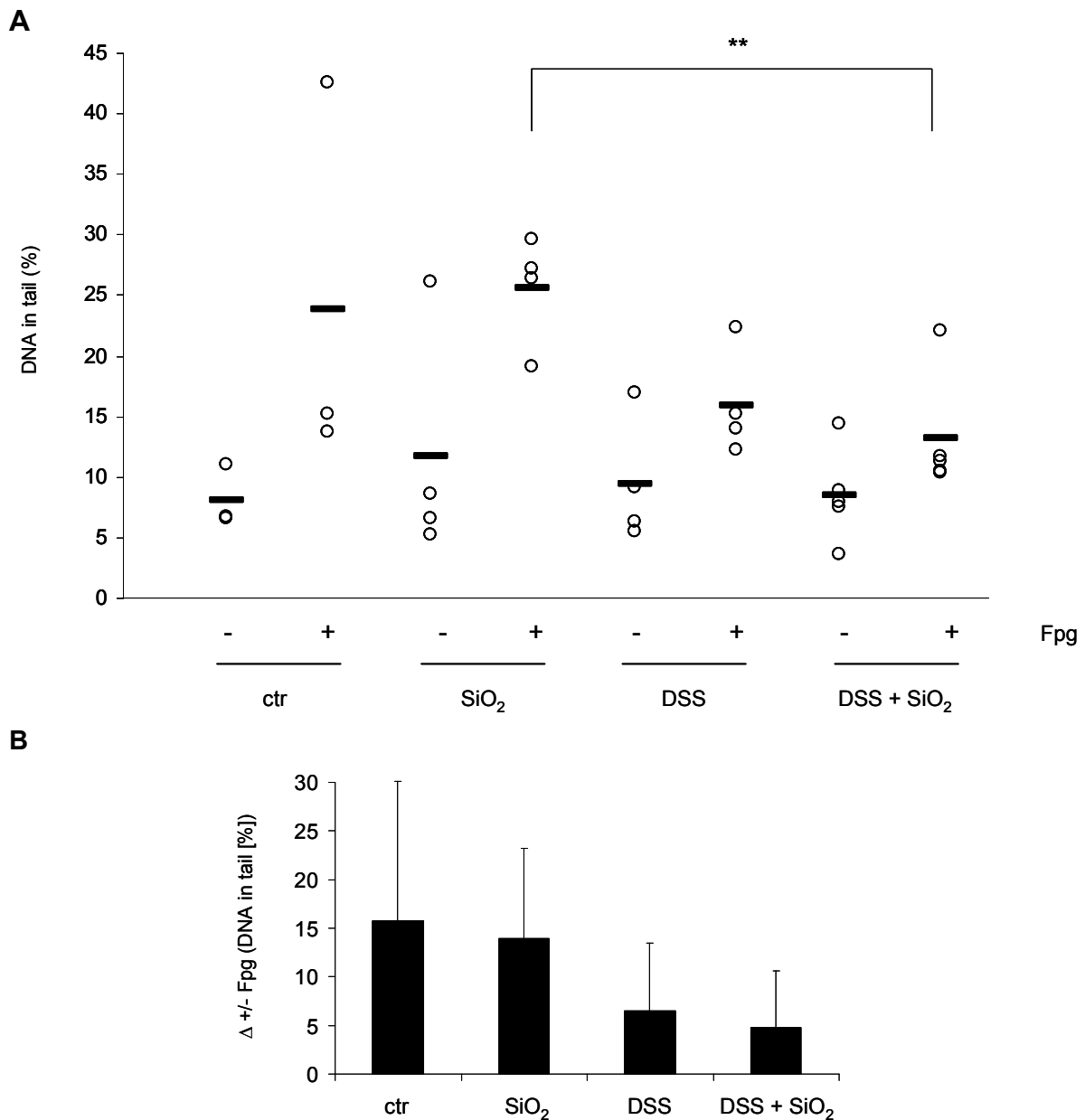


**Figure 5.9 DNA strand breakage and oxidative DNA damage in murine colonic tissue using *in vivo* Fpg-comet assay in an acute colitis model.** DNA strand breakage and oxidative DNA damage were determined in whole murine colonic tissue using the *in vivo* Fpg-modified comet assay (A). The total amount of oxidative DNA damage is depicted as  $\Delta$ Fpg, calculated by the difference between + Fpg and – Fpg (B). Treated mice were fed with either DSS to induce acute colitic symptoms, SiO<sub>2</sub> or both DSS and SiO<sub>2</sub>. ctr=control, DSS=dextrane sulphate sodium. Values are expressed as, n=3 (ctr), n=4 (SiO<sub>2</sub>, DSS) and n=5 (DSS+SiO<sub>2</sub>).

\*\* p < 0.01

Slightly elevated levels of oxidative lesions were observed after a SiO<sub>2</sub> containing diet, although they did not reach a statistical significance. Remarkably, in the presence of Fpg, the % of tail DNA was found to be significantly lower in the DSS-SiO<sub>2</sub> group when compared to the SiO<sub>2</sub> groups (Figure 5.9 A). However, no significant reduction was found for the  $\Delta$ Fpg values indicating that there was no significant reduction of oxidative DNA damage (Figure 5.9 B). The absolute levels of DNA damage in the DSS and DSS-SiO<sub>2</sub> groups of the acute colitis study were comparable to the damage in the corresponding groups of the chronic study, but revealed higher interindividual variations.

Moreover, IHC staining of the respective colonic tissue did not show marked differences in staining for 8-OHdG within the nuclei, as shown by representative images in Figure 5.10.

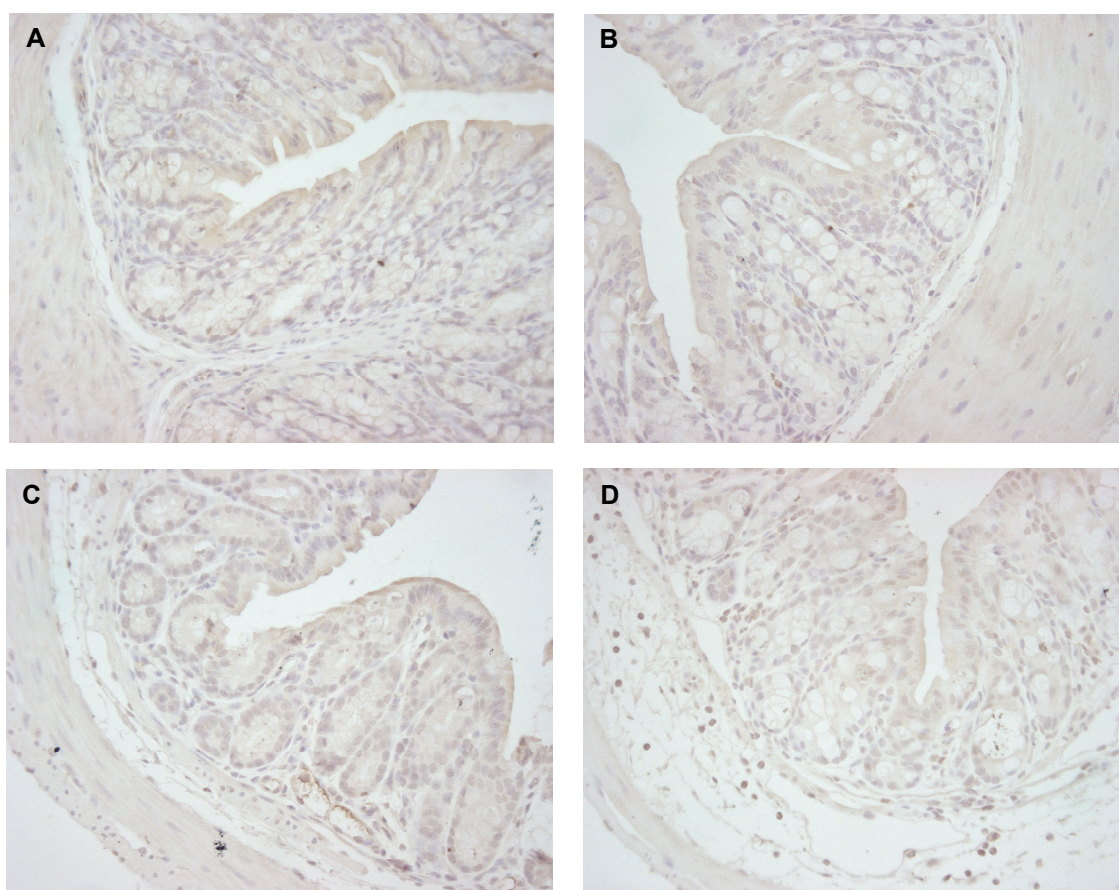


**Figure 5.10 Immunohistochemical analysis of 8-hydroxydeoxyguanosine in a murine colonic tissue in an acute colitis model.** Representative images of colonic sections, obtained from controls (A), mice after receiving SiO<sub>2</sub> enriched-chow (B) DSS treated mice receiving normal chow (C) or DSS treated mice receiving SiO<sub>2</sub> enriched-chow (D), stained with an antibody against 8-OHdG (original magnification  $\times$  400). n=3 (ctr), n=4 (SiO<sub>2</sub>, DSS) and n=5 (DSS+SiO<sub>2</sub>).

## 5.4 Discussion

In this study we evaluated the DNA damaging potential of SiO<sub>2</sub> in the presence or absence of neutrophils on intestinal epithelial cells *in vitro*, as well as in a colitic mouse model *in vivo*.

Our *in vitro* model for intestinal inflammation consisted of a co-culture of Caco-2 cells and human primary neutrophils (PMN) at direct cell-cell contact. The model is similar to the one introduced by Vermeer and co-workers (Vermeer *et al.*, 2004) and an established model in our laboratory to address effects of PMN on alveolar epithelial cell lines (Knaapen *et al.*, 1999, 2002a, 2006; Boots *et al.*, submitted). The presently applied co-incubation model allowed us to investigate the effect of activated neutrophils on the genome integrity of human intestinal cells and by varying the number of neutrophils present, different degrees of neutrophilic inflammation could be simulated. Importantly, we used non-confluent undifferentiated Caco-2 cells, which are still capable of cell division and differentiation. As such the influence of a neutrophilic inflammation on the potential genotoxic effects of SiO<sub>2</sub> could be addressed in an optimal manner, since intestinal inflammation is marked by the presence of hyperproliferative epithelial cells (Huang *et al.*, 1997; Arai *et al.*, 1999). Our results clearly show the potential of activated PMN to induce both DNA strand breakage and oxidative lesions in Caco-2 cells. Interestingly, this effect was shown to be dependent on both the number of PMN present and their activation.

A likely explanation for the observed PMN-driven DNA damage is the marked ROS production which is initiated during the respiratory burst of these inflammatory cells. Indeed, it is known that increased ROS formation also occurs in the inflamed tissue of patients suffering from ulcerative colitis (Babbs, 1992) accompanied by a reduced antioxidant potential, as lower levels of glutathione (Sido *et al.*, 1998). Since an increased amount of superoxide anion radicals could be found after activation of neutrophils alone or in the co-culture, we hypothesise that these ROS are the main cause of DNA damage in the Caco-2 cells.

Our previous studies demonstrated the potential of SiO<sub>2</sub> alone to induce oxidative lesions in Caco-2 cells after 4 hours incubation (Gerloff *et al.*, 2009). In the present work, we adapted the application of this nanoparticle to the co-incubation model and determined possible interference of PMN and SiO<sub>2</sub> on DNA damage in the co culture. Surprisingly, the SiO<sub>2</sub> particles alone now induced only significant DNA

strand breaks, but no oxidative lesions. The most likely explanation for this apparent discrepancy between the results of both studies is the difference in treatment time and cell culture conditions. In the present study, to adapt to the conditions of the co-incubation model a shorter incubation time was applied and all experiments were performed in HBSS instead of serum free cell culture media in order to minimise scavenging effects of culture medium constituents. Interestingly, the effects of SiO<sub>2</sub> were not enhanced in the co-incubation, i.e. when neutrophils were also present. Current results indicate that the SiO<sub>2</sub> particles do not activate the neutrophils to induce comparable DNA damage as detected in the presence of PMA, but that the presence of neutrophils in fact decreases the potential of SiO<sub>2</sub> to induce DNA damage in Caco-2 cells.

SiO<sub>2</sub>-induced ROS formation by PMN was determined by two independent methods. No potential of SiO<sub>2</sub> to induce neutrophilic burst could be revealed. This absence correlates nicely with the observed absence of DNA damage within the co-incubation model. The observed abrogation of the DNA damaging effect of SiO<sub>2</sub> in the presence of PMN may be explained by the increased number of total cells in culture (i.e. a 3-fold number of PMN), which thereby reduces the particle number dose per Caco-2 cell. The SiO<sub>2</sub> might preferentially interact with the phagocytosing PMN and thereby the amount of particles faced by Caco-2 cells is reduced, which in turn leads to reduced direct SiO<sub>2</sub> effects on Caco-2 cells. Moreover, the neutrophils are known to contain various antioxidants including superoxide dismutase (Zakhireh *et al.*, 1979), which may scavenge to moderate oxidative effects of the SiO<sub>2</sub> to the Caco-2 cells.

The actual influence of SiO<sub>2</sub> on DNA integrity *in vivo* was investigated in a mouse model of colitis via the application of SiO<sub>2</sub> in the chow. The polysaccharide DSS was used for induction of experimental colitis as it reduces the integrity of the mucosal barrier by causing a direct toxicity to gut epithelial cells (Gaudio *et al.*, 1999; Wirtz and Neurath, 2007). Our *in vivo* comet assay analyses of fresh whole colonic tissue in this model surprisingly revealed reduced DNA lesions after SiO<sub>2</sub> ingestion in both healthy and colitic animals compared to control animals fed a SiO<sub>2</sub>-free diet. The finding that DNA strand breaks were markedly reduced in the colitic mice leads to the assumption that DNA repair mechanisms might be upregulated in colitis. Such upregulation would be in accordance with the results of a previous study performed by Wessels and co-workers in our lab in an experimental model of pulmonary

exposure to nanoparticles (Wessels *et al.*, in press). In this study, no induction of DNA strand breaks or oxidative lesions could be detected in the lungs of mice upon inhalation of spark generated carbon nanoparticles, while several genes regulating DNA repair enzymes tended to be upregulated within this tissue.

In our current study however, immunohistochemical staining of 8-OHdG revealed a clear induction of oxidative lesions in the DNA of epithelial cells after treatment with SiO<sub>2</sub> or DSS. Moreover, the intensity of the induced staining tended to be slightly lower after combined DSS-SiO<sub>2</sub> treatment compared to treatment with either SiO<sub>2</sub> or DSS alone. The discrepancies between the immunohistochemical findings and the comet assay data might lie within the fact that not only epithelial cells are analysed by the latter method, but whole colon tissue. Thus, this also includes other cell types present in the colon, including infiltrated immune cells or small muscle cells, which might lead to a “dilution” of the overall determined effect. Moreover, one should take into account that the *in vivo* comet assay method requires processing time to isolate cells and nuclei from the tissue homogenates, during which potential artefacts may be induced. In contrast, IHC staining allows for the specific detection of 8-OHdG formation in individual cells.

Caco-2 cells, although isolated from a colon adenocarcinoma, form an apical brush border and microvilli upon differentiation (Chantret *et al.*, 1988) and thus show several properties of the small intestine. To investigate the influence of ingested SiO<sub>2</sub> on the gene integrity of the small intestine *in vivo*, the comet assay was also performed in whole small intestinal tissue. In line with our findings within the colonic tissue, no DNA damage was detectable in the small intestine after chronic ingestion of SiO<sub>2</sub>. In contrast to a short-term study of Hong *et al.* (2005) who administered DSS in the drinking water for 48 hours, we also could not find any oxidative DNA damage in whole tissue samples of the small intestine after DSS treatment in our chronic study by Fpg-modified comet-assay analysis.

To address whether the observations were due to the chronic exposure conditions we also performed an acute colitis study. Comparably to our results of the chronic study, no induction of DNA strand breaks or oxidative lesions were found in colons of DSS treated mice. However, oxidative DNA damage tended to be increased after treatment with SiO<sub>2</sub> alone, although this did not reach statistical significance and may be due to the limited number of animals investigated. Remarkably, the oxidative DNA damage in the SiO<sub>2</sub> treatment group was significantly

higher than the damage found in the DSS+SiO<sub>2</sub> treatment group when the absolute amount of strand breaks plus oxidative lesions were considered (Figure 5.9 A), whereas IHC staining for 8-OHdG lesions did not show marked differences within the four treatment groups. However, the comet assay results are in concordance to our *in vitro* results, where the DNA damaging potential of SiO<sub>2</sub> seemed to be reduced in an inflammatory environment. The mechanisms of these *in vivo* effects require further investigation in view of their relevance for hazard and risk assessment of ingested SiO<sub>2</sub> and other nanoparticles, but also because of potential preventive or therapeutic strategies in patients suffering from inflammatory bowel diseases.

As already mentioned it should be emphasised that the *in vivo* comet assay used in our study reflects alterations in the whole tissue. Therefore it determines not exclusively the DNA damage of epithelial cells which are considered relevant target cells for colon carcinogenesis (Itzkowitz *et al.*, 2004). The DNA damage measured by the *in vivo* comet assay also may reflect integrity changes in endothelial cells, smooth muscle cells or, most importantly inflammatory cells, which might dilute a possible damage of the epithelial DNA. Earlier studies detected increased levels of 8-hydroxydeoxyguanosine (8-OHdG) in isolated colonic mucosal cells of DSS treated rats by HPLC (Tardieu *et al.*, 1998) or in whole colonic rat tissue, measured by quantitative immunohistochemistry (Hong *et al.*, 2005). The latter finding could be confirmed in our chronic colitis model for treatment with DSS, but not after co-treatment with DSS and SiO<sub>2</sub>. This suggests that the *in vivo* comet assay of whole tissue might not be sensitive or specific enough to detect slight alterations in epithelial DNA damage. Additionally, Westbrook *et al.* (2009) could detect systemic DNA damage after chronic DSS treatment in mice, as found in peripheral leukocytes, detected with the alkaline comet assay during acute colitis. However they also reported a slight decrease of DNA strand breaks during remission cycles, in concordance with the observations in our current study of chronic colitis.

Here we highlighted the effects of amorphous SiO<sub>2</sub>, possibly present in food or pharmaceuticals, on the genome integrity of the healthy or inflammatory intestinal epithelium *in vitro* and *in vivo*. We analysed the effects of activated human primary neutrophils on the genome integrity of Caco-2 cells in an *in vitro* model of intestinal inflammation. The induction of oxidative lesions was dependent on the amount of activated inflammatory cells and associated with the neutrophilic burst. In the presence of SiO<sub>2</sub> no significant neutrophil-activation was detected, as measured by



reactive oxygen species formation. In line with these observations, the concurrent incubation of Caco-2 cells with neutrophils and SiO<sub>2</sub> did not lead to an augmented DNA damage when compared to the effect of SiO<sub>2</sub> alone. We further analysed the DNA damaging properties of ingested SiO<sub>2</sub> on the intestine in a DSS-induced colitic mouse model. DSS alone did not induce DNA strand breakage in the colons in both acute and chronic colitis studies. Treatment with SiO<sub>2</sub> in healthy or colitis mice also did not lead to a significant enhancement of DNA damage measured by the *in vivo* Fpg-comet assay, whereas slight induction of 8-OHdG lesions was shown in immunohistochemical staining in the chronically, but not in the acutely treated colons. We conclude that the risk of SiO<sub>2</sub> ingestion on the genome integrity of the intestine is low, also in the inflamed gut, taken into account that a rather high concentration was used. Importantly however, slightly increased oxidative lesions were found locally after chronic SiO<sub>2</sub> treatment. Moreover, systemic or long-term damage could not be excluded, and extrapolation of our current results to the human situation is limited and should be done with caution. Concern about the potential genotoxic hazard of nanoparticles in food was recently expressed on the basis of the investigations by Trouiller and co-workers, who showed marked systemic DNA damage and mutagenesis in mice after oral uptake of TiO<sub>2</sub> nanoparticles (Trouiller *et al.*, 2009). In contrast to our investigations no data were provided in their study on local (geno)toxic effects in the intestine. In our present study, the mice chow contained 0.1 mass % of SiO<sub>2</sub> (estimated daily intake: 200 mg/kg body weight), which is in the range of the concentrations of TiO<sub>2</sub> within the drinking water as applied by Trouiller *et al.* (2009). The different methods of administration of the tested particles also need to be considered in the interpretation of both studies for risk assessment purposes. An appropriate extrapolation of our current findings to human risk assessment requires a thorough evaluation of both quantitative (mass and number dose) and qualitative (size, aggregation/agglomeration, etc.) particle properties in consumer products such as food and beverages. Presently such information is still very limited.

## **Acknowledgements**

This study was financially supported by a grant from the German Research Council (Deutsche Forschungsgemeinschaft - Graduate College GRK-1427).

## **Declaration**

The manuscript is currently in preparation.

All experimental *in vitro* work, processing of the isolated tissue samples for the *in vivo* Fpg comet assay and the IHC staining as well as the performance and analysis of the *in vivo* Fpg comet assay was performed by Kirsten Gerloff. The impact on authoring this paper can be estimated in total with 90%.

## 5.5 References

- Arai N, Mitomi H, Ohtani Y, Igarashi M, Kakita A, Okayasu I. Enhanced epithelial cell turnover associated with p53 accumulation and high p21WAF1/CIP1 expression in ulcerative colitis. *Mod Pathol* 1999;12(6):604-11
- Ashwood P, Thompson RP, Powell JJ. Fine particles that adsorb lipopolysaccharide via bridging calcium cations may mimic bacterial pathogenicity towards cells. *Exp Biol Med (Maywood)* 2007;232(1):107-17.
- Babbs CF. Oxygen radicals in ulcerative colitis. *Free Radic Biol Med* 1992;13(2):169-81
- Boots AW, Gerloff K, van Berlo F, Ledermann K, Haenen GRMM, Bast A, Albrecht C, Schins RPF. Neutrophils augment LPS-mediated pro-inflammatory signaling in human lung epithelial cells, submitted
- Chantret I, Barbat A, Dussaulx E, Brattain MG, Zweibaum A. Epithelial polarity, villin expression, and enterocytic differentiation of cultured human colon carcinoma cells: a survey of twenty cell lines. *Cancer Res* 1988;48(7):1936-42
- Chaudhry Q, Scotter M, Blackburn J, Ross B, Boxall A, Castle L, Aitken R, Watkins R. Applications and implications of nanotechnologies for the food sector. *Food Addit Contam Part A Chem Anal Control Expo Risk Assess* 2008;25(3):241-58
- Cooper HS, Murthy SN, Shah RS, Sendergran DJ. Clinicopathologic study of dextran sulphate sodium experimental murine colitis. *Lab Invest* 1993;69(2):238-249
- Desai MP, Labhsetwar V, Amidon GL, Levy RJ. Gastrointestinal uptake of biodegradable microparticles: effect of particle size. *Pharm Res* 1996;13(12):1838-45
- Donaldson K, Tran L, Jimenez LA, Duffin R, Newby DE, Mills N, MacNee W, Stone V. Combustion-derived nanoparticles: a review of their toxicology following inhalation exposure. *Part Fibre Toxicol* 2005;2:10
- Driscoll KE, Deyo LC, Carter JM, Howard BW, Hassenbein DG, Bertram TA, 1997. Effects of particle exposure and particle-elicited inflammatory cells on mutation in rat alveolar epithelial cells. *Carcinogenesis* 18: 423-430.
- Duffin R, Tran L, Brown D, Stone V, Donaldson K. Proinflammogenic effects of low-toxicity and metal nanoparticles in vivo and in vitro: highlighting the role of particle surface area and surface reactivity. *Inhal Toxicol* 2007;19(10):849-56
- Fatahzadeh M. Inflammatory bowel disease. *Oral Surg Oral Med Oral Pathol Oral Radiol Endod* 2009;108(5):e1-10
- food.gov.uk homepage:  
<http://www.food.gov.uk/safereating/chemsafe/additivesbranch/enumberlist> (May 2010)
- Gaudio E, Taddei G, Vetusch A, Sferra R, Frieri G, Ricciardi G, Caprilli R. Dextran sulfate sodium (DSS) colitis in rats: clinical, structural, and ultrastructural aspects. *Dig Dis Sci* 1999;44(7):1458-75
- Gerloff K, Albrecht C, Boots AW, Förster I, Schins RPF. Cytotoxicity and oxidative DNA damage by nanoparticles in human intestinal Caco-2 cells. *Nanotoxicol* 2009; 3(4):355-364

- Gerloff K, Pereira D, Faria N, Boots AW, Förster I, Albrecht C, Powell JJ, Schins RPF. Influence of simulated gastrointestinal digestion on particulate mineral oxide- induced cytotoxicity and interleukin-8 regulation in differentiated and undifferentiated Caco-2 cells. In preparation
- Hillery AM, Jani PU, Florence AT. Comparative, quantitative study of lymphoid and non-lymphoid uptake of 60 nm polystyrene particles. *J Drug Target* 1994;2(2):151-6
- Hong MY, Turner ND, Carroll RJ, Chapkin RS, Lupton JR. Differential response to DNA damage may explain different cancer susceptibility between small and large intestine. *Exp Biol Med (Maywood)* 2005;230(7):464-71
- Huang N, Katz JP, Martin DR, Wu GD. Inhibition of IL-8 gene expression in Caco-2 cells by compounds which induce histone hyperacetylation. *Cytokine* 1997;9(1):27-36
- Itzkowitz SH, Yio X. Inflammation and cancer IV. Colorectal cancer in inflammatory bowel disease: the role of inflammation. *Am J Physiol Gastrointest Liver Physiol* 2004;287(1):G7-17
- Jani PU, McCarthy DE, Florence AT. Titanium dioxide (rutile) particle uptake from the rat GI tract and translocation to systemic organs after oral administration. *J Pharm* 1994;105(2):157-168
- Johnston CJ, Driscoll KE, Finkelstein JN, Baggs R, O'Reilly MA, Carter J, Gelein R, Oberdörster G. Pulmonary chemokine and mutagenic responses in rats after subchronic inhalation of amorphous and crystalline silica. *Toxicol Sci* 2000;56(2):405-13
- Jung HC, Eckmann L, Yang SK, Panja A, Fierer J, Morzycka-Wroblewska E, Kagnoff MF. A distinct array of proinflammatory cytokines is expressed in human colon epithelial cells in response to bacterial invasion. *J Clin Invest* 1995;95(1):55-65
- Knaapen AM, Seiler F, Schilderman PA, Nehls P, Bruch J, Schins RP, Borm PJ. Neutrophils cause oxidative DNA damage in alveolar epithelial cells. *Free Radic Biol Med* 1999;27(1-2):234-40
- Knaapen AM, Schins RP, Polat D, Becker A, Borm PJ. Mechanisms of neutrophil-induced DNA damage in respiratory tract epithelial cells. *Mol Cell Biochem* 2002a;234-235(1-2):143-51
- Knaapen AM, Albrecht C, Becker A, Höhr D, Winzer A, Haenen GR, Borm PJA, Schins RPF. DNA damage in lung epithelial cells isolated from rats exposed to quartz: role of surface reactivity and neutrophilic inflammation. *Carcinogenesis* 2002b;23:1111-1120
- Knaapen AM, Güngör N, Schins RP, Borm PJ, Van Schooten FJ. Neutrophils and respiratory tract DNA damage and mutagenesis: a review. *Mutagenesis* 2006;21(4):225-36
- Kucharzik T, Williams IR. Neutrophil migration across the intestinal epithelial barrier--summary of in vitro data and description of a new transgenic mouse model with doxycycline-inducible interleukin-8 expression in intestinal epithelial cells. *Pathobiology* 2002-2003;70(3):143-9
- Kunkel SL, Standiford T, Kasahara K, Strieter RM. Interleukin-8 (IL-8): the major neutrophil chemotactic factor in the lung. *Exp Lung Res* 1991;17(1):17-23
- Lomer MC, Harvey RS, Evans SM, Thompson RP, Powell JJ. Efficacy and tolerability of a low microparticle diet in a double blind, randomized, pilot study in Crohn's disease. *Eur J Gastroenterol Hepatol* 2001;13(2):101-6
- Lomer MC, Hutchinson C, Volkert S, Greenfield SM, Catterall A, Thompson RP, Powell JJ. Dietary sources of inorganic microparticles and their intake in healthy subjects and patients with Crohn's disease. *Br J Nutr* 2004;92(6):947-55
- MacDermott. Chemokines in the inflammatory bowel disease. *J Clin Immunol* 1999;19(5):266-72

- Mazzucchelli L, Hauser C, Zraggen K, Wagner H, Hess M, Laissue JA, Mueller C. Expression of interleukin-8 gene in inflammatory bowel disease is related to the histological grade of active inflammation. *Am J Pathol* 1994;144(5):997-1007
- Mitsuyama K, Toyonaga A, Sasaki E, Watanabe K, Tateishi H, Nishiyama T, Saiki T, Ikeda H, Tsuruta O, Tanikawa K. IL-8 as an important chemoattractant for neutrophils in ulcerative colitis and Crohn's disease. *Clin Exp Immunol* 1994;96(3):432-6
- Monteiller C, Tran L, MacNee W, Faux S, Jones A, Miller B, Donaldson K. The pro-inflammatory effects of low-toxicity low-solubility particles, nanoparticles and fine particles, on epithelial cells in vitro: the role of surface area. *Occup Environ Med* 2007;64(9):609-15
- Nanotechproject homepage  
<http://www.nanotechproject.org/inventories/consumer/browse/products/5107/> (April 2010)
- Oberdörster G, Oberdörster E, Oberdörster J. Nanotoxicology: an emerging discipline evolving from studies of ultrafine particles. *Environ Health Perspect* 2005;113(7):823-39
- Okayasu I, Hatakeyama S, Yamada M, Ohkusa T, Inagaki Y, Nakaya R. A novel method in the induction of reliable experimental acute and chronic ulcerative colitis in mice. *Gastroenterol* 1990;98(3):694-702
- Powell JJ, Faria N, Thomas-McKay E, Pele LC. Origin and fate of dietary nanoparticles and microparticles in the gastrointestinal tract. *J Autoimmun* 2010;34(3):J226-33
- Risom L, Møller P, Vogel U, Kristjansen PE, Loft S. X-ray-induced oxidative stress: DNA damage and gene expression of HO-1, ERCC1 and OGG1 in mouse lung. *Free Radic Res* 2003;37(9):957-66
- Rogler G, Andus T. Cytokines in inflammatory bowel disease. *World J Surg* 1998;22(4):382-9
- Schins RP, Knaapen AM. Genotoxicity of poorly soluble particles. *Inhal Toxicol* 2007;19 (Suppl 1):189-98
- Schmid K, Riediker M. Use of nanoparticles in Swiss Industry: a targeted survey. *Environ Sci Technol* 2008;42(7):2253-60
- Schneider JC. Can microparticles contribute to inflammatory bowel disease: innocuous or inflammatory? *Exp Biol Med (Maywood)* 2007;232(1):1-2
- Sido B, Hack V, Hochlehnert A, Lipps H, Herfarth C, Dröge W. Impairment of intestinal glutathione synthesis in patients with inflammatory bowel disease. *Gut* 1998;42(4):485-92
- Singh S, Shi T, Duffin R, Albrecht C, van Berlo D, Höhr D, Fubini B, Fenoglio I, Martra G, Borm PJA, Schins RPF. Endocytosis, oxidative stress and IL-8 expression in human lung epithelial cells upon treatment with fine and ultrafine TiO<sub>2</sub>: role of particle surface area and of surface methylation of the particles. *Toxicol Applied Pharmacol* 2007;222:141-151
- Speit G, Schütz P, Bonzheim I, Trenz K, Hoffmann H. Sensitivity of the FPG protein towards alkylation damage in the comet assay. *Toxicol Lett* 2004;146(2):151-8
- Tardieu D, Jaeg JP, Cadet J, Embvani E, Corpet DE, Petit C. Dextran sulfate enhances the level of an oxidative DNA damage biomarker, 8-oxo-7,8-dihydro-2'-deoxyguanosine, in rat colonic mucosa. *Cancer Lett* 1998;134(1):1-5

- Tiede K, Boxall AB, Tear SP, Lewis J, David H, Hasselov M. Detection and characterization of engineered nanoparticles in food and the environment. *Food Addit Contam Part A Chem Anal Control Expo Risk Assess* 2008;25:795-821
- Trouiller B, Reliene R, Westbrook A, Solaimani P, Schiestl RH. Titanium dioxide nanoparticles induce DNA damage and genetic instability in vivo in mice. *Cancer Res* 2009;69(22):8784-9
- Unfried K, Albrecht C, Klotz LO, von Mikecz A, Grether-Beck S, Schins RPF. Cellular responses to nanoparticles: target structures and mechanisms. *Nanotoxicol* 2007;1:52-71
- Vermeer IT, Henderson LY, Moonen EJ, Engels LG, Dallinga JW, van Maanen JM, Kleinjans JC. Neutrophil-mediated formation of carcinogenic N-nitroso compounds in an in vitro model for intestinal inflammation. *Toxicol Lett* 2004;154(3):175-82
- Wessels A, Van Berlo D, Boots AW, Gerloff K, Scherbart A, Cassee FR, Gerlofs-Nijland ME, Van Schooten FJ, Albrecht C, Schins RPF. Oxidative stress and DNA damage responses in rat and mouse lung to inhaled carbon nanoparticles. In press, *Nanotoxicology*
- Westbrook AM, Wei B, Braun J, Schiestl RH. Intestinal mucosal inflammation leads to systemic genotoxicity in mice. *Cancer Res* 2009;69(11):4827-34
- Wirtz S, Neurath MF. Mouse models of inflammatory bowel disease. *Adv Drug Deliv Rev* 2007;59(11):1073-83
- Zakhireh B, Block LH, Root RK. Neutrophil function and host resistance. *Infection* 1979;7(2):88-98

## CHAPTER 6

---

### 6 General Discussion

Presently, very little is known about potential toxic, genotoxic or pro-inflammatory effects of food-relevant metal oxide nanoparticles (NP) in the human intestine. This thesis aimed to contribute to a better understanding of possible adverse effects and their underlying mechanisms of several of these materials, thus leading to improved hazard and risk assessment.

As hardly any information on the extent of NP usage in food and, if indeed used, the characteristics of these materials is available, the first intention of this work was to determine the toxic and DNA damaging potential of a choice of particles that might already find their way in modern food products (**Chapter 2**). The use of nano-sized titanium dioxide ( $\text{TiO}_2$ ) is already described, and patents exist describing its potential for use in confectionary products, but the actual size and structure of the applied materials remains unclear (Chaudhry *et al.*, 2008; Bouwmeester *et al.*, 2009; Mars Inc.'s US Patent US 5741505). Amorphous silicon dioxide ( $\text{SiO}_2$ ) is known to induce DNA fragmentation, increased influx of PMN and cytotoxicity in rat lungs upon subchronic inhalation (Johnston *et al.*, 2000), whereas hardly any evidence on possible adverse health effects in the intestine has been reported. Accordingly, amorphous  $\text{SiO}_2$  has a long-standing use in pharmaceuticals (US Patent US 2002/0025964 A1), and general  $\text{SiO}_2$  use in food is already described (Chaudhry *et al.*, 2008; Schmid and Riediker, 2008; homepage nanotechproject.org). Zinc oxide (ZnO) and magnesium oxide (MgO) both can be used in food packages as well as in food directly (Chaudhry *et al.*, 2008; homepage nanotechproject.org). Carbon black (CB) was chosen as a model of environmental nanoparticles; diesel exhaust e.g. contains carbonaceous nanoparticles and (I) these can be inhaled and subsequently transported into the gastrointestinal tract upon mucociliary clearance or (II) may deposit on vegetables grown on fields close to high-traffic roads or upon transportation (Dybdahl *et al.*, 2003).

Upon treatment of Caco-2 cells with this selection of NP, a clear potential of ZnO and  $\text{SiO}_2$  could be found to induce both cytotoxicity as well as DNA strand breakage and oxidative lesions, respectively, associated with induction of intracellular

oxidative stress, as further confirmed by reduction of the intracellular GSH content (**Chapter 2**). The adverse effects that could be determined are depicted in Figure 6.1. A DNA damaging potential of TiO<sub>2</sub> upon processing by light was already shown for various cells lines and confirmed in the present study using Caco-2 cells, but obviously photoactivation is not an issue within the human intestine (Nakagawa *et al.*, 1997; Sayes *et al.*, 2006; Johnston *et al.*, 2009). Comparison of three samples of TiO<sub>2</sub> and ZnO respectively, each featuring different specific surface areas (SSA), revealed no relationship between the DNA damaging potential and a varying SSA for both materials tested. However, cytotoxicity appeared to be elevated when using the high-SSA TiO<sub>2</sub> samples.

To follow-up on this study two additional TiO<sub>2</sub> particles were included and all five samples were analysed for crystallinity, primary particle size, SSA and aggregation/agglomeration (**Chapter 3**). Two samples contained both anatase and rutile and were found to have a similar SSA, in contrast to three pure anatase powders with one having a very low and two a very high SSA respectively. Interestingly, only the anatase-rutile containing particles caused mild cytotoxicity and DNA oxidation under exclusion of illumination. Similarly to the first study (**Chapter 2**), the effects could not be explained by the different SSA of the samples. The results indicated that cytotoxic and DNA damaging properties of TiO<sub>2</sub> in Caco-2 cells are at least in part driven by their chemical composition. This highlights the need for thorough evaluation and labelling of the TiO<sub>2</sub> species within the final (food) product.

As SiO<sub>2</sub> and ZnO were found to be the most cytotoxic and DNA damaging particles (**Chapter 2**), their solubility and aggregational/agglomerational potential was further determined, as well as their uptake onto differentiated Caco-2 cells (**Chapter 4**). ZnO was found to be absorbed more effectively, and upon analysis of possible uptake mechanisms both microtubule-dependent and clathrin/AP2-mediated endocytosis did not seem to be of major importance in both systems. This suggests that further research is needed to discriminate between actual uptake into versus adhesion onto the cells. Moreover, phagocytosis, macropinocytosis or diffusion might play a role, always depending on the particle properties and the exposed cell type (Unfried *et al.*, 2007). The influence of gastrointestinal digestion was simulated by means of pH changes (**Chapter 4**), and both materials were found to be highly aggregated/agglomerated before and after the simulated digestion. For this study, undifferentiated as well as differentiated Caco-2 cells were used to test cytotoxic and



pro-inflammatory effects of both the native and digestion-simulated (DS) particles. Pre-treatment under gastrointestinal conditions was found to markedly reduce the ability of both materials to generate acellular reactive oxygen species. However, native versus DS particles showed comparable effects on cell viability. ZnO decreased viability of both undifferentiated and differentiated cells in a dose and time dependent manner, whereas surprisingly SiO<sub>2</sub> was only cytotoxic to undifferentiated cells. Interestingly, interleukin-8 (IL-8) secretion after SiO<sub>2</sub> treatment appeared lower in differentiated compared to undifferentiated cells, whereas the secretion following ZnO incubation was markedly higher in the differentiated Caco-2 cells. The digestion simulation treatment of the particles did not affect their ability to induce IL-8 mRNA expression and secretion.

In **Chapter 5**, an inflammatory intestinal condition was simulated by incubating Caco-2 cells with primary human neutrophils, important phagocytes in the innate immune response. The effect of the PMN on the genome integrity of the intestinal cells and the influence of SiO<sub>2</sub> on this system was evaluated. When activated with PMA, neutrophils strongly induced DNA strand breakage and oxidative lesions in Caco-2 cells, going along with generation of superoxide anion radicals (Figure 6.1). SiO<sub>2</sub> however did not induce the oxidative burst of the PMN, and surprisingly the presence of SiO<sub>2</sub> in the co-culture appeared to even reduce the DNA damaging potential of PMN. Current *in vitro* findings might actually provide some insight to not only the adverse, but also potential beneficial effects associated with oral exposure to specific types of NP. Therefore, the significance of these interesting findings was additionally evaluated *in vivo*. Mouse studies were performed to determine the impact of ingested SiO<sub>2</sub> in the healthy and colitic gut. Chronic and acute colitis symptoms were induced by treatment with dextrane sulphate sodium (DSS). Immunohistochemical staining revealed an induction of oxidative lesions in the colonic epithelium of SiO<sub>2</sub> or DSS treated mice in the chronic, but not in the acute colitis experiment. Interestingly the co-treatment of SiO<sub>2</sub> and DSS did not induce 8-OHdG. Contrary, the *in vivo* comet assay, an assay well known for its high sensitivity for quantification of both overall DNA strand breakage and oxidative lesions (Liao *et al.*, 2009), revealed neither elevated levels of DNA strand breaks nor enhanced oxidative lesions in the colitic colon, regardless of SiO<sub>2</sub> treatment. Moreover, in specific circumstances the damage appeared even alleviated compared to the control animals (in the chronic study) or compared to the SiO<sub>2</sub> treated mice (in

the acute study). Direct interactions between SiO<sub>2</sub> and DSS can be excluded as an explanation for this, since time-staggered treatment of both substances was performed. Notably, the *in vivo* comet assay did not only include epithelial cells into the analysis, but also infiltrated immune or smooth muscle cells e.g., thus most likely leading to a dilution effect in determining epithelial DNA strand break alteration. However, in future experiments, the use of more sophisticated models of colitis (e.g. knock out animals that develop spontaneous colitic symptoms, such as STAT3 deficient or VILLIN-HA x CL4-TCR mice) might add valuable information about these mechanisms (Westendorf *et al.*, 2006; Reindl *et al.*, 2007). Not surprisingly, no effect was observed in the small intestinal tissue after chronic colitis induction, as colitis usually only affects the large intestine.

Taken together, the present studies demonstrated a cytotoxic and/or DNA damaging potential of a variety of food relevant NP, and a simulated gastro- and intestinal digestion did not influence the cytotoxic potential of SiO<sub>2</sub> and ZnO. However, both materials strongly induced pro-inflammatory cytokine secretion that might lead to a subsequent infiltration and activation of neutrophils *in vivo*. Ongoing experiments on mouse colonic tissues will focus on this matter. The genotoxic potential of activated PMN towards human intestinal cells was demonstrated by elevated levels of DNA strand breakage and oxidative lesions, but SiO<sub>2</sub> clearly did not trigger this effect *in vitro*.

It should be emphasised that in all studies performed in the framework of this thesis, relatively high concentrations were chosen. The actual amount of ingested particles for consumers is considered to be markedly lower. The predominantly applied dose in the *in vitro* studies was 20 µg/cm<sup>2</sup>. Considering an exemplary intestinal surface area of 200 m<sup>2</sup> (Wells *et al.*, 1995) which equates to 2,000,000 cm<sup>2</sup>, our dose represents a single dose of 40 g particles (assuming that all material distributes equally over this system). Lomer and colleagues calculated an average daily TiO<sub>2</sub> (micro)particle intake of around 2.7 mg and a daily ingestion of 4.5 mg mixed silicates per person (Lomer *et al.*, 2004), which is expected to increase dramatically, but is still around 5000 times lower compared to the *in vitro* doses used in the present studies. However, ingested particles do not immediately disperse throughout the whole intestine, and the small intestine is the first segment of the gut facing the particles. It is more specialised for uptake than the colon and therefore might be burdened more than other intestinal tissues. Furthermore, a daily ingestion

of particles can lead to accumulation. This has already been shown for microparticles by the presence of so-called pigment cells (PC), mainly mature macrophages located at the base of Peyer's patches that contain particle-filled lysosomes (Thoree *et al.*, 2008). Up to now these PC were mainly challenged with microparticles and are found widely unreactive, but an increase of NP in our diet, accompanied by elevated uptake (Desai *et al.*, 1996) and an increased intrinsic reactivity (Oberdörster *et al.*, 2005) might rapidly increase the amount of accumulated particles and possibly alter the activity of PC. Therefore, single application of relatively high doses enables a first screening and discrimination of the hazardous potential of the various materials tested. As no effects were found after treatment with MgO and CB (**Chapter 2**), even at these relatively high doses, further approaches focused on TiO<sub>2</sub> (**Chapter 3**), ZnO (**Chapter 4**) and SiO<sub>2</sub> (**Chapter 4, 5**).

Contrasting to various findings in the lung *in vitro* and *in vivo*, we could not find any relation of the SSA with the toxicity of TiO<sub>2</sub> in the Caco-2 cells (Oberdörster *et al.*, 2005; Monteiller *et al.*, 2007; Johnston *et al.*, 2009). In our hands, this effect was found to mainly depend on the chemical composition, as the anatase-rutile containing particles were more reactive than pure anatase, when photoactivation was avoided. This effect however was in line with the studies from Gurr and colleagues (Gurr *et al.*, 2005) and Grassian *et al.* (2007). The present study is the first to confirm this phenomenon to be true for particle treatment of intestinal cells. A thorough validation of the material properties herewith appears to be of major importance.

Agglomeration/aggregation of nanoparticles is a well-known issue, and nearly all studies report this instance, if particles were used without certain stabilisation. For the present studies it was deliberately refrained from stabilising the particles in suspension, as no information is available on the properties of particles or their stabilisation in food or within the human body. However, this raises the question if working with merely aggregated/agglomerated materials actually means analysis of nanoparticle behaviour. This issue is currently discussed controversial amongst scientists, but the aim of this thesis was not to analyse an artificial system but to approximate the *in vivo* situation. Herein, analysis and characterisation of NP within the body is presently complicated and aggregational behaviour not clearly described. Additionally even aggregated/agglomerated nanoparticles still feature a higher SSA compared to their micro-sized counterparts, and were found to induce

stronger oxidative and pro-inflammatory effects in lung epithelial cells (Singh *et al.*, 2007).

The simulation of gastrointestinal digestion was a first approach to study altered NP behaviour by means of physiological pH changes. For ongoing studies this assay clearly can be modified to even more resemble the *in vivo* situation. For example, certain enzymes might be included to the buffers, such as pepsin to the gastric buffer, or artificial bile and glycoproteins such as mucin to the intestinal buffer (Zhao *et al.*, 1998; Sripanyakorn *et al.*, 2009). Nevertheless, this was the first study performed to analyse the influence of gastrointestinal pH changes on NP toxicity, and even though the ROS generating potential appeared reduced, it was even more surprising that no alteration in cytotoxicity or the pro-inflammatory potential could be found. These experiments also enabled us to conclude that the behaviour and toxic potential of particles used for “conventional” cell treatment is close to physiological particle behaviour, as we couldn’t find significant differences in treatment of DS or native particles. It will be interesting to determine the influence of the digestion simulation on the DNA damaging potential of the materials, even before extending the buffers with enzymes or (glyco)proteins.

Various other methods can be considered in the hazard screening of NP for the GI tract. For instance, investigations on the uptake of NP into the intestinal epithelium can be further enhanced by using a transwell system. Herein, cells grow on a permeable membrane to form a confluent cell layer, and are in contact with cell culture media within an underlying well and directly upon the cells. Using this system, differentiated cells express an apical, i.e. luminal aligned, and a basal side. This model allows studying not only particle uptake, but also active particle transport. Therefore, the cells would be incubated apically, which equals the physiological situation. After a certain period, the media on the basal side could then be analysed for the amounts of particles by quantification of the respective element via ICP-OES, as described in **Chapter 4**, or other methods, such as electron microscopy. Gullberg *et al.* developed an *in vitro* M-cell model by co-culturing Caco-2 cells and B-cell lymphoma Raji cells, whereupon the epithelial cells express various M-cell markers and an altered morphology (Gullberg *et al.*, 2000). This model could be used to compare to the uptake capacity of “normal” differentiated Caco-2 cells and to further evaluate the underlying mechanisms, for example by use of specific uptake inhibitors (e.g. cytochalasin D to inhibit actin polymerisation) (Quaddoumi *et al.* 2004).

The co-incubation model of Caco-2 cells and PMN was first used as an in vitro model for intestinal inflammation by Vermeer and co-workers (2004), based on preceding studies using co-incubation models of primary human neutrophils and lung epithelial cell lines in the same laboratory to address the role of inflammation in pulmonary toxicity (Borm *et al.*, 1997; Knaapen *et al.*, 1999). In inflammatory bowel diseases such as UC, a clear correlation exists between the amount of infiltrated neutrophils and the grade of local inflammation (Mazzucchelli *et al.*, 1994; Mitsuyama *et al.*, 1994). Epithelial cells in active UC are known to be hyperproliferative (Huang *et al.*, 1997; Arai *et al.*, 1999), which is simulated in this assay by the use of semiconfluent, proliferating Caco-2 cells. However, studies on undifferentiated Caco-2 cells always need to be viewed critically, as they feature various properties of cancer cells. In future experiments, this co-culture model could be modified to investigate the influence of repeated incubation of a confluent Caco-2 cell layer, reflecting the healthy intestinal epithelium, with activated PMN to simulate an inflammatory onset. It will be interesting to determine whether this would lead to an altered permeability of the cell layer, when Caco-2 cells are grown in a transwell system, and whether this would influence NP toxicity and their pro-inflammatory potential, e.g. by determination of the transepithelial resistance (TEER) or intercellular communication (connexins). Investigation of the mRNA regulation of DNA repair enzymes (e.g. apurinic/aprimidinic endonuclease [APE/Ref-1], 8-oxoguanine DNA glycosylase [OGG1], DNA-polymerase  $\alpha$  [DNA-pol- $\alpha$ ]) or markers for oxidative stress (such as heme oxygenase 1 [HO-1]) are further approaches for both the existing and the modified model.

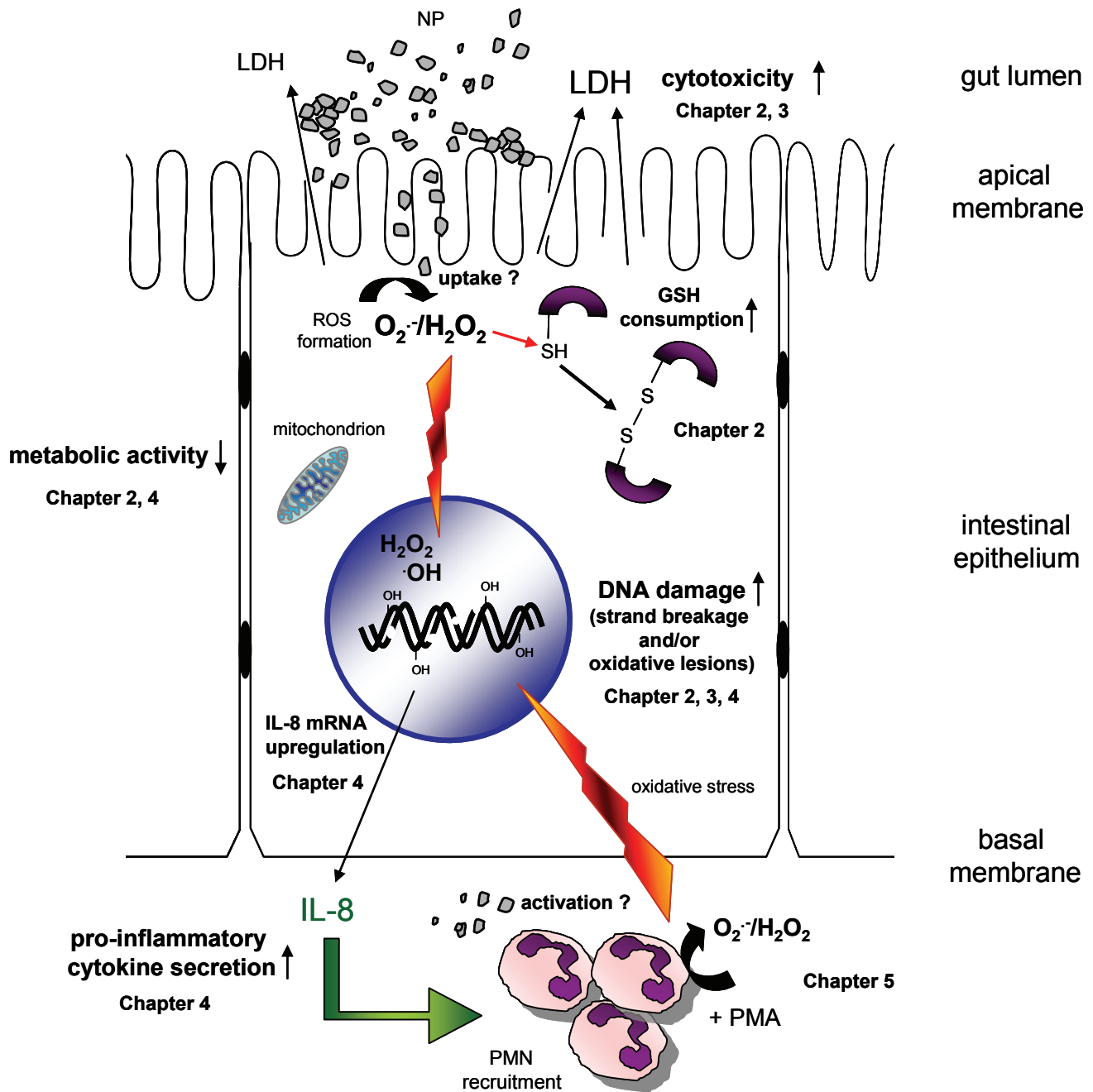


**Figure 6.1 Overview of the various possible adverse NP effects as determined in the present thesis.** Specific NP were found to cause cytotoxicity (LDH leakage following membrane damage and/or decreased mitochondrial metabolic activity), oxidative stress (consumption of glutathione [GSH] and induction of oxidative lesions, as depicted by DNA-associated OH-groups), DNA strand breakage and the mRNA expression and secretion of the pro-inflammatory cytokine interleukin-8 (IL-8). IL-8 is implicated in the recruitment of neutrophils (PMN) from the blood capillaries. PMN were found to induce DNA strand breakage and oxidative lesions in intestinal epithelial cells upon activation with phorbol myristate acetate (PMA), but not upon treatment with specific NP ( $SiO_2$ ).

## 6.1 Conclusions

Taken together, the present thesis contributes to our understanding about possible hazards of food relevant nanoparticles, a knowledge which currently is rather limited. The potential of TiO<sub>2</sub>, SiO<sub>2</sub> and ZnO to induce cyto- and/or genotoxicity in a human intestinal epithelial cell line was clearly demonstrated. The induction of oxidative stress was shown by reduction of the intracellular antioxidant glutathione and oxidative DNA damage induction. Ongoing studies should be performed to further confirm the importance of oxidative stress by the use of antioxidants (reduced oxidative lesions expected) or depletion of glutathione (increased oxidative lesions expected). In view of current research interest and focus on antioxidant applications in food, it may also be interesting to use non-toxic NP for pharmaceutical and nutraceuticals applications. For example, various antioxidants such as quercetin might be taken up more efficiently when coated with or bound to certain nanomaterials, thus leading to a more directed uptake to the target tissues and increased bioavailability (Boots *et al.*, 2008; Lopes *et al.*, 2010).

For TiO<sub>2</sub>, it was shown that the hazardous potential was merely dependent on the chemical composition, and not on the SSA, as previously expected. Presently it is still too preliminary to recommend the preferential use of pure anatase particles and avoidance of the more reactive rutile-anatase particles in the food sector. However further screening of various TiO<sub>2</sub> formulations is advisable. Furthermore, the present work demonstrated that the physiological pH changes throughout digestion processes did not alter the cytotoxic and pro-inflammatory potential of SiO<sub>2</sub> and ZnO for the evaluated effects. The reduction of the ROS activating potential in the cell-free system further points towards an even reduced reactivity within the human body. This hypothesis was further underlined by the performed *in vivo* study. No DNA damaging effect of ingested SiO<sub>2</sub> was found in the colitic murine intestine. An *in vitro* intestinal inflammation model confirmed these findings. Moreover, SiO<sub>2</sub> appears to even provide certain beneficial effects when inflammatory cells are present, both *in vitro* and *in vivo*. This is an important observation in view of using NP in therapeutic or molecular preventive medicine approaches, and currently ongoing investigations focus on this topic.

A further aspect of the current thesis relates to the specific methods used. The *in vitro* assays developed and used, especially the gastrointestinal assay (**Chapter 4**)

and the co-culture model (**Chapter 5**), further provide tools for general *in vitro* screening of NP that are considered for oral uptake, either in food or for medical purposes. Therefore, the present work also contributes to animal alternative testing (3R concept: 'reduction, refinement, replacement' of animal experiments) (Richmond, 2002).

The broad diversity of engineered nanomaterials and their manifold use complicates a reliable hazard assessment. Nowadays, their widely unpredictable behaviour necessitates an individual evaluation for each particle (*case-by-case-approach*) in each target tissue (*target-by-target-approach*), depending on the application and main uptake route. The findings reported in this thesis offer insights into the hazard and possible mechanisms of some of the main food relevant NP within the intestinal epithelium.



## 6.2 References

- Arai N, Mitomi H, Ohtani Y, Igarashi M, Kakita A, Okayasu I. Enhanced epithelial cell turnover associated with p53 accumulation and high p21WAF1/CIP1 expression in ulcerative colitis. *Mod Pathol* 1999;12(6):604-11
- Boots AW, Haenen GR, Bast A. Health effects of quercetin: from antioxidant to nutraceutical. *Eur J Pharmacol* 2008;585(2-3):325-37
- Borm PJA, Knaapen AM, Schins RPF, Godschalk RWL, Van Schooten FJ. Neutrophils amplify the formation of DNA-adducts by benzo[a]pyrene in lung target cells. *Environ Health Perspect* 1997;105 (5): 1089-93
- Bouwmeester H, Dekkers S, Noordam MY, Hagens WI, Bulder AS, de Heer C, ten Voorde SE, Wijnhoven SW, Marvin HJ, Sips AJ. Review of health safety aspects of nanotechnologies in food production. *Regul Toxicol Pharmacol* 2009;53:52
- Chaudhry Q, Scotter M, Blackburn J, Ross B, Boxall A, Castle L, Aitken R, Watkins R. Applications and implications of nanotechnologies for the food sector. *Food Addit Contam Part A Chem Anal Control Expo Risk Assess* 2008;25(3):241-58
- Desai MP, Labhasetwar V, Amidon GL, Levy RJ. Gastrointestinal uptake of biodegradable microparticles: effect of particle size. *Pharm Res* 1996;13(12):1838-45
- Dybdahl M, Risom L, Møller P, Autrup H, Wallin H, Vogel U, Bornholdt J, Daneshvar B, Dragsted LO, Weimann A, Poulsen HE, Loft S. DNA adduct formation and oxidative stress in colon and liver of Big Blue rats after dietary exposure to diesel particles. *Carcinogenesis* 2003;24(11):1759-66
- Grassian VH, Adamcakova-Dodd A, Pettibone JM, O'shaughnessy PT, Thorne PS. Inflammatory response of mice to manufactured titanium dioxide nanoparticles: comparison of size effects through different exposure routes. *Nanotoxicol* 2007;1:211-226
- Gullberg E, Leonard M, Karlsson J, Hopkins AM, Brayden D, Baird AW, Artursson P. Expression of specific markers and particle transport in a new human intestinal M-cell model. *Biochem Biophys Res Commun* 2000 Dec;279(3):808-13
- Gurr JR, Wang AS, Chen CH, Jan KY. Ultrafine titanium dioxide particles in the absence of photoactivation can induce oxidative damage to human bronchial epithelial cells. *Toxicology* 2005;213(1-2):66-73
- Huang N, Katz JP, Martin DR, Wu GD. Inhibition of IL-8 gene expression in Caco-2 cells by compounds which induce histone hyperacetylation. *Cytokine* 1997;9(1):27-36
- Johnston CJ, Driscoll KE, Finkelstein JN, Baggs R, O'Reilly MA, Carter J, Gelein R, Oberdörster G. Pulmonary chemokine and mutagenic responses in rats after subchronic inhalation of amorphous and crystalline silica. *Toxicol Sci* 2000;56(2):405-13
- Knaapen AM, Seiler F, Schilderman PA, Nehls P, Bruch J, Schins RP, Borm PJ. Neutrophils cause oxidative DNA damage in alveolar epithelial cells. *Free Radic Biol Med* 1999;27(1-2):234-40
- Liao W, McNutt MA, Zhu WG. The comet assay: a sensitive method for detecting DNA damage in individual cells. *Methods* 2009; 48(1):46-53

- Lomer MC, Hutchinson C, Volkert S, Greenfield SM, Catterall A, Thompson RP, Powell JJ. Dietary sources of inorganic microparticles and their intake in healthy subjects and patients with Crohn's disease. *Br J Nutr* 2004;92(6):947-55
- Lopes CM, Martins-Lopes P, Souto EB. Nanoparticulate carriers (NPC) for oral pharmaceuticals and nutraceuticals. *Pharmazie* 2010;65(2):75-82
- Mars Inc.'s US Patent US 5741505
- Mazzucchelli L, Hauser C, Zraggen K, Wagner H, Hess M, Laissue JA, Mueller C. Expression of interleukin-8 gene in inflammatory bowel disease is related to the histological grade of active inflammation. *Am J Pathol* 1994;144(5):997-1007
- Mitsuyama K, Toyonaga A, Sasaki E, Watanabe K, Tateishi H, Nishiyama T, Saiki T, Ikeda H, Tsuruta O, Tanikawa K. IL-8 as an important chemoattractant for neutrophils in ulcerative colitis and Crohn's disease. *Clin Exp Immunol* 1994;96(3):432-6
- Monteiller C, Tran L, MacNee W, Faux S, Jones A, Miller B, Donaldson K. The pro-inflammatory effects of low-toxicity low-solubility particles, nanoparticles and fine particles, on epithelial cells in vitro: the role of surface area. *Occup Environ Med* 2007;64(9):609-15
- Nakagawa Y, Wakuri S, Sakamoto K, Tanaka N. The photogenotoxicity of titanium dioxide particles. *Mutat Res* 1997;394(1-3):125-32
- <http://www.nanotechproject.org/inventories/consumer/browse/> (May 2010)
- Oberdörster G, Oberdörster E, Oberdörster J. Nanotoxicology: an emerging discipline evolving from studies of ultrafine particles. *Environ Health Perspect* 2005;113(7):823-39
- Qaddoumi MG, Ueda H, Yang J, Davda J, Labhasetwar V, Lee VH. The characteristics and mechanisms of uptake of PLGA nanoparticles in rabbit conjunctival epithelial cell layers. *Pharm Res* 2004;21(4):641-8
- Reindl W, Weiss S, Lehr HA, Förster I. Essential crosstalk between myeloid and lymphoid cells for development of chronic colitis in myeloid-specific signal transducer and activator of transcription 3-deficient mice. *Immunology* 2007;120(1):19-27
- Richmond J. Refinement, reduction, and replacement of animal use for regulatory testing: future improvements and implementation within the regulatory framework. *ILAR J* 2002;43 Suppl:S63-8
- Sayes CM, Wahi R, Kurian PA, Liu Y, West JL, Ausman KD, Warheit DB, Colvin VL. Correlating nanoscale titania structure with toxicity: a cytotoxicity and inflammatory response study with human dermal fibroblasts and human lung epithelial cells. *Toxicol Sci* 2006;92(1):174-85
- Schmid K, Riediker M. Use of nanoparticles in Swiss Industry: a targeted survey. *Environ Sci Technol* 2008;42(7):2253-60
- Singh S, Shi T, Duffin R, Albrecht C, van Berlo D, Höhr D, Fubini B, Martra G, Fenoglio I, Borm PJ, Schins RP. Endocytosis, oxidative stress and IL-8 expression in human lung epithelial cells upon treatment with fine and ultrafine TiO<sub>2</sub>: role of the specific surface area and of surface methylation of the particles. *Toxicol Appl Pharmacol* 2007;222(2):141-51
- Sripanyakorn S, Jugdaohsingh R, Dissayabutr W, Anderson SH, Thompson RP, Powell JJ. The comparative absorption of silicon from different foods and food supplements. *Br J Nutr*. 2009 Sep;102(6):825-34

- Thoree V, Skepper J, Deere H, Pele LC, Thompson RP, Powell JJ. Phenotype of exogenous microparticle-containing pigment cells of the human Peyer's patch in inflamed and normal ileum. *Inflamm Res*. 2008 Aug;57(8):374-8
- Unfried K, Albrecht C, Klotz LO, von Mikecz A, Grether-Beck S, Schins RPF. Cellular responses to nanoparticles: target structures and mechanisms. *Nanotoxicol* 2007;1:52-71
- US Patent US 2002/0025964 A1
- Vermeer IT, Henderson LY, Moonen EJ, Engels LG, Dallinga JW, van Maanen JM, Kleinjans JC. Neutrophil-mediated formation of carcinogenic N-nitroso compounds in an in vitro model for intestinal inflammation. *Toxicol Lett* 2004;154(3):175-82
- Wells CL, Jechorek RP, Erlandsen SL. Inhibitory effect of bile on bacterial invasion of enterocytes: possible mechanism for increased translocation associated with obstructive jaundice. *Crit Care Med* 1995;23(2):301-7
- Westendorf AM, Fleissner D, Deppenmeier S, Gruber AD, Bruder D, Hansen W, Liblau R, Buer J. Autoimmune-mediated intestinal inflammation-impact and regulation of antigen-specific CD8+ T cells. *Gastroenterology* 2006;131(2):510-24
- Zhao LG, Wu XX, Han EK, Chen YL, Chen C, Xu DQ. Protective effect of YHI and HHI-I against experimental acute pancreatitis in rabbits. *World J Gastroenterol* 1998;4(3):256-259



### 6.3 Summary

The toxicological mechanisms of nanoparticles (NP) in the respiratory tract are relatively well understood and are thought to arise mainly from their unique ability to generate reactive oxygen species (ROS). NP are characterised by a size range between 1 and 100 nm and can directly induce intracellular oxidative stress, e.g. resulting in cell death or oxidative DNA damage. Induction of pro-inflammatory signalling pathways, which is also triggered by ROS, can initiate or exacerbate inflammatory events by recruitment and activation of phagocytes such as neutrophils or macrophages. NP induced oxidative stress and inflammation in the lung is known to play a role in various lung diseases including chronic obstructive pulmonary disease (COPD) and asthma. Elevated DNA strand breakage and oxidative DNA damage by ROS is implicated in carcinogenesis and may provide an explanation for the associations between inhalation of ambient particulate matter, diesel exhaust particles or nano-sized metal oxide particles and lung cancer.

Industrial applications of nano-sized materials in food and food products have increased dramatically. However, possible adverse effects of particles in the human intestine are poorly investigated to date and these may play a role in chronic inflammatory bowel diseases or bowel cancer.

In the present thesis, a selection of five NP relevant as likely food additives or contaminants (e.g. for use in food packaging) was analysed for the potential to induce cytotoxicity and DNA damage in the widely used human intestinal epithelial cell line Caco-2. Carbon black, a model for environmental NP, as well as magnesium oxide did only slightly reduce the metabolic activity of the cells, and no DNA damaging potential was found. In contrast, titanium dioxide (TiO<sub>2</sub>) revealed both cytotoxic and light-dependent DNA damaging potential. Upon detailed particle characterisation, these effects on intestinal cells were found to be mainly driven by the crystalline structure of the different TiO<sub>2</sub> samples and less on their particle size or specific surface area, both being major factors in TiO<sub>2</sub> induced lung toxicity.

Silicon dioxide (SiO<sub>2</sub>) and zinc oxide (ZnO) were both found to induce not only strong cytotoxic effects in Caco-2 cells, but also oxidative stress accompanied by induction of (oxidative) DNA damage: Moreover, they showed a strong potential to upregulate the pro-inflammatory cytokine interleukin-8, which is known as a potent recruitment and activating factor for neutrophils. Both materials tended to form aggregates and/or agglomerates in suspension and were found to be taken up into Caco-2 cells independent of microtubule- and clathrin/AP2-mediated endocytosis. A simulated gastrointestinal digestion procedure was established; however, this treatment did not alter the cytotoxic or pro-inflammatory potentials of both SiO<sub>2</sub> and ZnO. This is relevant information for hazard assessment, when these particles are used in food products and as such enter the human intestinal tract.

Potential interactions between NP and neutrophils were investigated using a co-culture-model of freshly isolated primary human neutrophils with Caco-2 cells. In this model enhanced superoxide anion production by the neutrophils was observed and, in association with this, increased DNA damage and oxidative lesions in the Caco-2 cells. However, SiO<sub>2</sub> did not directly activate the neutrophils, and no induction of DNA strand breakage was detected when SiO<sub>2</sub> was applied in the co-culture model. The effect of ingested SiO<sub>2</sub> was therefore also determined *in vivo* in healthy as well as colitis induced mice. The induction of DNA strand breakage and oxidative lesions were analysed by using the highly sensitive Fpg-modified comet assay and immunohistochemical staining. Interestingly, SiO<sub>2</sub> only appeared to induce slight oxidative DNA damage after chronic but not after acute treatment and played no role in the modification of the genome integrity in colitic colons.

Taken together, the present thesis contributed to a better understanding of various adverse effects of relevant NP in the intestinal epithelium and thus offers valuable information for improved hazard and risk assessment. Furthermore, specific experimental models used in the framework of this thesis may serve as tools to screen for the potential hazards of novel engineered NP for which oral exposure can be anticipated.

## 6.4 Zusammenfassung

Die toxikologischen Mechanismen von Nanopartikeln (NP) im Respirationstrakt sind heutzutage verhältnismäßig gut untersucht. Diese besonders kleinen Materialien, charakterisiert durch eine Größenverteilung von 1-100 nm in ein oder mehr Dimensionen, weisen üblicherweise ein hohes Potenzial zur Generierung reaktiver Sauerstoffspezies auf. Diese wiederum sind häufig Ursache für die zelltoxischen, inflammatorischen und DNA-schädigenden Effekte von NP. DNA-Strangbrüche sowie oxidative DNA-Schäden spielen eine entscheidende Rolle in der Kanzerogenese, und die Inhalation von Feinstäuben, Dieselabgasen oder Nano-Metalloxiden stellt ein erhöhtes Risiko zur Entstehung von Lungentumoren dar.

Eine NP-induzierte Freisetzung von proinflammatorischen Zytokinen kann zudem zur Auslösung und/oder Exazerbation entzündlicher Erkrankungen führen, wobei die Rekrutierung und Aktivierung von Phagozyten wie neutrophilen Granulozyten (Neutrophilen) oder Makrophagen eine entscheidende Rolle spielen. Es konnte gezeigt werden, dass durch NP induzierter oxidativer Stress sowie Entzündungsreaktionen auch eine Rolle bei der Pathologie chronisch-entzündlicher Lungenerkrankungen wie Asthma oder chronisch obstruktiver Lungenerkrankung (chronic obstructive pulmonary disease, COPD) spielen.

Bereits seit Jahrzehnten werden größere, so genannte Mikropartikel als Zusatzstoffe für Nahrungsmittel verwendet, häufig ohne mengenmäßige Einschränkungen. Die veränderten chemischen und physikalischen Eigenschaften derselben Substanzen in Nano-Größe könnten jedoch zu unvorhersehbaren gesundheitlichen Risiken führen, würden diese Partikel in Nahrungsmitteln Verwendung finden. Bereits heutzutage wird umfangreich Forschung betrieben, die zu einer weiten Nutzung von NP in alltäglichen Lebensmitteln, aber auch in so genannten „functional foods“ oder auch Verpackungsmaterialien führen sollen. Vereinzelt sind derartige Produkte bereits auf dem Markt. Die Reaktivität dieser Partikel im menschlichen Körper und mögliche damit verbundene gesundheitliche Risiken sind derzeit jedoch noch weitgehend unerforscht. Besonders im menschlichen Darm könnten NP, vergleichbar mit der Lunge, eine Rolle bei der Entstehung von Darmkrebs oder chronisch entzündlichen Darmerkrankungen wie Colitis Ulzerosa spielen.

In der vorliegenden Arbeit wurden fünf verschiedene NP untersucht, die möglicherweise eine Rolle als Lebensmittel-Zusatzstoff oder in Verpackungsmaterialien für Lebensmittel spielen könnten. Ihr zelltoxisches sowie DNA-schädigendes Potenzial auf den Darm wurde zunächst an der vielfach genutzten humanen intestinalen Epithelzelllinie Caco-2 analysiert.

Es konnte gezeigt werden, dass sowohl Magnesiumoxid als auch Kohlenstoffpartikel, die als Modell für Feinstaub verwendet werden, nur einen schwachen Einfluss auf die metabolische Aktivität der Zellen sowie kein DNA-schädigendes Potenzial aufwiesen. Dagegen führte eine Belastung mit Titandioxid ( $\text{TiO}_2$ ) sowohl zu einer dosisabhängigen Zelltoxizität als auch zu lichtabhängiger Erhöhung von DNA-Strangbrüchen. Fünf verschiedene  $\text{TiO}_2$ -Partikel wurden daraufhin vergleichend untersucht und die Materialeigenschaften detailliert charakterisiert. Hierbei zeigte sich, dass das toxische Potenzial hauptsächlich von der kristallinen Struktur der Partikel abhing, nicht jedoch von der Partikelgröße oder der spezifischen Oberfläche, welche als wichtigster Faktor der Partikelreaktivität in der Lunge bekannt ist.

Des Weiteren konnte gezeigt werden, dass Siliziumdioxid ( $\text{SiO}_2$ ) und Zinkoxid ( $\text{ZnO}$ ) nicht nur starke Zelltoxizität, sondern auch ein hohes Maß an oxidativem Stress, verbunden mit einer Erhöhung von (oxidativen) DNA-Schäden hervorriefen. Das zytotoxische Potenzial war dabei jedoch abhängig vom Differenzierungsstatus der Zellen. Beide Materialien induzierten zudem die mRNA-Expression und Proteinsekretion von Interleukin-8, einem proinflammatorischen Zytokin, welches besonders bei der Rekrutierung und Aktivierung von Neutrophilen aus dem Blutkreislauf eine Rolle spielt, welche nach Aktivierung erhöhte Mengen an reaktiven Sauerstoffspezies produzieren.

Sowohl  $\text{SiO}_2$  als auch  $\text{ZnO}$  wurden von den Caco-2 Zellen über Mikrotubuli- und Clathrin/AP2-vermittelte Endozytose-unabhängige Mechanismen aufgenommen. Zudem zeigte sich, dass beide Partikel in Suspension in hohem Maß zur Bildung von Aggregaten und/oder Agglomeraten neigten. Ein simulierter pH-abhängiger gastrointestinaler Verdau der Partikel führte zudem zu keiner signifikanten Veränderung des zytotoxischen sowie proinflammatorischen Potenzials der Partikel. Dieses Ergebnis ist besonders relevant für eine Einschätzung möglicher Gesundheitsrisiken, da die verwendete Methode das Verhalten der Partikel im Organismus realistischer widerspiegelt als herkömmliche *in vitro* Partikelauflösungen.

Um den Einfluss von  $\text{SiO}_2$  auf den inflammatorischen Darm vertiefend zu untersuchen, wurde ein Koinkubationsmodell aus Caco-2 Zellen und frisch isolierten humanen Neutrophilen verwendet. Aktivierte Neutrophile zeigten dabei eine signifikante Generierung reaktiver Sauerstoffspezies und induzierten sowohl DNA-Strangbrüche als auch oxidative DNA-Schäden in den Caco-2 Zellen.  $\text{SiO}_2$  dagegen führte nicht zu einer Aktivierung der Neutrophilen, und die DNA-Schädigung in Caco-2 Zellen war zudem sogar leicht verringert im Verhältnis zu einer  $\text{SiO}_2$ -Inkubation ohne Kokultur mit Neutrophilen. Um diesen wesentlichen Effekt genauer zu untersuchen wurde sowohl gesunde als auch akut bzw. chronisch an Colitis erkrankten Mäusen  $\text{SiO}_2$ -angereichertes Futter verabreicht. In allen Gruppen wurde keine Induktion von DNA-Schäden im Gesamtkolongewebe nach  $\text{SiO}_2$ -Behandlung nachgewiesen. Immunhistochemische Analysen in Kolon-Gewebeschnitten zeigten dagegen eine leichte Erhöhung oxidativer Läsionen sowohl in  $\text{SiO}_2$ -behandelten gesunden Tieren als auch nach Colitis-Induktion im chronischen Modell.

Die vorliegende Arbeit leistet einen wichtigen Beitrag zum besseren Verständnis möglicher Risiken von NP in Lebensmitteln und deren Auswirkungen auf das Darmepithel. Die Ergebnisse dieser Arbeit tragen somit zu einer verbesserten Risikoabschätzung und damit erhöhten Lebensmittelsicherheit bei. Zudem können die hier beschriebenen experimentellen Modelle als *in vitro* Methoden zum Screening von neuartigen NP hinsichtlich potenzieller Gesundheitsrisiken verwendet werden.

## 6.5 Abbreviations

8-OHdG	8-hydroxydeoxyguanosine
°C	degree Celsius
Ag	Silver
Al <sub>2</sub> O <sub>3</sub>	alumina
AP2	adaptor protein 2
APC	adenomatous polyposis coli
APE/Ref-1	apurinic/apyrimidinic endonuclease
AU	arbitrary units
BCA	bicinchonnic acid- and copper(II) sulphate solution
BET	Brunauer-Emmett-Teller
BSA	bovine serum albumin
CB	carbon black
CD	Crohn's disease
cDNA	complementary DNA
CGD	chronic granulomatous disease
CIN	chromosomal instability
cm <sup>2</sup>	square centimetres
COPD	chronic obstructive pulmonary disease
CPH	1-hydroxy-3-carboxy-pyrrolidine
CRC	Colorectal cancer
CXCR	CXC chemokine receptor
DC	dendritic cells
DC assay	detergent compatible assay
DFO	deferoxamine
DLS	dynamic light scattering
DMSO	dimethyl sulfoxide
DNA	Deoxyribonucleic acid
DNA-pol- $\alpha$	DNA-polymerase $\alpha$
DPBS	Dulbecco's Phosphate Buffered Saline
DPP4	dipeptidylpeptidase 4
DS	digestion-simulated
DSMZ	Deutsche Sammlung von Mikroorganismen und Zellkulturen
DSS	dextrane sulphate sodium
DTNB	5,5'-dithiobis-(2-nitrobenzoic acid)
Duox	dual oxidases
EDTA	ethylenediaminetetraacetic acid disodium salt dehydrate
EFSA	European Food Safety Authority
ELISA	Enzyme-linked immunosorbent assay
ENP	engineered nanoparticles
E-number	Europe-number (for food additives)
EPR	Electron paramagnetic resonance
F	fine
FCS	fetal calf serum
FDA	Food and Drug Administration
Fe <sub>3</sub> O <sub>4</sub> , Fe <sub>2</sub> O <sub>3</sub>	iron oxides
Fpg	formamidopyrimidine glycosylase
G	gauss
GALT	gut-associated lymphoid tissue
G-CSF	granulocyte-colony stimulating factor
GI	gastrointestinal
GSFA	Codex General Standard for Food Additives
GSH	glutathione
GSSG	glutathione disulfide

## Abbreviations

GTPase	guanosine triphosphate hydrolase
h	hours
HBSS	Hanks' Balanced Salt Solution
HEI	Health Effects Institute
HEPES	4-(2-hydroxyethyl)-1-piperazineethanesulfonic acid
HNO <sub>3</sub>	nitric acid
HO·	hydroxyl radical
HO-1	heme oxygenase 1
HOCl	hypochlorous acid
H <sub>2</sub> O <sub>2</sub>	inflammatory bowel diseases
HRTEM	High-resolution transmission electron microscopy
HSA	high surface area
hZTL1	human ZnT-like transporter 1
IBD	inflammatory bowel diseases
ICAM-1	the intercellular adhesion molecule 1
ICDD	International Centre for Diffraction Data
ICP-OES	inductively coupled plasma optical emission spectrometry
IEL	intraepithelial lymphocytes
IHC	immunohistochemistry
IL-1 $\beta$	interleukin-1 $\beta$
IL-8	interleukin-8
iNOS	inducible nitric oxide synthase
IU/ml	International Units per milliliter
IVCAB	<i>in vivo</i> comet assay buffer
LDH	Lactate dehydrogenase
Lgr5	Leucine-rich repeat-containing G-protein coupled receptor 5
LMP	low melting point
LP	lamina propria
LPS	lipopolysaccharide
kDa	kilodaltons
kg	kilograms
kHz	kilohertz
kV	kilovolt
M	molar
m <sup>2</sup>	square metres
m $\phi$	macrophages
mA	milliampere
M-cells	microfold cells
MDR1	Multi drug resistant 1
MEM	Minimum essential Medium
mG	milligauss
mg	milligrams
MgO	magnesium oxide
min	minutes
MLN	mesenteric lymph nodes
mM	millimolar
mm	millimetres
MPO	myeloperoxidase
mRNA	messenger ribonucleic acid
MSI	microsatellite instability
NADPH	nicotinamide adenine dinucleotide phosphate
NF- $\kappa$ B	nuclear factor- $\kappa$ B
ng	nanograms
nm	nanometer
NO·	nitric oxide
NP	nanoparticles



Ns	nano-sized
O <sub>2</sub> <sup>-</sup>	superoxide anion radical
<sup>1</sup> O <sub>2</sub>	singlet oxygen
OGG1	8-oxoguanine DNA glycosylase
ONOO <sup>-</sup>	peroxynitrite anion
PAF	platelet activating factor
PAMP	particulate matter
PBS	phosphate buffered saline
PC	pigment cells
PCR	polymerase chain reaction
PMA	phorbol myristate acetate
PMN	polymorphonuclear neutrophils
PP	Peyer's patches
ppm	parts-per-million
PSP	poorly soluble low toxicity particles
qRT-PCR	quantitative Real-Time reverse-transcription PCR
RLU	relative light units
RNS	reactive nitrogen species
Ro19-8022	[R]-1-[(10-Chloro-4-oxo-3-phenyl-4H-benzo[a]quinolizin-1-yl)-carbonyl]-2-pyrrolidinemethanol
ROS	reactive oxygen species
rpm	revolutions per minute
SCC	sporadic colorectal carcinoma
SD	standard deviation
SiO <sub>2</sub>	silicon dioxide
SOD	superoxide dismutase
SPF	specific pathogen-free
SSA	specific surface area
STAT3/4	activator of transcription 3/4
TD <sub>50</sub>	median toxic dose
TEER	transepithelial resistance
TEM	transmission electron microscopy
Th1/2	type 1/2 helper cell
TiO <sub>2</sub>	titanium dioxide
TLR	Toll-like receptors
TNF- $\alpha$	tumor necrosis factor- $\alpha$
Tris	tris(hydroxymethyl)aminomethane
UC	ulcerative colitis
UV	ultraviolet
V	Volt
W	Watt
WST-1	water-soluble tetrazolium salt
WT	wild type
XRD	X-ray diffraction
$\mu$ m	micrometer
ZnO	zinc oxide



## Publications

### First author papers

**Gerloff K**, Albrecht C, Boots AW, Förster I, Schins RPF. Cytotoxicity and oxidative DNA damage by nanoparticles in human intestinal Caco-2 cells.  
*Nanotoxicology* 2009; 3(4): 355-364

**Gerloff K**, Fenoglio I, Carella E, Albrecht C, Boots AW, Förster I, Roel P.F. Schins. Specific surface area independent effects of titanium dioxide particles in human intestinal Caco-2 cells.  
*Submitted*

**Gerloff K**, Pereira DIA, Faria NJR, Boots AW, Förster I, Albrecht C, Powell JJ, Schins RPF. Influence of simulated gastrointestinal digestion on particulate mineral oxide-induced cytotoxicity and interleukin-8 regulation in differentiated and undifferentiated Caco-2 cells  
*In preparation*

**Gerloff K**, Winter M, Boots AW, Van Berlo D, Kolling J, Albrecht C, Förster I, Schins RPF. In vitro and in vivo investigations on the effect of amorphous silica on DNA damage in the inflamed intestine.  
*In preparation*

## Co-author papers

- Van Berlo D, Haberzettl P, **Gerloff K**, Li H, Scherbart AM, Albrecht C, Schins RP. Investigation of the cytotoxic and proinflammatory effects of cement dusts in rat alveolar macrophages.  
*Chem Res Toxicol* 2009;22(9):1548-58
- Wessels A, Van Berlo D, Boots AW, **Gerloff K**, Scherbart AM, Cassee FR, Gerlofs-Nijland ME, Van Schooten FJ, Albrecht C and Schins RPF. Oxidative stress and DNA damage responses in rat and mouse lung to inhaled carbon nanoparticles.  
*In press, Nanotoxicology*
- Van Berlo D\*, Wessels A\*, Boots AW, Wilhelmi V, Scherbart AM, **Gerloff K**, Albrecht C, Schins, RPF. \*equal contribution. Neutrophil-derived oxygen species contribute to oxidative stress and DNA damage induction by respirable quartz particles.  
*Submitted*
- Boots AW, **Gerloff K**, Van Berlo D, Ledermann K, Haenen G, Bast A, Albrecht C and Schins RPF. Neutrophils augment LPS-mediated pro-inflammatory signalling in human lung epithelial cells.  
*Submitted*
- Van Berlo D, Albrecht C, Wessels A, Wilhelmi V, Scherbart AM, **Gerloff K**, Hellack B, Huaux F, Boots A and Schins RPF. Role of phagocyte-derived reactive oxygen species (ROS) in fibrosis induced by respirable quartz.  
*In preparation*
- Winter M, Lehr HA, **Gerloff K**, Schins RPF, Buer J, Westendorf AM\* and Förster I\*. \*equal contribution. Oral uptake of amorphous SiO<sub>2</sub> nanoparticles exacerbates experimental inflammatory bowel disease.  
*In preparation*

## Presentations

### Oral presentations

DNA damage in human colon cells by nanoparticles and activated neutrophils. 3<sup>rd</sup> Symposium of the GRK 1427 "Nanoparticles and the gastrointestinal tract". 5-6 March 2009, Düsseldorf, Germany.

Nanoparticle-activated neutrophils cause oxidative DNA damage in human colon epithelial cells. 50<sup>th</sup> Annual meeting of the German Society for Toxicology and Pharmacology (DGPT). 10-12 March 2009, Mainz, Germany.

### Poster presentations

**Gerloff K**, Boots A, Förster I, Albrecht C, Schins R. Effects of engineered nanoparticles on oxidative stress and DNA damage in human colon epithelial cells-lines. 1<sup>st</sup> Symposium of the GRK 1427 "Food, gut, and the immune system: A challenge in environmental medicine".  
4-5 October 2007, Düsseldorf, Germany

**Gerloff K**, Boots A, Förster I, Albrecht C, Schins R. Oxidative stress and DNA damage in human colon epithelial cells by engineered nanoparticles. 49<sup>th</sup> Annual meeting of the German Society for Toxicology and Pharmacology (DGPT).  
11-13 March 2008, Mainz, Germany

**Gerloff K**, Boots A, Förster I, Albrecht C, Schins RPF. Oxidative stress and DNA damage in human colon epithelial cells by engineered nanoparticles. NANOTOX2008, 2<sup>nd</sup> International Nanotoxicology Conference.  
7-10 September 2008, Zurich, Switzerland

**Gerloff K**, Boots A, Förster I, Albrecht C, Schins RPF. Oxidative stress and DNA damage in human colon epithelial cells by engineered nanoparticles. 2<sup>nd</sup> Symposium of the GRK 1427 "Nutrition and Health: Intestinal Effects of Food Compounds."  
3-4 April 2008, Düsseldorf, Germany

**Gerloff K**, Boots AW, Winter M, Förster I, Albrecht C, Schins RPF. Oxidative DNA damage by nanoparticles in human intestinal Caco-2 cells in the presence or absence of neutrophils. Eurotox-46<sup>th</sup> Congress of the European Societies of Toxicology  
13-16 September 2009, Dresden

**Gerloff K**, Boots AW, Winter M, Förster I, Albrecht C, Schins RPF. Oxidative DNA damage by nanoparticles in human intestinal Caco-2 cells in the presence or absence of neutrophils. 4<sup>th</sup> Symposium of the GRK 1427 "Endocrine Disruptors: Mode of action and exposure assessment."  
8-9 October 2009, Düsseldorf

**Gerloff K**, Pereira D, Faria N, Förster I, Albrecht C, Powell JJ, Schins RPF. Simulated gastric conditions do not influence nanoparticle-induced effects on cytotoxicity and Interleukin-8 release from human intestinal cells. 51<sup>st</sup> Annual meeting of the German Society for Toxicology and Pharmacology (DGPT).  
23-25 March 2010, Mainz, Germany

**Gerloff K**, Fenoglio I, Carella E, Albrecht C, Boots AW, Förster I, Roel P.F. Schins. Specific surface area independent effects of titanium dioxide particles in human intestinal Caco-2 cells. Nanotoxicology 2010  
2-4-June 2010



## Danksagung

Ich danke Herrn Professor Dr. Josef Abel für die Übernahme des Erstgutachtens.

Ebenso bin ich Herrn Professor Dr. Manfred Braun für die Übernahme des Zweitgutachtens dankbar.

Besonders möchte ich mich bei Dr. Roel Schins für die Bereitstellung dieses spannenden Themas und die Aufnahme in seine Arbeitsgruppe bedanken. Sein Engagement, die Anregungen und viele interessante Gespräche sowie die Freiheiten, die mir zur Ausgestaltung dieser Arbeit gewährt wurden, haben maßgeblich zum Gelingen beigetragen.

Zudem bedanke ich mich vielmals bei Frau Dr. Catrin Albrecht, die jederzeit zu hilfreichen Anregungen und Diskussionen sowie Unterstützung jeglicher Art bereit war und immer ein freundliches Wort für jeden hat.

Allen Kollegen und Mit-Doktoranden in der Arbeitsgruppe, Damien van Berlo, Bryan Hellack, Julia Kolling, Maja Rohling, Agnes Scherbart, Anton Wessels und Verena Wilhelmi möchte ich besonders für das tolle Arbeitsklima, die gute Zusammenarbeit und die Hilfsbereitschaft danken. Zudem bedanke ich mich bei Frau Dr. Agnes Boots für viele interessante und produktive Diskussionen und die Freundschaft.

Mein Dank für die Unterstützung im Laboralltag gilt Frau Kirstin Ledermann, Frau Christel Weishaupt und Frau Gabriele Wick.

Frau Professor Dr. Irmgard Förster und Meike Winter danke ich für die gute Zusammenarbeit und die jederzeit entgegengebrachte Hilfsbereitschaft.

Der Aufnahme in das Graduiertenkolleg 1427 und die allzeit gute Betreuung durch Frau Professor Dr. Regine Kahl, Frau Professor Dr. Charlotte Esser, Herrn PD Dr. Wim Wätjen und Frau Bennat verdanke ich viele interessante Erfahrungen durch die Teilnahme an verschiedensten Kursen und Veranstaltungen sowie die Ermöglichung meines Forschungsaufenthaltes in Cambridge. Allen Mitgliedern des GRK bin ich für die tolle Zeit und den guten Zusammenhalt dankbar.

Zudem bedanke ich mich herzlich bei Herrn Professor Dr. Jonathan Powell für die freundliche und offene Aufnahme als Gast in seiner Arbeitsgruppe. Die große Hilfsbereitschaft und die gute Arbeitsatmosphäre durch Dr. Dora Pereira, Dr. Nuno Faria,

## *Danksagung*

Bianca Mergler sowie allen anderen Kollegen ermöglichten mir eine überaus lehrreiche, spannende und abwechslungsreiche Zeit!

Ich möchte allen Kollegen und Mitarbeitern des IUF für die gute und angenehme Zusammenarbeit danken, insbesondere Herrn PD Dr. Klaus Unfried und seiner gesamten Arbeitsgruppe für die Hilfsbereitschaft in Laborfragen und die stets freundliche Atmosphäre.

Bei Dr. Ivana Fenoglio und Emanuele Carella bedanke ich mich für die gute und unkomplizierte Kooperation.

Allen meinen Freunden, auch und besonders Henrike an „vorderster Front“ danke ich für den Rückhalt und die Unterstützung. Catrin, Katharina und Simone, ihr habt unsere gemeinsame Zeit zum Abenteuer und unvergesslich gemacht!

Besonderer Dank gilt meinen Eltern, meiner Schwester und meiner gesamten Familie. Ihr habt mich jederzeit unterstützt und seid immer für mich da! Und natürlich Bodo, mein Fels in der Brandung, auf den ich mich immer verlassen kann!



## **Eidesstattliche Erklärung**

Hiermit versichere ich, dass ich die vorliegende Arbeit eigenständig verfasst und keine anderen als die angegebenen Quellen und Hilfsmittel verwendet habe. Ferner versichere ich, dass ich weder an der Heinrich-Heine-Universität Düsseldorf noch an einer anderen Universität versucht habe, diese Dissertation einzureichen. Ebenso habe ich bisher keine erfolglosen Promotionsversuche unternommen.

Düsseldorf, den 19.05.2010

---

Kirsten Britta Gerloff